Louisiana Transportation Research Center

Final Report 567

Development of Guidelines for Transportation of Long Prestressed Concrete Girders

by

Jonathan C. McGormley, P.E., S.E.
Richard E. Lindenberg, P.E., S.E

Wiss, Janney, Elstner Associates

4101 Gourrier Avenue | Baton Rouge, Louisiana 70808
(225) 767-9131 | (225) 767-9108 fax | www.ltrc.lsu.edu

TECHNICAL REPORT STANDARD PAGE

1. Report No.	2. Government Accession No.	3. Recipient's Catalog No.
FHWA/LA.16/567		

4. Title and Subtitle	5. Report Date
Development of Guidelines for Transportation of Long Prestressed Concrete Girders	December 2016
	6. Performing Organization Code LTRC Project Number: 10-5ST State Project Number: 30000138

7. Author(s)	8. Performing Organization Report No.
Jonathan C. McGormley, P.E., S.E. Richard E. Lindenberg, S.E.	

9. Performing Organization Name and Address	10. Work Unit No.
Wiss, Janney, Elstner Associates, Inc. 330 Pfingsten Road, Northbrook, IL 60062	11. Contract or Grant No.

12. Sponsoring Agency Name and Address	13. Type of Report and Period Covered
Louisiana Department of Transportation and Development P.O. Box 94245 Baton Rouge, LA 70804-9245	**Final Report** **May 2011-March 2016**
	14. Sponsoring Agency Code

15. Supplementary Notes

Conducted in Cooperation with the U.S. Department of Transportation, Federal Highway Administration

16. Abstract

This research study investigates the behavior of two long prestressed concrete girders during lifting and transportation from the precast yard to the bridge site, with a particular focus on cracking concerns during transport. Different response measurements were recorded, including dynamic strains, dynamic accelerations, rigid body motion measurements, thermal, and girder location using GPS tracking. The monitoring results indicate that higher tensile strain events occurred during transport of the girders than during lifting of the girders at the yard or bridge site. Local events during transportation of both girders produced strains that exceeded the theoretical cracking strain determined by the research team. Potential cracking events were not associated with high dynamic accelerations; instead, they occurred at low-speed (<10 mph) sharp turns (90 deg. with tight radii) where the jeep tongue was attached to the girder. Based on analysis of the girders in this study and previous related research, cracking strains were readily experienced during girder transport and prior to erection. This research presents technical data obtained from two long prestressed concrete girders during transport and handling.

17. Key Words	18. Distribution Statement
Long prestressed concrete girders; transport; torsion; bending; cracking; buckling; stability; instrumentation	**Unrestricted. This document is available through the National Technical Information Service, Springfield, VA 21161.**

19. Security Classif. (of this report)	20. Security Classif. (of this page)	21. No. of Pages	22. Price
N/A	N/A	113	

Project Review Committee

Each research project will have an advisory committee appointed by the LTRC Director. The Project Review Committee is responsible for assisting the LTRC Administrator or Manager in the development of acceptable research problem statements, requests for proposals, review of research proposals, oversight of approved research projects, and implementation of findings.

LTRC appreciates the dedication of the following Project Review Committee Members in guiding this research study to fruition.

LTRC Manager

Walid R. Alaywan, Ph.D., P.E.
Sr. Structures Research Engineer

Members

Jenan Nakhlé, P.E., DOTD Bridge Design
Gill Gautreau, P.E., DOTD Bridge Maintenance
Mike Ricca, P.E., DOTD Construction
Alden Allen, P.E., DOTD Bridge Design
Michael Boudreaux, P.E., LTRC
Art Aguirre, P.E., FHWA

Directorate Implementation Sponsor

Janice P. Williams, P.E.
DOTD Chief Engineer

Development of Guidelines for Transportation of Long Prestressed Concrete Girders

by

Jonathan C. McGormley, P.E., S.E.
Richard E. Lindenberg, P.E., S.E

Wiss, Janney, Elstner Associates
330 Pfingsten Road
Northbrook, IL 60062

LTRC Project No. 10-5ST
State Project No. 30000138

conducted for

Louisiana Department of Transportation and Development
Louisiana Transportation Research Center

The contents of this report reflect the views of the author/principal investigator who is responsible for the facts and the accuracy of the data presented herein. The contents do not necessarily reflect the views or policies of the Louisiana Department of Transportation and Development, the Federal Highway Administration, or the Louisiana Transportation Research Center. This report does not constitute a standard, specification, or regulation.

December 2016

ABSTRACT

Prior research has recognized that long girder transportation is fundamentally complex. Most research on girder stability and cracking prior to erection has focused on lifting of long girders, as this has been traditionally viewed as the most critical action—with respect to loading—in the life of the girder. In these studies, researchers aimed to provide a methodology to avoid cracking and loss of stiffness during lifting of long girders.

This research study investigated the behavior of two long prestressed concrete girders during lifting and transportation from the precast yard to the bridge site, with a particular focus on cracking and stability concerns during transport. Different response measurements were recorded, including dynamic strains, dynamic accelerations, thermal, and rigid body motion measurements, while the girders were tracked using a global positioning system (GPS). The monitoring results indicate that girder transport produced more severe tensile strain events than those measured during lifting of the girders at the yard or bridge site. Local transport events for both girders caused strains to exceed the theoretical cracking strain determined by the research team. Contrary to initial assumptions, potential cracking events were not associated with high dynamic accelerations, but instead occurred at low-speed (<10 mph) sharp turns (90 deg. with tight radii) where the trailer (jeep) tongue was attached to the girder. Cracks were not visually observed, but changes in girder response were noted as an indication that localized concrete cracking occurred.

While most of the previous research in girder handling focused on avoiding cracking events, based on analyses of the girders in this study and previous related research work, cracking strains were readily experienced during girder lifting and transport. These findings have implications for how long prestressed concrete girders should be handled to avoid cracking. Some of the greatest tensile strains imposed on the girders were the result of controllable events (i.e., tight turning radii), and not due to a less controllable phenomenon such as roadway super-elevation along the delivery route. This research identified the jeep tongue loading as a critical component in the transportation process, one that should likely be considered as part of any long girder transportation evaluation.

ACKNOWLEDGMENTS

The author gratefully acknowledges the financial support provided by the Louisiana Transportation Research Center (LTRC) and the Louisiana Department of Transportation and Development (DOTD).

The researchers would like to acknowledge the assistance of Gulf Coast Pre-Stress (GCP), Pass Christian, Mississippi, for their participation in this project. The GCP staff were helpful and accommodating during the fabrication and transport portions of the project, enabling the researchers to complete their work within the project schedule.

The authors also acknowledge the assistance of WJE staff Mohamed ElBatanouny, John Fraczek, Steve Lauer, Todd Nelson, Roger Pelletier, and Brian Santosuosso. Through their efforts, this project was a success.

Finally, special thanks are due to Dr. Walid Alaywan (LTRC), senior structures research engineer, for the project management of this research as well as providing valuable articles pertaining to the literature search.

IMPLEMENTATION STATEMENT

By identifying the loading effects caused by the rear jeep tongue on long prestressed concrete girders during transport, the potential for cracking of these girders can be reduced. The link between the tongue forces and girder cracking had not been previously documented in published research. Through this research, recommendations to mitigate girder cracking during transportation were presented that include the application of tongue forces by the designer during transportation stress evaluation and changes in transport procedures by the precaster.

TABLE OF CONTENTS

ABSTRACT iii
ACKNOWLEDGMENTS v
IMPLEMENTATION STATEMENT vii
TABLE OF CONTENTS ix
LIST OF TABLES xi
LIST OF FIGURES xiii
INTRODUCTION 1
Literature Review 1
DOTD-BDI Research 4
Department of Transportation Design Guidance 5
Ohio Department of Transportation 5
Washington Department of Transportation 6
Industry Software 6
PGSuper 6
OBJECTIVE 9
SCOPE 11
METHODOLOGY 13
Instrumentation Program 13
Selection and Description of Girders 13
Instrumentation 15
Sensor Information 17
Sensor Information - Periodic Monitoring 18
Sensor Information Dynamic Monitoring 20
Data Acquisition Equipment 26
Girder Fabrication 27
Laboratory Testing 30
Compressive Strength 30
Creep and Shrinkage 31
Modulus of Elasticity 32
Coefficient of Thermal Expansion 33
Evaluating the Potential of Cracking 33
Periodic Monitoring 35
Strains at Prestressing Release 35
Time Dependent Concrete Properties: Creep and Shrinkage 36
Camber and Sweep Measurements 38

Dynamic Monitoring During Girder Transport and Lifting 40
Trailer Support and Operation 40
Girder Loading 42
Evaluation of Measured Strain Data for Cracking 44
Dynamic Monitoring During Girder Transport: *Girder 1 - Ft. Buhlow Route* 45
Dynamic Monitoring During Girder Transport: *Girder 2 - Lake Charles Route* 58
Dynamic Monitoring During Other Notable Events 64
Dynamic Monitoring During Prestress Transfer 65
Dynamic Monitoring During Lifting 67
Observations from Girder Transportation and Lifting 68
Finite Element Analysis 70
Development of 3D Model 71
Variation of Girder Roll Angle versus Girder Length 73
Variation of Jeep Tongue Lateral Force versus Girder Length 74
Comparison of BT-72 and LG-54 Girders 76
Modal Response Analysis of Girders 77
DISCUSSION OF RESULTS 81
State of Strain 81
Girder Stability 82
Transportation Strains 83
Lifting Strains 85
Girder Properties 86
CONCLUSIONS 87
RECOMMENDATIONS 89
ACRONYMS, ABBREVIATIONS, AND SYMBOLS 91
REFERENCES 93
APPENDIX *(See online version for Appendix)* 95

LIST OF TABLES

Table 1 Girders moment of inertia and effective prestressing force 14
Table 2 Casting and transportation overview 15
Table 3 Girder 1 instrumentation during transportation 17
Table 4 Girder 2 instrumentation during transportation 17
Table 5 Girder 1 instrumentation summary 18
Table 6 Girder 2 instrumentation summary 18
Table 7 Girder 1 data acquisition channel information 27
Table 8 Girder 2 data acquisition channel information 27
Table 9 Compressive strength results at 7 days 31
Table 10 Creep and shrinkage test results 32
Table 11 Modulus of elasticity 33
Table 12 Coefficient of thermal expansion 33
Table 13 Measured and calculated strains at release in microstrain 35
Table 14 Calculated strains at release in microstrain 35
Table 15 Camber and sweep measurements versus analytical predictions 40
Table 16 Surface strains of selected transportation events based on high girder acceleration 50
Table 17 Surface strains of selected transportation events based on high girder strains 53
Table 18 Surface strains of selected transportation events based on high girder acceleration 61
Table 19 Surface strains of selected transportation events based on high girder strains 62
Table 20 Surface strains during road surface irregularity transportation events 65
Table 21 Measured and calculated transfer strains for Girder 1 66
Table 22 Transfer strains of Girder 1 before and after lifting from prestressing bed using embedded strain gages 66
Table 23 Surface strains of lifting events at yard and site 68

LIST OF FIGURES

Figure 1 Instrumented cross-sections (i.e., A, B, C, D, and E) from BDI instrumentation work 5
Figure 2 ODOT suggest locations for shipping strands 5
Figure 3 PGSuper input form view for "Lifting and Shipping" 7
Figure 4 Factor of safety versus end support location during lifting 8
Figure 5 End view of Girder 1 (BT-72) shortly after removal from casting bed 14
Figure 6 End view of Girder 2 (LG-54) during loading for transport 15
Figure 7 Instrumented mid-span girder cross-section as represented on the instrumentation plan for Girder 2 16
Figure 8 Micro Measurements EGP-5-350 embedded strain gage installed prior to casting 19
Figure 9 Laser mounted on girder end for camber measurements 20
Figure 10 Laser target with dots marking recorded laser points 20
Figure 11 BDI external stain transducer with adjacent externally bonded thermocouple for coarse thermal corrections and redundant strain gage (Girder 2 shown) 21
Figure 12 Comparison of strain recorded by BDI gages and surface strain gages at Section B for Girder 2 22
Figure 13 Thermocouple (blue wire) placed adjacent to embedded strain gage (Section B) 23
Figure 14 View of IMU installation on girder: a) external mounting of enclosure; and b) inside enclosure with IMU (yellow box) and digital to analog converter 24
Figure 15 View of IMU output: a) heading response through 90° turn; and b) roll response about the longitudinal axis during the turn 25
Figure 16 Photograph from on-board camera during I-10 turn 26
Figure 17 Stressed prestressing laid out for Girder 1 in the form beds at Gulf Coast Pre-Stress 29
Figure 18 Concrete placement from the chute of a buggy into the forms for Girder 1 29
Figure 19 Attempted rotational stiffness testing of Hydra-Steer trailer at GCP yard 30
Figure 20 Experimental and analytical creep results 31
Figure 21 Change of strain in Girder 1 due to creep and shrinkage 38
Figure 22 Schematic of camber and sweep measurements using laser 39
Figure 23 Typical girder transport setup with Girder 2 crab turning (note that tongue is engaged) 41
Figure 24 Isometric diagram of Hydra-steer trailer 41
Figure 25 Turning configurations of Hydra-steer trailer 42

Figure 26 Front steering of rear trailer (note tongue disengaged) 42
Figure 27 Girder 2 moved for loading using gantry crane..... 43
Figure 28 Loading of girder on truck with gantry crane..... 43
Figure 29 Tie down of girder at rear jeep tongue 44
Figure 30 FFT of vertical and lateral acceleration at midspan vertical gyro unit..... 45
Figure 31 Overview of route of Girder 1 with relative speed along the route overlaid (red > 55 mph; green < 10 mph) 46
Figure 32 Evaluation of route characteristics using synchronized data and time lapse video from Girder 2..... 47
Figure 33 Overview of route of Girder 1 showing accelerations with selected events noted (color contours: green < 0.05 g to red > 0.25 g) 49
Figure 34 Selected event G1-A1 as shown on a map with colorized data output along route..... 51
Figure 35 Overview of route of Girder 1 showing girder top flange strain differentials with selected events noted (color contours: green < 100 microstrain to red > 300 microstrain) 52
Figure 36 Comparison of transport data at noted top flange differential strain events in Pass Christian 55
Figure 37 First turn out of yard without jeep tongue mounted on Girder 1 (upper photo) and Girder 2 (lower photo)..... 56
Figure 38 Girder 1 (upper photo) and Girder 2 (lower photo) crabbing during a turn onto I-10 with jeep tongue engaged 56
Figure 39 Comparison between (a) top flange strain differential; (b) lateral and vertical acceleration at midspan; and (c) lateral roll angle at mid-span..... 57
Figure 40 Overview of route of Girder 1 with relative speed along the route overlaid (red > 55 mph; green < 10 mph) 58
Figure 41 Overview of route of Girder 2 showing accelerations with selected events noted (color contours: green < 0.05 g to red > 0.25 g)..... 60
Figure 42 Overview of route of Girder 2 showing girder top flange strain differentials with selected events noted (color contours: green < 100 microstrain to red > 300 microstrain)..... 63
Figure 43 Girder transport during a high strain event going around a tight radius turn with the tongue attached..... 64
Figure 44 Erection of Girder 1 onto the bridge bearings..... 67
Figure 45 3D Model of BT72 Girder..... 72
Figure 46 Typical FEM output results..... 73
Figure 47 Midspan cross-section showing displaced shape and lateral deflection..... 73

Figure 48 Effect of roll angle at midspan and girder length on peak tensile strains..... 74
Figure 49 Girder model to examine effect of lateral loading at jeep tongue support 75
Figure 50 Comparison of tongue force variation on different length girders 75
Figure 51 Comparison of roll angle variation on different type girders 76
Figure 52 Comparison of variation tongue force on different type girders 77
Figure 53 Modal analysis of first four modes of 130-ft long BT-72 78
Figure 54 Modal analysis of first four modes of 130-ft. long LG-54 78
Figure 55 Change in cross section strains during turning event without tongue engaged..... 84
Figure 56 Change in cross section strains during turning event with tongue engaged..... 84

INTRODUCTION

Prestressed concrete girders are an economical superstructure system for bridges and are used in about 24 percent of the bridges in the United States *[1]*. With the advent of higher strength concrete and more efficient cross sections, the use of long (> 100 ft.) prestressed concrete girders has become commonplace. Routinely, girders exceeding 150 ft. in length and depths of 6 ft. are now specified. Such long span girders require special considerations during manufacturing, transporting, handling, and erecting.

Many of the forces associated with construction of precast prestressed concrete girders are well understood. Less is known, however, about the forces a girder is subjected to during transport. While girders are designed for strong axis loading conditions and, thus, can readily accommodate such loading during transportation, they are typically braced in-service and, hence, may have inadequate resistance to lateral or lateral-torsional load effects before bracing is installed. As a result, girders have arrived on jobsites exhibiting visual cracks indicative of weak axis bending or torsion. In other instances, trucks transporting girders have rolled as the girders laterally buckled. These transportation problems can delay construction while the girders are repaired or replaced, and possibly lead to a reduction in service life if moisture and chlorides infiltrate unrepaired cracked girders.

The Louisiana Department of Transportation and Development (DOTD) has observed these transportation problems with long prestressed concrete girders. Building on research into girder stability design by Laszlo et al., and estimations of transportation stresses by Mast, the DOTD instrumented two 150-ft. long prestressed bulb-tees during transport in an effort to assess the forces on the girders *[2 - 6]*. Transportation of these instrumented girders resulted in weak axis cracking. The current research project was initiated to further investigate the causes of cracking during transportation and included monitoring of transportation-related strains in two additional long prestressed concrete girders.

Literature Review

Stability of long prestressed girders has been a focus of a number of studies since their introduction in the early 1960s. Mast's 1989 seminal work is probably the most cited paper for lifting of long-span prestressed concrete girders *[3]*. This work, along with a second part of the study published in 1993 serve as, the Precast/Prestressed Concrete Institute, PCI's recommendations to girder designers on stability and cracking prior to installation, respectively *[4, 5, 7]*. In his work, Mast simplified the stability effects caused by girder geometry as it relates to lateral and torsional stiffness. Based on this work, stability was quantified by comparing the height of the roll axis (i.e., the axis defined through the girder

support points, about which the girder rolls), versus the sweep deflection of the girder, assuming the full gravity load was applied in the weak-axis direction.

In 1993, Mast revisited lateral stability of girders with a focus on transportation *[4, 5]*. This work provides much of the theory and information still relied upon by the precast industry. The essential point of this work established the likelihood of lateral buckling of long concrete girders as minimal because of their high torsional stiffness; therefore, it is recommended to assume rigid torsional behavior in the roll stability analysis of girders. Mast tested static tilt angles of full-size girders to failure, and in that process, evaluated cracking, stability, and ultimate capacity. He found that girders generally started cracking and losing stiffness at tilt angles between 5 and 10 degrees. Failure typically occurred when the tilt angle exceeded 20 degrees.

When a girder cracks, its stiffness is reduced, affecting its deflections. Mast developed a simplified relationship between cracked (effective) and uncracked girder stiffnesses based on tilt angle. For tilt angles that produce top flange tensile stresses in excess of $7.5\sqrt{f'_c}$, the commonly accepted modulus of rupture per the American Concrete Institute (ACI) building code, ACI 318-14, the effective stiffness can be calculated as follows *[8]*:

$$I_{eff} = I_g/(1 + 2.5\theta_{max}) \quad (1)$$

where,
I_{eff} = Effective moment of inertia,
I_g = Gross moment of inertia, and
θ_{max} = tilt angle at which cracking occurs.

From Mast, it was found that girders supported from below, as they are during transportation, have sufficient torsional stiffness but overall less roll angle stiffness due to the flexible supports. This can lead to long span girders rolling sideways and subsequently buckling laterally. The factor of safety against instability is defined as the ratio of the resisting moment arm to the applied overturning moment arm as follows:

$$FS = \frac{r(\theta_{max} - \propto)}{\overline{z_o}\theta_{max} + e_i + y\theta_{max}} \quad (2)$$

where,
FS = factor of safety,
θ_{max} = tilt angle at which cracking occurs,
r = Kθ/w, Kθ = rotational spring constant of support (roll stiffness),
w = self-weight of girder,

$\bar{z_o}$ = deflection of the center of gravity of the girder due to bending about the weak axis caused by self-weight over a simple support,
ei = initial eccentricity of the center of gravity of the girder,
$\propto$ = super-elevation angle or tilt angle of support, and
y = height of center of gravity of girder above roll axis.

Mast proposed similar factors of safety when lifting girders, which are used as the basis for the equations in the PCI Design Handbook *[7]*.

Laszlo et al. point out the importance of lateral loads and super-elevation considerations during transport *[2]*. They also recommend temporary post-tensioning as a possible aid to reduce tensile stresses. Zureick et al. studied the stability of long prestressed bridge girders considering sweep and thermal effects *[9]*.

Cojocaru revisited research on girder stability work performed by Mast on lifting and provided an updated methodology using a nonlinear section analysis approach *[10]*. The basis of this approach was born from a classic solution to the lifting of doubly symmetric girders developed by Plaut et. al. *[11]*. Cojocaru investigated the performance of this updated approach and subsequently modified the method to allow for inclination and height of lift supports. Finite element modeling verification was also included in this work. Because beam imperfections are the main concern when lifting a beam, Cojocaru also performed a statistical study to review the effects of beam imperfections.

Stratford and Burgoyne reviewed girder stability through their work published in 1999 and 2002 *[12, 13, 14]*. In their work, three states of support for girders are defined as: (1) simply supported, (2) hanging, and (3) transported. This work focused more on lateral buckling, as it reviewed cross-sections from Europe that have minimal-to-no upper flange width when compared to precast bridge shapes commonly found in the US. Therefore, the lateral and torsional stiffness of such cross-sections are much smaller than their counterparts in the US. Stratford and Burgoyne indicated that, for such girders, lifting is the most critical support state as there is no restraint against rigid body motion (i.e., rotation). A series of non-dimensional buckling loads for the different support states was also developed in this work:

$$w_{cr} = k\frac{\sqrt{GJEI_y}}{L^3}. \quad (3)$$

where,
G = shear modulus,

J = St. Venant's torsion constant,
E = Young's modulus,
Iy = moment of inertia about the minor axis,
L = beam length, and
k = constant, equal to 28.5 for simply supported and 16.5 for the transported beam.

The authors present a more detailed solution for the case of the hanging girder *[12, 13]*.

It is noted that all of the above research, as well as other recent research by Weigel et al., Consolazio and Hamilton, and Hill et al. aimed to prevent instability and cracking (at least limit it) while handling and shipping long prestressed concrete girders *[15 - 17]*. Code-based guidance provided in the PCI Design Handbook and PCI Bridge Design Manual are essentially a reorganization of Mast's research into girder stability *[8, 18]*.

DOTD-BDI Research

In October 2006, Bridge Diagnostics, Inc. (BDI) instrumented two girders for DOTD and transported them in the same way as for this research project. The girders measured approximately 150 ft. in length and were monitored during transportation and erection. Strain gages were installed on the four girder flange tips at five cross-sections along the girder (Figure 1), consistent with the strain gage setup utilized in this research.

The transportation route included traveling along Interstate 20, where the girders reached speeds exceeding 60 mph, as well as being subjected to several sharp turns and uneven roadway surfaces. The data collected during this research indicates large recorded tensile strains occurred in both girders during various sharp turns (90 deg. with tight radii) with the highest strains recorded during a low speed U-turn at the bridge site. BDI researchers noted, "large weak-axis bending forces were primarily due to the synchronization of steering between the front and rear." It was also noted that higher strains were recorded in one girder due to the presence of a longitudinal crack in the girder top flange. The results from the BDI tests led to the initiation of this current research to further investigate the behavior of long girders during transportation *[6]*.

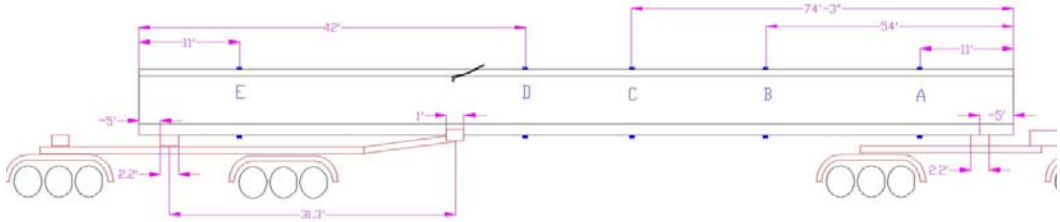

Figure 1
Instrumented cross-sections (i.e., A, B, C, D, and E) from BDI instrumentation work

Department of Transportation Design Guidance

Several Departments of Transportation (DOTs) have developed guidelines for safe handling and shipping of long prestressed girders. This section highlights such guidelines by two DOTs.

Ohio Department of Transportation

The Ohio Department of Transportation (ODOT) enables designers to include shipping strands in their designs as shown in Figure 2. These permanent strands are located in the top flange of the beam. ODOT notes, in their detail, that these strands are to be debonded for the entire length of the beam except for the last 10 ft. of the beam, and that they should be cut via a block-out in the top flange after handling operations are complete.

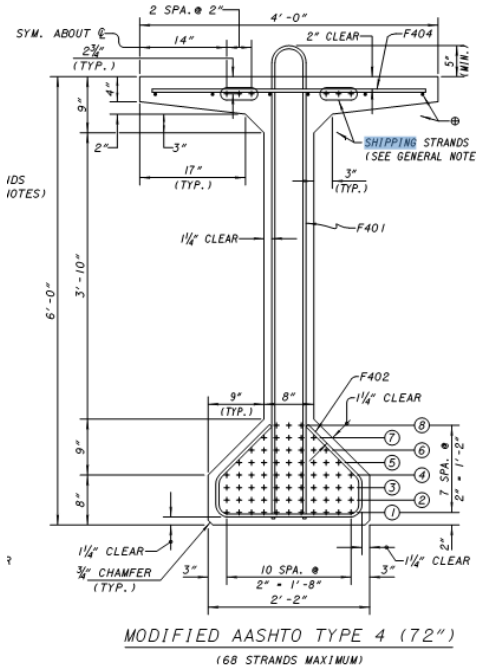

Figure 2
ODOT suggest locations for shipping strands

Washington Department of Transportation

The Washington Department of Transportation (WSDOT) includes a section within their design manual on girder transport *[19]*. They provide the following requirements and recommendations for designers.

- Use an additional impact factor of 20 percent during transport, while not including an impact factor for lifting.
- Consider the shipping route and its feasibility for transporting the girder(s).
- Place support locations in-board of the ends a minimum length equal to the depth of the girder.
- Minimize girder overhangs and make equal.
- Check lateral stability of the girder during shipping that considers the roll stiffness of girder supports.

Industry Software

PGSuper

PGSuper is a precast prestressed bridge girder design software sponsored by the Washington, Texas, and Kansas State Departments of Transportation and is available to be used for other state DOT designs *[20]*. The objective of the software is to provide the ability to design and check strength, service, and detailing criteria. In particular, there is a design module within the software that checks bridge girders for stresses and stability during lifting and transportation.

The WSDOT version of the software contains supplemental checks for lifting and transportation. Figure 3 shows an input view for the software from the "Lifting and Shipping" section. As seen in the figure, this is a very general representation of the transport support. One observation from a review of this software is that there is no provision to enter data for the jeep tongue attachment into this form or elsewhere within the software.

The software includes the standard BT-72 and LG-54 girder cross-sections used in this research; however, the specific prestressing configurations used in the research girders were not available. For example, test Girder 1 had 50 straight prestressing strands, and some of these were debonded. The design generated within the WSDOT configuration of PGSuper, required use of a combination of straight and harped strands. An example output from the software for checks for cracking and failure is shown in Figure 4. Because the dominant concern for cracking is length between the support points as presented in Mast's research, this figure shows that the factor of safety to prevent cracking is improved considerably by moving the supports inboard, up to a certain point.

In review of the WSDOT site, it is apparent that transportation remains a challenge for designers as observed from the following question on their frequently asked questions section on their website:

> *Question: I'm designing a long span girder and I just can't get the Spacing Between Truck Supports for Hauling, Girder Support Configuration, and Maximum Girder Weight specification checks to pass. What can I do?*
>
> *Answer: At design time it is difficult to know what actual equipment will be used to transport a girder. The Fail status simply means the design fails to satisfy the design criteria. In this case, the maximum allowable distance between supports, the maximum allowable leading overhang, and the maximum girder weight are highly dependent on the actual hauling equipment. The design criteria are based on rules of thumb.*
>
> *If you find yourself in this situation, call your local fabricators and haulers and let them help you decide if it is practical to transport your girders.*

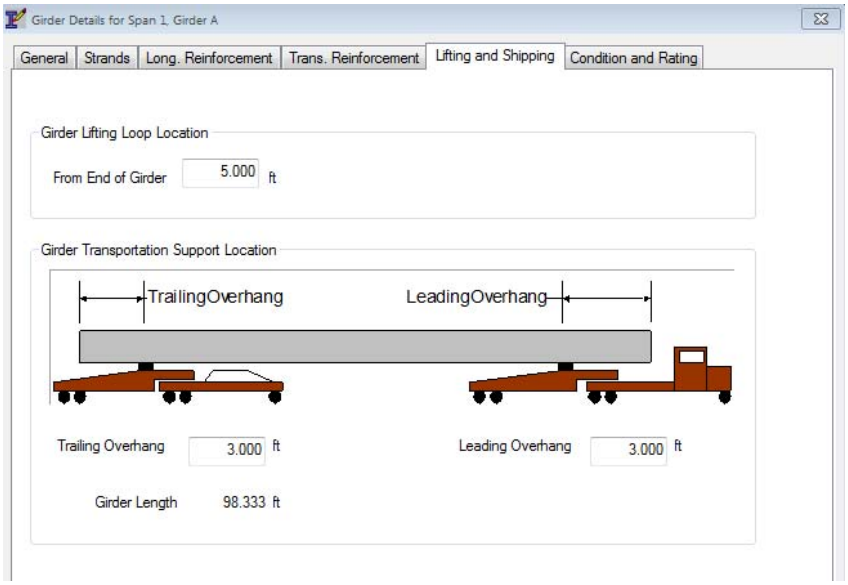

Figure 3
PGSuper input form view for "Lifting and Shipping"

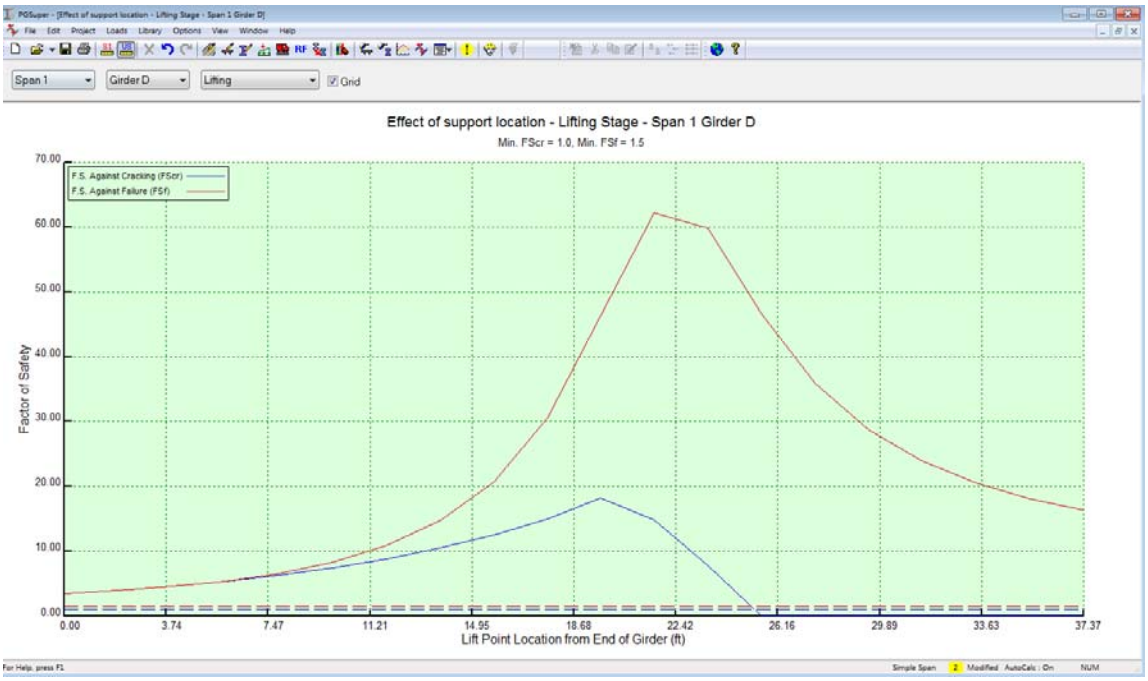

Figure 4
Factor of safety versus end support location during lifting

OBJECTIVE

The objective of this research was to develop guidelines that DOTD can apply to the future design and transportation of long prestressed concrete bridge girders to avoid cracking. The guidelines would define acceptable methods of girder support during transportation, recommend safe girder response limits during transportation, suggest road conditions/geometries to be avoided on transportation routes, and advocate design changes to improve girder shipping performance.

SCOPE

This research examined the behavior of two long-span prestressed concrete girders during transportation and lifting at the yard and bridge site. A key aspect of this study was to determine if cracking events occur before erecting the girders and to investigate the reason for those events. Thus, cross sections in each girder were instrumented with sensors to measure the following responses from initial girder casting to transport of the girder to the bridge site:

- Concrete strains;
- Accelerations—multi-axial;
- Roll and estimated deflections; and
- Temperature.

From detailed analyses of these results, suggested recommendations to better quantify the loads causing cracking and to reduce the potential for cracking were developed for long girders during transportation.

METHODOLOGY

The increasingly longer and slenderer prestressed precast concrete girders used in today's bridge structures are more susceptible to cracking and instability during handling and shipping. Unfortunately, the forces associated with transporting girders are not well defined, in part because they depend on a number of different parameters. The following research work plan was implemented to quantify transportation forces experienced by precast concrete girders and to develop applicable transportation guidelines and design changes to avoid cracking and instability.

Instrumentation Program

Selection and Description of Girders

Due to past long girder performance issues, DOTD subsequently placed a moratorium on the design of new long-span precast concrete girders. Therefore, for this research, it was necessary to select from already designed bridge projects that still required fabrication and transport of long girders within the research study period. The following two projects and girder sections were identified:

- Girder 1 - LA71B Fort Buhlow Bridge, Alexandria, LA: BT-72 girder with a length of 130 ft. Figure 5 is a photograph showing an end view of the girder shortly after casting.

- Girder 2 - I-210 over Cove Lane Bridge, Lake Charles, LA: LG-54 girder with a length of 130 ft. Figure 6 is a photograph of the end view of the girder just prior to loading for transport.

Cross section details and properties for each of the girders are provided in Appendix A. The gross moment of inertia and effective prestress force of each girder are shown in Table 1. A comparison of the studied girders notes a greater moment of inertia contributing to larger weak axis bending resistance and a significantly larger amount of effective prestressing force for Girder 2 (LG-54). Table 2 provides the casting and erection dates, along with the total time from fabrication until transportation and erection.

Figure 5
End view of Girder 1 (BT-72) shortly after removal from casting bed

Table 1
Girders moment of inertia and effective prestressing force

Girder	Strong axis moment of inertia (in^4)	Weak axis moment of inertia (in^4)	Weak axis to strong axis inertia ratio	Effective Prestressing at midspan (kips)
Girder 1: 130 ft. BT-72	545,857	37,634	0.07	1,425
Girder 2: 130 ft. LG-54	344,586	70,877	0.21	2,235

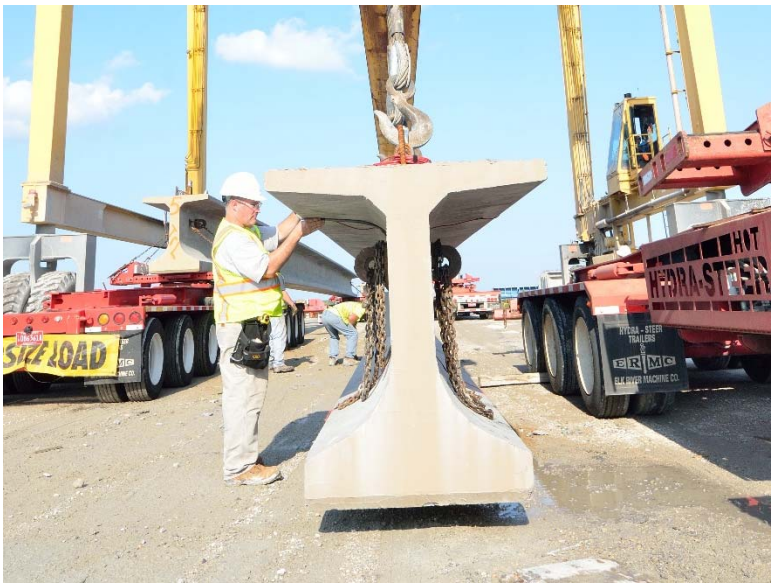

Figure 6
End view of Girder 2 (LG-54) during loading for transport

Table 2
Casting and transportation overview

Girder	Date Cast	Date Transported & Erected	Total Days Until Transport/Erection
Girder 1: 130 ft. BT-72	Nov. 30, 2011	July 3, 2013	581
Girder 2: 130 ft. LG-54	July 12, 2014	September 23, 2014	73

Instrumentation

Detailed instrumentation plans were developed based on a review of previous monitoring and parametric analyses of earlier DOTD-funded research. The purpose of the instrumentation was to monitor the behavior of the girders during transportation and lifting to detect and identify any events that may lead to cracking of the girders during these construction stages. In addition, periodic monitoring and a creep study for Girder 1 were also incorporated into the research plan to have a better understanding of the total state of strain in the girders at the time of transportation. The periodic monitoring plan included the installation of demountable mechanical strain gages (DEMEC) at multiple cross sections, along with field camber and sweep measurements.

The transportation instrumentation plan included installing dynamic strain, inertial measurement (acceleration and rotation), and temperature sensors at several critical cross sections in each girder as outlined in Table 3 and Table 4. The cross sections included both

girder ends and midspan, as well as the cross section where the jeep tongue contacted the girder. As shown in Figure 7, each cross section was instrumented with four strain gages (two at the bottom flange tip and two at the top flange tip) and one inertial measurement sensor, except for the tongue location where no inertial measurement sensor was installed. For Girder 1, these strain gages were typically embedded, while for Girder 2, they were externally applied. The midspan section was also instrumented with four temperature sensors. Girder 1 was instrumented with two additional temperature sensors to measure ambient temperature and temperature within the data acquisition enclosure. At the midspan cross-section (B) and tongue cross-section (D), additional redundant gages were installed on both test girders for purposes of testing gage types.

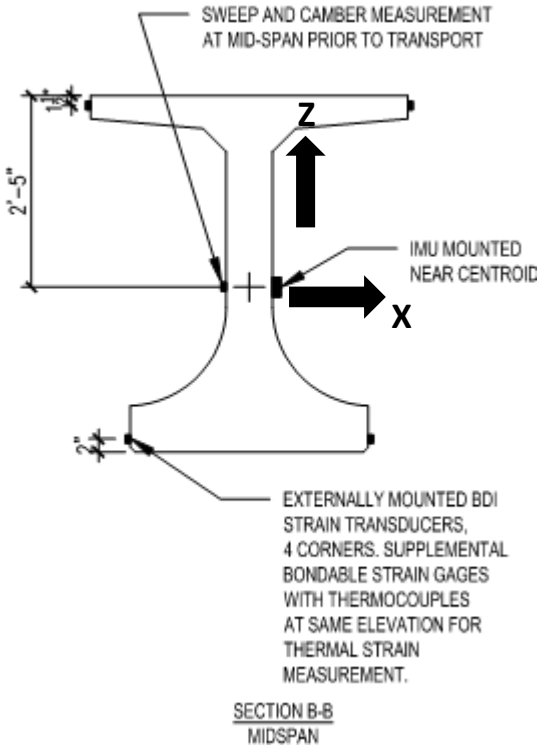

Figure 7
Instrumented mid-span girder cross-section as represented on the instrumentation plan for Girder 2

Additional measurements (displacements, geolocation, and photographic data) were also recorded during different transportation stages. A description of the use of each sensor, reason for selection, interface with data acquisition, and sampling rates are described next. In addition, Appendix B includes product information for the various sensors.

Table 3
Girder 1 instrumentation during transportation

Cross Section Label	**Location**	Sensor Type		
		Strain	Inertial	Temperature
A	Jeep End: 10 ft. from end	4	1	—
B	Midspan: 65 ft. from end	4	1	4
D	Tongue: 32 ft. from jeep end	4	—	—
C	Tractor End: 10 ft. from end	4	1	—

Table 4
Girder 2 instrumentation during transportation

Cross Section Label	**Location**	Sensor Type		
		Strain	Inertial	Temperature
A	Jeep End: 5 ft. from end	4	1	—
B	Midspan: 65 ft. from end	4	1	4
D	Tongue: 32 ft. from jeep end	4	—	—
C	Tractor End: 5 ft. from end	4	1	—

Sensor Information

The research utilized a variety of sensors to capture girder behavior during various phases of fabrication while in the yard, as well as dynamic behavior while the girder was being lifted or transported. Sensors were chosen for their ability to measure the desired behavior while remaining within the project budget. Each sensor type and time of sensor installation is listed in Table 5 for Girder 1 and Table 6 for Girder 2.

Table 5
Girder 1 instrumentation summary

Gage	Type	Installed Before
EGP-5-350	Dynamic Strain	Casting
Thermocouples	Temperature	Casting
DEMEC	Static Strain	Release
Displacement	Displacement	Release
Roll & yaw	Tilt (deg.)	Transport
Pitch	Orientation (deg.)	Transport
Acceleration	Acceleration	Transport
GPS	Geolocation	Transport
BDI Strain Transducer	Dynamic Strain	Transport

Table 6
Girder 2 instrumentation summary

Gage	Type	Installed Before
Roll & yaw	Tilt (deg.)	Transport
Pitch	Orientation (deg.)	Transport
Acceleration	Acceleration	Transport
GPS	Geolocation	Transport
BDI Strain Transducer	Dynamic Strain	Transport

Sensor Information - Periodic Monitoring

Girder 1 was chosen to capture representative long-term strain, as well as periodic measurements of sweep and camber, while still in the precast yard.

Concrete Strain Measurements. Strain losses from creep and shrinkage after casting are known to be several hundred microstrain, as widely reported in the literature. DEMEC gages were used to measure static strains of Girder 1 while in the yard. Although DEMEC gages have less accuracy than conventional strain gages, they offer economical and reasonable long-term stability without being affected by drift. These gages were placed at the ends and quarter points along the girder on the girder flange tips.

Embedded concrete strain gages were also installed in Girder 1 near each end and midspan (Sections A, B, and C) before concrete casting. The EGP-5-350 embedded sensor manufactured by Micro-Measurements is a 350 Ohm strain gage with a 4-in. gage length covered with a cementitious coating. The embedded gages were used to measure concrete strains prior to and after strand release, as well as during lifting and transport. The embedded gages provided protection from damage during fabrication, storage, and transport. They were also less susceptible to thermal gradients when the girder was directly exposed to the sun.

The gages were tied between prestressing strands or mild steel reinforcement using fiberglass dowels as shown in Figure 8.

Figure 8
Micro Measurements EGP-5-350 embedded strain gage installed prior to casting

Displacement Measurements. For Girder 1, a laser and target system was utilized at various stages of fabrication to measure overall length change, static camber, and static sweep. The laser and targets were temporarily secured using stainless steel drop-in anchors on the top side of the Girder 1 top flange near the tips. The laser and length target were installed at opposite ends of the girder, with a grid target installed at the midspan. Figure 9 shows the laser mounted on the girder top flange, with the associated laser target shown in Figure 10. Sweep and camber were measured using the grid target with the change in position of the laser beam on the target providing a measure of sweep and camber. A permanent dot was placed on the grid target for each measurement. These measurement sets were completed after fabrication and after storage prior to transport. Figure 10 shows the laser target with dots marking recorder laser points.

A high strength aircraft cable was also used for a traditional camber measurement. Tapcon screws were installed at each end of the girder and the cable was strung between the two with a weight hung from one end. This technique was utilized for the first series of measurements after casting, but was not repeatable in later measurements due to corrosion of the wire and missing weights that occurred during the approximate 19-month storage period of the girder.

Figure 9
Laser mounted on girder end for camber measurements

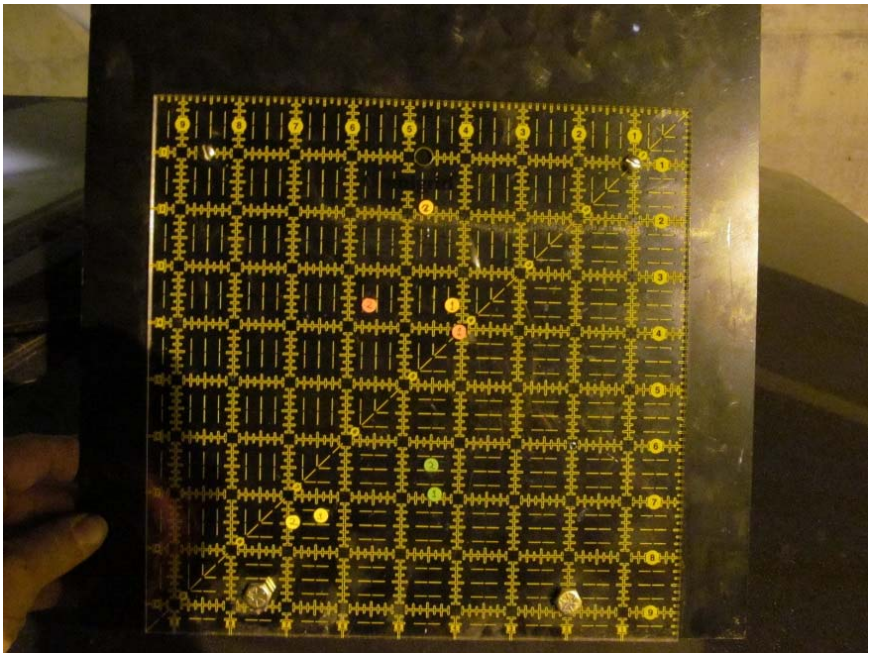

Figure 10
Laser target with dots marking recorded laser points

Sensor Information Dynamic Monitoring

Concrete Strain Measurements. For Girder 1, dynamic monitoring of strains during lifting and transportation were performed using a combination of the Micro Measurements EGP-5-350 embedded concrete gages discussed above and BDI external strain transducers. The EPG-5-350 gages were used to monitor the strains at Sections A, B, and C, while the

BDI external strain transducers were installed to monitor strains at the tongue mounting point (Section D). A redundant pair of BDI gages were also installed at Section B to compare midspan strains with the embedded strain gages. For Girder 2, only external strain transducers were utilized. BDI transducers were installed at all four girder cross sections described in the instrumentation plan. The BDI transducers were installed by bonding the transducer to the concrete surface using epoxy prior to lifting the girder at the yard for transportation. Figure 11 shows the BDI installation. These sensors are more susceptible to ambient temperature changes; therefore, only short-term events were considered.

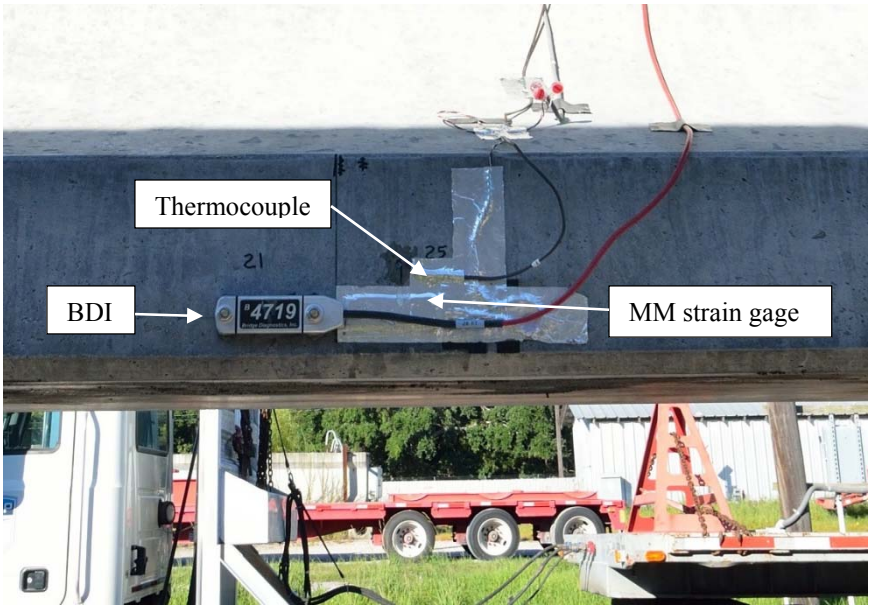

Figure 11
BDI external stain transducer with adjacent externally bonded thermocouple for coarse thermal corrections and redundant strain gage (Girder 2 shown)

Externally bonded Micro Measurements (MM) 20CBW-350 with a 2-in. gage length and 350-ohm resistance were also installed on Girder 2 at midspan (Section B) to provide redundancy and a comparison with the BDI sensor results. The change of strain recorded by both sensor types during an event (Event G2-S2 is shown in Figure 12) gave a similar response, with the difference in recorded strain value limited to 10 microstrain. The only notable difference between the two gage types is that BDI gages are more susceptible to temperature change, as they are made of aluminum. Therefore, for long-term monitoring, data collected using BDI gages were coarsely corrected for temperature effects using adjacent thermocouples bonded to the concrete flange.

Comparison of the BDI gage response data versus the embedded gage data for Girder 1 proved more difficult, as the gages were located at different points in the girder. As it was desired to compare the strains at the surface, the embedded strain data was transposed to the surface using the methods described in Appendix C.

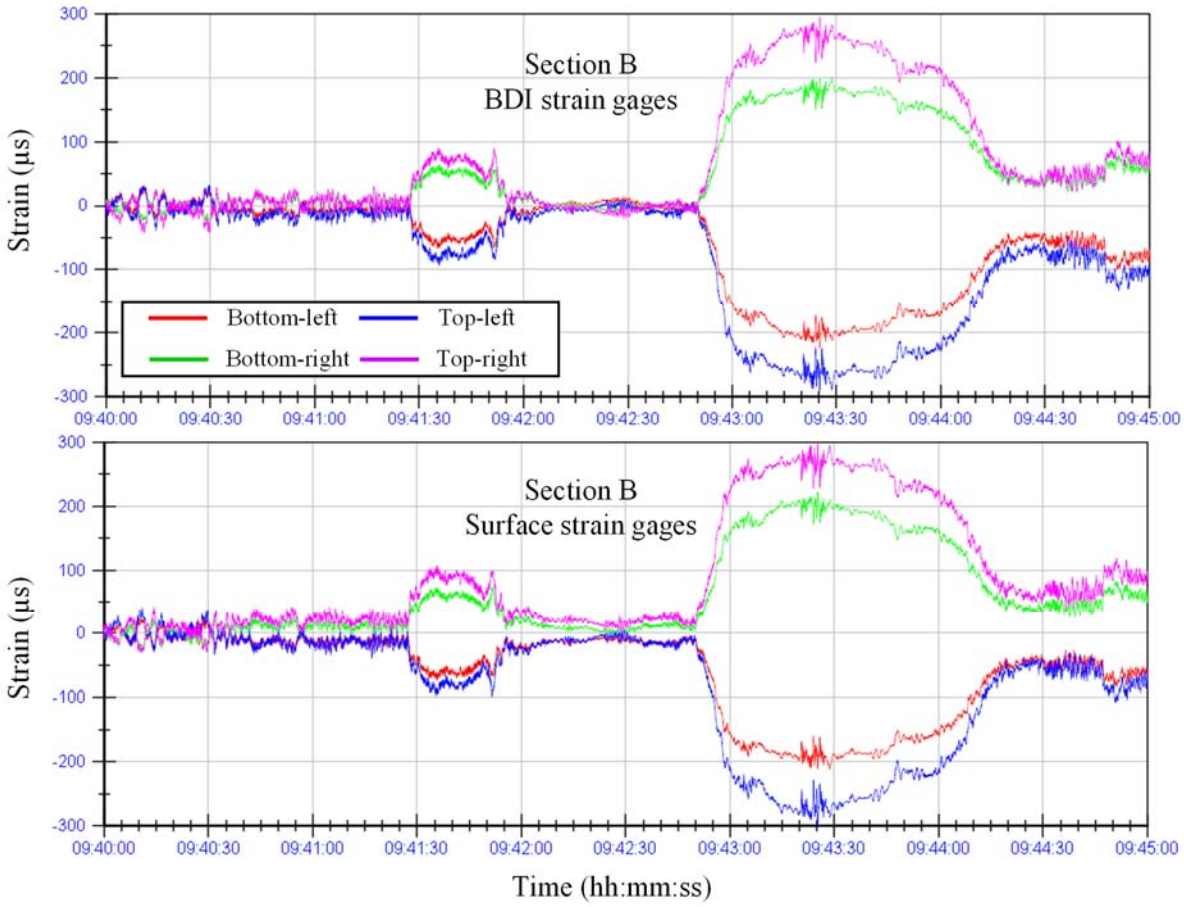

Figure 12
Comparison of strain recorded by BDI gages and surface strain gages at Section B for Girder 2

Temperature Measurements. For Girder 1, Type T thermocouples were installed on the reinforcement as shown in Figure 13 at Section B adjacent to the embedded strain gages to measure temperature gradients across the girder cross section. For Girder 2, the thermocouples were placed adjacent to the BDI transducers at Section B.

Figure 13
Thermocouple (blue wire) placed adjacent to embedded strain gage (Section B)

Inertial Measurement. Memsic VG350 vertical gyro units, which are also referenced as inertial measurement units (IMU), were used to measure dynamics related to girder transport and lifts. These units utilize a MEMS-based inertial sensor to provide three-dimensional acceleration, orientation (i.e., roll, pitch, and yaw), and roll rates. The systems were coupled to a Memsic NAV-DAC440 that converted the VG350 serial digital data signal into nine BNC analog voltage outputs. Each inertial unit provided orientation information relative to a vertical gravity reference. The VG350 was epoxied onto the vertical surface of the girder web near its centroidal axis. To provide protection from the elements, as well as protection for the NAV-DAC440 and associated connections, the instrumentation was housed in an enclosure that was attached with stainless steel drop-in anchors and sealed along the perimeter. A typical installation from the exterior and interior of the enclosure is shown in Figure 14.

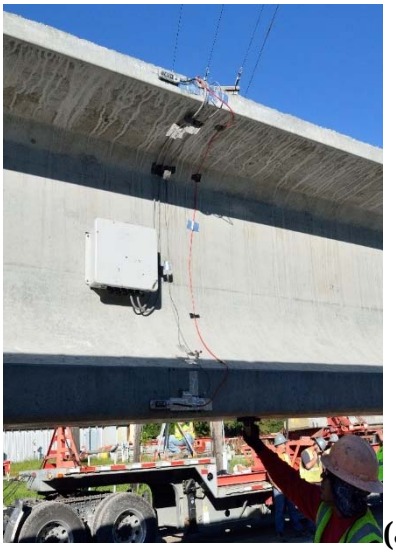
(a)

(b)

Figure 14
View of IMU installation on girder: a) external mounting of enclosure; and b) inside enclosure with IMU (yellow box) and digital to analog converter

The inertial measurement units were installed at the ends and midspan (Sections A, B, and C) to provide information on the response of the middle of the girder relative to its supported ends.

The acceleration response is consistent with conventional accelerometers but, through utilization of on-board processing, angular measurements can also be provided. An example output of the girder going around a 90° turn is provided in Figure 15. Roll rate data is also outputted by these units, but these data were not analyzed within this research. The units are typically specified for dynamic applications on land, consistent with this research application.

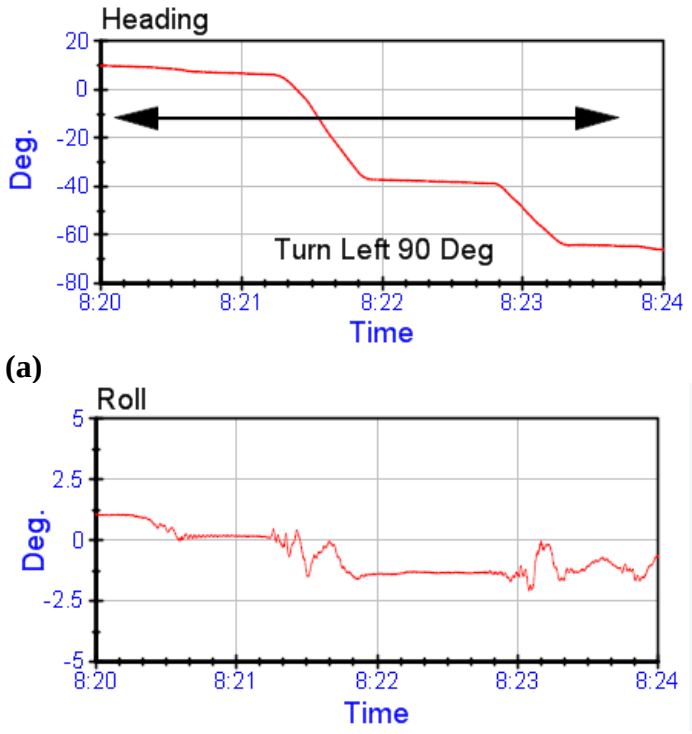

Figure 15
View of IMU output: a) heading response through 90° turn; and b) roll response about the longitudinal axis during the turn

Geolocation Measurements. The geolocation of both girders was tracked and recorded on Apple iPhones from a chase car. During transport, the girders were observed from the chase car at a distance of approximately 30 yards.

On-Board Camera. Each girder had photo imagery systems mounted as a part of the study. The camera was installed such that full field view of the girder during transportation was captured, as shown in Figure 16.

Figure 16
Photograph from on-board camera during I-10 turn

Data Acquisition Equipment

A Campbell Scientific CR9000X data acquisition system was utilized to collect and store strain, inertial behavior, and temperature measurements. The data acquisition equipment was stored in a weather resistant enclosure. For Girder 1, the data acquisition system was powered by a 2000-watt gasoline powered generator during transportation. For Girder 2, the data acquisition system was powered with two deep-cycle (marine) batteries. In both cases, the enclosure was securely strapped to the jeep end to prevent movement during transportation, and temporarily relocated on top of the girder during yard and site lifting operations.

The data acquisition system scanned the data at 100 Hz. The number of channels and their interface with the data acquisition system are shown in Table 7 and Table 8 for Girder 1 and Girder 2, respectively.

Table 7
Girder 1 data acquisition channel information

Gage	Type	Number of Channels of Data	Min Scan Rate	Comment
EGP-5-350	Dynamic Strain	12	100 Hz	Full Bridge completion
Thermocouples	Temperature	6	0.5 Hz	
DEMEC	Static Strain	20 static	Static	
Roll and yaw	Tilt (deg.)	3 locations x 2=6	100 Hz	
Pitch	Orientation (deg.)	3 locations x 1=3	100 Hz	
Acceleration	Acceleration	3 locations x 3=9	100 Hz	
GPS	Geolocation	1	10 sec	
BDI Strain Transducer	Dynamic Strain	6	100 Hz	Full bridge completion
Static Measurement		Static=20		EGPs, Thermocouples, & DEMEC
Transportation Measurement		Dynamic=43		All except DEMEC

Table 8
Girder 2 data acquisition channel information

Gage	Type	Number of Channels of Data	Min Scan Rate	Comment
BDI Strain Transducer	Dynamic Strain	16	100 Hz	Full Bridge completion
Thermocouples	Temperature	4	0.5 Hz	
Roll and yaw	Tilt (deg.)	3 locations x 2=6	100 Hz	
Pitch	Orientation (deg.)	3 locations x 1=3	100 Hz	
Acceleration	Acceleration	3 locations x 3=9	100 Hz	
GPS	Geolocation	1	10 sec	
Transportation Measurement		Dynamic=39		

Girder Fabrication

Gulf Coast Pre-Stress (GCP) fabricated the test girders for this project. They are a large precaster located in Pass Christian, Mississippi, on the banks of Bay St. Louis with ready access to US-90 and I-10 beyond. Established in 1967, they specialize in the fabrication of square pile, triangular pile, spun-cast cylinder pile, sheet pile, bridge girders, platforms, and walkways.

Fabrication of Girder 1 occurred in November 2011 consistent with the drawings provided by GCP, which are presented in Appendix A.

At the time of arrival at their yard, prestressing had already been arranged for the BT-72 girders destined for the Ft. Buhlow project. Stressed prestressing strand spanned the length of several girders in a single long bed as shown in Figure 17. Individual girders were formed using end forms positioned along the length of the casting bed. Forms for the girder sides were lowered on one side and fully removed from the other side for ready access to install instrumentation.

Instrumentation was installed over a full day. Once instrumentation was complete, the side forms were installed for casting on the afternoon of November 29, 2011, when several girders were cast in a row (Figure 18). GCP placed and finished the concrete in accordance with industry standard practices.

After steam curing overnight, the girder was ready for stripping the next morning based on cylinder testing performed by GCP. The researchers requested that, prior to cutting the prestressing, they be permitted to install the DEMEC points for static strain measurements. GCP agreed but advised this was outside of standard operating procedures and there would be some concern for development of shrinkage or thermal cracks if the sensor installation process extended the time prior to release. To minimize this risk, the DEMEC points were installed under the tarps while steam curing continued.

Once instrumentation installation was complete, initial static strain, camber, and sweep measurements were performed. The prestressing steel was cut using a torch at approximately 4:30 p.m. on November 30, 2011. An additional set of strain, camber, and sweep measurements were collected after release. The girder was lifted out of the form beds approximately one hour later and positioned on supports so that finishers could repair surface blemishes prior to storage. The girder was inspected for cracks prior to any surface corrections. Over 50 small cracks were observed in the top flange of the girder consistent with thermal cracking. An inspection after finishing and storage in the yard approximately 19 months later found no evidence of these cracks. It is noted that this type of hairline crack is usually superficial and, therefore, does not affect the structural properties of the member.

The researchers also reviewed the trailer scheduled for girder transport. GCP utilizes air-sprung ERMC Hydra-Steer trailers to transport the girders to construction sites. Mast and PCI design documents recommend a technique adopted from Mast's research to obtain a value for the trailer's rotational stiffness. While in the yard, the researchers worked with the precaster on possible concepts to test the rotational stiffness of the trailer. Mast's approach was not viable for the precasters operations, so a scheme to drive the girder onto blocking of different heights was attempted (Figure 19). Review of the data proved unreliable in

calculating a stiffness. The researchers understand Mast's concern was with coil springs, and the newer air ride systems would appear to mitigate some issues. Ultimately, the researchers were unable to obtain a rotational stiffness for the trailer within the research.

Figure 17
Stressed prestressing laid out for Girder 1 in the form beds at Gulf Coast Pre-Stress

Figure 18
Concrete placement from the chute of a buggy into the forms for Girder 1

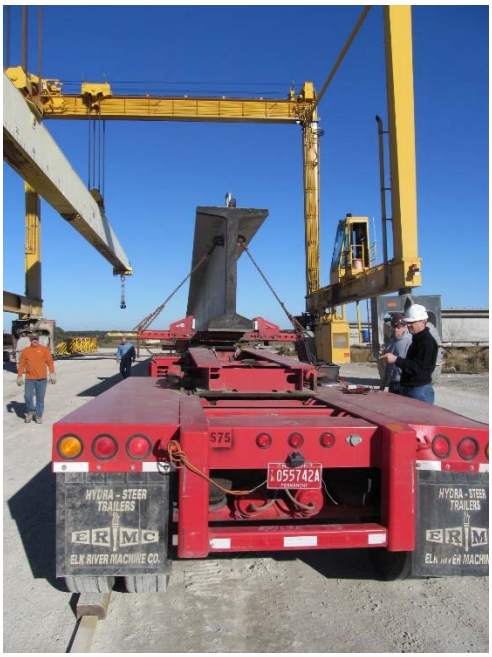

Figure 19
Attempted rotational stiffness testing of Hydra-Steer trailer at GCP yard

Laboratory Testing

Because Girder 1 had remained in the yard for approximately19 months after casting before being shipped to the bridge site, the effects of concrete creep and shrinkage on the girder were greater than if the girder had been shipped soon after it was fabricated. A laboratory testing program was subsequently developed to produce mix-specific concrete creep data for use in this study. All the laboratory tests were conducted on concrete cylinders prepared by GCP using the same mix design for Girder 1. Mix design information and test results for Girder 1 are located in Appendix A. Girder 2 mix design information is also provided in Appendix A.

Compressive Strength

WJE performed compressive strength testing in accordance with ASTM C39, *Standard Test Method for Compressive Strength of Cylindrical Concrete Specimens,* and creep testing in accordance with ASTM C-512*, Standard Test Method for Creep of Concrete in Compression.* A total of six 6-x-12-in. cylinders were received from Gulf Coast Pre-Stress. Two cylinders were tested for compressive strength at an age of 7 days with the results shown in Table 9.

Table 9
Compressive strength results at 7 days

Sample	Compressive Strength (psi)
1	8,170
2	8,160
Average	**8,170***

*Rounded to the nearest 10 psi

Creep and Shrinkage

Four cylinders were loaded at 7 days to a load of 69,300 lbs, approximately 30 percent of their ultimate strength, to measure creep and shrinkage. The testing was completed at a relative humidity of 50 percent. The average creep and shrinkage results of all samples are shown in Table 10. Figure 20 shows the creep and shrinkage test results compared to creep predication models found in the literature and standards. It is noted that the Branson creep prediction model matched well with the experimental results *[21]*.

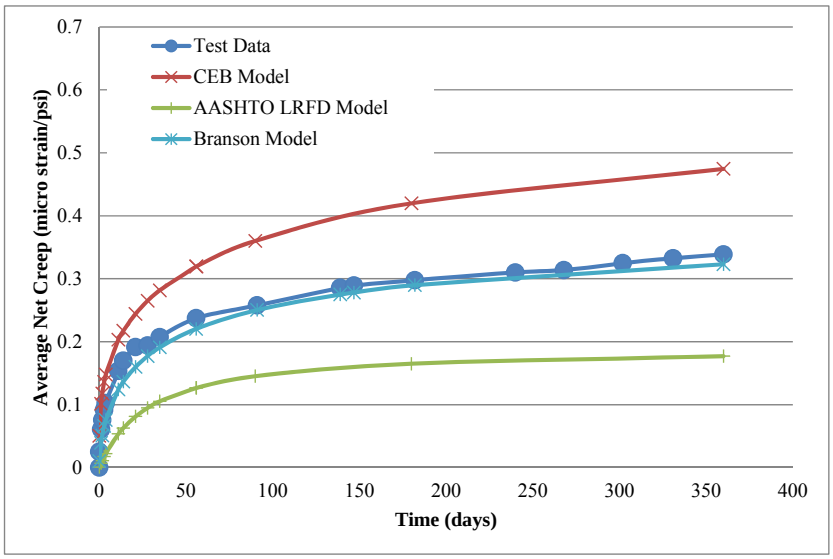

Figure 20
Experimental and analytical creep results

Table 10
Creep and shrinkage test results

Time (days)	Specific Creep (microstrain/psi)	Creep Coefficient
0.00	0.000	0.000
0.10	0.025	0.133
1.00	0.061	0.321
2.00	0.076	0.401
3.00	0.092	0.486
4.00	0.102	0.543
11.00	0.153	0.814
14.00	0.170	0.901
21.00	0.191	1.014
28.00	0.194	1.029
35.00	0.207	1.099
56.00	0.237	1.258
91.00	0.258	1.367
139.00	0.285	1.514
147.00	0.289	1.534
182.00	0.298	1.580
240.00	0.310	1.645
268.00	0.314	1.664
302.00	0.325	1.722
331.00	0.332	1.763
369.00	0.339	1.797

Modulus of Elasticity

The Modulus of Elasticity was measured using the 6-x12-in. cylinders. For Sample 1, the modulus of elasticity was calculated at 7 days based on instantaneous strain measurements during initial creep testing in accordance with ASTM C512 *Standard Test Method for Creep of Concrete in Compression*. The load level at which the modulus of elasticity was calculated was 30 percent of the ultimate capacity of the sample. For Sample 2, the static modulus of elasticity was calculated based on instantaneous strain measurements in accordance with ASTM C469 *Standard Test Method for Static Modulus of Elasticity and Poisson's Ratio of Concrete in Compression.* As required by this standard, the load level for Sample 2 was 40 percent of the ultimate capacity of the sample. The difference in the two measured moduli of elasticity is slight and may be attributed to the age of the second sample (approximately 19 months) at the time of the test at which the measurement was taken. The results of the modulus of elasticity can be found in Table 11.

Table 11
Modulus of elasticity

Sample	Modulus of Elasticity (psi)
1	5.3×10^6
2	5.9×10^6

Coefficient of Thermal Expansion

The Coefficient of Thermal Expansion was measured using DEMEC points. After calibrating the gage to a standard bar at ambient conditions, the samples were measured at ambient. The samples were then acclimated to a temperature of 140°F inside an oven and measured within the oven. This process was repeated for a second time and the results averaged as presented in Table 12.

Table 12
Coefficient of thermal expansion

Sample	Coefficient of Thermal Expansion (1/°F)
1	8.04×10^{-6}
2	6.96×10^{-6}
Average	7.50×10^{-6}

Evaluating the Potential of Cracking

The primary goal of this study is to determine whether events occur during typical transportation and lifting operations for long-span girders that cause cracking. Therefore, an estimate of the theoretical concrete cracking strains was determined in order to perform comparisons with the measured data.

ACI 318-14 defines modulus of rupture of concrete and modulus of elasticity as *[8]:*

$$f_r = 7.5\sqrt{f_c'} \tag{4}$$

$$E = 33 w_c^{1.5} \sqrt{f_c'} \tag{5}$$

Units in lb/ft^3 for w_c and psi for f'_c

Therefore, per ACI 318, concrete will crack at a flexural strain of 132 microstrain (f_r/E), assuming concrete unit weight of 145 lb/ft^3.

The American Association of State Highway and Transportation Officials (AASHTO) LRFD (2013) has similar definitions for concrete modulus of rupture and modulus of elasticity as

per ACI 318 *[22]*. The equations of AASHTO LRFD (2013) Articles C5.4.2.4 and C5.4.2.6 estimate E_c and f_r only from the square root of compressive strength as follows:

$$E_c = 33,000 K_1 w_c^{1.5} \sqrt{f_c'} \quad (6)$$

$$f_r = 0.24 \sqrt{f_c'} \quad (7)$$

K_1 correction factor for source of aggregate to be taken as 1.0 unless determined by physical testing

Units in kip/ft^3 for w_c and ksi for f'_c

Using AASHTO's definitions, and assuming normal weight concrete of 0.145 kip/ft^3, concrete will crack at the same flexural strain.

The above referenced ACI and AASHTO cracking strain definitions are suitable for normal strength concrete. However, for high strength concrete, such as the concrete used in this research, AASHTO suggests a higher limit for modulus of rupture as shown in equation 8 *[22]*. No provisions for modulus of elasticity of high early strength concrete are included in AASHTO. Therefore, the CEB-FIP Model Code 1990 was used to estimate modulus of elasticity of high early strength concrete in this study as shown in equations (9) and (10) *[23]*.

$$f_r = 0.37 \sqrt{f_c'} \quad (8)$$

where,
f'_c= compressive strength of concrete (ksi)

$$E_c = 21.5 \left(\frac{f_c'}{10}\right)^{1/3} \quad (9)$$

where,
E_c = Modulus of elasticity of concrete (GPa),
f'_c= compressive strength of concrete (MPa)

$$E_c = 3{,}117 \left(\frac{f_c'}{1{,}450}\right)^{1/3} \quad (10)$$

where,
E_c = Modulus of elasticity of concrete (ksi),
f'_c= compressive strength of concrete (psi)

Using the above definitions, and assuming concrete compressive strength of 10,000 psi, approximating strength at the time of transport, concrete will crack at a flexural strain of 197 microstrain. It is noted that the estimated concrete modulus of elasticity using CEB-FIP Model is equal to 5,930 ksi, which is very similar to the measured values shown in Table 11. Therefore, concrete strains between 130 and 200 microstrain indicate a potential for cracking with strains over 200 microstrain suggesting cracking is likely.

Periodic Monitoring

The behavior of the girder prior to transportation was evaluated by instrumenting Girder 1 to obtain strain, sweep, and camber changes between transfer of prestressing force and time of transportation.

Strains at Prestressing Release

Strains were measured in Girder 1 just prior to and immediately after cutting the strands. These strains were compared to analytically calculated strains as shown in Table 13. The measured modulus of elasticity, shown in Table 11 and similar to the calculated modulus using CEB-FIP Model, was used to calculate the composite section properties for the analytically calculated strains. As shown in Table 13, the analytical results match well with the measured strains.

For Girder 2, strains at transfer were not measured; however, similar to Girder 1, analytical strains at transfer were calculated using the same modulus of elasticity. The analytical strains for Girder 2 are shown in Table 14.

Appendix D shows the analytical procedure used to calculate transfer strains of both girders.

Table 13
Measured and calculated strains at release in microstrain

Strain	A- Top	A-Bot.	B-Top	B-Bot.	D-Top	D-Bot.	C-Top	C-Bot.
Girder 1 DEMEC*	41*	-657*	-109*	-554*	NA	NA	27*	-610*
Girder 1 Analytical	39	-551	-101	-498	-47	-550	39	-551

*Average value of two strain gages

Table 14
Calculated strains at release in microstrain

Strain	A- Top	A-Bot.	B-Top	B-Bot.	D-Top	D-Bot.	C-Top	C-Bot.
Girder 2 Analytical	-51	-698	-170	-599	-150	-618	-51	-698

*Average value of two strain gages

Time Dependent Concrete Properties: Creep and Shrinkage

Change of strain due to creep and shrinkage was estimated through periodic monitoring of Girder 1 during fabrication and after the approximately 19 months of storage (from transfer of prestress force on November 30, 2011, to just prior to transport on July 2, 2013). The long-term strain monitoring results are shown in Figure 21. As can be seen in this figure, the strains changed significantly, on the order of 300 microstrain, between the time of prestressing force release and transport. This change is attributed primarily to creep and shrinkage of the concrete.

The measured top strains at Section A (girder end) increased from 41 microstrain to an average of 251 microstrain. Although, this value (251 microstrain) exceeds the cracking strain value previously defined in this report, the strain associated with creep and shrinkage was not restrained. Therefore, cracking stresses were not associated with strain changes due to creep and shrinkage. Furthermore, these strain changes occurred over a sufficient period of time that creep effects prevented the onset of cracking. A visual inspection prior to transport, approximately 19 months after casting, found no concrete cracks even though cracking, as previously indicated, had been observed a few hours after release of the strands. These numerous hairline cracks along the top flange were superficial and were subsequently covered with a parge coat prior to shipment. This routine process fills bugholes and minor cracks. Thus, at the time of transportation, the research team and the state inspector did not identify cracks in either girder.

Monitoring during transportation was intended to identify measured strains exceeding anticipated cracking thresholds. Therefore, to allow for true comparisons between measured and cracking strains, a state of strain was assumed since a large amount of creep and shrinkage had occurred. Because the creep and shrinkage strains were judged not to contribute to cracking concerns, gage readings were reset, at the time of transport, to the measured concrete strains at transfer before lifting and transporting the girder as further discussed in the “Dynamic Monitoring during Girder Transport and Lifting” section. For Girder 2 these readings were set to the calculated strains, an approach verified by comparing calculated and measured strains in Girder 1.

Other considerations related to creep and shrinkage are prestress losses and long-term deflection changes. The effect of prestress loss on the state of the strain in the top flange was determined analytically using the AASHTO LFRD (2013) Specifications. Estimated losses in the prestressing due to creep and shrinkage were calculated to be 11.4 ksi and 5.6 ksi, respectively. This resulted in a small change in the calculated state of strain equal to 15 microstrain in Girder 1 after approximately 19 months. This result is consistent with the approach of resetting the concrete strains to the time at transfer.

Using the laboratory creep and shrinkage test results, an estimate of the creep and shrinkage prestress losses using the PCI equations was performed. As creep and shrinkage were measured simultaneously during the laboratory testing, separation of the measurements was required prior to estimating the prestress losses. For this purpose, it was assumed that the ratio between creep and shrinkage is the same as the ratio between creep and shrinkage losses (2:1) calculated using AASHTO LRFD approach. Thus, a creep coefficient of 1.198 (calculated from Table 10) was used to calculate prestress loss due to creep while a shrinkage strain of approximately 350 microstrain was used to calculate prestress loss due to shrinkage. A correction factor for the difference in the relative humidity between the laboratory test and the approximated actual condition at the storage site is included in the above estimated strain. Estimated prestress losses for creep and shrinkage were 17.6 ksi and 10.2 ksi, respectively. A significant difference can be observed between the two approaches, which highlights the high variability of prestress losses estimates. The change in the state of strain at the top flange of Girder 1 was calculated for the second set of prestress losses as 20 microstrain.

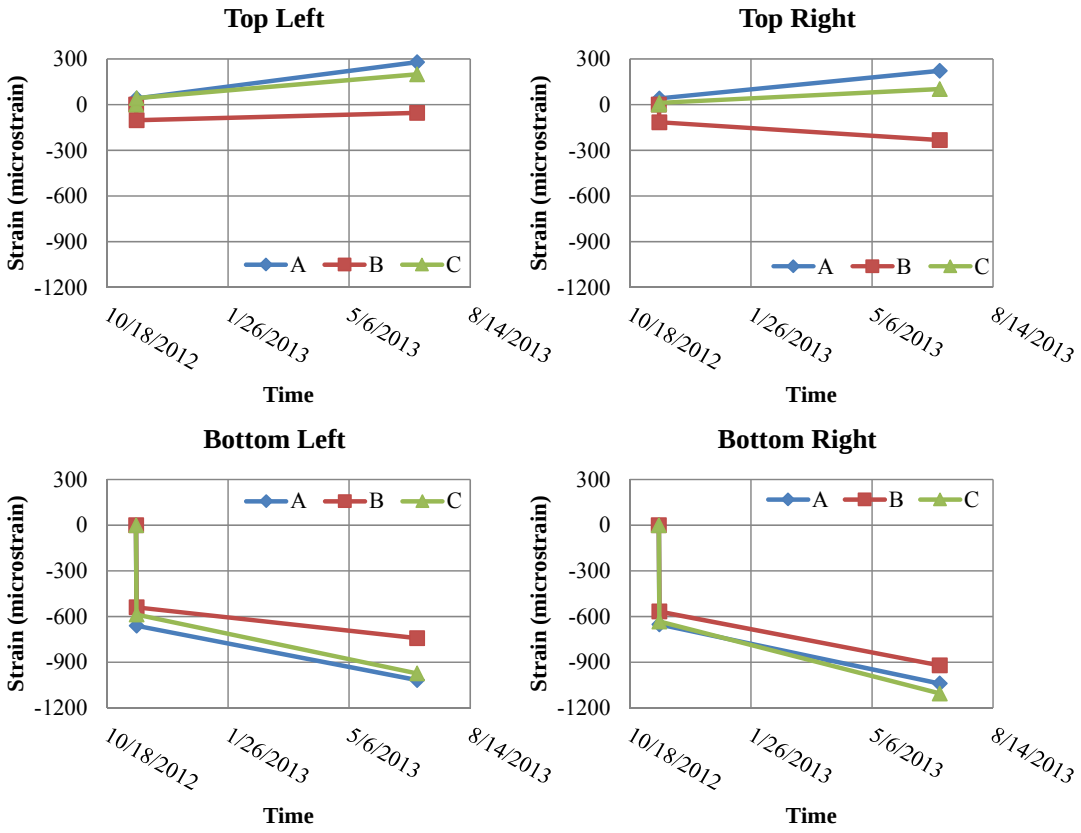

Figure 21
Change of strain in Girder 1 due to creep and shrinkage

Camber and Sweep Measurements

Camber and sweep estimates were performed on Girder 1 utilizing the laser system. This was done to avoid defining a wire tension and applying corrections for wire sag. The measurements were performed by installing a laser mount with a laser at one end of the girder and target mounts at the other end and at midspan of the girder. Measurements were recorded on top of the girder flange near the tips to estimate girder sweep. To estimate sweep and camber, the target was first setup at the end of the girder and the location marked on the target. The target was then moved to midspan and the intermediate point was marked on the target. Accounting for known differences in the mounting of the target and by applying the theorem of similar triangles, the camber and sweep were calculated. Figure 22 shows the position of the laser and the two target positions for calculating camber and sweep. A consideration with these measurements is that the camber and sweep are calculated at the top of the girder and not at the centroidal axis. A second set of measurements was conducted using aircraft cable for verification of the first set of measurements, and the results were observed to be comparable.

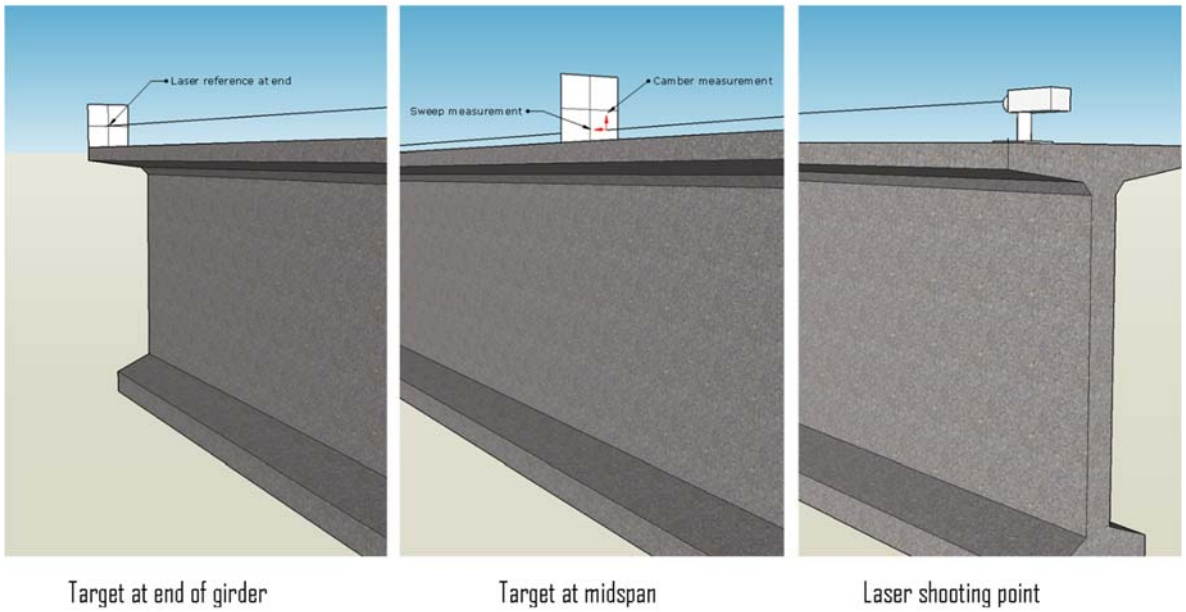

Figure 22
Schematic of camber and sweep measurements using laser

Table 15 shows the recorded camber and sweep values using laser measurements, as well as estimates based on the strain gage readings. Camber was also calculated using the girder moment of inertia and prestressing force on the girder. However, theoretical sweep calculations were not performed as the prestressing force was assumed to be equally distributed laterally in a girder with a symmetric cross section. As indicated in Table 15, the strain measurements provided a lower estimate of long-term camber and an upper estimate of long-term sweep. This strain behavior is attributed to gage drift that can affect long-term strain measurements, as well as differences in environmental conditions. These effects were not accounted for in these estimates. A significant difference between the measured and calculated sweep was also observed and is attributed to environmental conditions during girder storage at the yard including temperature and moisture.

Table 15
Camber and sweep measurements versus analytical predictions

	After Release (in.)	19 Months
Camber (positive up)		
Theoretical	2.2	5.3
Estimated (Strain)	2.0	3.1
Measured (Laser)	2.7	4.8
Measure (Wire)	2.7	—
Sweep (positive to right)		
Theoretical	—	—
Estimated (Strain)	0.3	2.4
Measured (Laser)	1.0	0.5

Dynamic Monitoring During Girder Transport and Lifting

The focus of this research was measuring the behavior of girders during transport to identify events and responses indicative of cracking in the girders. DOTD's previous experience with shipping long girders had identified transportation as a key generator of cracking issues. Measurements were also taken during selected lifts to compare with analytical model results and to take advantage of this available opportunity. Each of the girders traveled a similar route with the same trailer support. Each shipment took approximately 7 hours and resulted in the collection of several gigabytes of measurement data. Detailed discussions of the collected data are presented in this section.

Trailer Support and Operation

Both girders were supported in similar fashion as shown in Figure 23. A three-axle tractor pulling a fifth-wheel, three-axle trailer supported the front end of the girder that was positioned on a rotating bunk. A Hydra-steer six-axle (Figure 24), rear jeep supported the back end of the girder. The rear Hydra-steer jeep provides considerable maneuverability, permitting the single driver/operator to efficiently steer the girder through a variety of navigation routes. The rear jeep is capable of operating in different steering configurations based on the navigation circumstances required. These steering configurations are shown in Figure 25. As observed during the two tests, once the driver is out of the yard and before operating at speeds exceeding 10 mph, the jeep tongue is hydraulically raised for trailer steering stability. In this configuration, the driver is capable of crab steering the girder only as shown in Figure 25. Where greater maneuverability is required, such as when operating within the yard or at the construction site, the driver can use either front steering or hinged steering. The use of front steering was more commonly observed when the tongue was not attached. Figure 26 shows this condition.

A single driver both drove and operated the rear jeep steering during transport of both girders. The rear jeep is typically operated through a wireless controller, but can also be wired. This was required during the transport of Girder 1 due to a malfunctioning wireless controller.

Figure 23
Typical girder transport setup with Girder 2 crab turning (note that tongue is engaged)

It was observed that during transport the driver would start the trip with the rear jeep tongue disengaged to take a tight turn out of the precast yard onto a small two-lane road. The driver then engaged the tongue by exiting the cab, lifting the tongue hydraulically, and securing it with chains. The tongue was then left in place for the remainder of the journey to the bridge site. For Girder 1, the tongue was disengaged for further maneuvering once it arrived at the site.

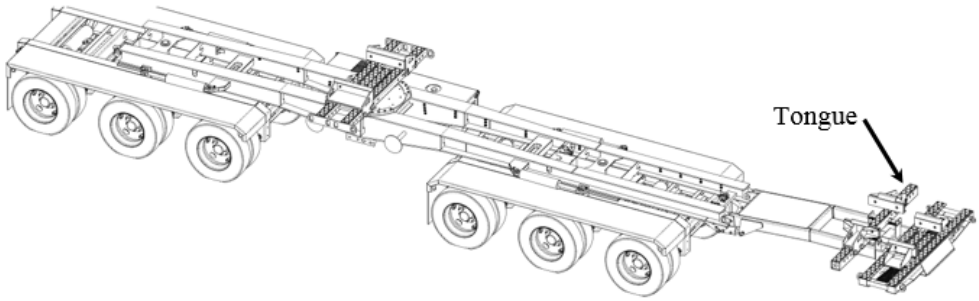

Figure 24
Isometric diagram of Hydra-steer trailer

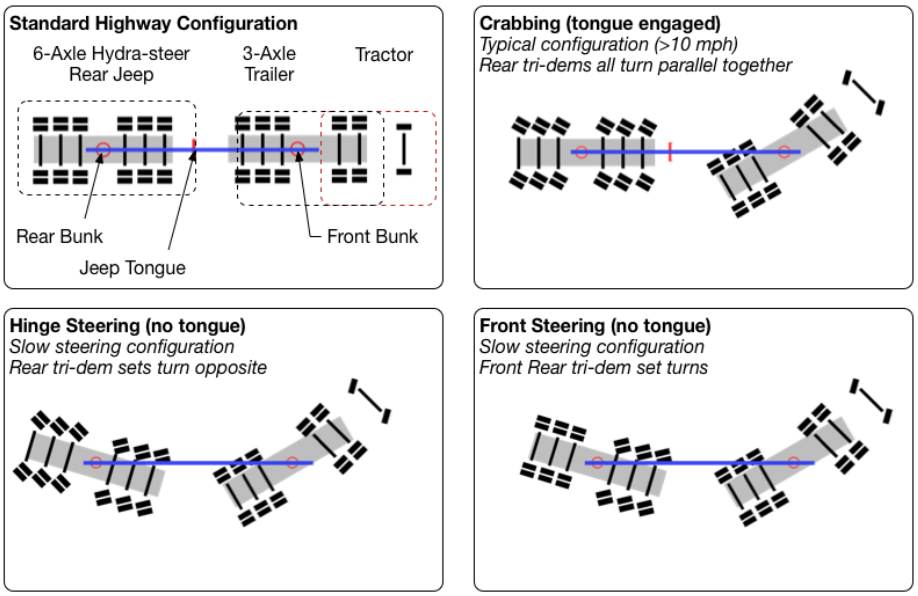

Figure 25
Turning configurations of Hydra-steer trailer

Figure 26
Front steering of rear trailer (note tongue disengaged)

Girder Loading

On the day prior to transport, the girders were lifted from their long-term storage supports using a rolling gantry crane, as shown in Figure 27, and placed on the trucks for transport, as shown in Figure 28. The girder ends were positioned such that a pair of tie-down block-outs were centered over the supports. Inserts were placed in the block-outs and attached to the trailer frames using chains. When the jeep tongue was engaged, it was attached to the girder using a single block-out insert with chains as shown in Figure 29.

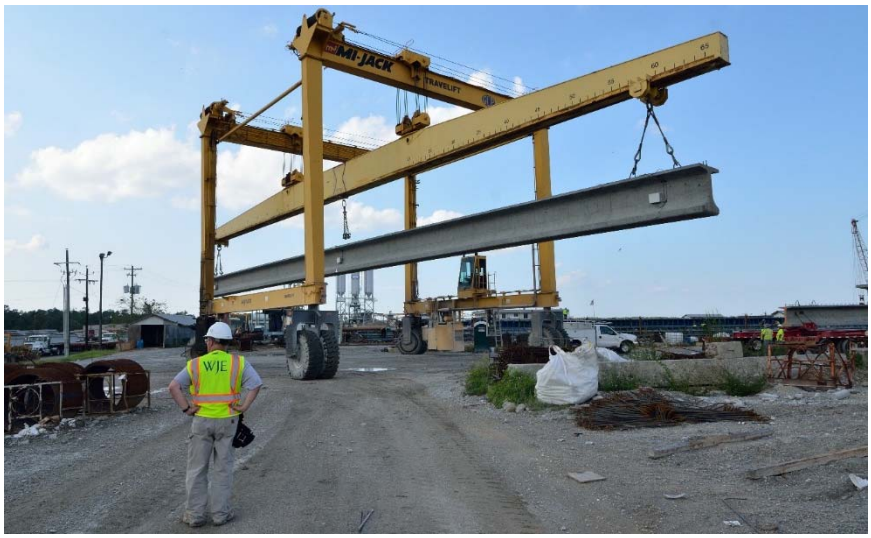

Figure 27
Girder 2 moved for loading using gantry crane

Figure 28
Loading of girder on truck with gantry crane

Figure 29
Tie down of girder at rear jeep tongue

Evaluation of Measured Strain Data for Cracking

The estimated cracking thresholds stated above are assumed by the researchers to be static strains, whereas concrete cracking response can be several times higher for higher frequency responses. Collected strain response data were compared to the estimated cracking threshold at the static strain levels by smoothing the strain data with a 10-second running average algorithm in event analysis, and selecting the average strain value at a particular event time consisting of an approximately 0.1-second window. Researchers looked to determine the relative maximum/minimum responses for selected events.

A Fast Fourier Transform (FFT) analysis of the vertical and lateral frequency response for the full 8-hour transport of Girder 2 was performed and is presented in Figure 30. The FFT indicates that the lateral responses were commonly occurring at 0.7 Hz. Thus, to obtain a running static average, multiple response cycles were averaged over a 10-second period. Based on a review of multiple smoothing levels, this was judged to appropriately represent a static loading condition for the girder.

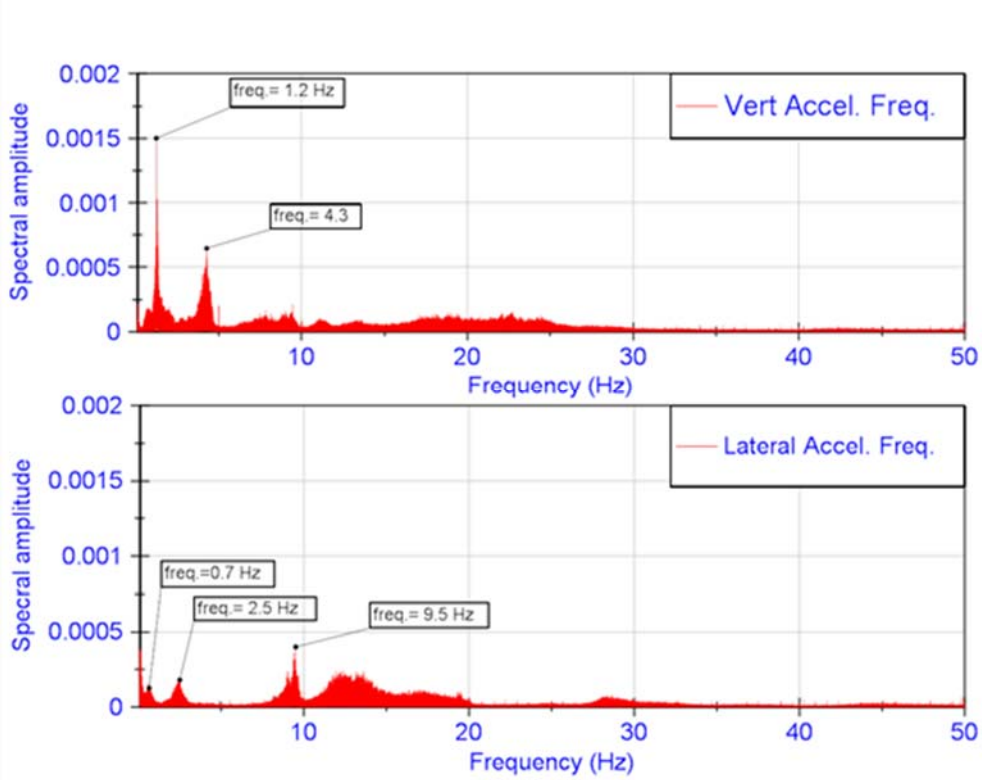

Figure 30
FFT of vertical and lateral acceleration at midspan vertical gyro unit

Dynamic Monitoring During Girder Transport: *Girder 1 - Ft. Buhlow Route*

Date: July 3, 2013
Start: Pass Christian, Mississippi
End: Alexandria / Ft. Buhlow, Louisiana
Length: 480 miles
Duration: 8 a.m. to 3 p.m., 7 hours
Weather: Morning- Pass Christian: Overcast and raining, little wind, 73 deg. F; Mid-day- Baton Rouge: Sunny, 85 deg. F; Late afternoon- Alexandria: Sunny, 90 deg. F

The transport of Girder 1 started on a rainy July morning destined for the new Fort Buhlow Bridge (US 71) crossing the Red River. A map of the overall journey is shown in Figure 31, which shows a color contour plot of the relative transport speed across the full length of transport. Measured speeds based on geolocation and time varied from stopped to over 70 mph. As shown by the speed map figure, the transport was operated along most of the route at highway speeds except in Pass Christian, Mississippi and Baton Rouge, Louisiana. The roadway conditions varied significantly over the girder transport route. The beginning portions of the route included gravel surfaces within GCP's yard and at turns approaching US 90. The paved roadway sections between the yard and US 90 were generally flat with one

elevated railroad crossing. From US 90, the route consisted mostly of higher speed (i.e., 45 mph and higher) paved asphalt and concrete riding surfaces (i.e., causeway and bridges). Route characteristics included flat off-road, local roads, arterial routes, highway, interstate, ramps, railroad crossings, and intersections.

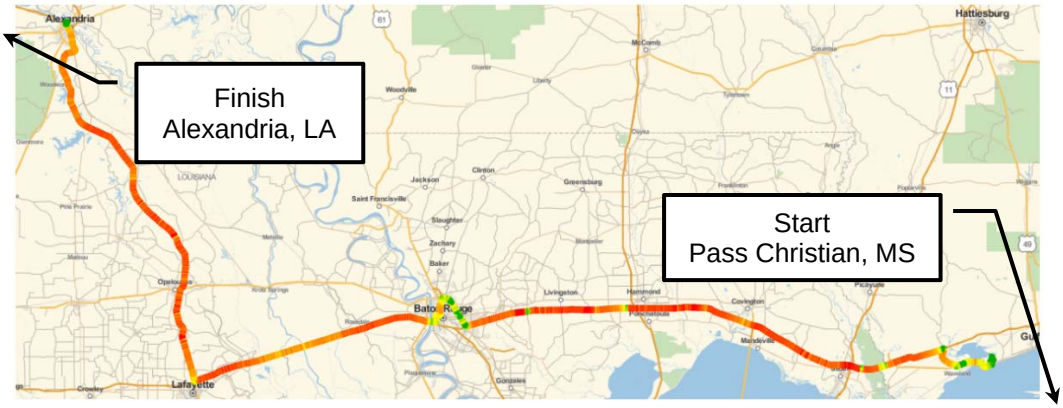

Figure 31
Overview of route of Girder 1 with relative speed along the route overlaid (red > 55 mph; green < 10 mph)

The first girder experienced an unexpected issue shortly after leaving the yard, where the wireless system that controls the rear jeep malfunctioned. This required the transport to stop on US 90 for more than one hour. While diagnosing the issue, the driver repeatedly operated and tested his controls while the truck and girder were stationary. This resulted in some of the highest strain events, which will be discussed below. GCP eventually remedied the problem by installing a wired control for the driver to operate. Once transport resumed, the weather cleared, producing a sunny and warm day while traveling across Louisiana.

Given the vast amount of data collected during the transportation record, only selected high-girder acceleration and strain events, shown in Table 16 and Table 17, are discussed. These selected events were developed through multiple data interrogation methods, including reviewing maximums for each of the channels. One methodology used for data interrogation was data fusion of time lapse video, three dimensional (3D) strain mapping of gage data onto a representative 3D model, and classic plots as shown in Figure 32 below. This provided clearer insight into the type of events causing significant girder responses. The tables show the values of each of the cross section strain gages and inertial measurement units at the selected time of maximum strain or acceleration. As discussed earlier, strain in each gage was set equal to the value of strain measured after prestress transfer. This was done to exclude the change in strain that happens due to temperature change as well as from creep and shrinkage during storage of the girder at the yard.

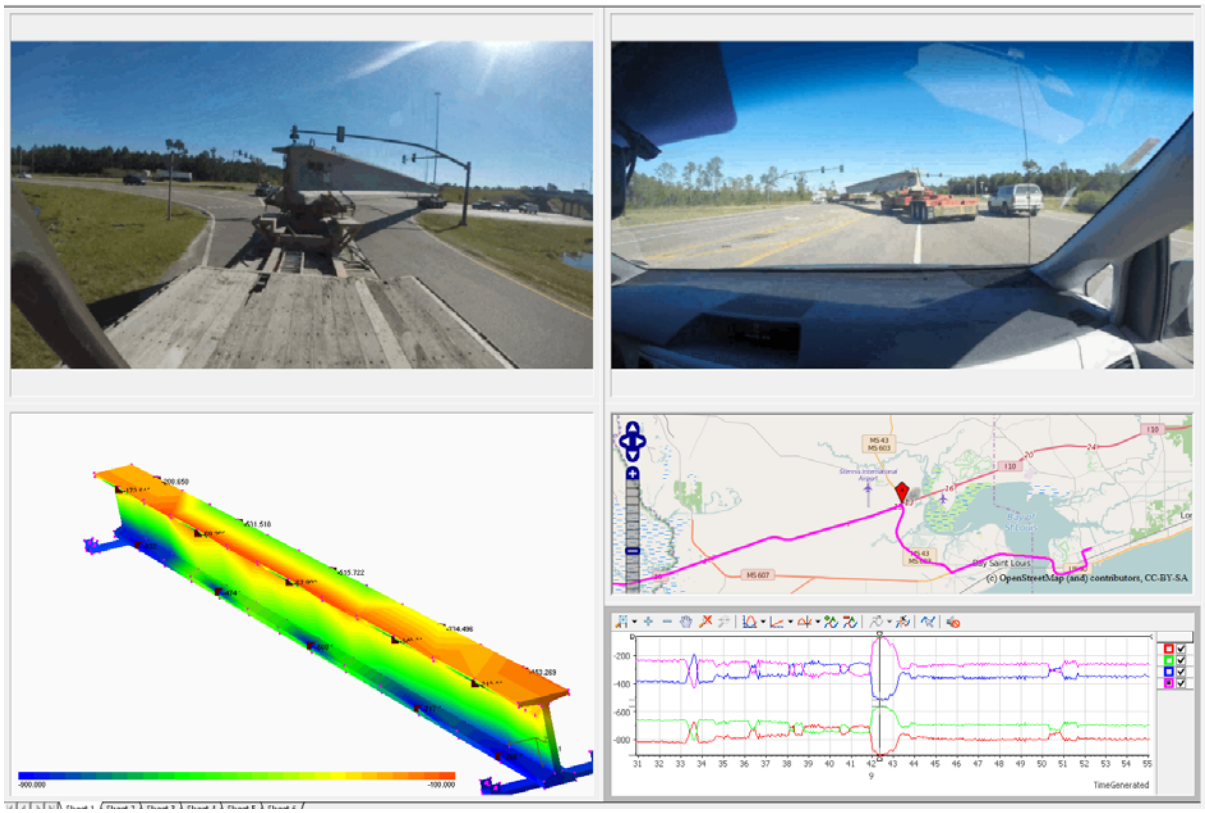

Figure 32
Evaluation of route characteristics using synchronized data and time lapse video from Girder 2

Embedded strain gages were used in Girder 1; however, cracks are expected to first occur on the concrete surface. Therefore, the tables present interpolated strain at the surface of the flange, by assuming a linear change in the strain across the girder cross section, for purposes of cracking evaluation. The methodology of calculating surface strains is shown in Appendix C. BDI strain gages were installed at the tongue location (Section D). These sensors can be effected by temperature changes; therefore, the data in the tables are coarsely corrected for temperature at Section D. This was done by subtracting the change of strain due to temperature changes from the reported strain at each event. Graphical details of the raw data of the full transportation record and the selected events are provided in Appendix E.

Selected acceleration events were picked from the transportation record using the data fusion approach discussed above. However, unlike events affected by the roadway geometry that could be cross referenced with the time-lapse video record, many of the acceleration events did not have an obvious geometric cause, e.g. railroad crossing. Therefore, it was assumed that these events originated from bumps or depressions in the roadway surface, e.g. bridge deck joints, during transport.

Table 16 shows the strain response of Girder 1 during five selected acceleration events. Figure 33 shows the transportation record for acceleration along the route with the selected locations highlighted.

- Event G1-A1 (Girder 1, first acceleration event) occurred when the truck reached highway speed on US 90 in Mississippi and the girder acceleration in the Z-direction (vertical acceleration upward) exceeded 0.25 g for the first time.
- Event G1-A2 was associated with high acceleration on I-10 in the upward Z-direction.
- Event G1-A3 occurred during typical highway transportation and included high accelerations in the Z-direction and X-direction (lateral acceleration).
- Event G1-A4 was the peak acceleration in the upward Z-direction experienced by the girder during transportation on I-10 in Louisiana.
- Event G1-A5 was the peak lateral X-direction acceleration recorded during highway transportation in Louisiana. The highest tensile strains were associated with acceleration events at the girder end (Section A at rear jeep).

Based on the selected 200 microstrain cracking threshold and the AASHTO implied cracking strain of about 130 microstrain, no potential cracking events were observed during acceleration events. The highest recorded strain in Table 16 occurred at the rear jeep section (Section A) when the peak lateral acceleration of 0.44 g was recorded as Event G1-A5. The highest recorded strain at midspan (Section B) was below the potential cracking strain and occurred during event G1-A1with a vertical upward acceleration of 0.25 g and a roll of -1.9 deg. It is noted that the peak upward vertical acceleration of 0.42 g for event G1-A4 was not associated with the highest recorded strains. Essentially, no tensile strains were recorded at the tongue location (Section D) during these selected acceleration events.

When the measured accelerations near event G1-A1 are looked at in combination with top flange strain differential and roll angle, as shown in Figure 34, some findings are observed. Strain seems to moderately correlate at this location while roll does not. A further example of where roll does not correlate is shown Figure 34c where the girder crosses over a superelevated portion of roadway and experiences a large roll without associated acceleration or strain.

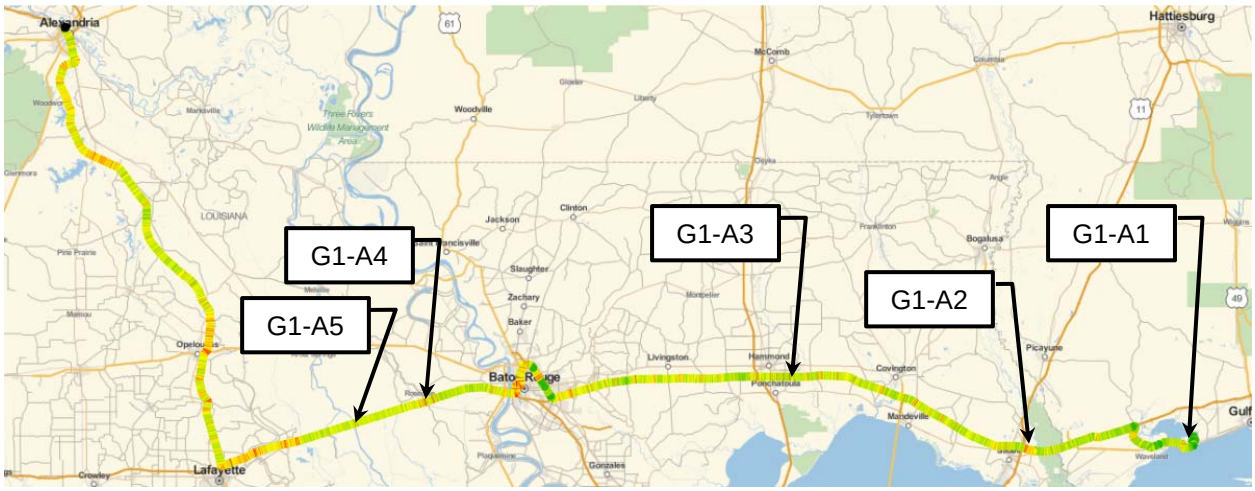

Figure 33
Overview of route of Girder 1 showing accelerations with selected events noted (color contours: green < 0.05 g to red > 0.25 g)

Table 16
Surface strains of selected transportation events based on high girder acceleration*

Event G1-A1		**Event G1-A2**		**Event G1-A3**		**Event G1-A4**		**Event G1-A5**	
10:40:00 to 10:42:00		11:33:00 to 11:36:00		12:11:00 to 12:18:00		13:38:00 to 13:40:00		13:51:00 to 13:53:00	
First occurrence: accelerations exceeding 0.25g		Acceleration in Z direction (highway)		Acceleration in Z and X directions (highway)		Peak acceleration: Z direction		Peak acceleration: X direction	
Section A		Section A		Section A		Section A		Section A	
20	62	-55	84	-59	99	-34	98	-41	119
-682	-629	-673	-649	-668	-644	-650	-639	-659	-648
AccZ = 0.46	AccX = 0.15	AccZ = 0.30	AccX = 0.02	AccZ = 0.48	AccX = 0.20	AccZ = 0.63	AccX = 0.08	AccZ = 0.18	AccX = 0.44
Roll = -2.3	Pitch = 1.6	Roll = -0.7	Pitch = -0.5	Roll = 0.0	Pitch = -0.2	Roll = -0.9	Pitch = -1.9	Roll = -0.6	Pitch = -0.8
Section B		Section B		Section B		Section B		Section B	
-370	55	-381	-31	-406	20	-275	-8	-305	-18
-633	-484	-568	-508	-590	-495	-585	-542	-569	-510
AccZ = 0.25	AccX = 0.07	AccZ = 0.27	AccX = 0.03	AccZ = 0.22	AccX = 0.25	AccZ = 0.42	AccX = -0.22	AccZ = 0.08	AccX = 0.22
Roll = -1.9	Pitch = 4.0	Roll = -0.1	Pitch = 0.9	Roll = 0.6	Pitch = 1.3	Roll = -0.3	Pitch = -0.6	Roll = 0.2	Pitch = 2.3
Section D		Section D		Section D		Section D		Section D	
-157	1	-146	-42	-174	-45	-141	-54	-158	-34
-787	-569	-787	-645	-817	-628	-757	-669	-773	-645
Section C		Section C		Section C		Section C		Section C	
20	55	44	44	62	56	75	85	84	72
-586	-638	-575	-646	-579	-650	-578	-647	-567	-646
AccZ = 0.21	AccX = 0.09	AccZ = 0.22	AccX = 0.08	AccZ = 0.30	AccX = 0.23	AccZ = 0.38	AccX = 0.13	AccZ = 0.11	AccX = 0.29
Roll = -2.5	Pitch = 1.7	Roll = -1.3	Pitch = -1.7	Roll = 0.2	Pitch = -0.2	Roll = -1.1	Pitch = -2.0	Roll = -0.5	Pitch = 0.8

Units: Strain in microstrain, Acceleration in g, and Roll and Pitch in degrees
AccZ = Vertical acceleration oriented with gravity (positive = upward acceleration of girder)
AccX = Lateral acceleration oriented normal to the girder web (positive = towards the driver's side)
* for each section, 4 strain measurements are reported in their respective cells: top left, top right, bottom left and bottom right.

a) Acceleration (Color contours: green < 0.05 g to red > 0.25 g).

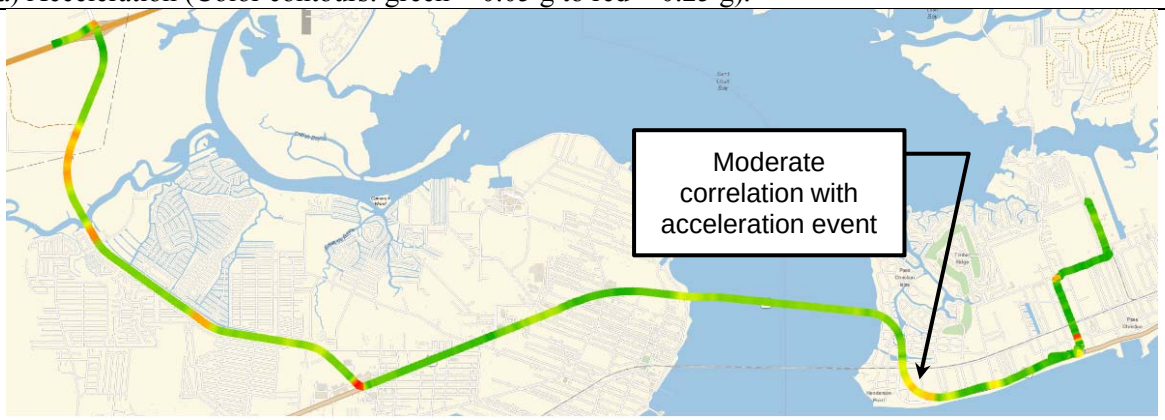

b) Top flange strain differential (Color contours: green < 100 microstrain to red > 300 microstrain)

c) Lateral roll (Color contours: green < 1 deg. to red > 5 deg.)

Figure 34
Selected event G1-A1 as shown on a map with colorized data output along route

The highest recorded strain events recorded during transportation are shown in Table 17. The events are shown along the route in Figure 35.

- Event G1-S1 was recorded during a slow right turn as the girder was leaving the yard without the tongue attached. This event provides a comparison with other events where the tongue was attached resulting in significantly higher strain responses.
- Event G1-S2 occurred during slow right turn on to US 90 with the tongue attached. This event demonstrated the significantly higher strains were induced into the top flange from turning events with the tongue engaged. Immediately after this turn, the driver stopped on US 90 to troubleshoot a problem with the rear jeep operation.
- Event G1-S3 occurred while the jeep was not moving, the operator actuated the rear jeep wheels for feedback while troubleshooting. This caused high strains in the girder as the jeep mechanism reacted off the girder.
- Event G1-S4 occurred during a slow left turn onto the on-ramp of I-10 in Mississippi with high roll (>3 deg.) and tongue force input apparent in the event.
- Event G1-S5 occurred during lifting of the girder with two cranes at the site and was caused by the roll of the girder.

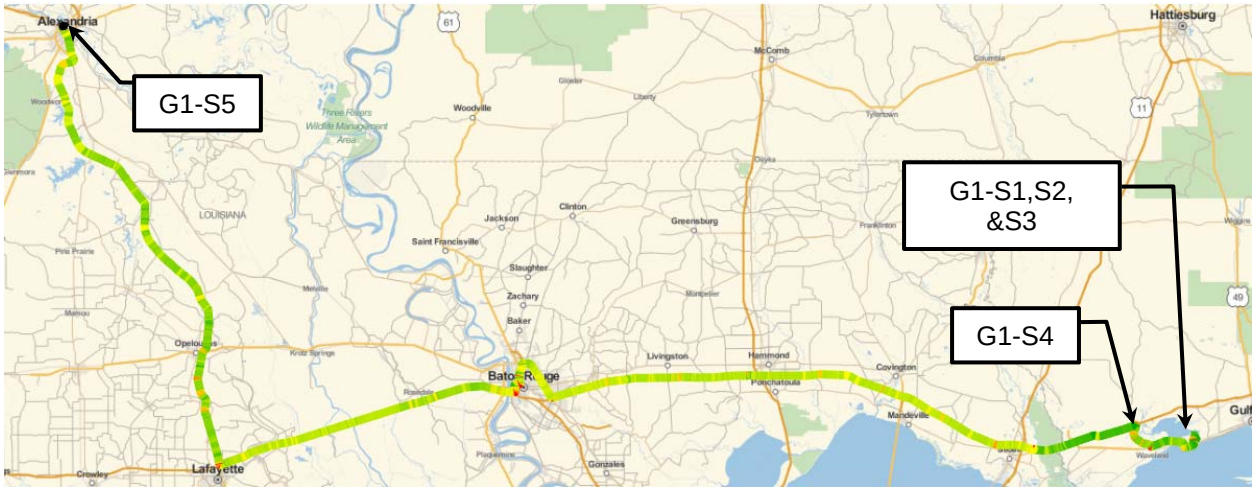

Figure 35
Overview of route of Girder 1 showing girder top flange strain differentials with selected events noted (color contours: green < 100 microstrain to red > 300 microstrain)

Table 17
Surface strains of selected transportation events based on high girder strains*

Event G1-S1		Event G1-S2		Event G1-S3		Event G1-S4		Event G1-S5	
07:58:00 to 08:03:00		08:20:00 to 09:20:00		10:06:00 to 10:08:00		10:59:30 to 11:01:30		16:00:00 to 16:25:00	
Yard exit		90 degree right turn onto US 90		Stationary jeep shift on US 90		90 degree left turn onto I-10		Site lift	
Section A		Section A		Section A		Section A		Section A	
-71	82	273	-123	153	-57	382	-141	31	103
-678	-637	-595	-722	-620	-700	-583	-707	-598	-637
AccZ = 0.015	AccX = 0.07	AccZ = 0.01	AccX = 0.12	AccZ = 0.01	AccX = 0.03	AccZ = 0.02	AccX = 0.014	AccZ = N/A	AccX = N/A
Roll= 1.9	Pitch = -0.2	Roll = 5.1	Pitch = -0.2	Roll = -1.9	Pitch = 0.4	Roll = -5.7	Pitch = 0.7	Roll = N/A	Pitch = N/A
Section B		Section B		Section B		Section B		Section B	
-214	-14	39	-459	-74	-304	-42	-447	-141	-152
-595	-507	-372	-747	-456	-640	-368	-747	-479	-586
AccZ = 0.016	AccX = 0.05	AccZ = 0.00	AccX = 0.09	AccZ = 0.003	AccX = 0.01	AccZ = 0.02	AccX = 0.05	AccZ = N/A	AccX = N/A
Roll = 2.4	Pitch = 1.3	Roll = 5.7	Pitch = 1.3	Roll = -1.3	Pitch = 1.8	Roll = -5.2	Pitch = 2.3	Roll = N/A	Pitch = N/A
Section D		Section D		Section D		Section D		Section D	
-115	-26	268	-464	123	-329	291	-505	-37	-31
-729	-604	-613	-1062	-626	-928	-629	-1095	-660	-801
Section C		Section C		Section C		Section C		Section C	
26	48	75	-17	58	1	82	-10	109	79
-584	-634	-551	-666	-562	-657	-549	-666	-549	-633
AccZ = 0.017	AccX = 0.06	AccZ = 0.01	AccX = 0.10	AccZ = 0.02	AccX = -0.04	AccZ = 0.02	AccX = 0.008	AccZ = N/A	AccX = N/A
Roll = 1.8	Pitch = -0.3	Roll = 5.1	Pitch = -0.2	Roll = -1.9	Pitch = 0.2	Roll = -6.2	Pitch = 1.0	Roll = N/A	Pitch = N/A

Units: Strain in microstrain, Acceleration in g, and Roll and Pitch in degrees
AccZ = Vertical acceleration oriented with gravity (positive = upward acceleration of girder)
AccX = Lateral acceleration oriented normal to the girder web (positive = towards the driver's side)
* for each section, 4 strain measurements are reported in their respective cells: top left, top right, bottom left and bottom right. Potential cracking events are highlighted by cracking threshold: 130 – 200 microstrain (yellow) and over 200 microstrain (green).

Potential cracking events, identified by strain above the selected 200 microstrain threshold, can be observed at the rear jeep section (Section A), and at the tongue location (Section D) for events G1-S2 and G1-S4. The highest recorded tensile strains occurred at the tongue location (Section D) and girder end (Section A) during the slow left turn onto I-10, event G1-S4, and were associated with a recorded roll angle of -5.2 deg. at Section B. The strain

behavior at Sections A and D are consistent with flexure created from a high-level of force being input by the tongue, as opposed to flexure from girder roll alone.

Figure 36 shows the relative differential top flange strain, acceleration, and lateral roll angle responses along the Pass Christian portion of the route. The high tensile strains recorded at Sections A and D during event G1-S2, G1-S3 and later in event G1-S4 are attributed to the effect of the jeep tongue which was not connected during event G1-S1 and where peak strains at these same cross sections were typically in compression or in low tension. Figure 37 and Figure 38 show the girder transport making the turn out of the yard (G1-S1) and onto I-10 (G1-S4), respectively.

While the jeep tongue is important for the stability of the trailer at speeds exceeding 10 mph, during maneuvering sharp turns (90 deg. with tight radii), if connected, the tongue exerts lateral force on the girder. This lateral force induces bending moment about the weak-axis of the girder, which can lead to high tensile strains and potential cracking. This phenomena was demonstrated while the truck was stopped on US 90 due to jeep controller issues. The results of the driver operating the rear jeep while the truck was stationary are observed in the strains recorded during event G1-S3. These strains were below the cracking strain threshold of 200 microstrain but above the AASHTO implied cracking strain of about 130 microstrain.

Lateral roll angle correlated well with high strains as shown in Figure 36c for this location; however, this was not always the case. For example, Figure 39 shows the transport traveling across a flyover with a large radius curve that was superelevated. The roll of the girder was significant, but the associated strain was relatively low, and the accelerations were only moderate.

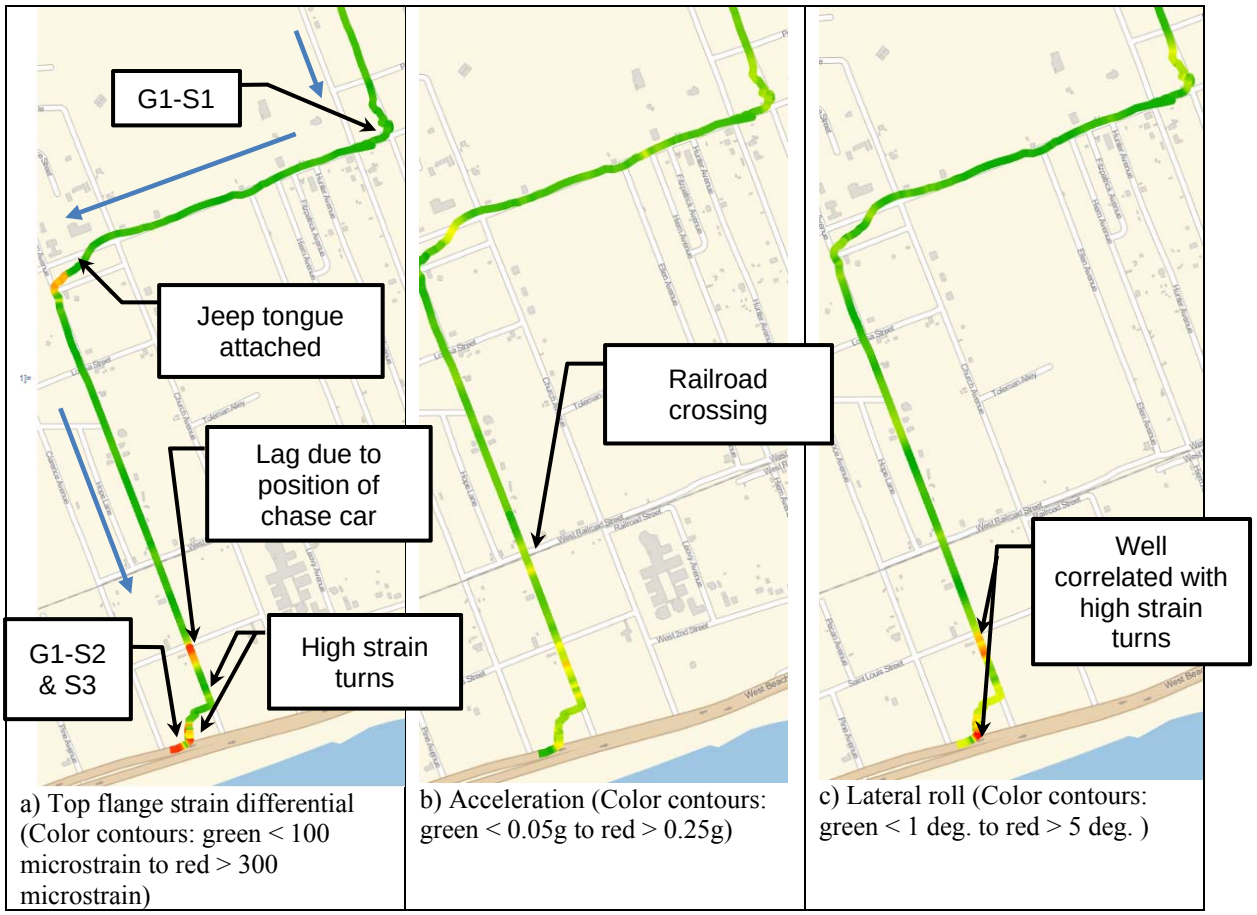

a) Top flange strain differential (Color contours: green < 100 microstrain to red > 300 microstrain)

b) Acceleration (Color contours: green < 0.05g to red > 0.25g)

c) Lateral roll (Color contours: green < 1 deg. to red > 5 deg.)

Figure 36
Comparison of transport data at noted top flange differential strain events in Pass Christian

Figure 37
First turn out of yard without jeep tongue mounted on Girder 1 (upper photo) and Girder 2 (lower photo)

Figure 38
Girder 1 (upper photo) and Girder 2 (lower photo) crabbing during a turn onto I-10 with jeep tongue engaged

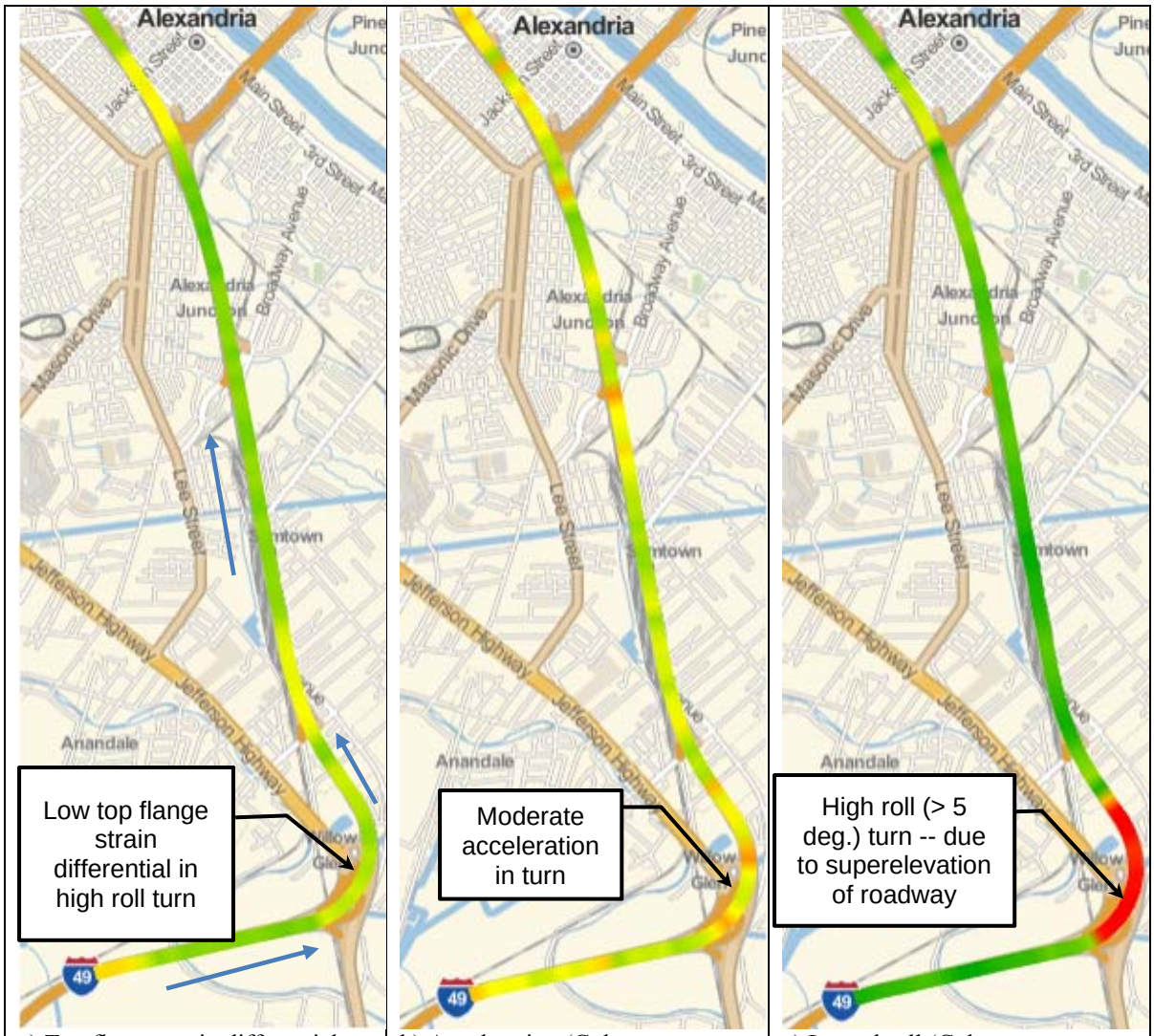

a) Top flange strain differential (Color contours: green < 100 microstrain to red > 300 microstrain)

b) Acceleration (Color contours: green < 0.05 g to red > 0.25 g)

c) Lateral roll (Color contours: green < 1 deg. to red > 5 deg.)

Figure 39
Comparison between (a) top flange strain differential; (b) lateral and vertical acceleration at midspan; and (c) lateral roll angle at mid-span

Dynamic Monitoring During Girder Transport: *Girder 2 - Lake Charles Route*

Date: September 23, 2014
Start: Pass Christian, Mississippi
End: Lake Charles, Louisiana
Length: 258 miles
Duration: 9 a.m. to 4 p.m., 7 hours
Weather: Morning- Pass Christian: Clear, Light wind, 69 deg. F; Mid-day- Baton Rouge: Sunny, 84 deg. F; Afternoon- Lake Charles: Sunny, High 84 deg. F

For nearly half its journey, Girder 2 covered much of the same route as Girder 1. After the girder made the first turn out of the yard, the driver raised the tongue into place and traveled the remainder of the journey with it raised. There were no mechanical or electrical issues on the trip to Lake Charles, Louisiana. The weather was clear and sunny throughout the day, and started warm and was hot by the end of the trip.

A map of the overall journey is shown in Figure 40 and shows a color contour plot of transport speed across the full length of traveled route. Measured speeds based on geolocation and time varied from stopped to over 60 mph. For the first half of the trip to Baton Rouge, roadway conditions for Girder 2 were the same as for Girder 1 (flat off-road at the yard, local roads, arterial routes, highway, interstate, ramps, railroad crossings, and intersections). Refer to Figure 37 and Figure 38 showing similar turns. In Baton Rouge, Girder 1 had exited I-10 due to lane restrictions which were subsequently removed during the Girder 2 passage. After Baton Rouge, Girder 2 traveled on high-speed paved asphalt and concrete riding surfaces until it exited at Lake Charles. The route from I-10 to the unpaved project site consisted of multiple turns on city streets.

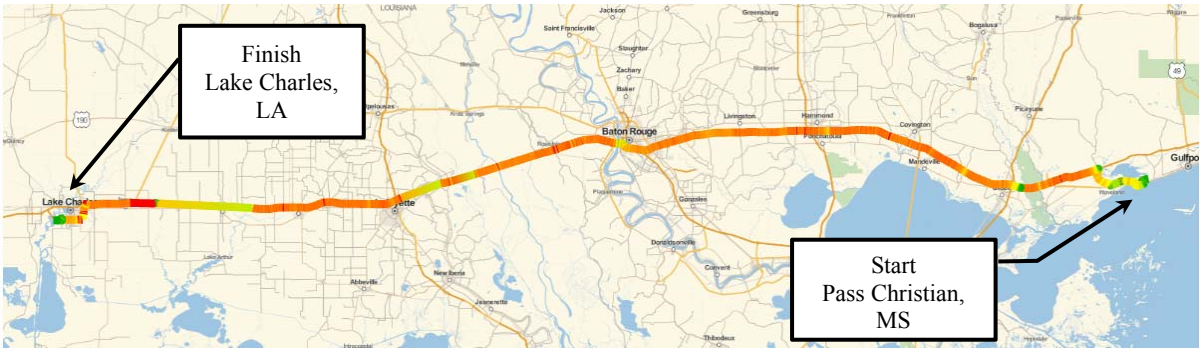

Figure 40
Overview of route of Girder 1 with relative speed along the route overlaid (red > 55 mph; green < 10 mph)

Similar to Girder 1, only selected high-girder acceleration and strain events, shown in Table 18 and Table 19, are discussed. These tables show the values for each strain gage and inertial measurement unit at a given cross section at the selected time of maximum strain or acceleration. Since the strain gages were installed on the girder just prior to transport, the strain in each gage or the measured response was offset equal to the calculated prestress transfer strains and gravity load strain. This provided a means to estimate whether the girder exceeded the cracking threshold during transport when the initial strains and measured strains were combined. All measurements were coarsely corrected for temperature effects by using the mean strain value at the start of the test as a reference value because external BDI strain gages were used. Graphical details of the raw data of the full transportation record and the selected events are provided in Appendix F.

Table 18 shows the strain response of Girder 2 during five selected acceleration events. These events are shown in Figure 41.

- Event G2-A1 occurred when the transportation truck reached high speed on I-10 in Mississippi and the girder acceleration in the Z-direction exceeded 0.25g.
- Event G2-A2 was associated with high acceleration in the Z-direction when the truck was exiting the highway at the rest stop located just over the Mississippi border into Louisiana.
- High acceleration in the Z-direction and X-direction were recorded during Event G2-A3 which occurred on I-10.
- Peak highway acceleration in the X-direction was recorded during Event G2-A4
- Peak highway acceleration in Z-direction was recorded during Event G2-A5.

As shown in Table 18, only compressive strains were observed during the acceleration events. The only exception is Event G2-A4, where a small tensile strain was recorded at the rear jeep section (Section A) when the peak lateral acceleration of -0.74g was recorded.

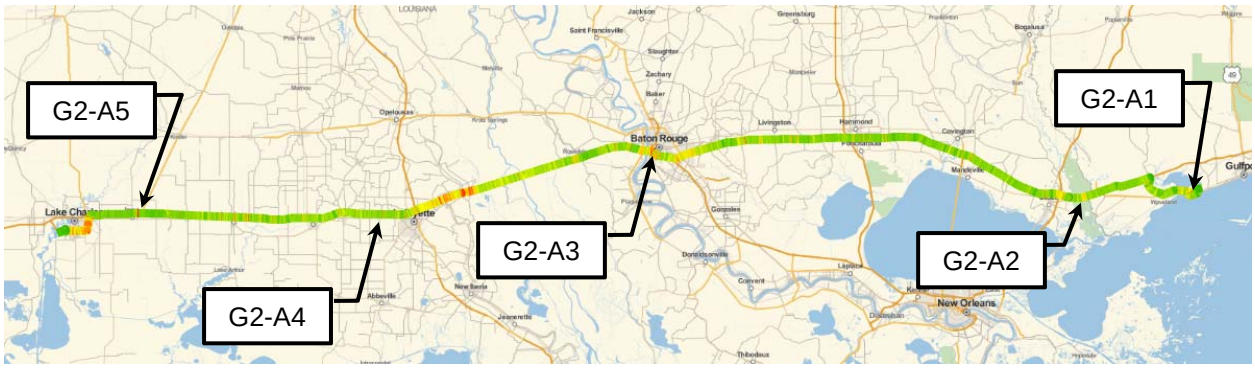

Figure 41
Overview of route of Girder 2 showing accelerations with selected events noted (color contours: green < 0.05 g to red > 0.25 g)

The highest recorded strain events during transport/lifting are shown in Table 19. Figure 43 shows the transport route with selected strain events.

- Event G2-S1 was recorded during slow right turn as the girder was leaving the yard. This event was selected for comparison with Girder 1, as well as for comparison to events when the tongue was engaged.
- Event G2-S2 occurred during slow left turn onto the on-ramp of I-10 in Mississippi. This event was caused by high roll of the girder and tongue force input from the jeep.
- Events G2-S3 and G2-S4 occurred in Louisiana during slow right turns. Both events were also caused by high roll of the girder and tongue force input from the jeep.
- Event G2-S5 occurred during lifting of the girder at the site by two cranes and was caused by roll of the girder.

Two potential cracking events can be observed when reviewing the table. Both potential cracking events (G2-S3 and G2-S4) occurred during slow right turns with potential cracking strains observed at midspan (Section B) and the tongue location (Section D). The highest recorded tensile strains were associated with the highest recorded average roll of -3.4 deg. with peak tensile strain measured at the tongue location (Section D).

Table 18
Surface strains of selected transportation events based on high girder acceleration*

Event G2-A1		Event G2-A2		Event G2-A3		Event G2-A4		Event G2-A5	
09:21:00 to 09:23:40		10:01:40 to 10:04:20		12:10:20 to 12:12:00		13:10:30 to 13:10:45		13:40:02 to13:40:42	
First occurrence: accelerations exceeding 0.25g		Acceleration in Z direction (I-10 exit ramp)		Acceleration in Z and X directions (I-10)		Peak acceleration: X direction (I-10)		Peak acceleration: Z direction (I-10)	
Section A		Section A		Section A		Section A		Section A	
-64	-90	-52	-26	-46	-25	-42	6	-46	-4
-687	-714	-684	-671	-703	-700	-702	-686	-717	-699
AccZ = 0.40	AccX = 0.13	AccZ = 0.31	AccX = 0.08	AccZ = 0.25	AccX = 0.17	AccZ = 0.17	AccX = 0.25	AccZ = 0.47	AccX = 0.16
Roll = 0.7	Pitch = 0.9	Roll = 1.3	Pitch = 2.6	Roll = -4.2	Pitch = 4.8	Roll = 1.4	Pitch = 0.3	Roll = 0.6	Pitch = -1.2
Section B		Section B		Section B		Section B		Section B	
-224	-159	-173	-124	-151	-232	-148	-103	-110	-78
-605	-571	-630	-562	-594	-601	-625	-548	-700	-600
AccZ = 0.24	AccX = 0.13	AccZ = 0.19	AccX = 0.03	AccZ = 0.21	AccX = 0.22	AccZ = 0.16	AccX = -0.42	AccZ = 0.44	AccX = 0.08
Roll = 0.6	Pitch = -0.6	Roll = 0.7	Pitch = 1.3	Roll = -4.0	Pitch = 5.1	Roll = 0.7	Pitch = -1.1	Roll = -0.1	Pitch = -2.5
Section D		Section D		Section D		Section D		Section D	
-138	-135	-105	-99	-123	-203	-113	-74	-116	-96
-554	-593	-542	-559	-479	-632	-498	-574	-525	-612
Section C		Section C		Section C		Section C		Section C	
-26	-113	-13	-48	-7	-51	-4	-38	-9	-34
-700	-724	-712	-701	-723	-724	-719	-714	-727	-719
AccZ = 0.60	AccX = 0.13	AccZ = 0.44	AccX = -0.05	AccZ = 0.42	AccX= -0.35	AccZ = 0.45	AccX = -0.74	AccZ = 0.65	AccX = -0.08
Roll = 0.3	Pitch = -1.1	Roll = -0.1	Pitch = 0.4	Roll = -5.2	Pitch = 6.0	Roll = -0.1	Pitch = -2.0	Roll = -1.2	Pitch = -3.5

Units: Strain in microstrain, Acceleration in g, and Roll and Pitch in degrees
AccZ = Vertical acceleration oriented with gravity (positive = upward acceleration of girder)
AccX = Lateral acceleration oriented normal to the girder web (positive = towards the driver's side)
* for each section, 4 strain measurements are reported in their respective cells: top left, top right, bottom left and bottom right. Potential cracking events are highlighted.

Table 19
Surface strains of selected transportation events based on high girder strains*

Event G2-S1		Event G2-S2		Event G2-S3		Event G2-S4		Event G2-S5	
08:55:00 to 09:00:00		09:40:00 to 09:45:00		14:28:00 to 14:34:00		14:40:00 to 14:44:00		15:40:00 to 15:45:00	
Yard exit		90 degree left turn onto I-10		90 degree right turn at site		90 degree right turn at site		Site lift	
Section A		Section A		Section A		Section A		Section A	
-128	-10	-10	-62	-189	-189	105	-162	-189	142
-723	-626	-626	-721	-846	-846	-628	-780	-846	-707
AccZ = 0.03	AccZ = 0.02	AccZ = 0.02	AccX = 0.03	AccZ = 0.02	AccZ = 0.02	AccZ = 0.04	AccX = -0.02	AccZ = 0.02	AccX = 0.02
Roll = 1.3	Roll = 1.6	Roll = 1.6	Pitch = 0.2	Roll = 0.3	Roll = 0.3	Roll = -2.8	Pitch = 0.1	Roll = 0.3	Pitch = 0.2
Section B		Section B		Section B		Section B		Section B	
-261	-320	-320	45	-265	-265	201	-517	-265	18
-671	-714	-714	-454	-794	-794	-379	-866	-794	-607
AccZ = 0.01	AccZ = 0.00	AccZ = 0.00	AccX = -0.01	AccZ = 0.00	AccZ = 0.00	AccZ = 0.01	AccX = -0.07	AccZ = 0.00	AccX = 0.00
Roll = 0.8	Roll = 0.7	Roll = 0.7	Pitch = -0.5	Roll = -0.6	Roll = -0.6	Roll = -3.4	Pitch = -1.1	Roll = -0.6	Pitch = -1.4
Section D		Section D		Section D		Section D		Section D	
-216	-317	-317	104	19	19	308	-498	19	18
-614	-714	-714	-365	-565	-565	-176	-1002	-565	-585
Section C		Section C		Section C		Section C		Section C	
-93	45	45	-100	-135	-135	27	-161	-135	-54
-720	-620	-620	-755	-863	-863	-653	-817	-863	-717
AccZ = 0.01	AccZ = 0.03	AccZ = 0.03	AccX = -0.08	AccZ = 0.00	AccZ = 0.00	AccZ = 0.01	AccX = -0.14	AccZ = 0.00	AccX = -0.09
Roll = 0.1	Roll = -0.8	Roll = -0.8	Pitch = -1.7	Roll = -1.5	Roll = -1.5	Roll = -4.1	Pitch = -2.2	Roll = -1.5	Pitch = -2.4

Units: Strain in microstrain, Acceleration in g, and Roll and Pitch in degrees
AccZ = Vertical acceleration oriented with gravity (positive = upward acceleration of girder)
AccX = Lateral acceleration oriented normal to the girder web (positive = towards the driver's side)
* for each section, 4 strain measurements are reported in their respective cells: top left, top right, bottom left and bottom right. Potential cracking events are highlighted: 130 – 200 microstrain (yellow) and over 200 microstrain (green).

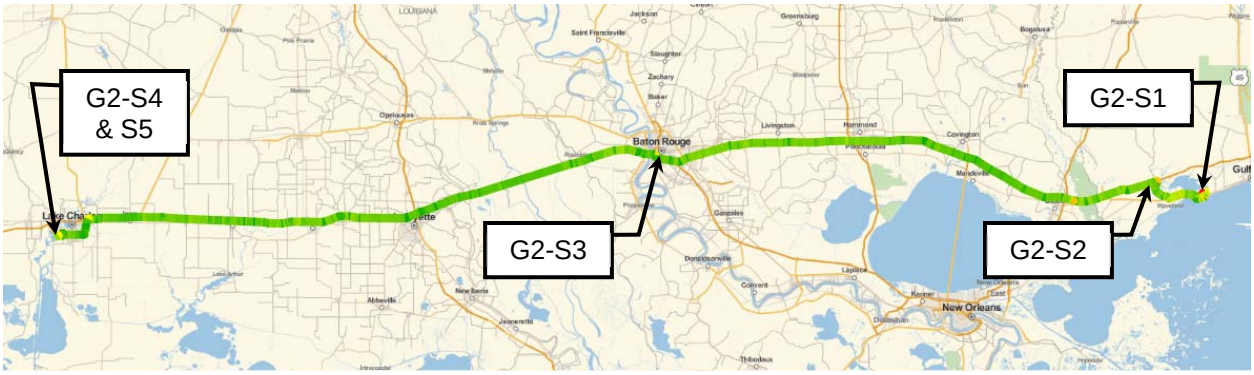

Figure 42
Overview of route of Girder 2 showing girder top flange strain differentials with selected events noted (color contours: green < 100 microstrain to red > 300 microstrain)

Higher tensile strains, likely exceeding the cracking strain, were recorded at the tongue location during event G2-S3 as compared to strains during event G2-S1. Similar to Girder 1, this can be attributed to the effect of the jeep tongue which was not connected during event G2-S1 (yard turn) and was connected during event G2-S3 (site turn).

The turn results for G2-S3 and G2-S4 are shown visually in Figure 43. The tight turns require the driver to operate the jeep, and this leads to the bending of the girder during maneuvering. Since the speed of the transport is very slow during transport, it does not result in a significant acceleration compared to other observed events during transport. The tight turning radius that results in girder bending does cause some girder roll, but not as high as from other events.

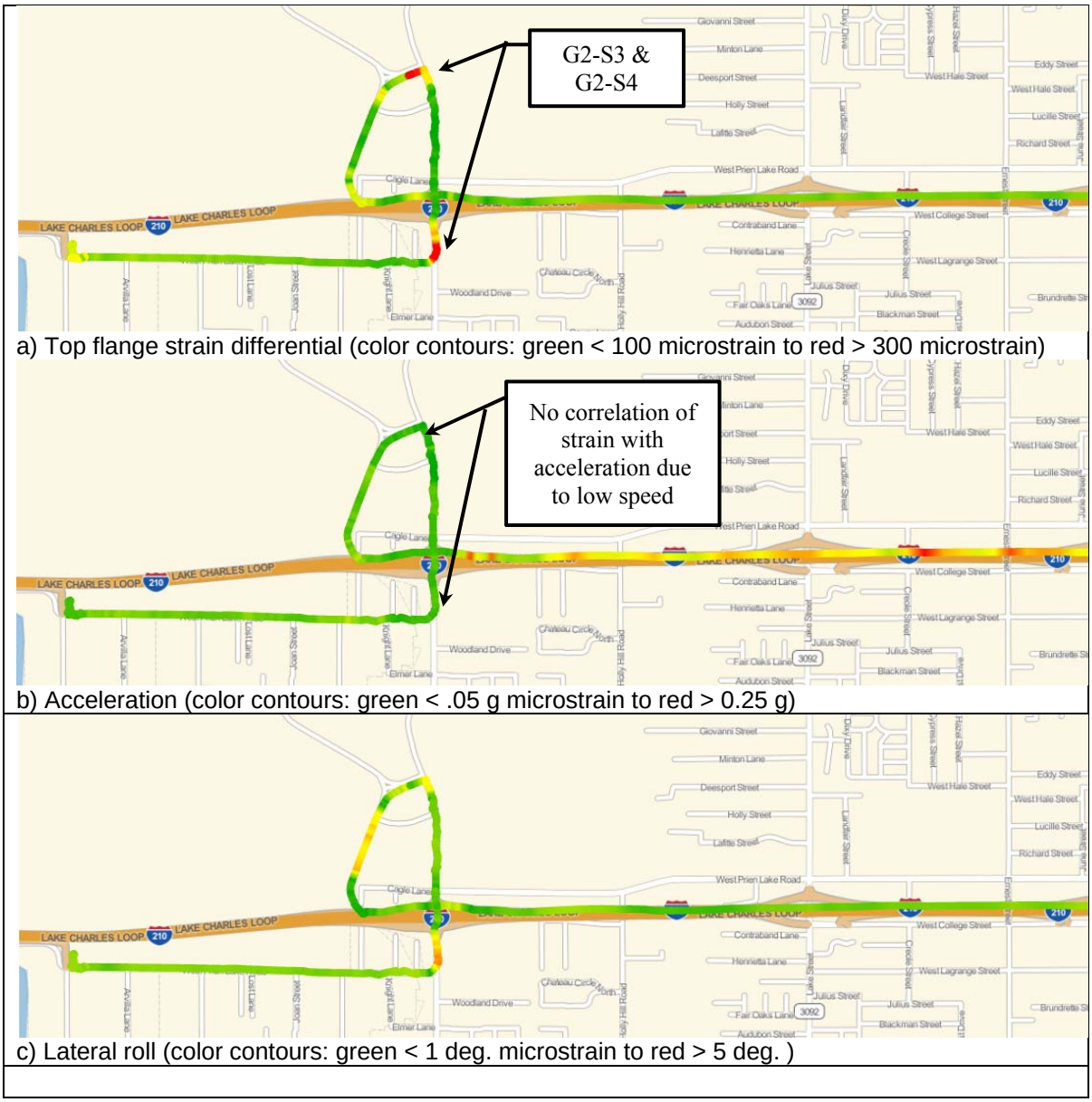

a) Top flange strain differential (color contours: green < 100 microstrain to red > 300 microstrain)

b) Acceleration (color contours: green < .05 g microstrain to red > 0.25 g)

c) Lateral roll (color contours: green < 1 deg. microstrain to red > 5 deg.)

Figure 43
Girder transport during a high strain event going around a tight radius turn with the tongue attached

Dynamic Monitoring During Other Notable Events

Table 20 shows the monitoring results of two notable events of interest. The first events is at a railroad crossing (refer to Figure 36b) while the second is at causeway crossing for both girders. As seen in the table, the measured strains were higher during the causeway crossing as compared to the railroad crossing. Although the road surface is more irregular during the railroad crossing, the speed of the truck was very slow and, therefore, did not result in high vertical accelerations and cracking strains. In general, recorded strains due to road surface irregularity were less than those measured during slow turns. No potential cracking strains

were observed during both events for both girders. No tensile strains were observed in Girder 2 during both events.

Table 20
Surface strains during road surface irregularity transportation events*

Girder 1				Girder 2			
08:26:00 to 08:28:00		01:42:00 to 01:44:00		9:12:00 to 09:14:00		12:32:00 to 12:34:00	
Railroad crossing		Causeway event		Railroad crossing		Causeway events	
Section A		Section A		Section A		Section A	
-42	60	-29	109	-112	-72	-49	-13
-666	-650	-666	-646	-732	-695	-705	-696
AccZ = 0.13	AccX = -0.01	AccZ = 0.25	AccX = -0.03	AccZ = 0.04	AccX = 0.00	AccZ = 0.45	AccX = 0.03
Roll = 0.0	Pitch = -0.4	Roll = -0.9	Pitch = -0.6	Roll = 0.2	Pitch = 1.2	Roll = 1.2	Pitch = -1.5
Section B		Section B		Section B		Section B	
-220	-66	-339	40	-229	-166	-193	-156
-562	-520	-599	-510	-646	-577	-628	-553
AccZ = -0.13	AccX = 0.07	AccZ = -0.05	AccX = 0.08	AccZ = -0.01	AccX = -0.00	AccZ = -0.09	AccX = 0.05
Roll = 0.6	Pitch = 1.1	Roll = -0.6	Pitch = 0.9	Roll = -0.4	Pitch = 0.0	Roll = 0.4	Pitch = -2.9
Section D		Section D		Section D		Section D	
-84	-72	-189	-46	-187	-146	-163	-140
-738	-650	-792	-634	-589	-596	-501	-572
Section C		Section C		Section C		Section C	
32	36	77	86	-75	-81	-3	-29
-578	-639	-578	-647	-718	-696	-722	-716
AccZ = 0.02	AccX = -0.01	AccZ = 0.11	AccX = 0.03	AccZ = 0.00	AccX = -0.09	AccZ = -0.27	AccX = -0.09
Roll = 0.1	Pitch = -0.5	Roll = -1.0	Pitch = -0.6	Roll = -1.1	Pitch = -0.8	Roll = -0.5	Pitch = -3.8

Units: Strain in microstrain, Acceleration in g, and Roll and Pitch in degrees
AccZ = Vertical acceleration oriented with gravity (positive = upward acceleration of girder)
AccX = Lateral acceleration oriented normal to the girder web (positive = towards the driver's side)
* for each section, 4 strain measurements are reported in their respective cells: top left, top right, bottom left, and bottom right.

Dynamic Monitoring During Prestress Transfer

The behavior of Girder 1 during prestress transfer and lifting from the prestressing bed was monitored using embedded strain gages and DEMEC gages. The measured and analytical strains are shown in Table 21 and indiate a reasonable agreement between all strains. However, higher strains were observed in the embedded strain gages as compared to the DEMEC gages and the analytical strains.

Continuous strain monitoring was performed during prestress transfer using embedded strain gages with results shown in Table 22 and Appendix E. It can be seen that full transfer of the prestressing force did not completely occur after the strands were cut. This is attributed to friction between the girder and the prestressing bed which prohibits the full transfer of the prestressing force to the girder. However, a permanent change in the strain, between 17 and 46 microstrain, was recorded once the girder was lifted from the forms. At this point, the full prestressing force was transferred to the concrete. A slight increase in strain was also observed after the lift, which can be attributed to the time-dependent concrete properties of creep and shrinkage.

Table 21
Measured and calculated transfer strains for Girder 1

Strain	A- Top	A-Bottom	B-Top	B-Bottom	D-Top	D-Bottom	C-Top	C-Bottom
Girder 1 Analytical	39	-551	-101	-498	-47	-550	39	-551
Girder 1 Measured DEMEC*	41	-657	-109	-554	__	__	27	-610
Girder 1 Measured (embedded)*	56	-673	-125	-562	__	__	24	-618

*Average value of two strain gages

Table 22
Transfer strains of Girder 1 before and after lifting from prestressing bed using embedded strain gages

Strain	A-Top	A-Bottom	B-Top	B-Bottom	D-Top	D-Bottom	C-Top	C-Bottom
After strands cut*	-20	-570	-142	-490	__	__	-2	-532
Immediately before lift*	10	-649	-143	-541	__	__	7	-596
Immediately after lift*	56	-673	-125	-562	__	__	24	-618
Change in strain due to lift	46	-24	18	-21	__	__	17	-22
45 min after lift*	62	-693	-127	-577	__	__	19	-636

*Average value of two strain gages

Dynamic Monitoring During Lifting

Monitoring was performed on each of the girders during the two lifts immediately prior to and after transportation (yard lift and site lift). The yard lift was monitored as the girders were moved from their storage position in the yard to the trailer in preparation for transport. The site lift occurred at the bridge site as the girders were raised off the truck before being set on their bearings (Figure 44). The recorded measurements during both girder lifts are shown in Table 23.

For Girder 1, tensile strains were recorded at the girder ends (Section A and Section C), during the initial yard lift. The tensile strains at the girder ends were higher during the site lift. No potential cracking strains were observed during both lifts for Girder 1. Similar to Girder 1, no potential cracking strains were observed during either lift for Girder 2 with tensile strains only recorded at the tongue location (Section D) and midspan (Section B) during the site lift. The tensile strain recorded at the girder end (Section A) is believed to have resulted from a false sensor reading, this sensor was potentially impacted prior to the lift.

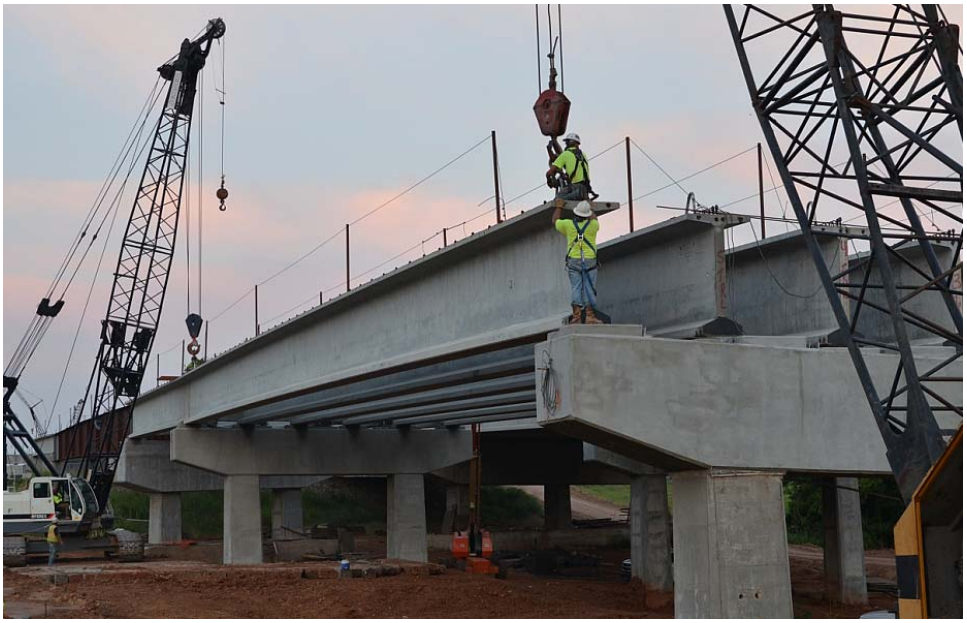

Figure 44
Erection of Girder 1 onto the bridge bearings

Table 23
Surface strains of lifting events at yard and site*

Girder 1				Girder 2			
Yard lift		**Site lift**		**Yard lift**		**Site lift**	
Section A		Section A		Section A		Section A	
50	77	31	103	-200	-163	-189	142[1]
-668	-649	-598	-637	-828	-793	-846	-707
AccZ = 0.17	AccX = 0.14	AccZ = N/A	AccX = N/A	AccZ = 0.02	AccX = 0.13	AccZ = 0.02	AccX = 0.02
Roll = 2.7	Pitch = 0.6	Roll = N/A	Pitch = N/A	Roll = 3.0	Pitch = 2.1	Roll = 0.3	Pitch = 0.2
Section B		Section B		Section B		Section B	
-140	-38	-141	-152	-410	-193	-265	18
-580	-477	-479	-586	-819	-626	-794	-607
AccZ = 0.16	AccX = 0.15	AccZ = N/A	AccX = N/A	AccZ = 0.01	AccX = 0.14	AccZ = 0.00	AccX = 0.00
Roll = 2.7	Pitch = -0.7	Roll = N/A	Pitch = N/A	Roll = 3.0	Pitch = 2.1	Roll = -0.6	Pitch = -1.4
Section D		Section D		Section D		Section D	
-68	-69	-37	-31	-320	-192	19	18
-665	-667	-660	-801	-731	-660	-565	-585
Section C		Section C		Section C		Section C	
44	39	109	79	-172	-193	-135	-54
-590	-642	-549	-633	-853	-817	-863	-717
AccZ = 0.1	AccX = 0.08	AccZ = N/A	AccX = N/A	AccZ = 0.11	AccX = -0.25	AccZ = 0.00	AccX = -0.09
Roll = 3.3	Pitch = -0.1	Roll = N/A	Pitch = N/A	Roll = 2.8	Pitch = 2.0	Roll = -1.5	Pitch = -2.4

Units: Strain in microstrain, Acceleration in g, and Roll and Pitch in degrees
[1] Appeared to be an bad reading from damage
AccZ = Vertical acceleration oriented with gravity (positive = upward acceleration of girder)
AccX = Lateral acceleration oriented normal to the girder web (positive = towards the driver's side)
* for each section, 4 strain measurements are reported in their respective cells: top left, top right, bottom left, and bottom right.

Observations from Girder Transportation and Lifting

1. Both girders traveled similar routes for the majority of their respective journeys, and similar responses were observed in both.
2. Higher tensile strains were observed in the top flange of Girder 1 as compared to Girder 2 considering the same turns. This is consistent with the smaller weak axis moment of inertia and lower prestressing force of Girder 1.
3. For both girders, events that caused high strains did not correspond to events with high acceleration. Alternatively, the highest measured strains occurred during tight turns at very low speeds where high roll angle values (>3 deg.) were recorded.

4. For both girders, the highest strains occurred at the measured cross section at the jeep tongue location (Section D). Based on general behavior and research, the critical cross section was thought to be at midspan due to sweep related effects, caused through either roadway super-elevation or accelerations during transport. However, prior transportation research through DOTD further confirmed the jeep tongue cross section as the critical location.
5. Girder travel over railroad crossings at slow speeds and causeway bridges at highway speeds did not result in any recordable cracking events.
6. Some of the highest recorded strains during transport of Girder 1 occurred when the girder was stationary on the side of the roadway and the driver was troubleshooting and testing the operation of the jeep controls (Event G1-S2).
7. Strain measurements exceeding potential cracking strain were observed during a few isolated events for both girders. These events occurred during high roll, slow speed events. No cracks were visually observed in the girders at the end of transportation.
8. For the same girder, higher tensile strains were observed during turns where the jeep tongue was attached. This highlights the effects the tongue force can exert on the girder.
9. For the two 130 ft. girders in this study, as well as the two 150 ft. girders in the prior DOTD study, the lift points and transport support points were all at the ends of the girder, approximately 5 ft. from the end for this study.
10. Drivers for both girders operated in the yard and left the yard through the first turn with the tongue of the jeep detached.
11. Strain measurements of the girder during lift operations were all noticeably lower than the peak transportation events.
12. Higher tensile strains were recorded during the site lift as compared to the yard lift. This was especially true for sections were potential cracking occurred during transport. Given, similarities between the two lifting cases, the girders should have had comparable responses during both lifts. The higher tensile strains during the site lift shows that the response of the girder changed due to transport, which could be an indication that the stiffness of the girder was reduced due to cracking. This is further supported by the strain gage data, which showed that likely cracking events occurred during transport.

Finite Element Analysis

Finite element models were generated to develop additional understanding of the behavior of the girders during transportation. Based on review of field measurements, it was determined that the predominant contributions to tensile strains in the girders were girder roll and the force input from the jeep tongue. As previously stated, the section with peak tensile strains was most commonly the cross section at the jeep tongue (Section D). The objective of the analysis work is to evaluate the contributions of girder roll angle and tongue force as a girder undergoes a turning event.

During the course of the research project, multiple analytical methods and software applications were considered and applied. The two issues encountered during this process were complexity of the modeling required and the ability of the finite element method (FEM) software to model the necessary behavior.

A number of analytical iterations and investigations were subsequently performed. Because of all the transport data collected, there was a desire to input acceleration and roll time history measurement data from each girder test, and then model and calibrate the analytical responses. This resulted in many hours of testing various techniques. As the analyses would have to be iterative, it would require hundreds or thousands of solution steps to adequately model an event measured in seconds. While an extensive effort was made to apply this approach, it was ultimately determined that an efficient means of executing this evaluation was not possible. Similarly, considerations for modeling the girder behavior linearly and nonlinearly were studied. However, modeling the nonlinear behavior of the girder at certain positions would require considerably more computational power and time. Thus, a more readily attainable objective of modeling the linear response of the girder at specific girder positions was ultimately applied.

Prior to using a detailed three-dimensional model for event simulation, the researchers investigated other successful techniques in the literature by Stratford et. al. and Cojocaru *,* respectively *[10, 12]*. The latter demonstrated that a frame model could readily be used; however, his development involved use of Abaqus software and a particular frame element capable of interpolating stress and strain for complex cross sections. Abaqus is an advanced FEM modeling software requiring specialized licensing. Other, more commercially available, FEM software such as RISA or SAP2000 were also considered. However, neither appeared to properly address the behavior of the girders. RISA could not model the cross section with the ability to report strains at particular points. While SAP2000 was capable of modeling detailed cross sections and outputting strains at particular points, it could not completely model torsional behavior using frame elements. A potential conceptual approach to address

the torsion issue is to replace the flange elements with shell elements capable of modeling the warping torsion aspect. Ultimately, it was decided this approach might result in inaccuracy due to the variable depth flanges.

Given the multiple approaches available, the researchers ultimately settled on a simpler approach for estimating the effects of roll and lateral tongue force on different length girders of a certain type by utilizing Autodesk Simulation Mechanical 2014 to perform the FEM modeling. A three-dimensional (3D) brick model was chosen to model the cross section geometry and obtain direct strain analysis results under loading. Considering the complexity of the transported girder system, multiple modeling techniques were investigated with the straight linear model chosen because the measurement data provided a known loading geometry. The need to perform a nonlinear analysis, where the girder analytical behavior is iterated as the load state and geometry changes, was then eliminated. Furthermore, because of the minimal change in dynamic acceleration in slow turns, the critical stress events can be approximated as static events.

Development of 3D Model

A 3D model of the BT-72 (Girder 1) was developed in the 3D modeling software Autodesk Fusion 360 and then imported into Autodesk Simulation Mechanical 2014, as shown in Figure 45. The model consisted of the girder, end bearing supports, and the tongue support. Prestressing was not considered in the model, as the problem was treated in a linear fashion where the principles of superposition could be applied against the assumed state of strain imposed by the prestressing. The cross-section was developed based on the drawings provided for Girder 1. Three models were developed to compare the behavior of different length girders: 100-ft., 130-ft., and 150-ft. long girders. In each of these models, the supports were 2 ft. inboard from the ends, and the tongue was 30 ft. from the end support, similar to the as-transported girders in this research. The support bunks were modeled as 4 in. thick by 24 in. long by the width of the girder. The tongue was modeled similarly as a 4-in. by 6-in. long element by the width of the girder.

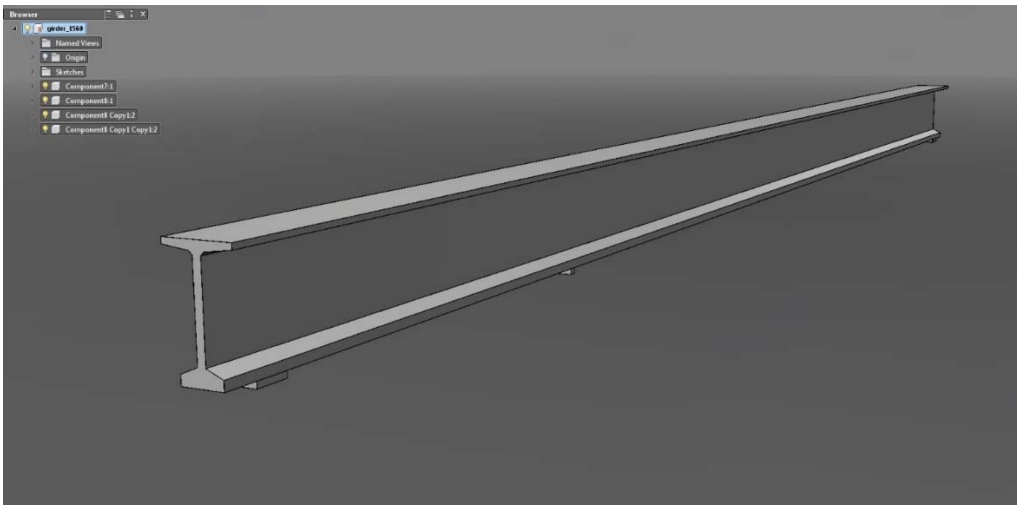

Figure 45
3D Model of BT72 Girder

After importing into Autodesk Simulation Mechanical 2014, each of the girders were meshed with brick elements between 6 and 9 in. sides. The concrete girder was modeled with a modulus of elasticity of 5,300 kip/in^2. The supports were modeled as a plastic element to provide for deformation flexibility using a material with a modulus of elasticity of 120 kip/in^2. Restraints were provided at each bunk support bottom surface. One end had all translations restrained and the other end had the vertical and lateral displacement restrained. As the entire surface was restrained, so too effectively was rotation, such as roll.

Two different sets of loadings were applied to each of the girder models. First, a gravitational load consistent with rotations of 2, 4, and 6 degrees at midspan. For example, for a 6 deg. roll at midspan, the gravitational scale factors were 0.10g oriented laterally to the girder, and -0.0055g in the vertical direction. This approach resulted in a slight uplift for the roll case. Note that this load case only examines the effect of the roll component, and not the addition of gravity causing self-weight strains. The objective was to estimate the additional strain due to roll, which would be considered additive to other load effects, such as self-weight and prestressing. The second set of load cases was the application of a lateral tongue force applied to the bottom of the tongue component at loads levels of 500, 2000, 5000, and 8000 lbs. The objective of this load case was to estimate the magnitude of the tongue force input. Examples of the 3D model and midspan cross section results are shown in Figure 46 and Figure 47.

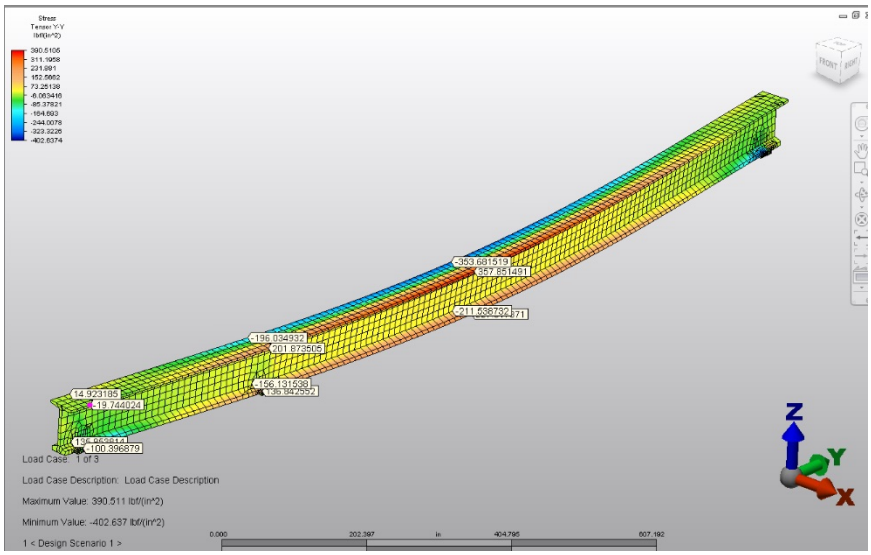

Figure 46
Typical FEM output results

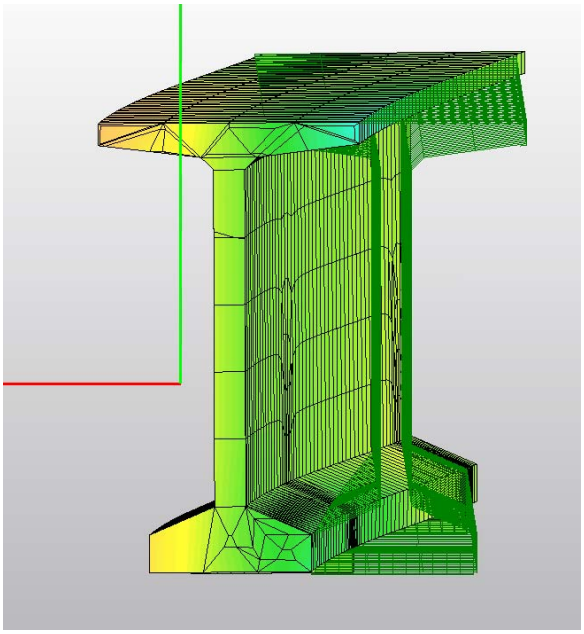

Figure 47
Midspan cross-section showing displaced shape and lateral deflection

Variation of Girder Roll Angle versus Girder Length

A parametric study was conducted to investigate the effect of roll angle and girder length on peak tensile strains. The loads were applied by varying gravity acceleration to apply only the component of acceleration attributed with roll. It was assumed that the girders were all supported near the ends to provide reasonable comparisons with the girders monitored in the

current research, as well as the previously discussed field measurements on 150 ft. girders. As shown in Figure 48, peak tensile strains increase with an increase of girder roll, as would be expected. In addition, longer girders have higher peak strains as compared to their shorter counterparts, as the girder roll causes a component of the girder's self-weight to be applied about the weak axis of inertia. This self-weight contribution increases strains in one corner of the girder's cross section and decreases it in the opposite corner. This result also agrees with the analytical model developed by Mast *[4]*.

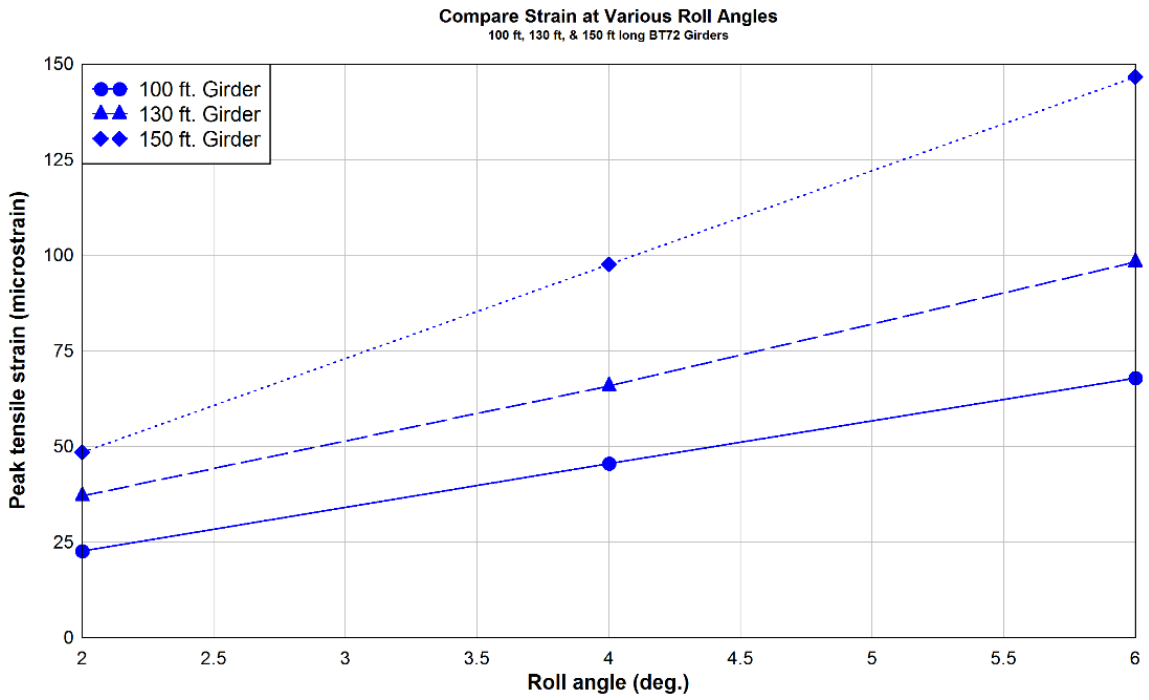

Figure 48
Effect of roll angle at midspan and girder length on peak tensile strains

Variation of Jeep Tongue Lateral Force versus Girder Length

A basic parametric analysis was performed to evaluate the influence of varying tongue force on different length girders. The jeep tongue is approximately 30 ft. from the girder end support. Based on field measurements, as well as prior DOTD research data, it was observed that the tongue force has a significant influence on strain measurements recorded at the tongue location and at midspan. Using the 3D model described above, a lateral load was applied at the bottom of the girder at the jeep tongue support location as shown in Figure 49. Results of the parametric study are shown in Figure 50.

Strains reported are only due to jeep tongue lateral loading and do not take into account stresses associated with prestressing. It can be seen that the girder length has minimal effect on peak tensile strains relative to the increase in tongue lateral force. However, it is

postulated that while the tensile strains from the tongue lateral load are somewhat invariant with girder length, the force will likely increase as the length of the girder increases due to the increased difficulty of maneuvering longer girders.

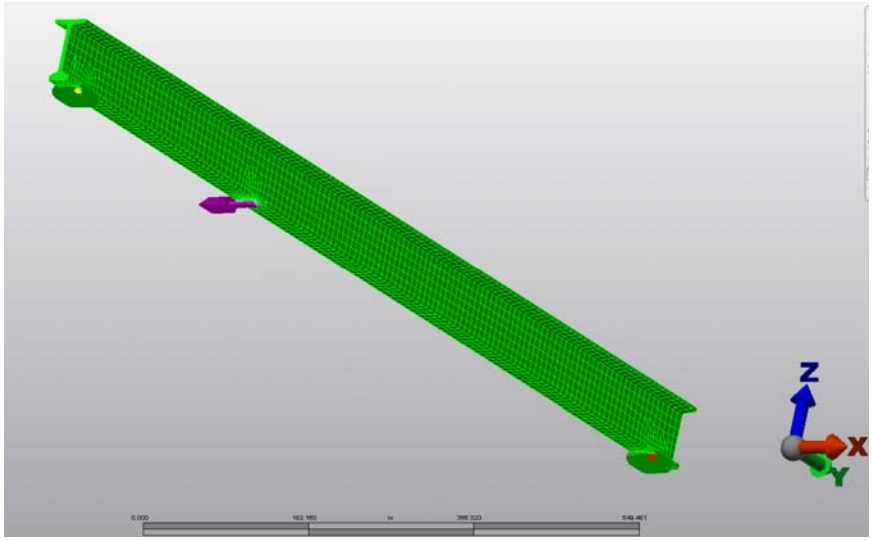

Figure 49
Girder model to examine effect of lateral loading at jeep tongue support

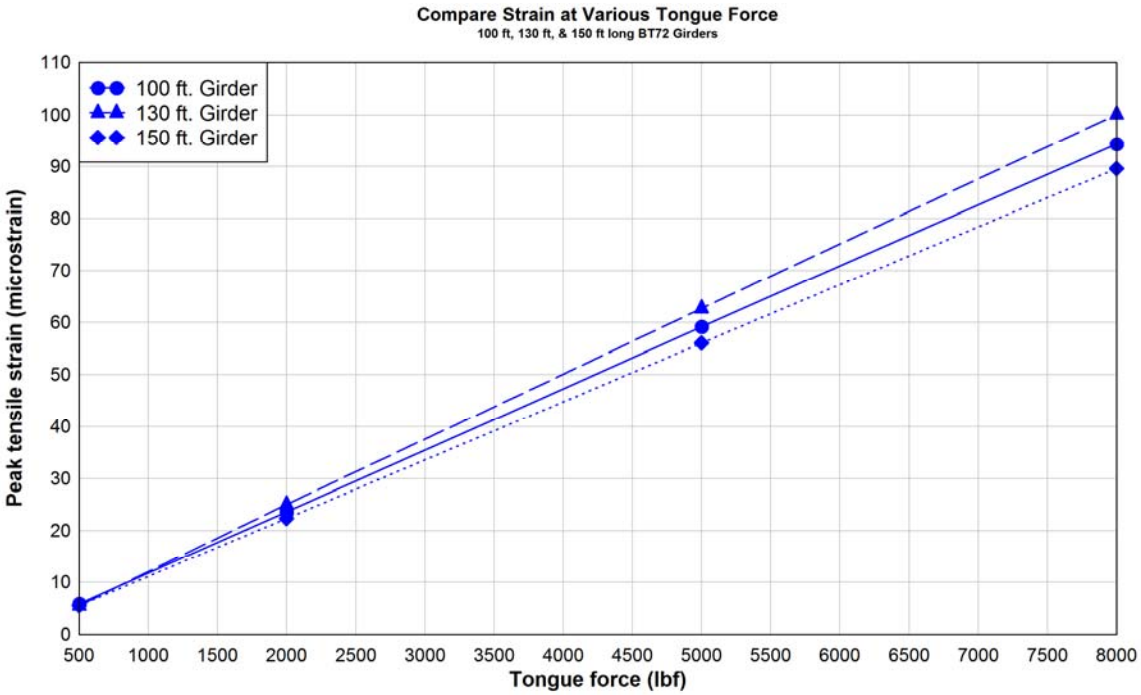

Figure 50
Comparison of tongue force variation on different length girders

Comparison of BT-72 and LG-54 Girders

A model of the 130 ft. long LG-54 girder was developed and compared to the BT-72 girder model. Support distances, restraint modeling, and material properties were kept the same as those specified for the BT-72. The objective of the model was to compare performance under the same loading conditions. Figure 51 shows the comparison of the BT-72 to the LG-54 for roll variation. Figure 51 compares the response of the different girder types with varying roll angle at midspan, while Figure 52 compares the response with varying tongue force.

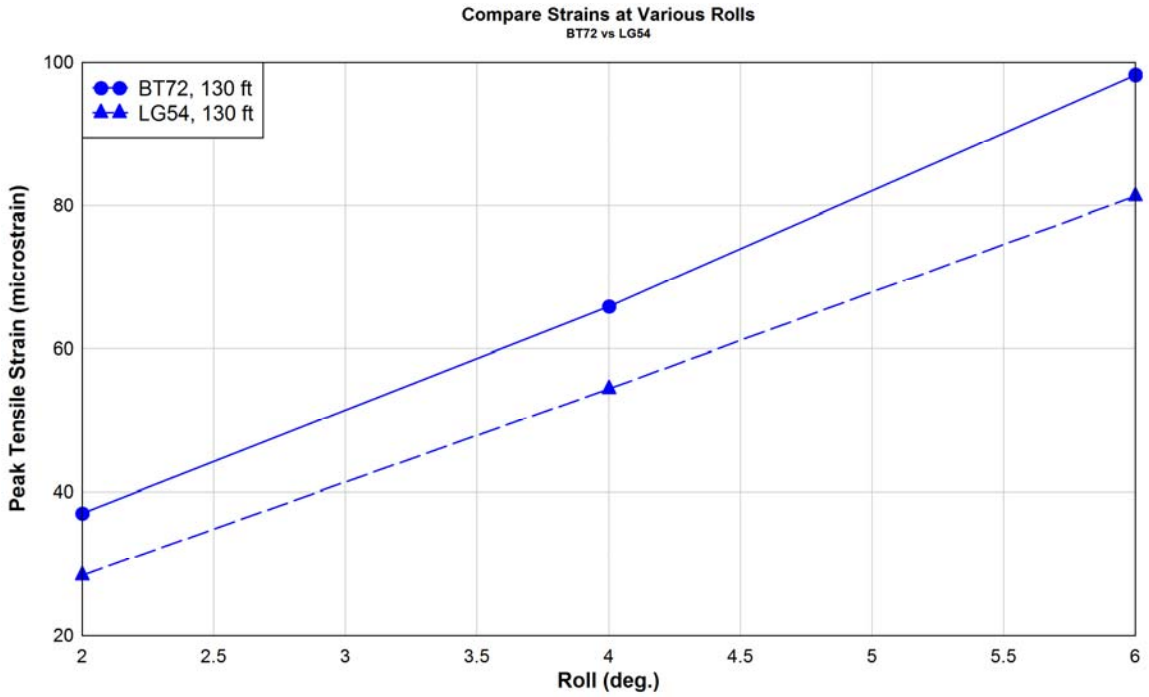

Figure 51
Comparison of roll angle variation on different type girders

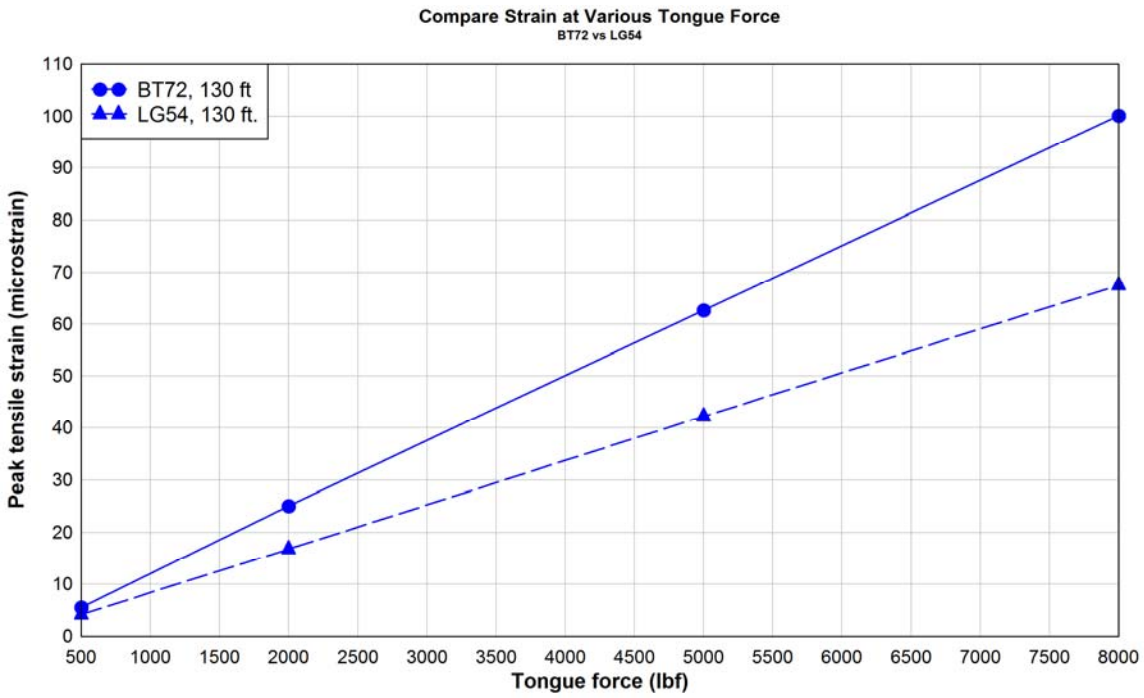

Figure 52
Comparison of variation tongue force on different type girders

Modal Response Analysis of Girders

A modal response analysis of the BT-72 and LG-54 shapes were performed as a part of the finite element study using the 130-ft. models to obtain estimated dominant frequency responses of the girders used in the research. Figure 53 and Figure 54 show the first four modes calculated in the finite element models using a linear analysis modal case with just the two end restraints supporting the girder. Figure 53 and Figure 54 show the BT-72 and LG-54 girders, respectively.

As seen in the figures, the modal response for the first four modes consist of the following modes:

Mode 1: 1st order lateral response mode
Mode 2: 1st order vertical response mode
Mode 3: 2nd order lateral response mode
Mode 4: 1st order torsional response mode

As expected, the modal responses of the BT-72 and LG-54 are quite similar. The differences were that the lateral and torsional modes for the LG-54 were at slightly higher frequencies and the vertical mode was slightly lower than those of the BT-72. As Figure 30 shows,

measured responses were noticeably lower, but seem consistent with expectations given that any flexibility within the trailer support would lead to lower associated frequencies.

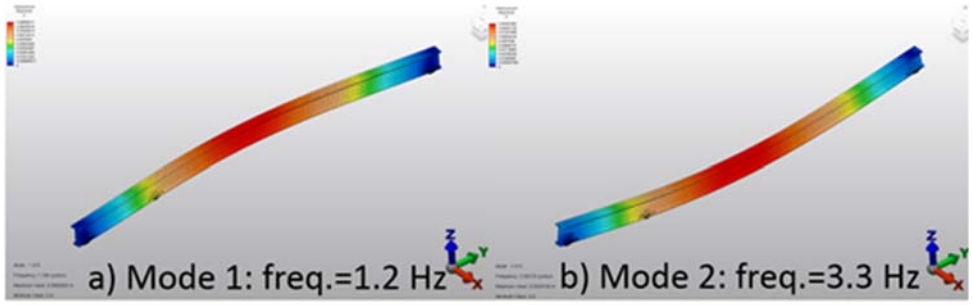

Figure 53
Modal analysis of first four modes of 130-ft. long BT-72

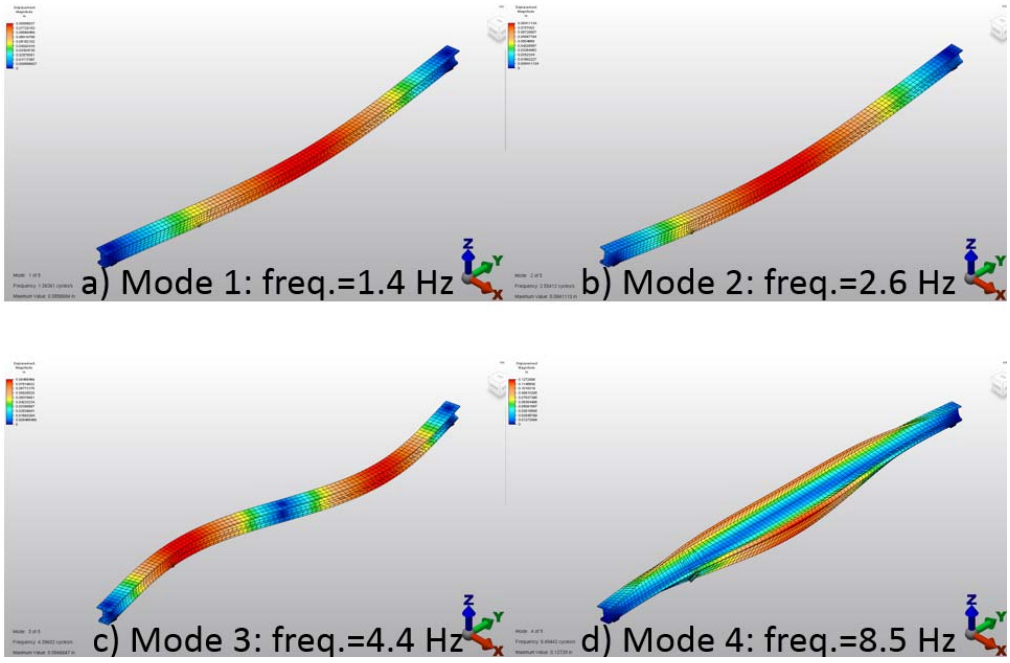

Figure 54
Modal analysis of first four modes of 130-ft. long LG-54

Observations from Finite Element Analyses

1. Peak tensile strains increase with an increase in roll angle at midspan.
2. As the girder length increases, the peak tensile strains associated with a given midspan roll angle increase.
3. Unlike roll angle, peak tensile strains are relatively insensitive to girder length versus the amount of lateral force imposed by the jeep tongue.
4. The jeep tongue force induces high flexure strains at that cross section.
5. The LG-54 with a larger weak axis moment of inertia performs substantially better that the BT-72 with increasing tongue force.

DISCUSSION OF RESULTS

State of Strain

Understanding the state of strain within a girder during transport is the fundamental challenge in the attempt to anticipate where cracks in the girder might occur. Girder strains can be grouped into: a) structurally-related strains due to self-weight and prestressing, as well as load-induced strains, and b) strains related to material properties, including creep, shrinkage and temperature effects. The following equation sums the potential contributors to the state of strain at any point at any girder cross section:

$$\boldsymbol{\varepsilon} = (\boldsymbol{\varepsilon_{SW}} + \boldsymbol{\varepsilon_{PS}} + \boldsymbol{\varepsilon_{ExtLoad}} + \boldsymbol{\varepsilon_{acc}})_{Structural} + \left(\boldsymbol{\varepsilon_{cr}} + \boldsymbol{\varepsilon_{sh}} + \boldsymbol{\varepsilon_{temp}}\right)_{Material} \quad (11)$$

where,
$\boldsymbol{\varepsilon_{SW}}$ is strain due to girder self-weight,
$\boldsymbol{\varepsilon_{PS}}$ is strain due to the internal prestressing of the girder,
$\boldsymbol{\varepsilon_{ExtLoad}}$ is strain due to externally applied loads, such as through a support or tongue,
$\boldsymbol{\varepsilon_{acc}}$ is strain due to inertial acceleration caused by the movement of the girder,
$\boldsymbol{\varepsilon_{cr}}$ is strain from creep,
$\boldsymbol{\varepsilon_{sh}}$ is strain from concrete shrinkage,
$\boldsymbol{\varepsilon_{temp}}$ is strain from temperature change.

Prestressed concrete properties at an early age affect the state of strain in the girder at prestress transfer, while time-dependent properties lead to changes in these strains. To study early age effects, strain measurements were recorded during prestress transfer of Girder 1. These measurements are significantly influenced by the geometrical properties of the girder and the early age concrete modulus of elasticity, such that a higher modulus will yield lower strains for the same stress state.

The time-dependent creep and shrinkage effects in Girder 1 were measured using cylinders collected from the same mix design used in casting the girders. Research has suggested a variety of anticipated creep behavior models, including the AASHTO LRFD Model, CEB-FIP Model, and Benson Model *[21 – 24]*. The laboratory measurements showed good agreement with both the CEB-FIP Model and the Branson creep model.

Although all the above factors contribute to the state of strain at any time, creep and shrinkage strains are generally regarded as autogeneous strains that occur without an accompanying stress unless some form of restraint resists the change. Their effects are manifested in prestress losses, which change the state of strain in the girder. However, the

effect of prestress losses on the top flange strains (strains of interest) in this research can be neglected. Therefore, for the prestressed girders considered in this research, the cause of cracking during transport was attributed to structural strains with the measured and calculated strains at transfer used as the baseline state of strain for Girder 1 and Girder 2, respectively, prior to transport. To determine cracking, measured strains were compared to the cracking strains of 132 to 200 microstrain determined for this research.

Girder Stability

Long span girders are typically designed to maximize bending capacity while minimizing self-weight; therefore, they tend to have a smaller weak-axis moment of inertia. A side effect of this shape design is a tendency of the girder to buckle in a lateral-torsional mode, or tip about its longitudinal or roll axis. This behavior can be caused by applied lateral loads, sweep in the girder due to fabrication, and shifts in lifting locations or support points. The buckling and roll behaviors result in weak axis bending of the girder such that, depending on the amount of lateral deflection, the concrete may crack.

Stability during lifting and transportation of the 130 ft. long BT-72 girder was studied. This girder was chosen because it has a smaller weak-axis moment of inertia when compared to the LG-54 used as Girder 2. Theories developed by Mast to evaluate stability of girders during lifting and during transportation were used. The approach followed is consistent with the PCI Design Handbook 6th edition *[3, 4,* 8*]*.

As discussed in Mast's papers, the main factors contributing to girder stability are the elastic stiffness properties of the girder, initial imperfections, location of lifting points, and properties of the support. The detailed calculations and list of assumptions used to calculate the maximum safe roll angle during lifting and transport of Girder 1 and Girder 2 are shown in Appendix G.

Based on Mast’s approach, the maximum safe roll angle for Girder 1 to avoid cracking is 6.3 degrees and the factor of safety against overturning during lifting and transportation is 2.0, which exceeds the recommended factor of safety by Mast of 1.5. Girder 2 has a higher safe roll angle of 12.5 degrees and factor of safety against overturning during lifting and transportation of 2.3 and 3.6, respectively.

For this study, no girder stability issues were observed during lifting and transporting of both girders. Although the average roll angle across Girder 1 (BT-72) and Girder 2 (LG-54) did not exceed the theoretical cracking roll angle, likely cracking events were observed during transportation of both girders. This measured cracking behavior is attributed to the combined

effect of roll angle and lateral force exerted by the jeep tongue not previously identified in the research.

Transportation Strains

A review of the overall transportation record for each of the test girders, as well as an examination of selected events observed to have produced large strain and/or acceleration readings, found that potential girder cracking events during transport occurred during slow moving turn events. Transportation at highway speeds, across long causeways, or over railroad tracks resulted in minimal concern for cracking or stability during this study.

The highest identified acceleration events shown for Girder 1 (Table 16) and Girder 2 (Table 18) resulted in noticeably lower strains than events selected based on the highest strains. Furthermore, the identified maximum strain events were accompanied by noticeably lower accelerations and high roll angles. In review of photos and time-lapse video, the high strain events were most often due to low-speed (<10 mph) turns at sharp angles or maneuvering of the rear jeep support while the truck was stationary. The latter was particularly obvious in review of the transportation record of Girder 1, Event G1-S2, as shown in Table 17 and Appendix E, where the truck was stationary but the driver adjusted the rear jeep during troubleshooting of a wireless controller problem. This event resulted in some of the highest strains and average roll angle in the entire transportation record for that girder.

The strains for the low-speed turns were also highest at the jeep tongue cross section. This is attributed to the lateral force the tongue exerts on the girders during maneuvering. The effect of the lateral force is clearly shown by comparing the results of the yard turn (events G1-S1 and G2-S1) where the tongue was detached (Figure 55) to a 90 degree turn event (events G1-S3 and G2-S3) where the tongue was attached (Figure 56). While both turns had comparable roll angles, the turn with the tongue attached yielded higher tensile strains, particularly at the tongue location. The finite element and stability analyses further demonstrates the effect of the tongue lateral force.

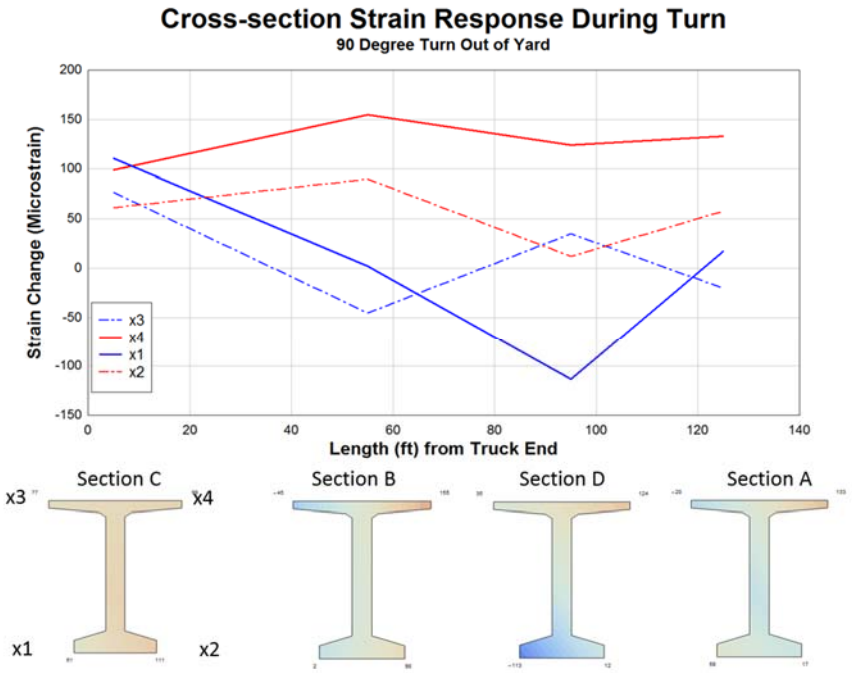

Figure 55
Change in cross section strains during turning event without tongue engaged

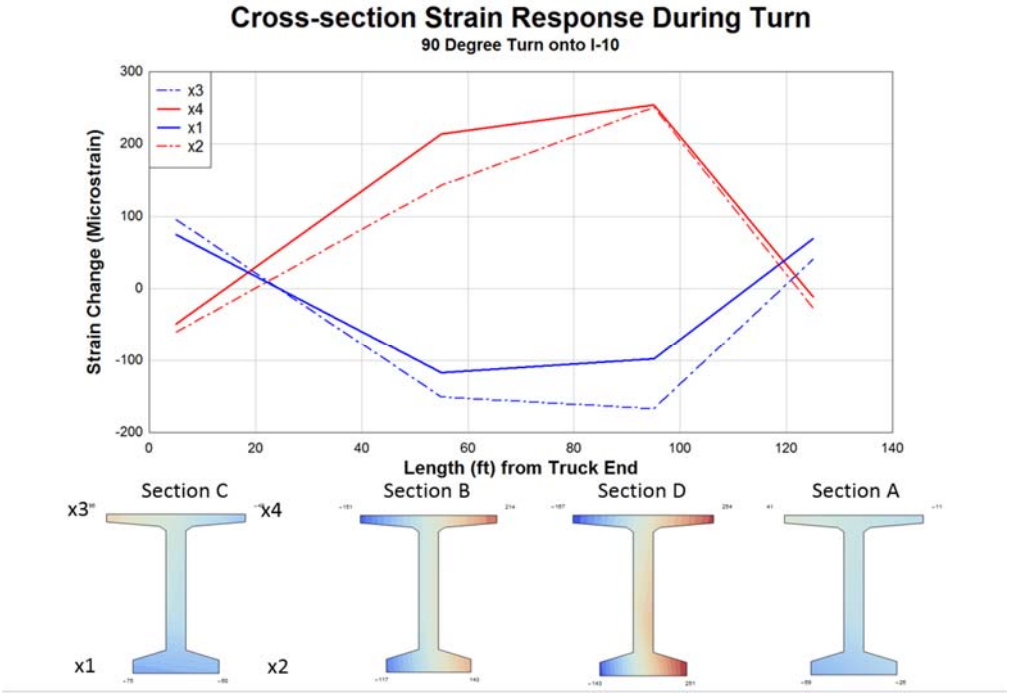

Figure 56
Change in cross section strains during turning event with tongue engaged

Previous girder transport research by DOTD showed similar results for the transportation of two 150 ft. long girders *[6]*. Here again, the highest events noted were at turns, and typically the highest strains were located at or near the jeep tongue. In one of these girders, a significant crack, potentially originating near the jeep tongue cross section, was observed early on during transportation.

Due to the high strains measured at the jeep tongue cross section and because these strains occurred during slow-speed turning events at a roll angle smaller than the theoretical cracking angle, it can be concluded that the operator of the jeep has a strong and unintended influence on the strains the girder will experience during transportation. In both the girders included in this research, as well as review of the prior DOTD research, strains in the girder exceeded likely cracking strains in the top flange during transportation.

The effect of the jeep tongue interaction with the girder has not been documented in previously published literature on this subject. Mast's work, which is highly regarded for girder lifting and transportation, only covers girder supports and classic response to weak-axis bending due to roll effects.

The jeep tongue support has a significant effect on girder strains. Currently, there is lack of data in the literature to help designers account for this loading during transportation. While girders of varying length appear to be relatively insensitive to changes in the jeep lateral force (assuming a constant distance between the jeep tongue and end support), the degree of maneuverability required to navigate a turn is related to girder length. Thus, more maneuvering of the jeep tongue and trailer is required for longer span girders, and this additional maneuvering likely results in larger tongue forces. When this tongue force is combined with the effects of roll from super-elevation, transport of long girders can become susceptible to concrete cracking.

Lifting Strains

The strains measured during yard and site lifts show a change in the behavior of the girders after transportation. As an example, higher strains were recorded during the site lift of Girder 1 when compared to strains measured in the yard lift. This suggests that cracking of the girder occurred sometime during transportation and that the post-cracked behavior was exhibited during the subsequent site lift.

Although cracks were not visually observed at the bridge site, it is still possible that cracks occurred but closed tight after the load that caused the cracks was removed. However, as

concrete is highly nonlinear under tensile strains, the stiffness of the girder at this crack will decrease allowing strains in this region to increase when loaded again.

Girder Properties

The girder design had a significant effect on the measured strains during girder transportation, particularly the weak-axis moment of inertia and the prestressing force and its layout. When comparing the two girders, Girder 1 has a smaller weak-axis moment of inertia, torsional constant, and safe roll angle as compared to Girder 2. This results in Girder 1 having higher roll angle values and higher tensile strains as compared to Girder 2. Considering the yard turn event that occurred in both girders, tensile strains were recorded in two of the four monitored sections (Sections A and C) in Girder 1 while no tensile strains were recorded in Girder 2. This indicates that the LG-54 cross section is more suitable for long girder transport applications than the BT-72 section which, as shown in this study, is more vulnerable to cracking during lifting and transport.

CONCLUSIONS

Prior research has recognized that girder transportation is fundamentally complex. Most of the research in the past has been focused on lifting of long girders, as this is traditionally seen as a more critical event in the life of the girder. This past research often focused on avoiding cracking during lifting of girders. However, based on the results of this research and the prior DOTD research for long-span girders, long girders experienced tensile strains during transportation that likely caused cracking. For the girders in this research, the transportation tensile strains were larger than the lifting strains. This indicates that during the final lift of the girder at the bridge site, cracked section properties should be considered.

Noted findings from this research include the following:

1. Transportation of long girders such as those studied in this research (130 ft. and longer) might lead to tensile strains that exceed the concrete cracking strain.
2. The change in girder behavior between lifts suggests the girders did crack.
3. High strain events in the transportation records of both girders were associated with low-speed (< 10 mph) maneuvers with high roll angle (> 3 deg.) and the presence of a lateral force from the jeep tongue.
4. The most critically loaded girder cross section was at the jeep tongue attachment.
5. Typical roadway conditions encountered during transportation did not necessarily relate to increases in tensile strain levels.
6. The highest recorded strains during the transportation of both girders occurred when the jeep tongue was attached to the girder during sharp turns. This fact emphasizes the importance of the steering system, which is driver controlled. It is noted that there is no feedback to the driver regarding the amount of force applied by the jeep tongue during such turns.
7. Girder shapes with higher prestressing force and lateral stiffness would be expected to be more resistant to cracking during transportation. This is shown in this research where the LG-54 section was judged to have better transportation performance over the BT-72 section based on the strain response from similar events. These parameters would likewise apply to other shapes in determining their relative performance during transportation.
8. Lifting the girders yielded lower tensile strains than the maximum recorded during transportation.

RECOMMENDATIONS

The results of this research study show that cracking and stability of long precast concrete girders (> 100 ft. in length) during transportation can be affected by both the designer and the precaster. The current research has shown that longer girders are at a greater risk for cracking and stability issues during transportation. However, this cracking risk can be mitigated to some extent. Accordingly, the following recommendations are presented:

1. If cracking is to be avoided, consideration must be given to all girder lifting and transportation events from fabrication through erection, with specified procedures in place for each of these events. Such girder-specific procedures could include when to attach and remove the jeep tongue based on travel speed and required turning radii, and prohibitions on moving the jeep when stationary.

2. Installation of force limitors or pressure sensors that either prohibit or warn the jeep operator when lateral forces applied by the jeep tongue against the girder exceed established thresholds.

3. Based on practices in place today, designers should assume that cracking strains would likely be experienced for longer girders in the upper flange at some point during transportation and consider tongue forces in evaluating transportation stresses.

4. Temporary post-tensioning of the top flange to create more compression strain could be a helpful mitigation strategy employed during transportation by bridge designers.

5. Selection by designers of more roll-tolerant girder cross sections that have been developed considering transportation-related strains.

6. Past research has suggested that strains could be reduced and stability of girders being lifted enhanced by moving lifting points inboard of the girder, such that the ends help counter act the weak-axis bending between lifting points. This same methodology could be considered for girder transportation. While there are other considerations for moving the trailer support points, there does appear to be an opportunity to move the rear support inboard of its current location.

Consideration should be given to expanding this research to include the following topics:

1. Measure the forces applied to girders through the jeep tongue using a variety of girder lengths.

2. Work with precasters and evaluate the effectiveness and safety of moving the rear jeep support closer to the girder midspan to reduce maneuvering stresses for long girders.

3. Use the transportation records collected for the test girders, develop a more sophisticated, non-linear model using advanced FEM software to aid in analytically evaluating girder performance.

4. Monitor additional girder transports to evaluate possible limitations on jeep tongue use or incorporation of temporary shipping prestressing installed on the girder top flange.

5. Develop a portable acceleration/roll monitor to be included with girder transport for the purposes of producing a transportation record of the girder for quality assurance purposes.

ACRONYMS, ABBREVIATIONS, AND SYMBOLS

AASHTO	American Association of State Highway and Transportation Officials
BDI	Bridge Diagnostic Inc.
cm	centimeter(s)
DOTD	Louisiana Department of Transportation and Development
FHWA	Federal Highway Administration
ft.	foot (feet)
in.	inch(es)
LTRC	Louisiana Transportation Research Center
lb.	pound(s)
m	meter(s)
PCI	Precast/Prestressed Concrete Institute
MEMS	Micro-electronic machinery
IMU	Inertial Measurement Unit
PCI	Precast/Prestressed Concrete Institute

REFERENCES

1. National Bridge Inventory (NBI). "Tables of Frequently Requested NBI Information: Deficient Bridges by State and Highway System," Federal Highway Administration (FHWA), 2014.

2. Laszlo, G., and Imper, R.R. "Handling and Shipping of Long Span Bridge Beams." PCI Journal 32(6), 1987, pp. 86-101.

3. Mast, R. F. "Lateral stability of long prestressed concrete beams-Part I." *PCI Journal*, 34(1), 1989, pp. 34-53.

4. Mast, R. F. "Lateral Stability of Long Prestressed Concrete Beams-Part II." *PCI Journal* 38(1), 1993, pp. 70-88.

5. Mast, R. F. "Reader Comments - Lateral Stability of Long Prestressed Concrete Beams-Part II." PCI Journal 39(1), 1994, pp. 96-100.

6. BDI. "Monitoring Live Load Forces on 150 Foot Pre-Stressed Bulb-T Girders during Transit and Installation." Final Report, Submitted to Louisiana Department of Transportation and Development (DOTD), 2007, pp. 132.

7. PCI Design Handbook, 6th ed., Precast/Prestressed Concrete Institute, Chicago, IL.

8. American Concrete Institute (ACI 318-14), "Building Code Requirements for Structural Concrete," ACI 318-11, ACI Committee 318, Farmington Hills, MI, 2014, 520 pp.

9. Zureick, A., Kahn, L., Will, K., Kalkan, I., Hurff, J., & Lee, J. H (2009). Stability of Precast Prestressed Concrete Bridge Girders Considering Sweep and Thermal Effects (pp. 1-119). GDOT.

10. Cojocaru, R. "Lifting Analysis of Precast Prestressed Concrete Beams." M.Sc. Thesis, Virginia Polytechnic Institute and State University, 2012, pp. 94.

11. Plaut, R. H., Moen, C. D., and Cojocaru, R. "Beam Deflections and Stresses during Lifting." AISC Engineering Journal, 49(4), 2012.

12. Stratford, T. J., Burgoyne, C. J., and Taylor, H.P.J. "The Stability Design of Long, Precast Concrete Beams." Proceedings of the Institution of Civil Engineers - Structures and Buildings, 119, Part 2, 1999, pp. 159-168.

13. Stratford, T. J., and Burgoyne, C.J. “Lateral Stability of Long Precast Concrete Beams.” Proceedings of the Institution of Civil Engineers - Structures and Buildings. 124, 1999, pp. 169-180.

14. Burgoyne, C. J., and Stratford, T. J. “Lateral Instability of Long-Span Prestressed Concrete Beams on Flexible Bearings." Structural Engineer 79(6), 2001.

15. Weigel, J.A., Seguirant, S.J., Brice, R., and Khaleghi, B. “Impact of High Performance Concrete on WSDOT Prestressed Concrete Girder Bridges: Part I – Pretensioned Girders.” TRB 2003 Annual Meeting CD-ROM. Washington, D.C., Transportation Research Board. 2003.

16. Consolazio, G. R., and Hamilton, H., III. “Lateral Bracing of Long-Span Florida Bulb-Tee Girders,” Structures Research Report, University of Florida Civil and Coastal Engineering, 2007.

17. Hill, C. D., Dick, J. S., and Tadros, M.K. “PCI Advisory on I-Girder Stability during Handling and Construction.” ASPIRE Magazine Online, Winter 2009, pp. 38-40.

18. PCI Bridge Design Manual, 3rd ed., Precast/Prestressed Concrete Institute, Chicago, IL.

19. Bridge Design Manual (LRFD). Washington State Department of Transportation, Bridge and Structures Office, 2011: 23-50.05.

20. PGSuper Overview. Washington State Department of Transportation, Bridge and Structures Office. Retried from URL http://www.wsdot.wa.gov/eesc/bridge/software/index.cfm?fuseaction=software_detail&software_id=47, August 1, 2015.

21. Branson, D.E., Christiason, M.L., “Time Dependent Concrete Properties Related to Design Strength and Elastic Properties, Creep, and Shrinkage,” ACI Special Publication, 27, 1971.

22. American Association of State Highway and Transportation Officials (AASHTO) 2013. AASHTO LRFD Bridge Design Specifications. Washington, D.C.: AASHTO.

23. Comité Euro-International du Béton (CEB) (1993). CEB-FIP Model Code 1990, Thomas Telford, London.

APPENDIX

Appendix A Properties of Girders
Appendix B Instrumentation Plan
Appendix C Transferring Embedded Strains to Surface Strains
Appendix D Estimated Analytical Strains
Appendix E Raw Data Event Plots for Girder 1
Appendix F Raw Data Event Plots for Girder 2
Appendix G Girders Stability Analysis

APPENDIX A. PROPERTIES OF GIRDERS

Table A. 1
Geometric properties of Girder 1: BT72

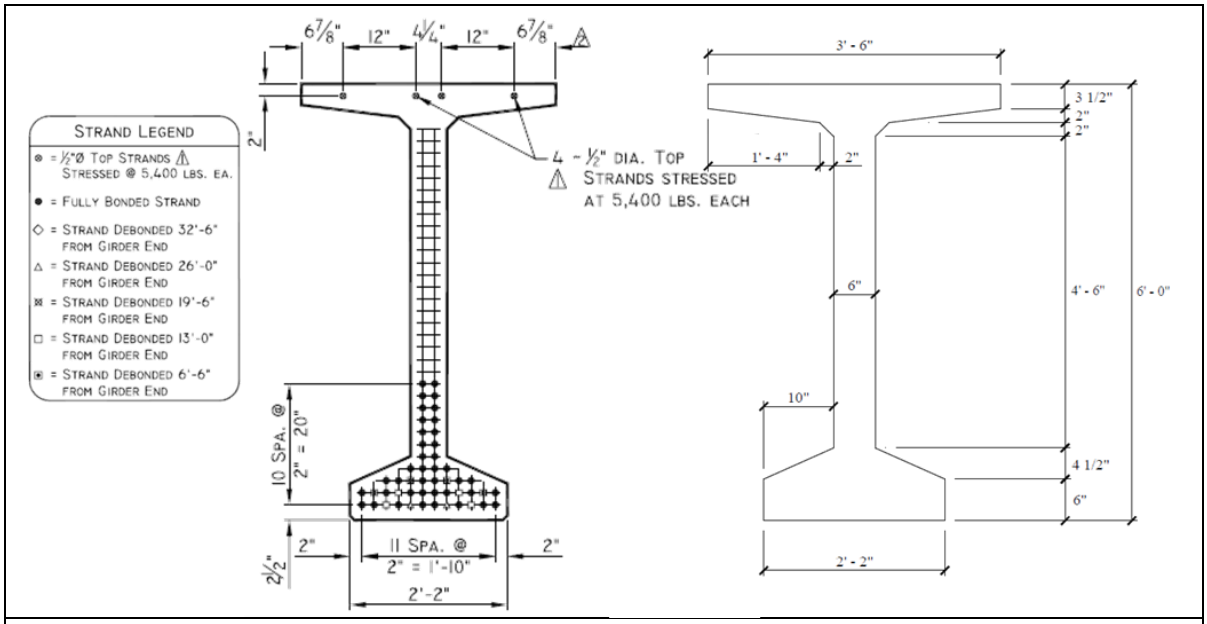

Gross section properties	
Area: Ac = 767 in^2	Center of gravity: CG = 36.6 in
Strong axis moment of inertia: Ix = 545,857 in^4	Weak axis moment of inertia: Iy = 37,634 in^4
Number of strands = 50	Strands per row = [12 12 8 4 2 2 2 2 2 2 2]
Strands diameter = 0.5 in	Area of one strand = 0.153 in^2
Guaranteed ultimate strength = 270 ksi	Modulus of elasticity = 29,000 ksi
Composite section properties at transfer	
Measured compressive strength= 8,170 psi	Measured modulus of elasticity = 5,930 ksi
Modular ratio = 4.9	Composite section area = 796.8 in^2
Midspan	**10 ft from ends**
CG = 35.5 in.	CG = 35.5 in.
Ix = 569,258.6 in^4	Ix = 569,258.6 in^4
Eccentricity of prestress force = 27.4 in.	Eccentricity of prestress force = 27.9 in.
Distance from centroid to bottom strain gage = 33.5 in.	Distance from centroid to bottom strain gage = 33.5 in.
Distance from centroid to top strain gage = 35.0 in.	Distance from centroid to top strain gage = 35.0 in.
Initial Prestress force = 1,549.1 kip	Initial Prestress force = 1,363.2 kip
Prestress losses = 113.7 kip	Prestress losses = 124.9 kip
Effective prestress force = 1,435.4 kip	Effective prestress force = 1,238.3 kip

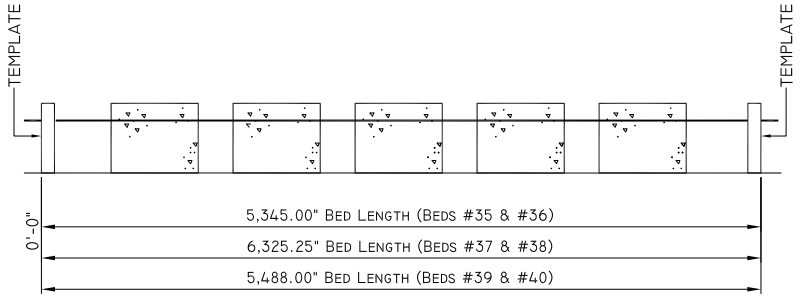

Elevation Diagram of Stressing Bed

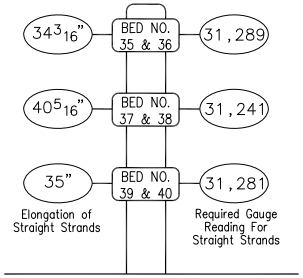

Prestressing of Straight Strands

1. String strands from anchor end to jacking end, occupying holes as shown in the Strand Pattern Elevation.
2. Tension all straight strands to 3,000 lbs. each.
3. Tension straight strands to full load by extending strands the amount shown as elongation.

Prestressing of Draped Strands

1. String Strand as shown in "Elevation of Template" and then pass over (1) hold-up device, under the first pair of hold-down devices and then over (2) hold-up device. Repeat process as required until strand passes over (N) hold-up device where it is then to pass through the template.
2. Tension all strands to 3,000 lbs. each
3. Elongate all strands to the amount shown.

No. Beams In Set Up	N	Drape Sequence
3	④	② ③
4	⑤	② ③ ④
5	⑥	② ③ ④ ⑤
6	⑦	② ③ ④ ⑤ ⑥
7	⑧	② ③ ④ ⑤ ⑥ ⑦

Sample Elongation Calculation

Strand Description:		0.5" dia. 270k Low-Relaxation
Casting Bed Number (Free Standing Form)		37 and 38
Bed length 'L' for straight strands		6325.25 in.
Area 'A' for 0.5" dia. 270k L/R strand		0.153 sq. in.
Modulus of elasticity 'E'		2.88E+007 p.s.i.
Initial tension 'P' 75% ultimate		30,980 lbs.
Initial tension less 3000 lbs.		27,980 lbs.

Elongation of straight strands		Gross	Net	Load (lbs)
elong = PL/AE	'basic'	40.160	40.160 in.	27,980
dead end seating	'des'	.125	.125 in.	0
live end seating	'les'	.375	0 in.	261
abutment movement	'am'	0	0 in.	0
initial pull		____	____	3000
		40.660 in.	40.285 in.	31,241

basic + des + am + bs + dc	40.285 in. (measured)
((basic + les) * (A*E))/L + 3000	31,241 lbs. (gauge reading)

NOTE: Elongation calculation shown is based on nominal strand area and modulus of elasticity. Actual elongation and gauge reading will be based on the actual strand area and modulus of elasticity from mill certificates from actual reels of prestressing strand used. Elongation is to be measured to the closest 1/8th of an inch.

Stress Transfer

1. Tendons shall be detensioned by a slow-heat cutting, using a low-oxygen flame. Heating shall be done with a low-oxygen flame (fairly large) played along the tendon for a minimum of 5". Tendons shall be heated in such a manner that the failure of the first wire in each tendon will occur after the torch has been applied for a minimum of five seconds.
2. The sequence for detensioning the tendons shall be in accordance with the detensioning sequence shown on this sheet which will keep the stresses nearly symmetrical about the axis of the girder.
3. Single strand detensioning shall be done at both ends of the bed and at all spaces between ends of girders simultaneously, unless otherwise directed.
4. Detension only when the concrete has reached the required minimum compressive cylinder strength of F'ci. (See Strand Patterns for Value of F'ci.)

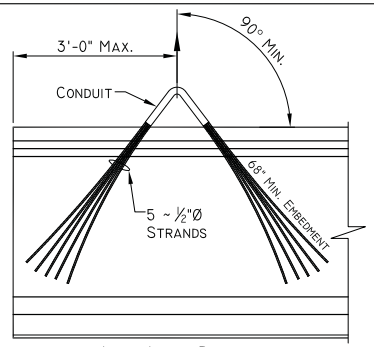

Lift-Loop Detail
For Vertical Lift Only

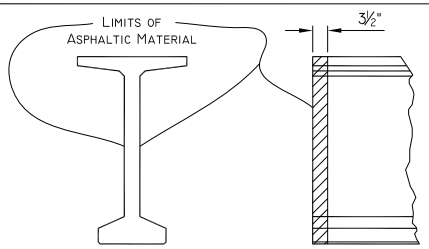

Bondbreaker at Continuity Diaphragm

NOTE:
Apply with a brush, asphaltic material to ends of girders as shown at continuity diaphragms where girders are embedded in concrete. Paint inside face of exterior girders and both sides of interior girders. Asphaltic material to meet ASTM D 1187 and applied according to manufacturer's recommendation.

General Notes

1. See GCP Sheets 9 thru 17 of 18 (Submittal #1) for Elevation of Template & Detensioning Sequence information not shown on this sheet.
2. All plain reinforcement to be as shown on GCP Sheet 18 of 18 (Submittal #1).
3. Steel reinforcement shall conform to ASTM A-615, Grade 60.
4. All strands shall be cut flush at each end of girder. Coat Expansion and Fixed Girder ends with (1) coat of Sika Sikadur 31 Hi-Mod Gel Epoxy Paste Adhesive, or approved equal. Coat continuity girder ends per Bondbreaker Detail this sheet.
5. Modulus of elasticity for ½"Ø 270k L/R Strand equals 2.88 x 10^7.
6. Girder lengths DO NOT include an allowance for elastic shortening.
7. Use ½"Ø 270k L/R strand and stress to 75% ultimate.
8. All girder lengths are measured along the centerline of girder.

Gulf Coast Pre-Stress, Inc. GCP Pass Christian, Miss.
Approved for Fabrication
5/12/2011

Submittal #1

Revision Legend

Mark	Date	Description	By

Gulf Coast Pre-Stress, Inc. GCP Pass Christian, Miss.

Contractor
Jensen Construction Company
Tulsa, Oklahoma

Engineer
State of Louisiana
Department of Transportation & Development

Stressing & Detensioning ~ Red River Bridge (BT-72 Girders)
Fort Buhlow Bridge & Approaches (U.S. 71/U.S. 165)
Rapides Parish, Louisiana
F.A.P. No. 0203(600) S.P. No. 840-43-0001

LDOTD

Job Number:	10-69
Drawing:	1069-StressA1
Sheet Number:	8 of 18
Date:	3/29/2011
Drawn By:	bec
Checked:	bjp

PATTERN P48-0

48 — TOTAL NUMBER OF 0.5" DIA. 270K L/R STRANDS STRESSED AT 30,980 LBS. EACH

0 — TOTAL NUMBER OF DRAPED STRANDS

4 — TOTAL NUMBER OF ½" DIA. TOP STRANDS STRESSED AT 5,400 LBS. EACH ⚠

F'c = 7,500 PSI
F'ci = 6,000 PSI
CLASS "Px"

GULF COAST PRE-STRESS, INC. GCP PASS CHRISTIAN, MISS.
APPROVED FOR FABRICATION
5/12/2011

STRAND LEGEND

- ⊗ = ½"Ø TOP STRANDS ⚠ STRESSED @ 5,400 LBS. EA.
- ● = FULLY BONDED STRAND
- ◇ = STRAND DEBONDED 32'-6" FROM GIRDER END
- △ = STRAND DEBONDED 26'-0" FROM GIRDER END
- ⊠ = STRAND DEBONDED 19'-6" FROM GIRDER END
- □ = STRAND DEBONDED 13'-0" FROM GIRDER END
- ⊡ = STRAND DEBONDED 6'-6" FROM GIRDER END

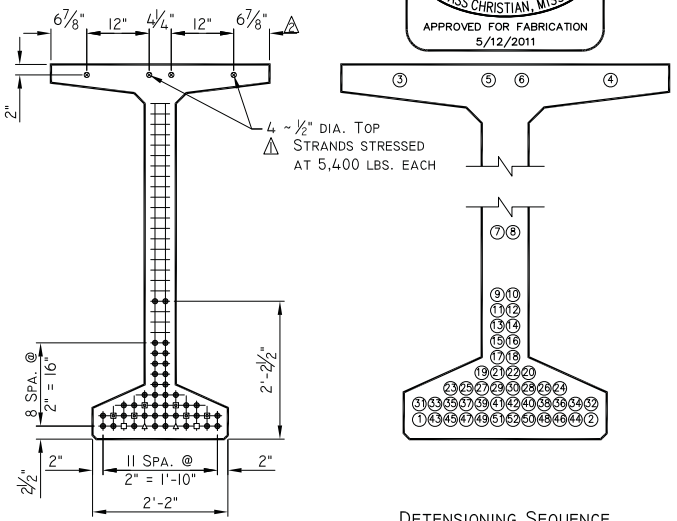

PATTERN P48-0

DETENSIONING SEQUENCE
PATTERN P48-0

PATTERN P50-0

50 — TOTAL NUMBER OF 0.5" DIA. 270K L/R STRANDS STRESSED AT 30,980 LBS. EACH

0 — TOTAL NUMBER OF DRAPED STRANDS

4 — TOTAL NUMBER OF ½" DIA. TOP STRANDS STRESSED AT 5,400 LBS. EACH ⚠

F'c = 7,500 PSI
F'ci = 6,000 PSI
CLASS "Px"

STRAND LEGEND

- ⊗ = ½"Ø TOP STRANDS ⚠ STRESSED @ 5,400 LBS. EA.
- ● = FULLY BONDED STRAND
- ◇ = STRAND DEBONDED 32'-6" FROM GIRDER END
- △ = STRAND DEBONDED 26'-0" FROM GIRDER END
- ⊠ = STRAND DEBONDED 19'-6" FROM GIRDER END
- □ = STRAND DEBONDED 13'-0" FROM GIRDER END
- ⊡ = STRAND DEBONDED 6'-6" FROM GIRDER END

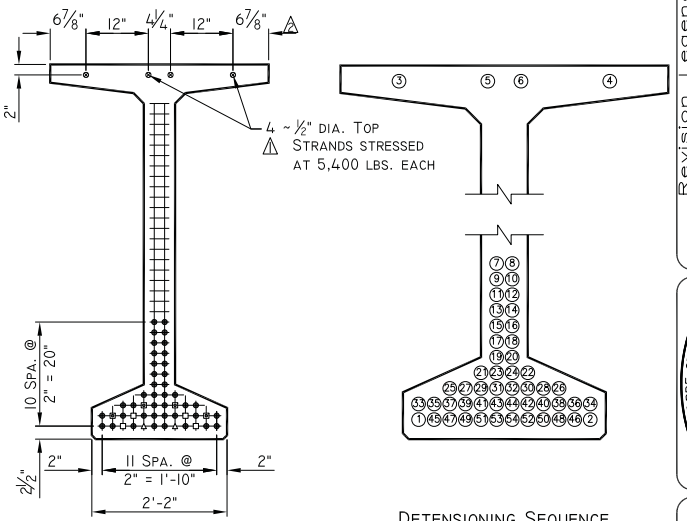

PATTERN P50-0

DETENSIONING SEQUENCE
PATTERN P50-0

Revision Legend			
Mark	Date	Description	By
⚠	5/9/11	adj. top strand diameter	bc
⚠	5/11/11	adj. top strand dim.	bc

GULF COAST PRE-STRESS, INC. GCP PASS CHRISTIAN, MISS.

Contractor
Jensen Construction Company
Tulsa, Oklahoma

Engineer
State of Louisiana
Department of Transportation & Development

Stressing & Detensioning ~ Red River Bridge (BT-72 Girders)
Fort Buhlow Bridge & Approaches (U.S. 71/U.S. 165)
Rapides Parish, Louisiana
F.A.P. No. 0203(600) S.P. No. 840-43-0001

LDOTD

Job Number: 10-69
Drawing: 1069-StressA10
Sheet Number: 17 of 18
Date: 3/29/2011
Drawn By: bec
Checked: bjp

SUBMITTAL #1

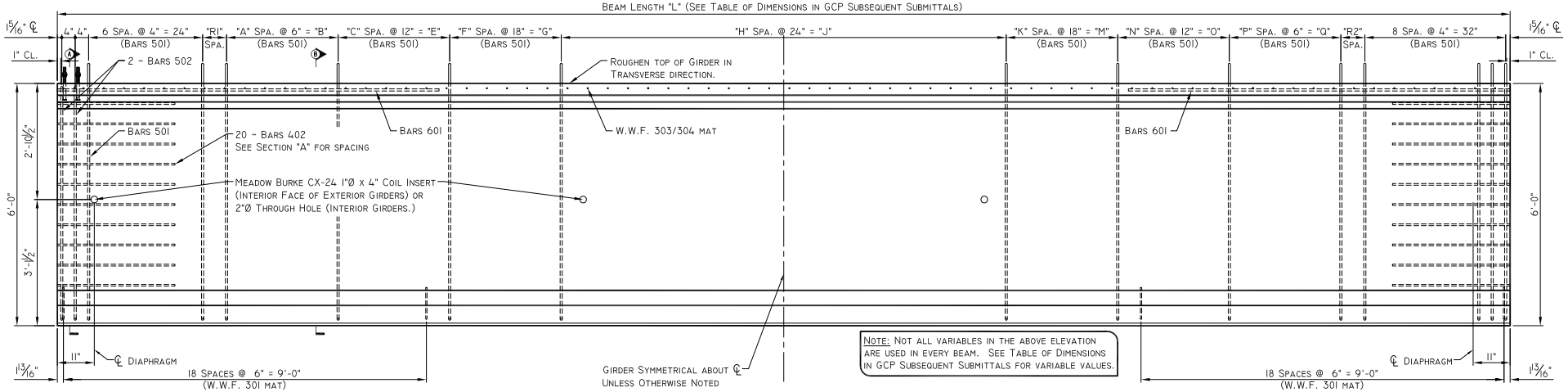

SHOWING FIXED & EXPANSION ENDS

REINFORCING LAYOUT ~ ELEVATION VIEW
BT-72 GIRDERS ~ SHOWING FIXED, EXPANSION & CONTINUITY ENDS
NTS

SHOWING CONTINUITY ENDS

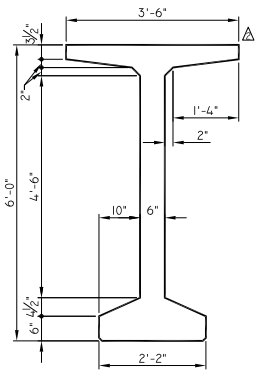

BT-72 GIRDER

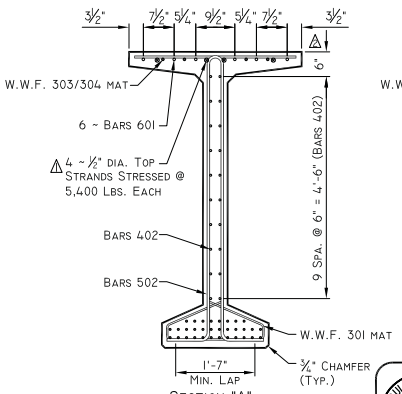

SECTION "A"

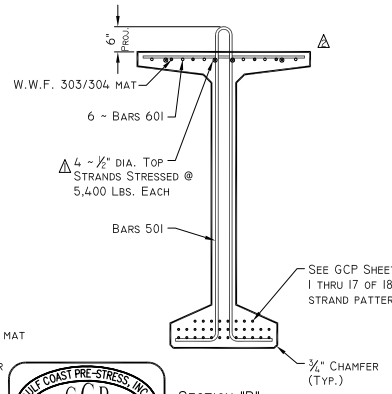

SECTION "B"

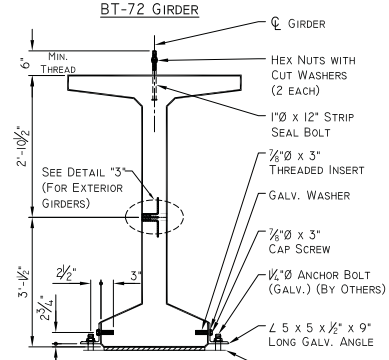

TYPICAL GIRDER END VIEW

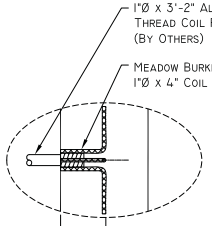

DETAIL "3"
SHOWING END DIAPHRAGM
INTERIOR FACE OF EXTERIOR GIRDERS

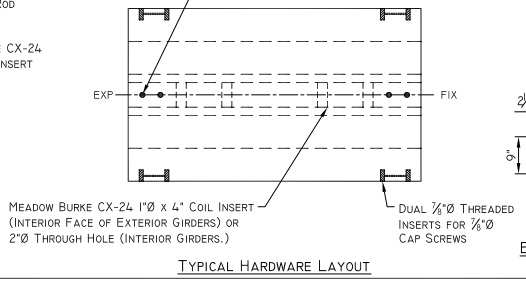

TYPICAL HARDWARE LAYOUT

* VARIES: SEE MISCELLANEOUS BEAM DETAILS SHEETS IN SUBMITTAL #2 FOR SKEWED END DETAILS

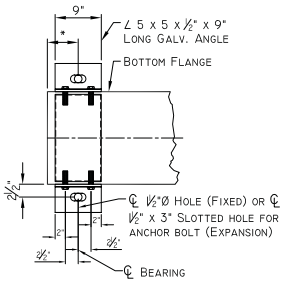

*PART PLAN @ END OF GIRDER
SHOWING BEARING ANCHOR DETAILS

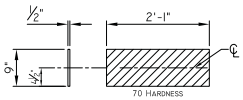

FIXED BEARING PAD, MARK P7
216 ~ REQUIRED

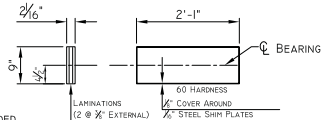

EXPANSION BEARING PAD, MARK L7
216 ~ REQUIRED

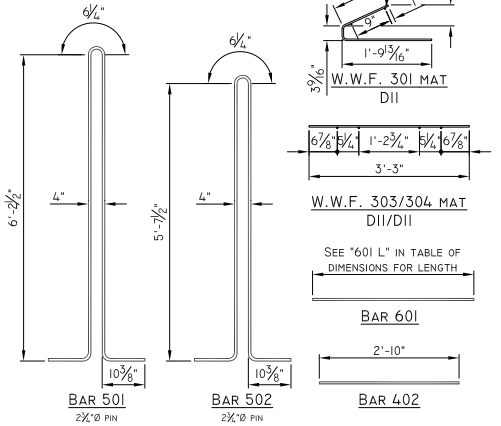

NOTES:

FABRICATION TOLERANCES, STRESSING, AND DETENSIONING OF THE GIRDERS SHALL BE AS SPECIFIED IN THE "MANUAL FOR QUALITY CONTROL FOR PLANTS AND PRODUCTION OF PRECAST-PRESTRESSED CONCRETE PRODUCTS (MNL-116 LATEST EDITION)" PUBLISHED BY PCI.

PRE-STRESSING STEEL SHALL BE ½" NOMINAL DIAMETER, UNCOATED, SEVEN-WIRE STRAND, GRADE 270k, CONFORMING TO ASTM DESIGNATION A-416. THE STRANDS SHALL BE LOW-RELAXATION WITH AN INITIAL APPLIED FORCE OF 31,000 LBS.

CONCRETE USED IN THE GIRDERS SHALL BE CLASS "P", "PM" OR "PX" (SEE TABLE OF DIMENSIONS IN GCP SUBMITTAL #2 - BASED ON RESPECTIVE STRAND PATTERNS).

PRE-STRESSED GIRDERS SHALL BE MAINTAINED IN AN UPRIGHT POSITION AT ALL TIMES DURING STORAGE AND HANDLING AND MUST BE SUPPORTED FROM POINTS WITHIN 3 FEET FROM GIRDER ENDS. DISREGARD OF THIS MAY LEAD TO COLLAPSE OF THE MEMBER.

STEEL REINFORCEMENT GIRDERS SHALL CONFORM TO ASTM DESIGNATION A-615, GRADE 60. DIMENSIONS SHOWN ON REINFORCING BAR DETAILS ARE OUT-TO-OUT OF BAR. REINFORCING STEEL SHALL BE FABRICATE TO CLOSE DIMENSIONAL TOLERANCES TO PROVIDE 1 INCH MINIMUM CLEARANCE FROM EDGE OF BAR TO FACE OF GIRDER.

APPROVED FOR FABRICATION
5/12/2011

Revision Legend

Mark	Date	Description	By
1	5/9/11	adj. top strand diameter	bc
2	5/11/11	adj. bars in top flange	bc

GULF COAST PRE-STRESS, INC. GCP PASS CHRISTIAN, MISS.

Contractor
Jensen Construction Company
Tulsa, Oklahoma

Engineer
State of Louisiana
Department of Transportation & Development

Beam Details ~ Red River Bridge (BT-72 Girders)
Fort Buhlow Bridge & Approaches (U.S. 71/U.S. 165)
Rapides Parish, Louisiana
F.A.P. No. 0203(600) S.P. No. 840-43-0001

LDOTD

Job Number: 10-69
Drawing: 1069-Beam2
Sheet Number: 18a of 18
Date: 3/29/2011
Drawn By: bec
Checked: bjp

Table of Dimensions ~ BT-72 Girders

Span	Beam Mark	Length	Strand Pattern	Diaphragm		Diaphragm Skew		Stirrup Spacing														Threaded Inserts				Skew		Blockout		601 "L"	Detail
				"D1"	"D2"	"X1"	"X2"	"R1"	"A"	"B"	"C"	"E"	"F"	"G"	"H"	"J"	"K"	"M"	"N"	"O"	"P"	"Q"	"R2"	"H1"	"H2"	"H3"	"H4"	"S1"	"S2"	"T1"	"T2"		
Span AS4	AS4-A	129'-10 3/16"	P50-0	43'-2 5/8"	86'-8 1/4"	-	-	8 1/8"	-	-	2	2'-0"	1	1'-6"	58	116'-0"	1	1'-6"	2	2'-0"	-	-	8 1/8"	-	-	-	-	-	-	-	-	28'-0"	23
	AS4-B	129'-10"	P38B-0	43'-2 5/16"	86'-7 1/16"	-	-	7 1/16"	-	-	2	2'-0"	1	1'-6"	58	116'-0"	1	1'-6"	2	2'-0"	-	-	7 1/16"	-	-	-	-	-	-	-	-	28'-0"	24
	AS4-C	129'-9 3/16"	P38B-0	43'-2 1/16"	86'-7 1/16"	-	-	7 1/4"	-	-	2	2'-0"	1	1'-6"	58	116'-0"	1	1'-6"	2	2'-0"	-	-	7 1/4"	-	-	-	-	-	-	-	-	28'-0"	24
	AS4-D	129'-8 3/8"	P38B-0	43'-1 13/16"	86'-6 15/16"	-	-	6 7/16"	-	-	2	2'-0"	1	1'-6"	58	116'-0"	1	1'-6"	2	2'-0"	-	-	6 7/16"	-	-	-	-	-	-	-	-	28'-0"	24
	AS4-E	129'-7 1/16"	P38B-0	43'-1 1/16"	86'-6 1/16"	-	-	6 1/2"	-	-	2	2'-0"	1	1'-6"	58	116'-0"	1	1'-6"	2	2'-0"	-	-	6 1/2"	-	-	-	-	-	-	-	-	28'-0"	24
	AS4-F	129'-6 3/4"	P50-0	43'-1 1/4"	86'-5 1/2"	-	-	6 1/16"	-	-	2	2'-0"	1	1'-6"	58	116'-0"	1	1'-6"	2	2'-0"	-	-	6 1/16"	-	-	-	-	-	-	-	-	28'-0"	25
Span AS5	AS5-A	65'-10 13/16"	P16-0	39'-4"	-	-	2 3/16"	8 1/8"	-	-	2	2'-0"	1	1'-6"	26	52'-0"	1	1'-6"	2	2'-0"	-	-	8 1/8"	-	-	7 1/4"	9 1/16"	-	9 7/16"	-	2 5/16"	22'-0"	26
	AS5-B	69'-1 3/16"	P16-0	39'-4 1/16"	-	-	2 3/16"	9 5/16"	-	-	2	2'-0"	-	-	29	58'-0"	-	-	2	2'-0"	-	-	9 5/16"	-	-	7 1/4"	9 1/16"	-	9 7/16"	-	2 5/16"	23'-0"	27
	AS5-C	72'-3 1/2"	P16-0	39'-4 1/8"	-	-	2 3/16"	4 7/16"	-	-	3	3'-0"	-	-	30	60'-0"	-	-	3	3'-0"	-	-	4 7/16"	-	-	7 1/4"	9 1/16"	-	9 7/16"	-	2 5/16"	24'-0"	27
Span AS7	AS7-A	110'-10 13/16"	P38B-0	41'-0 3/4"	76'-1 5/16"	2 1/8"	-	5 1/8"	-	-	3	3'-0"	-	-	43	86'-0"	3	4'-6"	7	7'-0"	8	4'-0"	5 1/8"	7 1/4"	8 5/16"	-	-	9 1/8"	-	2 1/8"	-	35'-0"	28
	AS7-B	107'-9 1/8"	P30A-0	37'-1 1/16"	72'-11 9/16"	2 1/8"	-	4 1/4"	-	-	3	3'-0"	-	-	41	82'-0"	3	4'-6"	8	8'-0"	8	4'-0"	4 1/4"	7 1/4"	9"	-	-	9 3/16"	-	2 1/8"	-	34'-0"	29
	AS7-C	104-7 1/8"	P30A-0	34'-9 3/8"	69'-9 7/16"	2 1/8"	-	3 3/8"	-	-	3	3'-0"	-	-	40	80'-0"	3	4'-6"	7	7'-0"	8	4'-0"	3 3/8"	7 1/4"	9"	-	-	9 1/4"	-	2 1/8"	-	33'-0"	29
	AS7-D	101'-5 1/16"	P30A-0	31'-7 1/16"	66'-8 5/16"	2 5/16"	-	5 1/2"	-	-	3	3'-0"	-	-	38	76'-0"	3	4'-6"	7	7'-0"	9	4'-6"	5 1/2"	7 1/4"	9"	-	-	9 3/8"	-	2 5/16"	-	32'-0"	29
	AS7-E	98'-3 15/16"	P30A-0	28'-6"	63'-6 1/2"	2 5/16"	-	4 1/16"	-	-	3	3'-0"	-	-	37	74'-0"	2	3'-0"	8	8'-0"	8	4'-0"	4 1/16"	7 1/4"	9 1/16"	-	-	9 1/16"	-	2 5/16"	-	31'-0"	30
Span AS8	AS8-A	119'-7 7/16"	P46-0	39'-9 1/2"	79'-10 1/16"	-	-	3 1/2"	9	4'-6"	4	4'-0"	-	-	51	102'-0"	-	-	3	3'-0"	-	-	3 1/2"	-	-	-	-	-	-	-	-	26'-0"	18
	AS8-B	119'-7 1/4"	P40-0	39'-9 7/16"	79'-9 15/16"	-	-	3 5/16"	11	5'-6"	3	3'-0"	-	-	51	102'-0"	-	-	3	3'-0"	-	-	3 5/16"	-	-	-	-	-	-	-	-	26'-0"	19
	AS8-C	119'-7"	P40-0	39'-9 3/8"	79'-9 1/16"	-	-	3 3/16"	11	5'-6"	3	3'-0"	-	-	51	102'-0"	-	-	3	3'-0"	-	-	3 3/16"	-	-	-	-	-	-	-	-	26'-0"	19
	AS8-D	119'-6 15/16"	P40-0	39'-9 5/16"	79'-9 5/8"	-	-	3 1/8"	11	5'-6"	3	3'-0"	-	-	51	102'-0"	-	-	3	3'-0"	-	-	3 1/8"	-	-	-	-	-	-	-	-	26'-0"	19
	AS8-E	119'-6 7/8"	P46-0	39'-9 5/16"	79'-9 9/16"	-	-	3 1/8"	11	5'-6"	3	3'-0"	-	-	51	102'-0"	-	-	3	3'-0"	-	-	3 1/8"	-	-	-	-	-	-	-	-	26'-0"	20
Span AS9	AS9-A	120'-1 1/16"	P44-0	39'-11 1/2"	80'-2 1/16"	-	-	9 1/16"	-	-	2	2'-0"	1	1'-6"	53	106'-0"	1	1'-6"	2	2'-0"	-	-	9 1/16"	-	-	-	-	-	-	-	-	26'-0"	8
	AS9-B	120'-0 3/8"	P34B-0	39'-11 1/8"	80'-1/4"	-	-	8 1/8"	-	-	2	2'-0"	1	1'-6"	53	106'-0"	1	1'-6"	2	2'-0"	-	-	8 1/8"	-	-	-	-	-	-	-	-	26'-0"	9
	AS9-C	119'-11 5/16"	P34B-0	39'-10 3/4"	80'-0 9/16"	-	-	8 5/16"	-	-	2	2'-0"	1	1'-6"	53	106'-0"	1	1'-6"	2	2'-0"	-	-	8 5/16"	-	-	-	-	-	-	-	-	26'-0"	9
	AS9-D	119'-10 5/16"	P34B-0	39'-10 7/16"	79'-11 7/8"	-	-	7 1/8"	-	-	2	2'-0"	1	1'-6"	53	106'-0"	1	1'-6"	2	2'-0"	-	-	7 1/8"	-	-	-	-	-	-	-	-	26'-0"	9
	AS9-E	119'-9 1/2"	P38C-0	39'-10 3/16"	79'-11 5/16"	-	-	7 1/16"	-	-	2	2'-0"	1	1'-6"	53	106'-0"	1	1'-6"	2	2'-0"	-	-	7 1/16"	-	-	-	-	-	-	-	-	26'-0"	9
	AS9-F	119'-8 3/4"	P38C-0	39'-9 5/16"	79'-10 7/8"	-	-	7 1/16"	-	-	2	2'-0"	1	1'-6"	53	106'-0"	1	1'-6"	2	2'-0"	-	-	7 1/16"	-	-	-	-	-	-	-	-	26'-0"	9
	AS9-G	119'-8 1/16"	P38C-0	39'-9 1/16"	79'-10 1/16"	-	-	6 3/4"	-	-	2	2'-0"	1	1'-6"	53	106'-0"	1	1'-6"	2	2'-0"	-	-	6 3/4"	-	-	-	-	-	-	-	-	26'-0"	9
	AS9-H	119'-7 5/16"	P34B-0	39'-9 1/16"	79'-10 1/16"	-	-	6 1/2"	-	-	2	2'-0"	1	1'-6"	53	106'-0"	1	1'-6"	2	2'-0"	-	-	6 1/2"	-	-	-	-	-	-	-	-	26'-0"	9
	AS9-I	119'-7 1/4"	P34B-0	39'-9 1/16"	79'-9 13/16"	-	-	6 5/16"	-	-	2	2'-0"	1	1'-6"	53	106'-0"	1	1'-6"	2	2'-0"	-	-	6 5/16"	-	-	-	-	-	-	-	-	26'-0"	9
	AS9-J	119'-6 15/16"	P34B-0	39'-9 5/16"	79'-9 5/8"	-	-	6 1/8"	-	-	2	2'-0"	1	1'-6"	53	106'-0"	1	1'-6"	2	2'-0"	-	-	6 1/8"	-	-	-	-	-	-	-	-	26'-0"	9
	AS9-K	119'-6 3/4"	P34B-0	39'-9 1/4"	79'-9 1/2"	-	-	6 1/16"	-	-	2	2'-0"	1	1'-6"	53	106'-0"	1	1'-6"	2	2'-0"	-	-	6 1/16"	-	-	-	-	-	-	-	-	26'-0"	9
	AS9-L	119'-6 1/16"	P44-0	39'-9 1/4"	79'-9 7/16"	-	-	6 1/16"	-	-	2	2'-0"	1	1'-6"	53	106'-0"	1	1'-6"	2	2'-0"	-	-	6 1/16"	-	-	-	-	-	-	-	-	26'-0"	10

Notes:

1. See GCP Sheets 8 thru 17 of 18 (Submittal #1) for Elevation of Stressing Bed and Detensioning Layout.
2. See GCP Sheets 3 thru 7 of 7 (Submittal #3) for Beam Details not shown on this sheet.
3. See GCP Sheets 18 & 18A of 18 (Submittal #1) for all plain reinforcement.
4. The Beam Mark End of the Girder is the Down Station End.
5. All Girder lengths are measured down the centerline.
6. Girder lengths DO NOT include an allowance for elastic shortening.

Gulf Coast Pre-Stress, Inc. GCP Pass Christian, Miss.
Approved for Fabrication
6/21/2011

Submittal #3

Revision Legend

Mark	Date	Description	By

Gulf Coast Pre-Stress, Inc. GCP Pass Christian, Miss.

Contractor
Jensen Construction Company
Tulsa, Oklahoma

Engineer
State of Louisiana
Department of Transportation & Development

Table of Dimensions ~ Red River Bridge (BT-72 Girders)
Fort Buhlow Bridge & Approaches (U.S. 71/U.S. 165)
Rapides Parish, Louisiana
F.A.P. No. 0203(600) S.P. No. 840-43-0001

LDOTD

Job Number: 10-69
Drawing: 1069-Table1
Sheet Number: 1 of 7
Date: 5/25/2011
Drawn By: bec
Checked: bjp

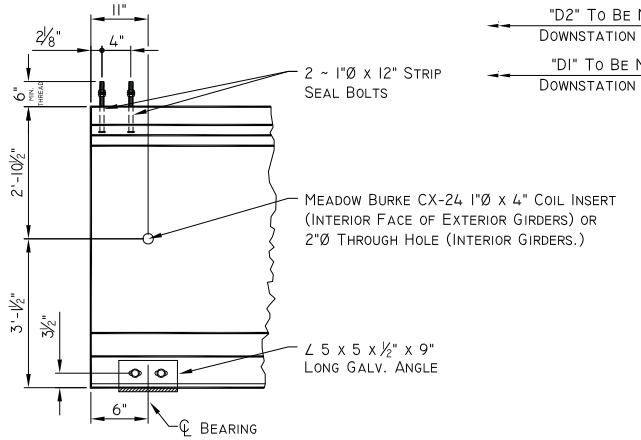

*End Elevation at Expansion & Fixed Bents for squared ends

*Note:
Above detail is for beams with a square end. For beams with a skewed end, use "End Skew Detail" and see Table of Dimensions for all variables
(i.e. Diaphragm Skews, Threaded Inserts & Sn Dimensions).

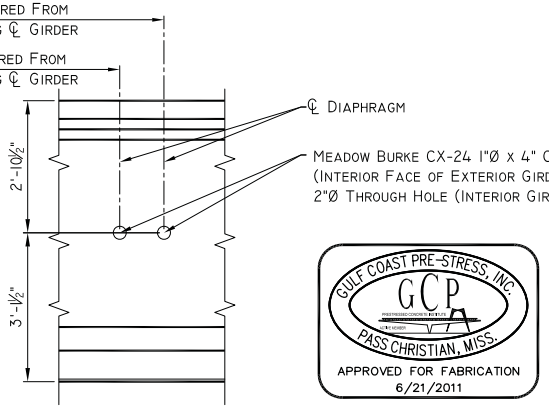

Mid Diaphragm Elevation Detail
BT-72 Girders

GULF COAST PRE-STRESS, INC. GCP PASS CHRISTIAN, MISS.
APPROVED FOR FABRICATION
6/21/2011

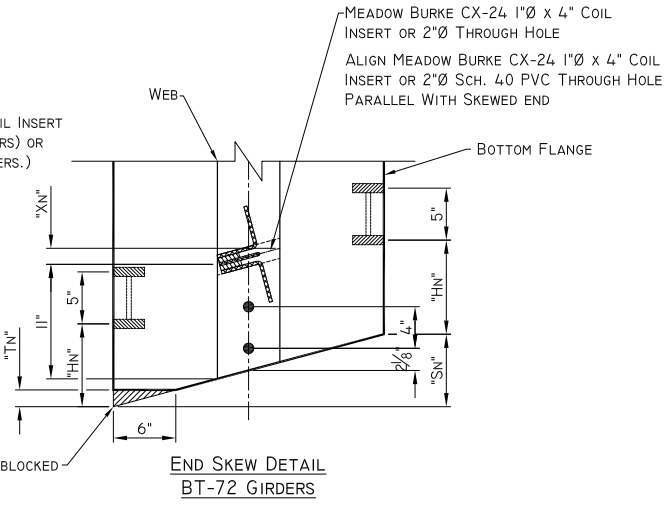

Hatched area to be blocked out with styrofoam
(Typical both ends)

End Skew Detail
BT-72 Girders

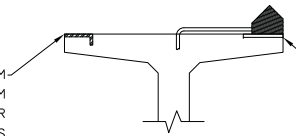

10 Gage Stay-In-Place Metal Form Clips 2" x 4" x 2" offset 6" from end then 12" O.C. thereafter (Interior Side Of Exterior Girders & Both Sides of Interior Girders.) (Supplied by Clearspan)

Dayton Superior C-24, Type 4-APR with bearing plate 45° Half-Hangers or Equal (S.W.L. = 6,000 lbs.) offset 12" from the Girder end then 36" O.C. Thereafter. (Exterior Side Of Exterior Girders.) (Supplied by Contractor)

Elevation of Top Flange
BT-72 Girders

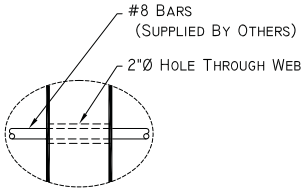

Diaphragm Through Hole Detail
Interior Girders

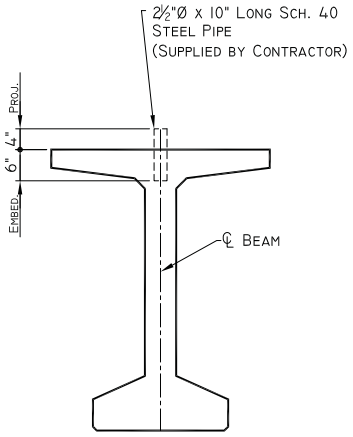

Typical Section

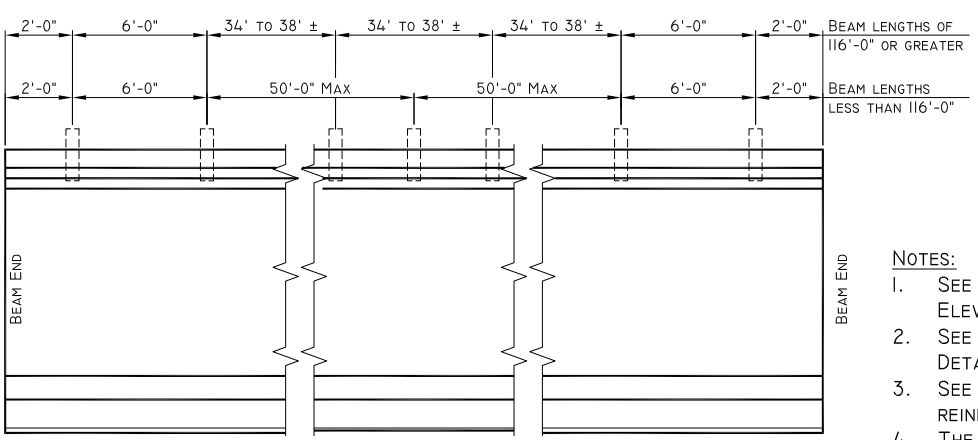

Safety Post Layout Detail ~ Elevation View
BT-72 Girders

Notes:
1. See GCP Sheets 8 thru 17 of 18 (Submittal #1) for Elevation of Stressing Bed and Detensioning Layout.
2. See GCP Sheets 4 thru 7 of 7 (Submittal #3) for Beam Details not shown on this Sheet.
3. See GCP Sheets 18 & 18A of 18 (Submittal #1) for all plain reinforcement.
4. The Beam Mark End of the Girder is the Down Station End.
5. All Girder lengths are measured down the centerline.
6. Girder lengths DO NOT include an allowance for elastic shortening.

Submittal #3

Revision Legend

Mark	Date	Description	By

GULF COAST PRE-STRESS, INC. GCP PASS CHRISTIAN, MISS.

Contractor
Jensen Construction Company
Tulsa, Oklahoma

Engineer
State of Louisiana
Department of Transportation & Development

Miscellaneous Beam Details ~ Red River Bridge (BT-72 Girders)
Fort Buhlow Bridge & Approaches (U.S. 71/U.S. 165)
Rapides Parish, Louisiana
F.A.P. No. 0203(600) S.P. No. 840-43-0001

LDOTD

Job Number:	10-69
Drawing:	1069-Detail1
Sheet Number:	3 of 7
Date:	5/25/2011
Drawn By:	bec
Checked:	bjp

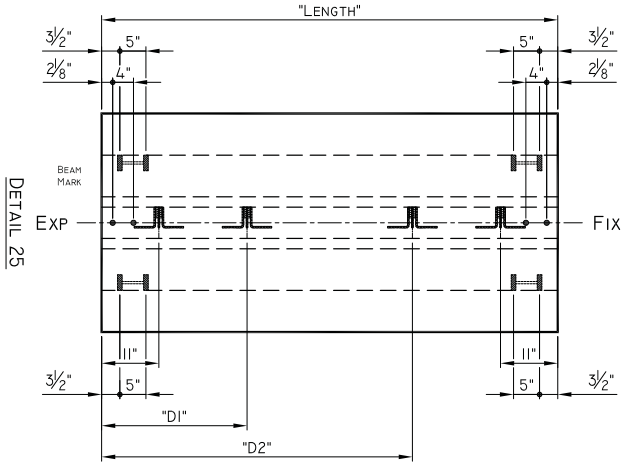

DETAIL 25

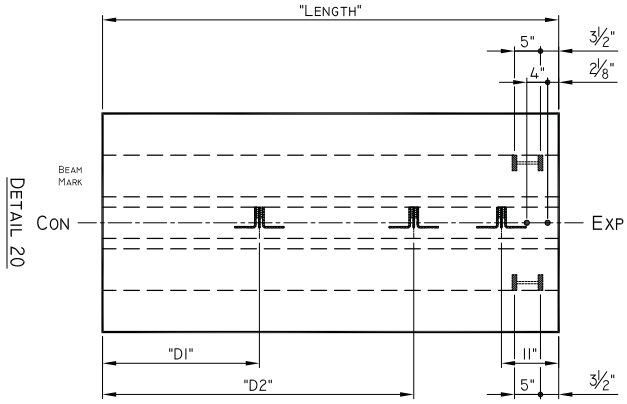

DETAIL 20

GULF COAST PRE-STRESS, INC.
PASS CHRISTIAN, MISS.
GCP
APPROVED FOR FABRICATION
6/21/2011

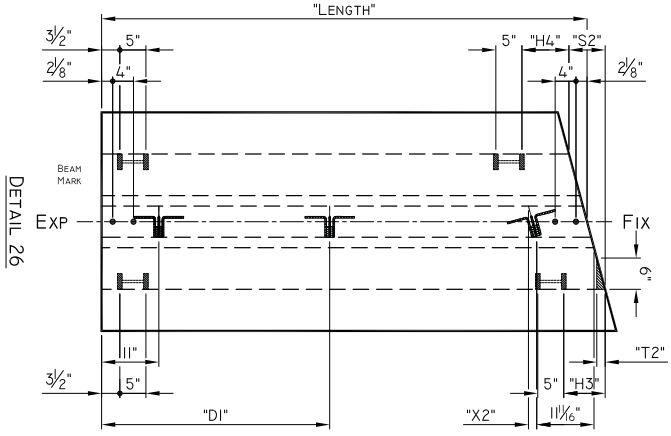

DETAIL 26

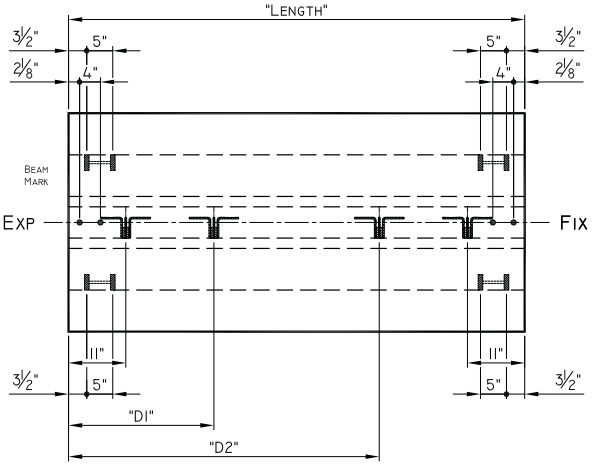

DETAIL 23

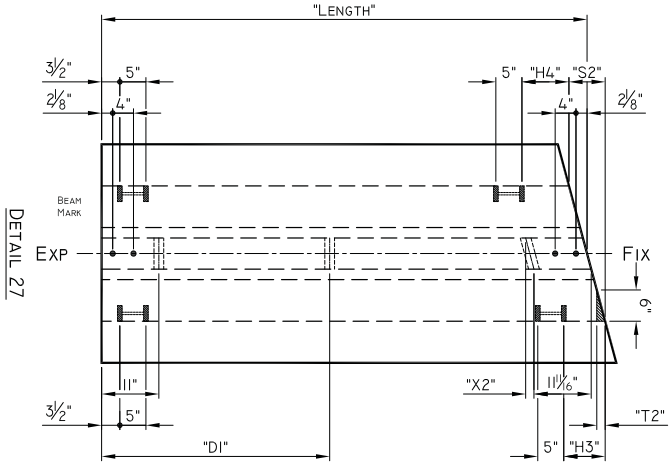

DETAIL 27

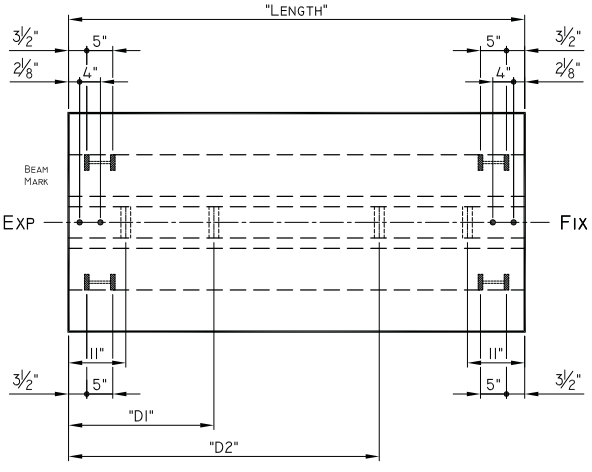

DETAIL 24

Checked:	Drawn By:	Date:	Sheet Number:	Drawing:	Job Number:
bjp	bec	5/25/2011	5 of 7	1069-Detail3	10-69

LDOTD

Engineer	Contractor
State of Louisiana Department of Transportation & Development	Jensen Construction Company Tulsa, Oklahoma

Miscellaneous Beam Details ~ Red River Bridge (BT-72 Girders)
Fort Buhlow Bridge & Approaches (U.S. 71/U.S. 165)
Rapides Parish, Louisiana
F.A.P. No. 0203(600) S.P. No. 840-43-0001

GULF COAST PRE-STRESS, INC.
GCP
PASS CHRISTIAN, MISS.

Revision Legend

Mark	Date	Description	By

Table A. 2
Geometric properties of Girder 2: LG54

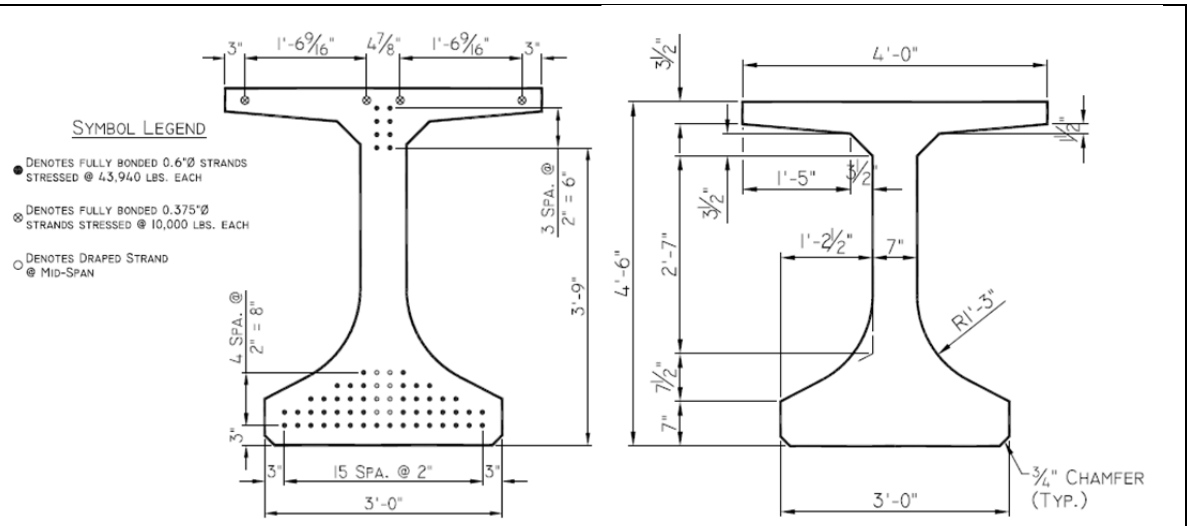

Gross section properties	
Area: Ac = 868 in^2	Center of gravity: CG = 25.1 in
Strong axis moment of inertia: Ix = 344,586 in^4	Weak axis moment of inertia: Iy = 70,877 in^4
Number of strands = 56	Strands per row = [16 16 12 8 4] Strands per row at ends = [16 14 10 6 2 2 2 2 2]
Strands diameter = 0.6 in	Area of one strand = 0.217 in^2
Guaranteed ultimate strength = 270 ksi	Modulus of elasticity = 29,000 ksi
Composite section properties at transfer	
Measured compressive strength= 8,170 psi	Measured modulus of elasticity = 5,930 ksi
Modular ratio = 4.9	Area = 915.8 in^2
Midspan	**10 ft from ends**
CG = 24.1 in.	CG = 24.4 in.
Ix = 361,188.0 in4	Ix = 353,499.7 in^4
Eccentricity of prestress force = 18.2 in.	Eccentricity of prestress force = 13.4 in.
Distance from centroid to bottom strain gage = 22.1 in.	Distance from centroid to bottom strain gage = 22.4 in.
Distance from centroid to top strain gage = 28.4 in.	Distance from centroid to top strain gage = 28.1 in.
Initial Prestress force = 2,460.8 kip	Initial Prestress force = 2,460.8 kip
Prestress losses = 226.7 kip	Prestress losses = 226.7 kip
Effective prestress force = 2,234.1 kip	Effective prestress force = 2,234.1 kip

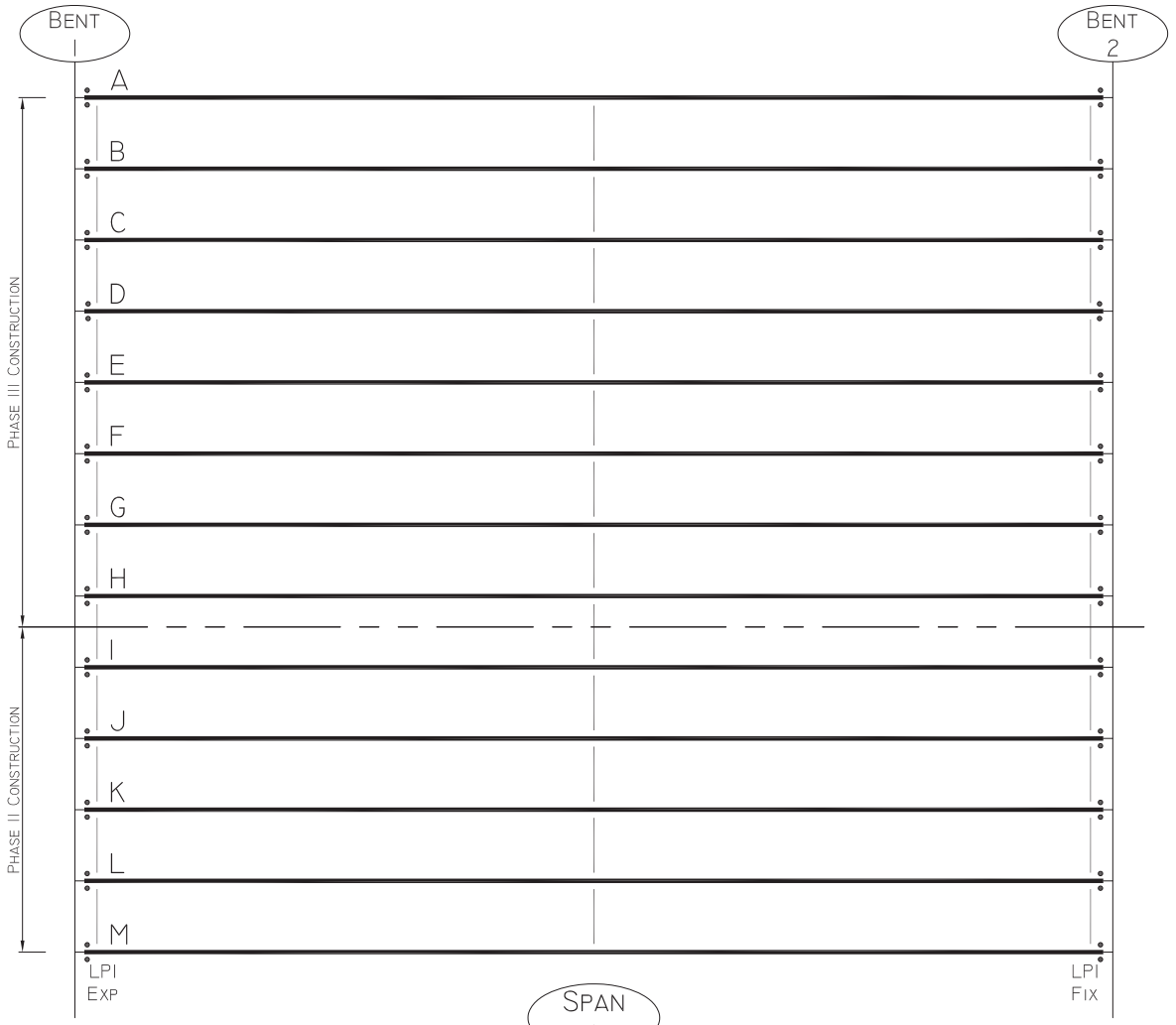

TYPE LG-54

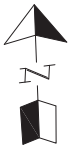

Revision Legend			
Mark	Date	Description	By

GCP

Contractor
Johnson Bros. Corp.
Lithia, Florida

Engineer
State of Louisiana
Department of Transportation
& Development

Framing Plan ~ LG-54 Beams
I-210 Over Cove Lane
State Project No. H.010151
Calcasieu Parish, Louisiana

LDOTD

GCP

APPROVED FOR FABRICATION
3-27-2014

CURRENT SET OF GCP SHOP DRAWINGS
AS OF 4-10-2014 △ A

I-210 OVER COVE LANE
STATE PROJECT NO. H.010151
CALCASIEU PARISH, LOUISIANA

LEGEND	
—•—•	= BEARING ASSEMBLY REQUIRED
EXP	= EXPANSION BEARING TYPE
FIX	= FIXED BEARING TYPE
LPI	= LAMINATED NEOPRENE BEARING PADS*

*SEE GCP BEARING PAD SUBMITTAL FOR INFORMATION

Job Number:	13-81
Drawing:	1381-Frame
Sheet Number:	1 of 8
Date:	3/6/2014
Drawn By:	dl
Checked:	bec

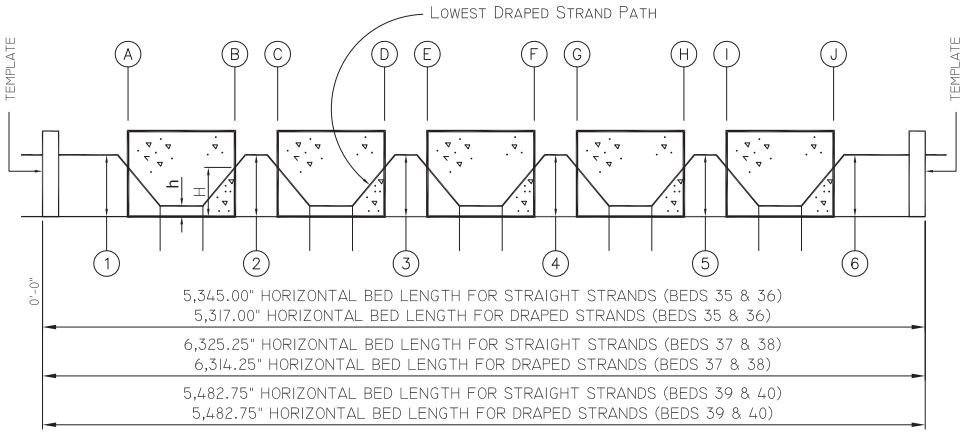

ELEVATION DIAGRAM OF STRESSING BED

APPROVED FOR FABRICATION
3-27-2014

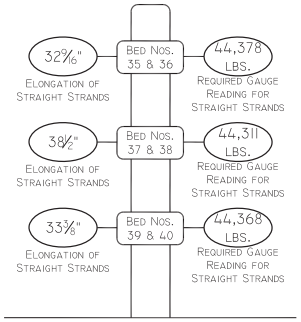

SEE "TABLE OF DIMENSIONS" FOR DRAPED STRAND ELONGATION.

Revision Legend			
Mark	Date	Description	By

PRESTRESSING OF STRAIGHT STRANDS

1. STRING STRANDS FROM ANCHOR END TO JACKING END, OCCUPYING HOLES AS SHOWN IN THE STRAND PATTERN ELEVATION.
2. TENSION ALL STRAIGHT STRANDS TO 6,000 LBS. EACH.
3. TENSION STRAIGHT STRANDS TO FULL LOAD BY EXTENDING STRANDS THE AMOUNT SHOWN AS ELONGATION.

PRESTRESSING OF DRAPED STRANDS

1. STRING STRAND AS SHOWN IN "ELEVATION OF TEMPLATE" AND THEN PASS OVER ① HOLD-UP DEVICE, UNDER THE FIRST PAIR OF HOLD-DOWN DEVICES AND THEN OVER ② HOLD-UP DEVICE. REPEAT PROCESS AS REQUIRED UNTIL STRAND PASSES OVER Ⓝ HOLD-UP DEVICE WHERE IT IS THEN TO PASS THROUGH THE TEMPLATE.
2. TENSION ALL STRANDS TO 6,000 LBS. EACH
3. ELONGATE ALL STRANDS TO THE AMOUNT SHOWN.

NO. BEAMS IN SET UP	N	DRAPE SEQUENCE
3	④	② ③
4	⑤	② ③ ④
5	⑥	② ③ ④ ⑤
6	⑦	② ③ ④ ⑤ ⑥
7	⑧	② ③ ④ ⑤ ⑥ ⑦

ELONGATION CALCULATION ~ BEDS 35 & 36

STRAND DESCRIPTION:			0.6"Ø 270K LOW-RELAXATION
CASTING BED NUMBER (FREE STANDING FORM)			35 & 36
BED LENGTH "L" FOR STRAIGHT STRANDS			5,345.00 IN.
AREA "A" FOR 0.6"Ø 270K L/R STRANDS			0.217 SQ. IN.
MODULUS OF ELASTICITY 'E'			2.88E+07 PSI
INITIAL TENSION 'P' 75% ULTIMATE			43,940 LBS.
INITIAL TENSION LESS 6,000 LBS.			37,940 LBS.
ELONGATION OF STRAIGHT STRANDS	GROSS	NET	LOAD (LBS.)
ELONG = PL/AE 'BASIC'	32.450	32.450 IN.	37,940
DEAD END SEATING 'DES'	0.125	0.125 IN.	0
LIVE END SEATING 'LES'	0.375	0.000 IN.	438
ABUTMENT MOVEMENT 'AM'	0.000	0.000 IN.	0
INITIAL PULL	-	-	6000
	32.950	32.575 IN.	44,378
BASIC + DES + AM		32.575 IN. (MEASURED)	
((BASIC + LES) * (A*E))/I + 6,000		44,378 (GAUGE READING)	

NOTE: ELONGATION CALCULATION SHOWN IS BASED ON NOMINAL STRAND AREA AND MODULUS OF ELASTICITY. ACTUAL ELONGATION AND GAUGE READING WILL BE BASED ON THE ACTUAL STRAND AREA AND MODULUS OF ELASTICITY FROM MILL CERTIFICATES FROM ACTUAL REELS OF PRE-STRESSING STRAND USED.

STRESS TRANSFER

1. TENDONS SHALL BE DETENSIONED BY A SLOW-HEAT CUTTING, USING A LOW-OXYGEN FLAME. HEATING SHALL BE DONE WITH A LOW-OXYGEN FLAME (FAIRLY LARGE) PLAYED ALONG THE TENDON FOR A MINIMUM OF 5". TENDONS SHALL BE HEATED IN SUCH A MANNER THAT THE FAILURE OF THE FIRST WIRE IN EACH TENDON WILL OCCUR AFTER THE TORCH HAS BEEN APPLIED FOR A MINIMUM OF FIVE SECONDS.
2. THE SEQUENCE FOR DETENSIONING THE TENDONS SHALL BE IN ACCORDANCE WITH THE DETENSIONING SEQUENCE SHOWN ON FABRICATION DETAILS WHICH WILL KEEP THE STRESSES NEARLY SYMMETRICAL ABOUT THE AXIS OF THE BEAM.
3. SINGLE STRAND DETENSIONING FOR PRODUCTS OF 36" IN HEIGHT OR LESS SHALL BE DONE AT BOTH ENDS OF BED ONLY. SINGLE STRAND DETENSIONING FOR PRODUCT HEIGHTS IN EXCESS OF 36" SHALL BE DETENSIONED AT BOTH ENDS OF BEDS AND ALL SPACES BETWEEN ENDS OF BEAMS SIMULTANEOUSLY.
4. DETENSION ONLY WHEN THE CONCRETE HAS REACHED THE REQUIRED MINIMUM COMPRESSIVE CYLINDER STRENGTH OF F'CI. (SEE FABRICATION DETAILS FOR VALUE OF F'CI.)

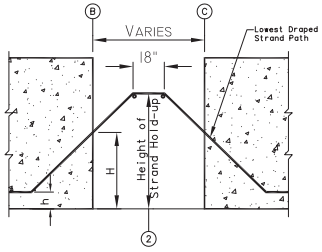

Detail of Strand Hold-up
Points ② thru ⑤

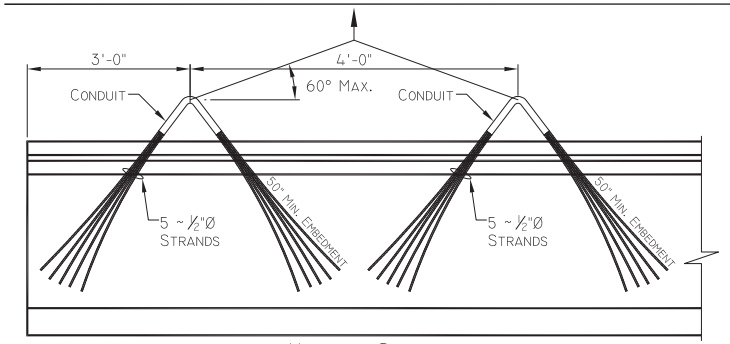

HANDLING DETAIL
FOR VERTICAL LIFT ONLY

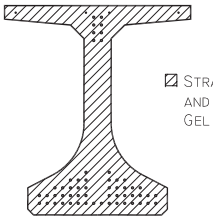

STRAND COATING DETAIL

☑ STRANDS SHALL BE CUT OFF FLUSH WITH THE CONCRETE FACE AND COATED WITH ONE (1) COAT OF SIKA SIKADUR 31 HI-MOD GEL EPOXY PASTES ADHESIVE, OR APPROVED EQUAL.

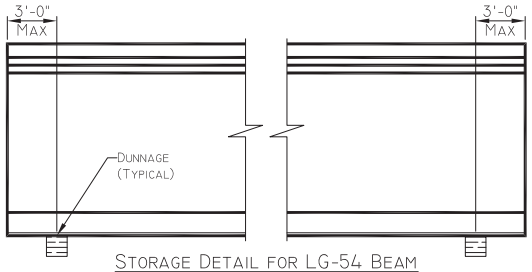

STORAGE DETAIL FOR LG-54 BEAM

Contractor
Johnson Bros. Corp.
Lithia, Florida

Engineer
State of Louisiana
Department of Transportation
& Development

Stressing and Detensioning Plan ~ LG-54 Beams
I-210 Over Cove Lane
State Project No. H.010151
Calcasieu Parish, Louisiana

LDOTD

Job Number:	13-81
Drawing:	1381-Stress
Sheet Number:	2 of 8
Date:	3/6/2014
Drawn By:	dl
Checked:	bec

LG-54 BEAMS

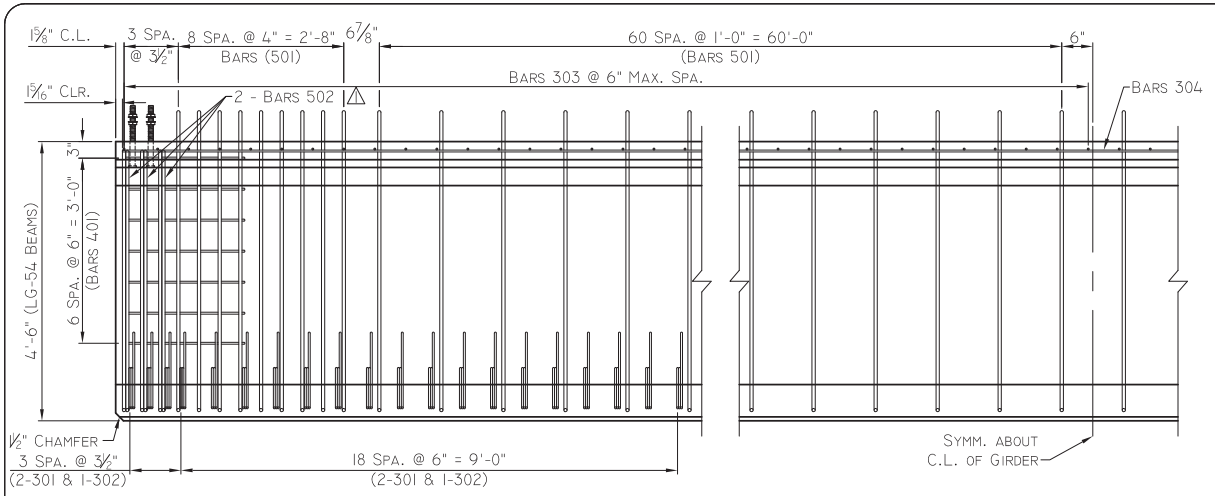

BEAM END ELEVATION
LG-54 BEAMS ~ NOT TO SCALE

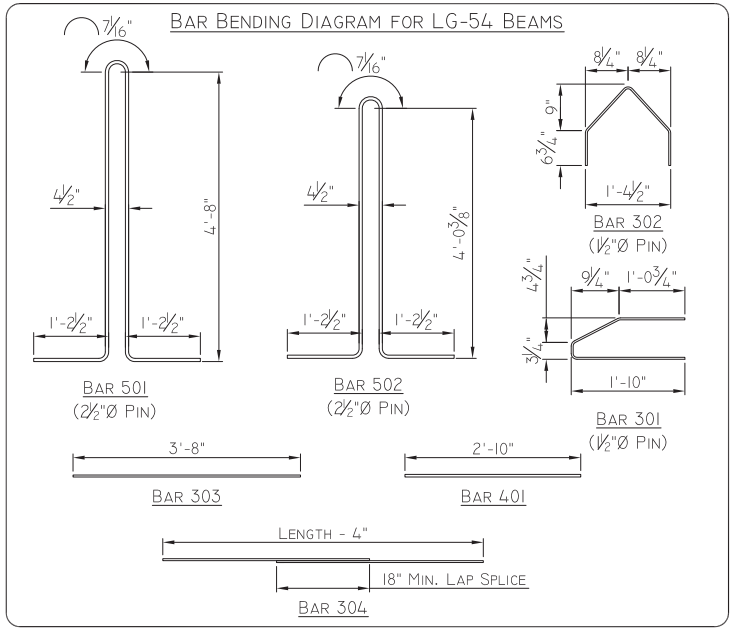

Revision Legend

Mark	Date	Description	By
△	2/25/14	added bars 502	bc

APPROVED FOR FABRICATION
3-27-2014

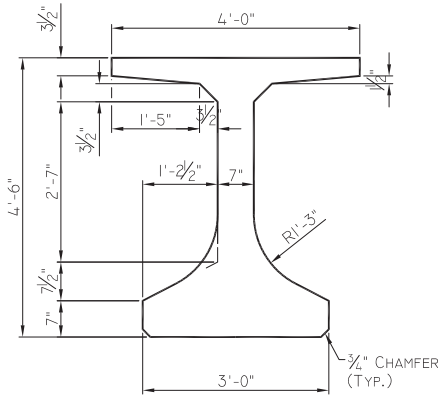

LG-54 BEAM

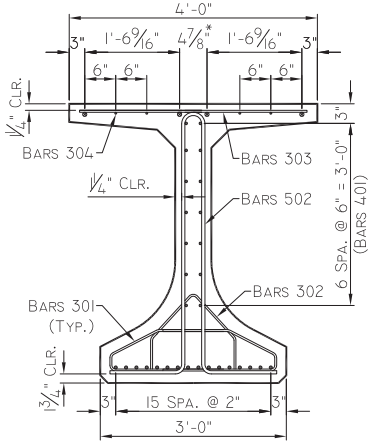

**SECTION AT BEAM END

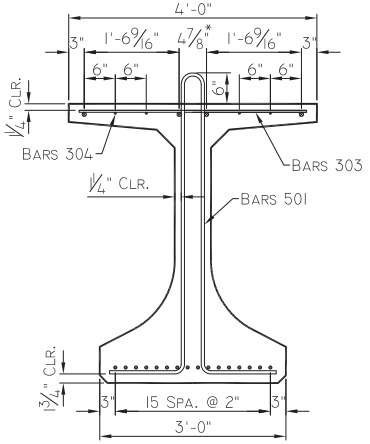

**SECTION NEAR CENTERLINE BEAM

*DENOTES TOP STRANDS

GENERAL NOTES:

FABRICATION TOLERANCES, STRESSING, AND DETENSIONING OF THE GIRDERS SHALL BE AS SPECIFIED IN THE "MANUAL FOR QUALITY CONTROL FOR PLANTS AND PRODUCTION OF PRECAST-PRESTRESSED CONCRETE PRODUCTS (MNL-116 LATEST EDITION)" PUBLISHED BY PCI.

PRE-STRESSING STEEL SHALL BE 0.6" NOMINAL DIAMETER, UNCOATED, SEVEN-WIRE STRAND, GRADE 270K, CONFORMING TO ASTM DESIGNATION A-416. THE STRANDS SHALL BE LOW-RELAXATION WITH AN INITIAL APPLIED FORCE OF 43,940 LBS.

CONCRETE USED IN THE GIRDERS SHALL BE CLASS "P(x) HPC" CONCRETE WITH A COMPRESSIVE STRENGTH OF F'ci 8,500 PSI AT RELEASE OF STRANDS AND F'c 10,000 PSI AT 28 DAYS.

PRE-STRESSED GIRDERS SHALL BE MAINTAINED IN AN UPRIGHT POSITION AT ALL TIMES DURING STORAGE AND HANDLING, SEE GCP STORAGE AND HANDLING DETAILS FOR SUPPORT LOCATIONS. DISREGARD OF THIS MAY LEAD TO COLLAPSE OF THE MEMBER.

STEEL REINFORCEMENT GIRDERS SHALL CONFORM TO ASTM DESIGNATION A-615, GRADE 60. DIMENSIONS SHOWN ON REINFORCING BAR DETAILS ARE OUT-TO-OUT OF BAR. REINFORCING STEEL SHALL BE FABRICATE TO CLOSE DIMENSIONAL TOLERANCES TO PROVIDE ¼" INCH MINIMUM CLEARANCE FROM EDGE OF BAR TO FACE OF GIRDER.

*GCP REQUEST TOP STRANDS BE SHIFTED LATERALLY AS SHOWN TO FACILITATE TYING OF STIRRUPS.

**THE SECTIONS SHOWN ARE GENERIC DETAILS. SEE GCP'S "FABRICATION DETAILS" FOR A SPECIFIC STRAND PATTERN.

LG-54 BEAMS

Contractor:
Johnson Bros. Corp.
Lithia, Florida

Engineer:
State of Louisiana
Department of Transportation
& Development

Reinforcement Details & General Notes ~ LG-54 Beams
I-210 Over Cove Lane
State Project No. H.010151
Calcasieu Parish, Louisiana

LDOTD

Job Number:	13-81
Drawing:	1381-Misc.
Sheet Number:	3 of 8
Date:	3/6/2014
Drawn By:	dl
Checked:	bec

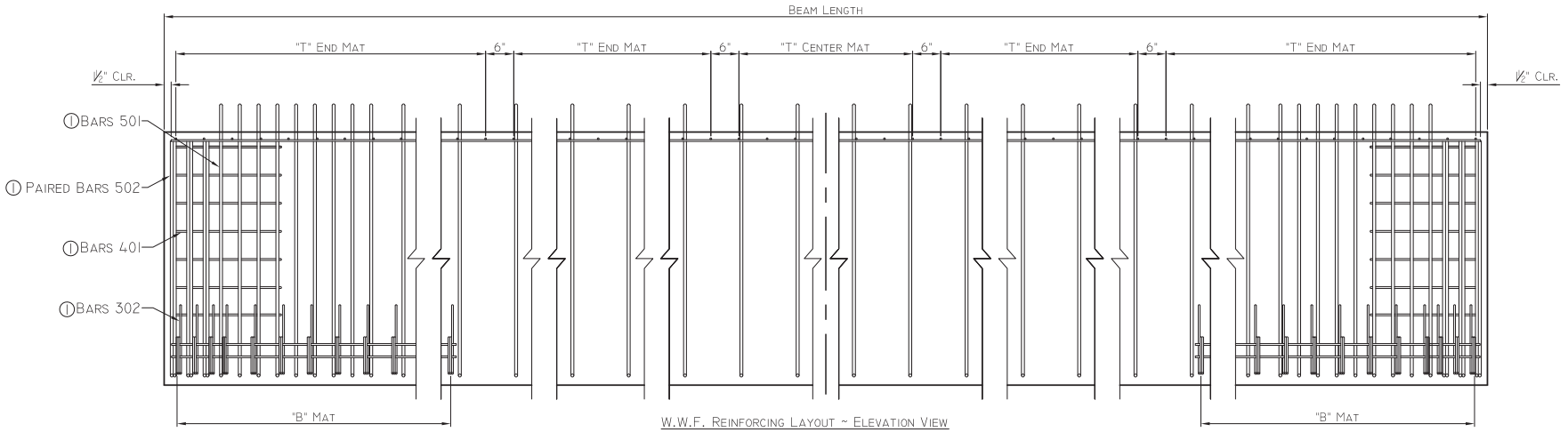

W.W.F. Reinforcing Layout ~ Elevation View
LG-54 Beams ~ Not to Scale

Notes:
① See "Reinforcement Details & General Notes" for information pertaining to mild reinforcing Bars 302, 401, 501, & 502.

Approved for Fabrication
3-27-2014

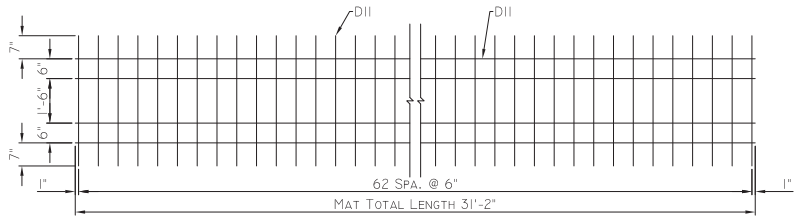

"T" Center Mat
Plan View

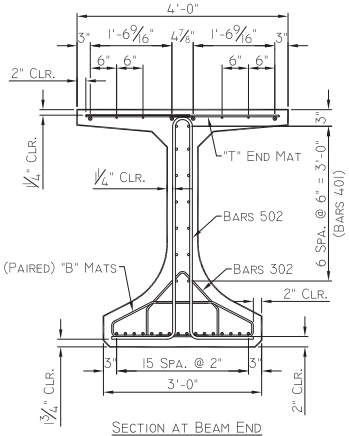

Section at Beam End

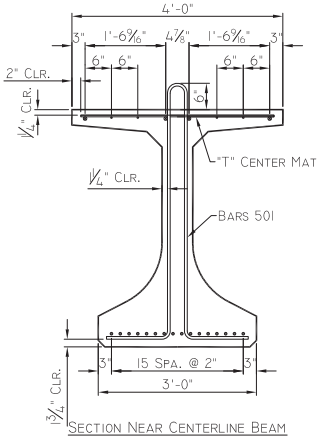

Section Near Centerline Beam

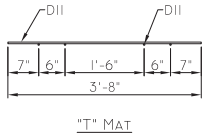

"T" Mat

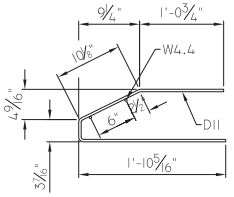

"B" Mat

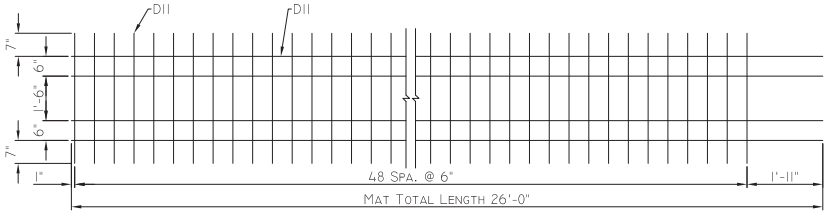

"T" End Mat
Plan View

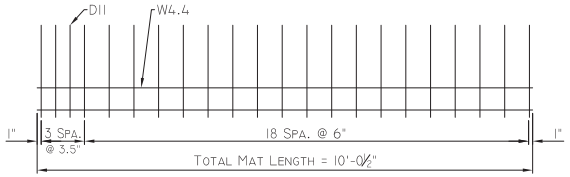

"B" Mat
Plan View

Revision Legend

Mark	Date	Description	By

Contractor:
Johnson Bros. Corp.
Lithia, Florida

Engineer:
State of Louisiana
Department of Transportation
& Development

W.W.F. Details ~ LG-54 Beams
I-210 Over Cove Lane
State Project No. H.010151
Calcasieu Parish, Louisiana

LDOTD

Job Number:	13-81
Drawing:	1381-Misc.
Sheet Number:	3a of 8
Date:	3/6/2014
Drawn By:	sj
Checked:	bec

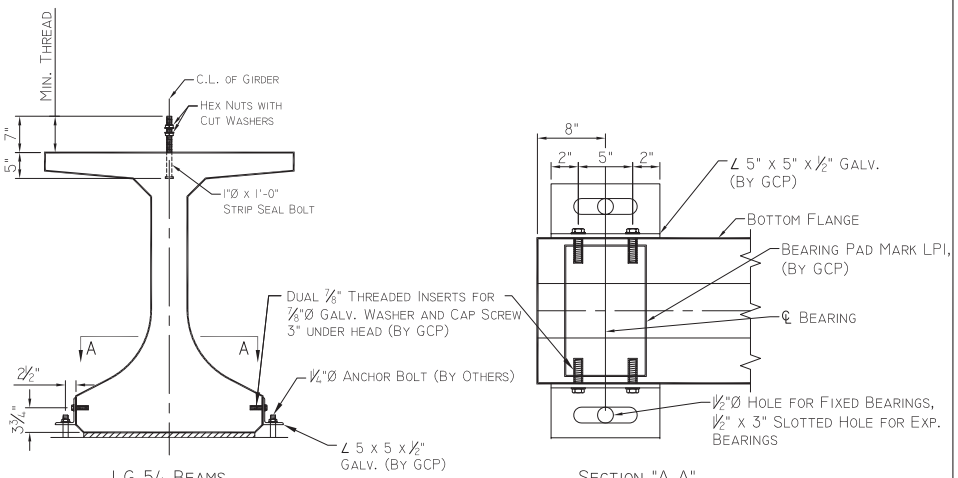

LG-54 BEAMS
END VIEW

SECTION "A-A"
LG-54 BEAMS

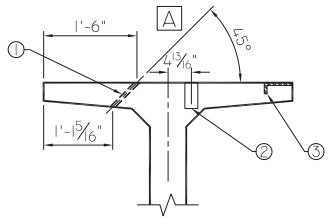

ELEVATION OF TOP FLANGE
BEAMS "A THRU G, J THRU M"

NOTES:

1. ⅝"Ø SCH 40 PVC INSERT OFFSET 1'-0" FROM BOTH ENDS OF BEAM AND A MAX. SPACING OF 36" O.C. THEREAFTER. (EXTERIOR SIDE OF EXTERIOR BEAMS)
2. SAFETY POST INSERT 2½" PVC PIPE SCHD. 40 (2.445" I.D.) x 5" LONG WITH BOTH ENDS DUCT TAPED FOR A CLEAN HOLE. OFFSET FROM BEAM END 2'-0" THEN 8'-0" O.C. THEREAFTER. (TYP.)
3. STAY-IN-PLACE METAL FORM CLIPS OFFSET 4" FROM END THEN 18" O.C. THEREAFTER. (BOTH SIDES OF INTERIOR BEAMS @ INTERIOR SIDE OF EXTERIOR BEAMS)

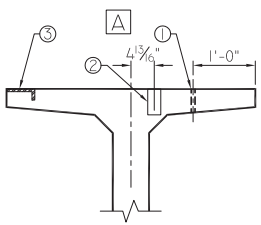

ELEVATION OF TOP FLANGE
LOOKING UPSTATION
BEAM "H"

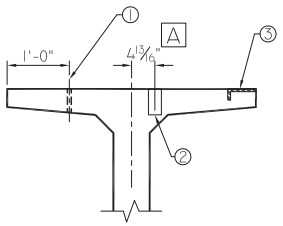

ELEVATION OF TOP FLANGE
LOOKING UPSTATION
BEAM "I"

APPROVED FOR FABRICATION
3-27-2014

Revision Legend

Mark	Date	Description	By
△	2/25/14	adjusted dimension to first strip seal bolt	bc
none	2/25/14	omitted information on elevation of top flange detail per reviewer's comments	bc
A	4/10/14	Adjusted note 2	sj
A	4/10/14	Changed safety post insert dimension	sj

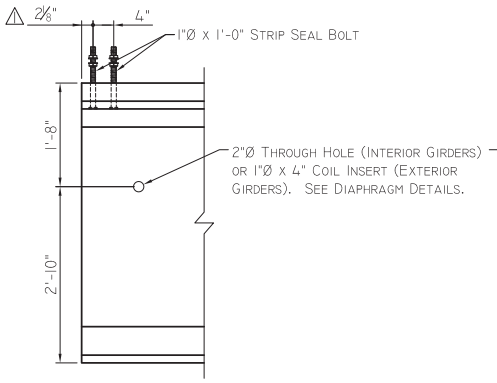

LG-54 BEAMS
ELEVATION VIEW @ BEAM END

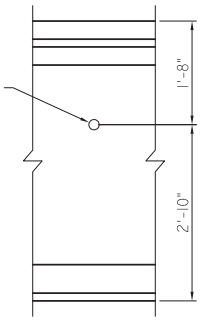

LG-54 BEAMS
ELEVATION VIEW @ BEAM C.L.

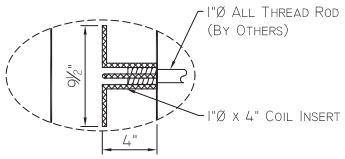

DIAPHRAGM COIL INSERT DETAIL
(EXTERIOR GIRDERS)

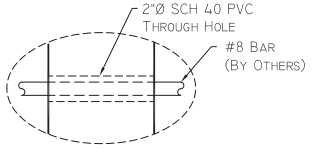

DIAPHRAGM THROUGH HOLE DETAIL
(INTERIOR GIRDERS)

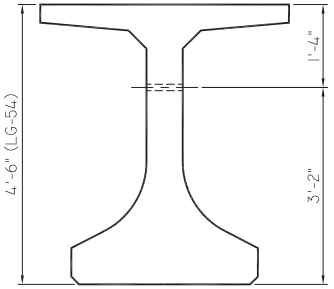

SECTION OF LG-54

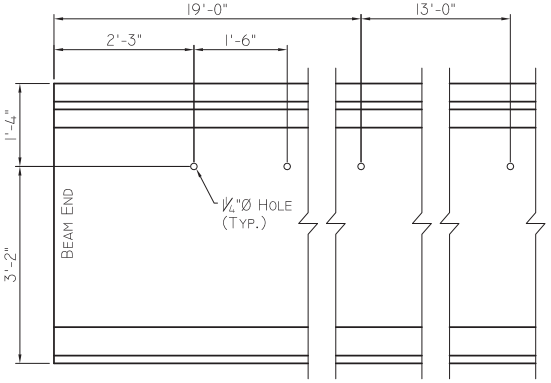

SIDE ELEVATION

LG-54 HANDLING HOLE DETAILS
TYPICAL EACH BEAM END

LG-54 BEAMS

Contractor
Johnson Bros. Corp.
Lithia, Florida

Engineer
State of Louisiana
Department of Transportation
& Development

Miscellaneous Details ~ LG-54 Beams
I-210 Over Cove Lane
State Project No. H.010151
Calcasieu Parish, Louisiana

LDOTD

Job Number: 13-81
Drawing: 1381-Misc.
Sheet Number: 4 of 8
Date: 3/6/2014
Drawn By: dl
Checked: bec

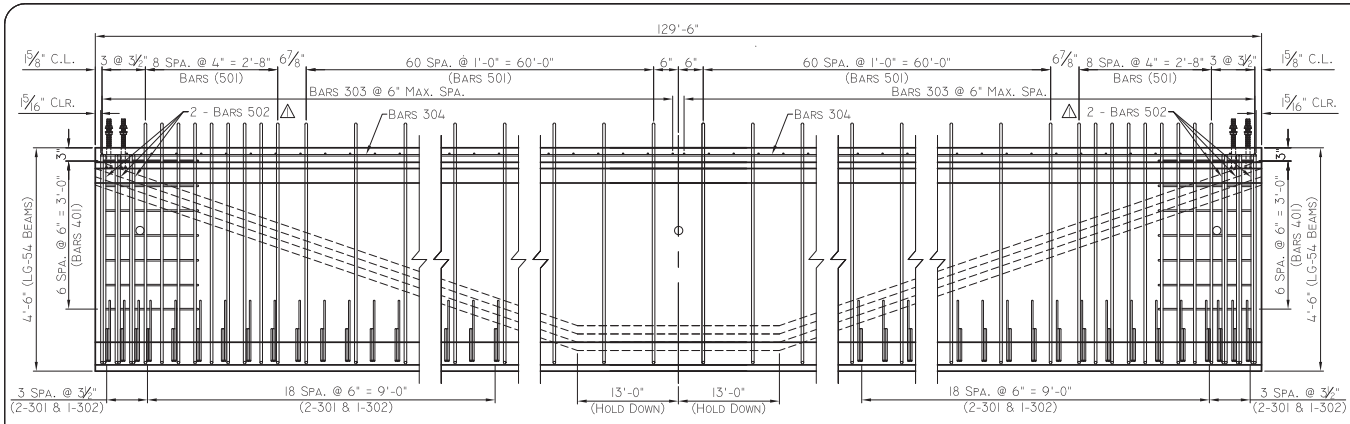

MILD REINFORCING LAYOUT ~ ELEVATION VIEW
LG-54 BEAMS ~ NOT TO SCALE

BEAM MARK

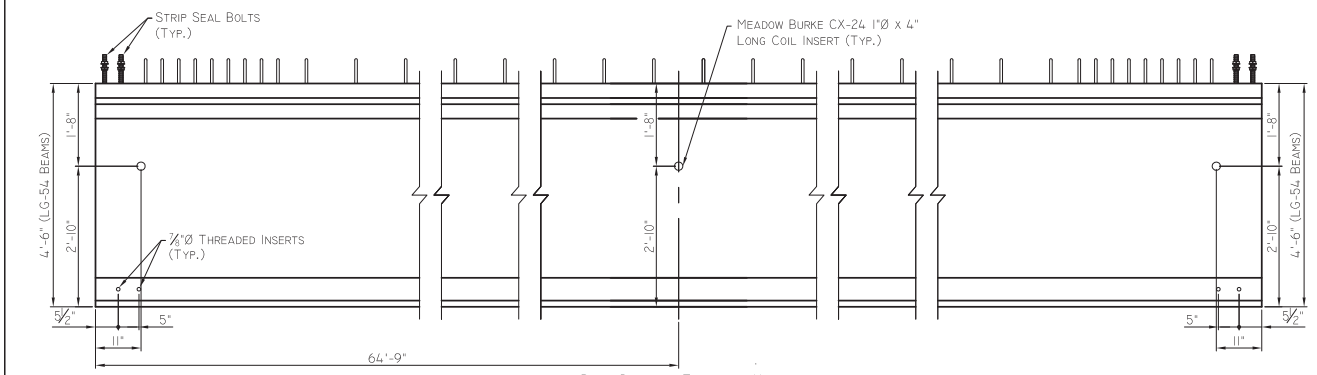

BEAM DETAIL ~ ELEVATION VIEW
LG-54 BEAMS ~ NOT TO SCALE

BEAM MARK

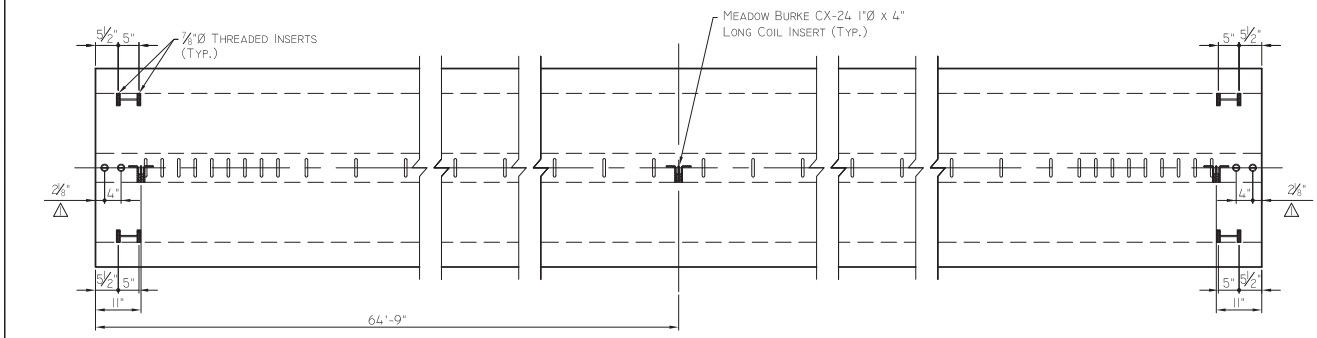

BEAM DETAIL ~ PLAN VIEW
LG-54 BEAMS ~ NOT TO SCALE

BEAM MARK

STRAND PATTERN P56-8

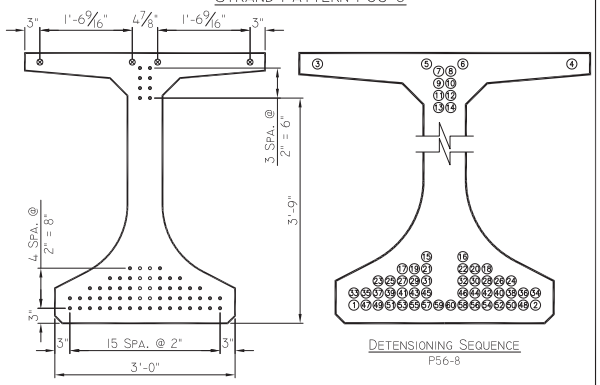

STRAND PATTERN P56-8

DETENSIONING SEQUENCE
P56-8

STRAND INFORMATION

- (56) TOTAL NUMBER OF 0.6"Ø 270K L/R STRANDS STRESSED @ 43,940 LBS. EACH
- (48) TOTAL NUMBER OF STRAIGHT STRANDS
- (4) TOTAL NUMBER OF 0.375"Ø TOP STRANDS STRESSED @ 10,000 LBS. EACH
- (8) TOTAL NUMBER OF DRAPED STRANDS

SYMBOL LEGEND

- ● DENOTES FULLY BONDED 0.6"Ø STRANDS STRESSED @ 43,940 LBS. EACH
- ⊗ DENOTES FULLY BONDED 0.375"Ø STRANDS STRESSED @ 10,000 LBS. EACH
- ○ DENOTES DRAPED STRAND @ MID-SPAN

DRAPED STRAND INFO.

H = 3'-9"
h = 5"

CONCRETE

F'c = 10,000 PSI
F'ci = 8,500 PSI

CAMBER LIMITS

2.742" - 3.429"

APPROVED FOR FABRICATION
3-27-2014

FABRICATION NOTES

1. FOR DETAILS NOT SHOWN ON THIS SHEET, SEE GCP'S "MISCELLANEOUS DETAILS" AND "MILD REINFORCING LAYOUT & GENERAL NOTES".
2. △ THE TOPS OF BEAMS SHALL BE ROUGH FLOATED AT APPROXIMATELY THE TIME OF INITIAL SET. THE ENTIRE BEAMS SHALL BE SCRUBBED TRANSVERSELY WITH A COURSE WIRE BRUSH TO REMOVE ALL LAITANCE AND PRODUCE A ROUGHENED SURFACE FOR BONDING SLAB.
3. BEAM LENGTHS SHOWN ARE MEASURED ALONG CENTERLINE OF BEAM. LENGTHS SHOWN DO NOT INCLUDE AN ALLOWANCE FOR ELASTIC SHORTENING.
4. THE DIRECTOR OF STRUCTURES, STATE BRIDGE ENGINEER SHALL BE NOTIFIED IF THE CAMBER OF THE BEAM IS NOT WITHIN THE LIMITS SHOWN.

BEAM SCHEDULE

SPAN NO.	MARK NO.	LENGTH			
1	I-A	129'-6"			

BEAM MARKS

I-A

REVISION LEGEND

Mark	Date	Description	By
△	2/25/14	adj. bars 502: dimension to strip seal bolt; note 2	bc

GCP

Contractor:
Johnson Bros. Corp.
Lithia, Florida

Engineer:
State of Louisiana Department of Transportation & Development

Fabrication Details ~ LG-54 Beams
I-210 Over Cove Lane
State Project No. H.010151
Calcasieu Parish, Louisiana

LDOTD

Job Number: 13-81
Drawing: 1381-Beam
Sheet Number: 5 of 8
Date: 3/6/2014
Drawn By: dl
Checked: bec

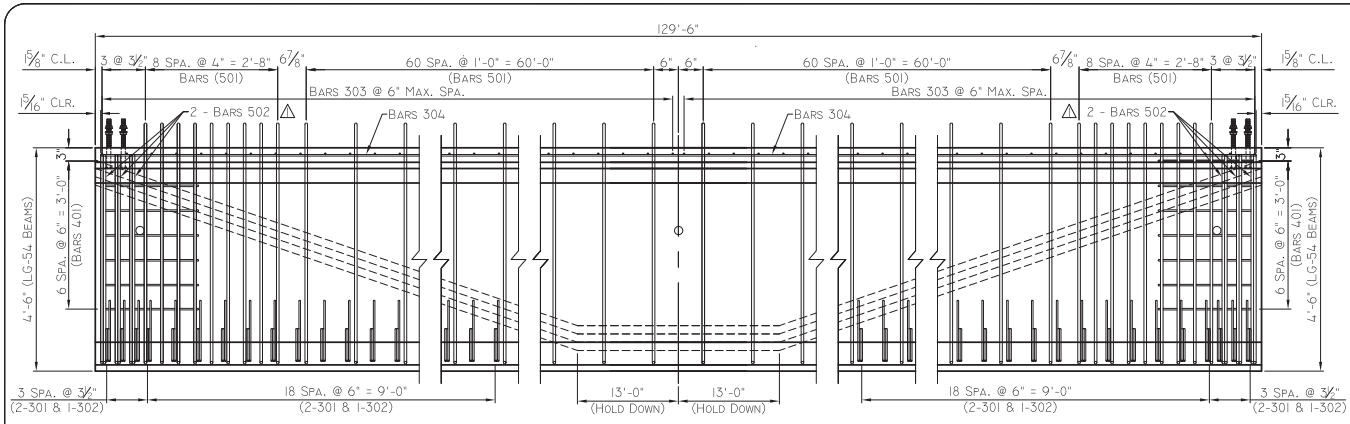

MILD REINFORCING LAYOUT ~ ELEVATION VIEW
LG-54 BEAMS ~ NOT TO SCALE

BEAM MARK

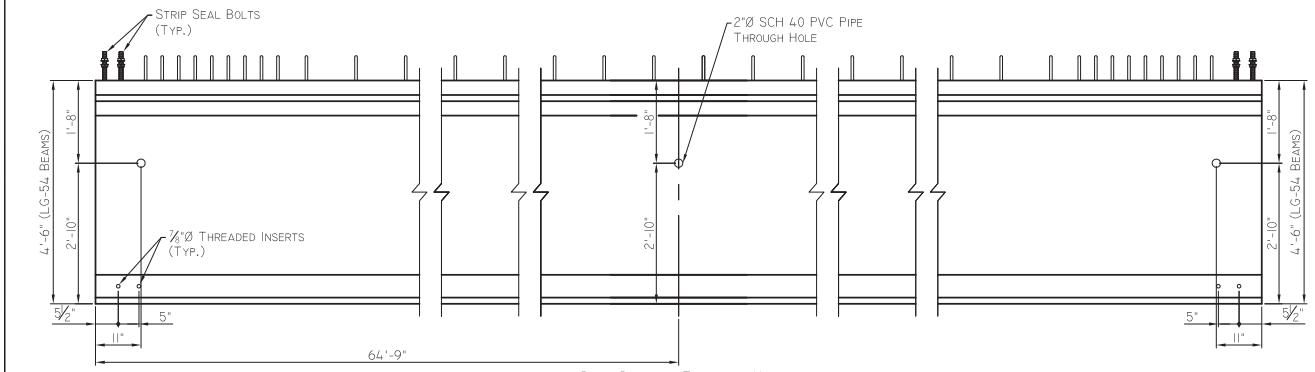

BEAM DETAIL ~ ELEVATION VIEW
LG-54 BEAMS ~ NOT TO SCALE

BEAM MARK

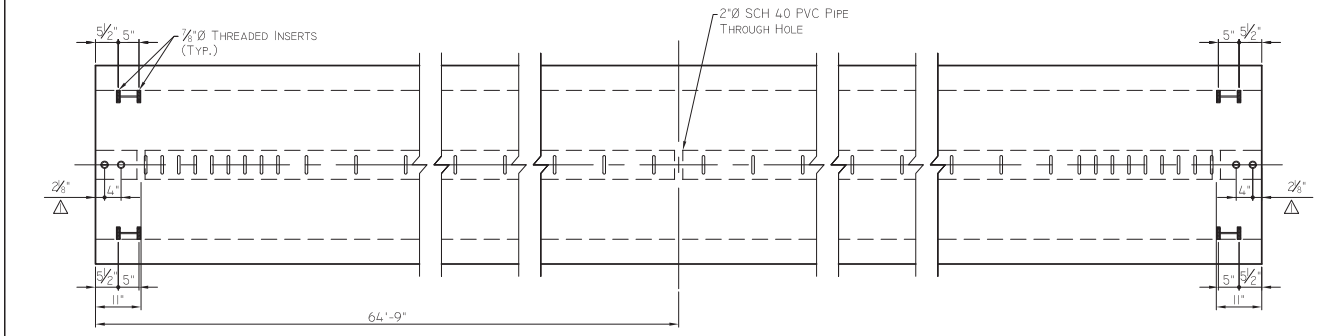

BEAM DETAIL ~ PLAN VIEW
LG-54 BEAMS ~ NOT TO SCALE

BEAM MARK

STRAND PATTERN P56-8

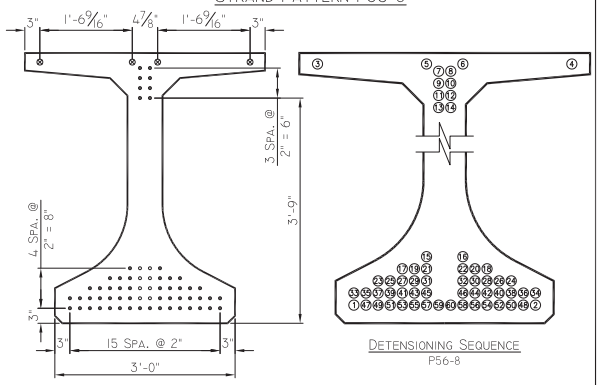

STRAND PATTERN P56-8

DETENSIONING SEQUENCE
P56-8

Mark	Date	Description	By
1	2/25/14	adj. bars 502: dimension to strip seal bolt; note 2	bc

Revision Legend

STRAND INFORMATION

- (56) TOTAL NUMBER OF 0.6"Ø 270K L/R STRANDS STRESSED @ 43,940 LBS. EACH
- (48) TOTAL NUMBER OF STRAIGHT STRANDS
- (4) TOTAL NUMBER OF 0.375"Ø TOP STRANDS STRESSED @ 10,000 LBS. EACH
- (8) TOTAL NUMBER OF DRAPED STRANDS

SYMBOL LEGEND

- ● DENOTES FULLY BONDED 0.6"Ø STRANDS STRESSED @ 43,940 LBS. EACH
- ⊗ DENOTES FULLY BONDED 0.375"Ø STRANDS STRESSED @ 10,000 LBS. EACH
- ○ DENOTES DRAPED STRAND @ MID-SPAN

DRAPED STRAND INFO.

H = 3'-9"
h = 5"

CONCRETE

F'c = 10,000 PSI
F'ci = 8,500 PSI

CAMBER LIMITS

2.742" - 3.429"

APPROVED FOR FABRICATION
3-27-2014

FABRICATION NOTES

1. FOR DETAILS NOT SHOWN ON THIS SHEET, SEE GCP'S "MISCELLANEOUS DETAILS" AND "MILD REINFORCING LAYOUT & GENERAL NOTES".
2. THE TOPS OF BEAMS SHALL BE ROUGH FLOATED AT APPROXIMATELY THE TIME OF INITIAL SET. THE ENTIRE BEAMS SHALL BE SCRUBBED TRANSVERSELY WITH A COURSE WIRE BRUSH TO REMOVE ALL LAITANCE AND PRODUCE A ROUGHENED SURFACE FOR BONDING SLAB.
3. BEAM LENGTHS SHOWN ARE MEASURED ALONG CENTERLINE OF BEAM. LENGTHS SHOWN DO NOT INCLUDE AN ALLOWANCE FOR ELASTIC SHORTENING.
4. THE DIRECTOR OF STRUCTURES, STATE BRIDGE ENGINEER SHALL BE NOTIFIED IF THE CAMBER OF THE BEAM IS NOT WITHIN THE LIMITS SHOWN.

BEAM SCHEDULE

SPAN NO.	MARK NO.	LENGTH			
1	I-B	129'-6"			
1	I-C	129'-6"			
1	I-D	129'-6"			
1	I-E	129'-6"			
1	I-F	129'-6"			
1	I-G	129'-6"			
1	I-H	129'-6"			
1	I-I	129'-6"			
1	I-J	129'-6"			
1	I-K	129'-6"			
1	I-L	129'-6"			

BEAM MARKS

I-B THRU I-L

Contractor:
Johnson Bros. Corp.
Lithia, Florida

Engineer:
State of Louisiana Department of Transportation & Development

Fabrication Details ~ LG-54 Beams
I-210 Over Cove Lane
State Project No. H.010151
Calcasieu Parish, Louisiana

LDOTD

Job Number:	13-81
Drawing:	1381-Beam
Sheet Number:	6 of 8
Date:	3/6/2014
Drawn By:	dl
Checked:	bec

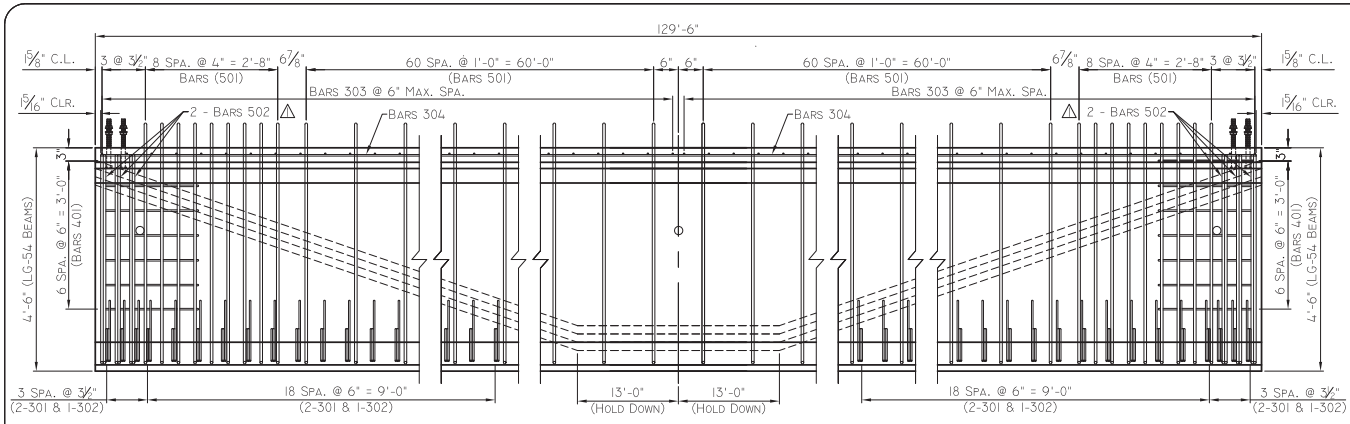

MILD REINFORCING LAYOUT ~ ELEVATION VIEW
LG-54 BEAMS ~ NOT TO SCALE

BEAM MARK

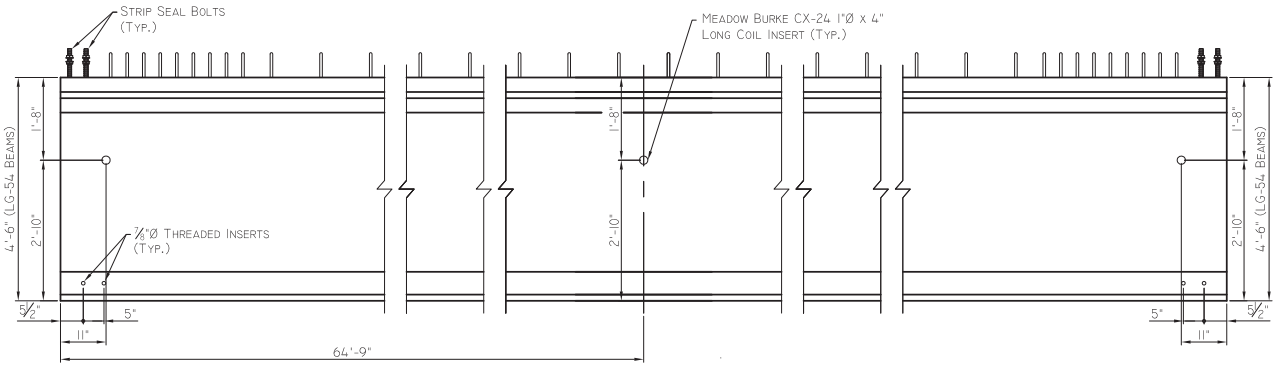

BEAM DETAIL ~ ELEVATION VIEW
LG-54 BEAMS ~ NOT TO SCALE

BEAM MARK

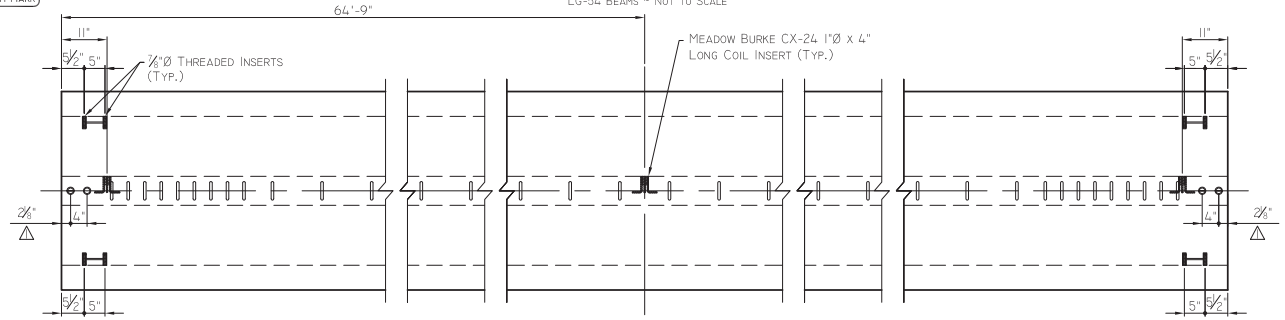

BEAM DETAIL ~ PLAN VIEW
LG-54 BEAMS ~ NOT TO SCALE

BEAM MARK

STRAND PATTERN P56-8

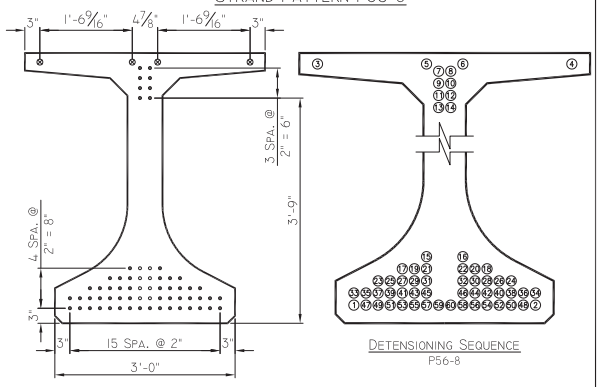

STRAND PATTERN P56-8

DETENSIONING SEQUENCE
P56-8

STRAND INFORMATION

- (56) TOTAL NUMBER OF 0.6"Ø 270K L/R STRANDS STRESSED @ 43,940 LBS. EACH
- (48) TOTAL NUMBER OF STRAIGHT STRANDS
- (4) TOTAL NUMBER OF 0.375"Ø TOP STRANDS STRESSED @ 10,000 LBS. EACH
- (8) TOTAL NUMBER OF DRAPED STRANDS

SYMBOL LEGEND

- ● DENOTES FULLY BONDED 0.6"Ø STRANDS STRESSED @ 43,940 LBS. EACH
- ⊗ DENOTES FULLY BONDED 0.375"Ø STRANDS STRESSED @ 10,000 LBS. EACH
- ○ DENOTES DRAPED STRAND @ MID-SPAN

DRAPED STRAND INFO.

H = 3'-9"
h = 5"

CONCRETE

F'c = 10,000 PSI
F'ci = 8,500 PSI

CAMBER LIMITS

2.742" - 3.429"

APPROVED FOR FABRICATION
3-27-2014

FABRICATION NOTES

1. FOR DETAILS NOT SHOWN ON THIS SHEET, SEE GCP'S "MISCELLANEOUS DETAILS" AND "MILD REINFORCING LAYOUT & GENERAL NOTES".
2. THE TOPS OF BEAMS SHALL BE ROUGH FLOATED AT APPROXIMATELY THE TIME OF INITIAL SET. THE ENTIRE BEAMS SHALL BE SCRUBBED TRANSVERSELY WITH A COURSE WIRE BRUSH TO REMOVE ALL LAITANCE AND PRODUCE A ROUGHENED SURFACE FOR BONDING SLAB.
3. BEAM LENGTHS SHOWN ARE MEASURED ALONG CENTERLINE OF BEAM. LENGTHS SHOWN DO NOT INCLUDE AN ALLOWANCE FOR ELASTIC SHORTENING.
4. THE DIRECTOR OF STRUCTURES, STATE BRIDGE ENGINEER SHALL BE NOTIFIED IF THE CAMBER OF THE BEAM IS NOT WITHIN THE LIMITS SHOWN.

BEAM SCHEDULE

SPAN NO.	MARK NO.	LENGTH			
1	1-M	129'-6"			

BEAM MARKS

1-M

REVISION LEGEND

Mark	Date	Description	By
1	2/25/14	adj. bars 502: dimension to strip seal bolt; note 2	bc

GCP

Contractor:
Johnson Bros. Corp.
Lithia, Florida

Engineer:
State of Louisiana Department of Transportation & Development

Fabrication Details ~ LG-54 Beams
I-210 Over Cove Lane
State Project No. H.010151
Calcasieu Parish, Louisiana

LDOTD

Job Number:	13-81
Drawing:	1381-Beam
Sheet Number:	7 of 8
Date:	3/6/2014
Drawn By:	dl
Checked:	bec

Table of Dimensions - Bed 35 & 36

Set Up No.	Beam Mark	Strand Pattern	Cast Length	Stationing For Stressing Bed Layout												Bed Elongation For D/S	**35 & 36** Bed Length D/S	Stressing Data Gauge Reading D/S
				Hold Up		Beam Start		Hold Down		Beam End		Hold Up						
					Station	Height							Station	Height				
1	1-A	P56-8	129'-6"	1	5'-0"	3'-10 3/4"	A	7'-3"	59'-0"	85'-0"	B	136'-9"	2	139'-0"	3'-10 3/16"	32 7/16"	5324.96"	44,380
	1-B	P56-8	129'-6"				C	141'-3"	193'-0"	219'-0"	D	270'-9"	3	273'-0"	3'-10 3/16"			
	1-C	P56-8	129'-6"				E	275'-3"	327'-0"	353'-0"	F	404'-9"	4	407'-0"	3'-10 3/4"			
2	1-D	P56-8	129'-6"	1	5'-0"	3'-10 3/4"	A	7'-3"	59'-0"	85'-0"	B	136'-9"	2	139'-0"	3'-10 3/16"	32 7/16"	5324.96"	44,380
	1-E	P56-8	129'-6"				C	141'-3"	193'-0"	219'-0"	D	270'-9"	3	273'-0"	3'-10 3/16"			
	1-F	P56-8	129'-6"				E	275'-3"	327'-0"	353'-0"	F	404'-9"	4	407'-0"	3'-10 3/4"			
3	1-G	P56-8	129'-6"	1	5'-0"	3'-10 3/4"	A	7'-3"	59'-0"	85'-0"	B	136'-9"	2	139'-0"	3'-10 3/16"	32 7/16"	5324.96"	44,380
	1-H	P56-8	129'-6"				C	141'-3"	193'-0"	219'-0"	D	270'-9"	3	273'-0"	3'-10 3/16"			
	1-I	P56-8	129'-6"				E	275'-3"	327'-0"	353'-0"	F	404'-9"	4	407'-0"	3'-10 3/4"			
4	1-J	P56-8	129'-6"	1	5'-0"	3'-10 3/4"	A	7'-3"	59'-0"	85'-0"	B	136'-9"	2	139'-0"	3'-10 3/16"	32 7/16"	5322.32"	44,380
	1-K	P56-8	129'-6"				C	141'-3"	193'-0"	219'-0"	D	270'-9"	3	273'-0"	3'-10 3/4"			
5	1-L	P56-8	129'-6"	1	5'-0"	3'-10 3/4"	A	7'-3"	59'-0"	85'-0"	B	136'-9"	2	139'-0"	3'-10 3/16"	32 7/16"	5322.32"	44,380
	1-M	P56-8	129'-6"				C	141'-3"	193'-0"	219'-0"	D	270'-9"	3	273'-0"	3'-10 3/4"			

Table of Dimensions - Bed 37 & 38

Set Up No.	Beam Mark	Strand Pattern	Cast Length	Stationing For Stressing Bed Layout												Bed Elongation For D/S	**37 & 38** Bed Length D/S	Stressing Data Gauge Reading D/S
				Hold Up		Beam Start		Hold Down		Beam End		Hold Up						
					Station	Height							Station	Height				
1A	1-A	P56-8	129'-6"	1	5'-0"	3'-10 3/4"	A	7'-3"	59'-0"	85'-0"	B	136'-9"	2	139'-0"	3'-10 3/16"	38 1/2"	6322.21"	44,311
	1-B	P56-8	129'-6"				C	141'-3"	193'-0"	219'-0"	D	270'-9"	3	273'-0"	3'-10 3/16"			
	1-C	P56-8	129'-6"				E	275'-3"	327'-0"	353'-0"	F	404'-9"	4	407'-0"	3'-10 3/4"			
2A	1-D	P56-8	129'-6"	1	5'-0"	3'-10 3/4"	A	7'-3"	59'-0"	85'-0"	B	136'-9"	2	139'-0"	3'-10 3/16"	38 1/2"	6322.21"	44,311
	1-E	P56-8	129'-6"				C	141'-3"	193'-0"	219'-0"	D	270'-9"	3	273'-0"	3'-10 3/16"			
	1-F	P56-8	129'-6"				E	275'-3"	327'-0"	353'-0"	F	404'-9"	4	407'-0"	3'-10 3/4"			
3A	1-G	P56-8	129'-6"	1	5'-0"	3'-10 3/4"	A	7'-3"	59'-0"	85'-0"	B	136'-9"	2	139'-0"	3'-10 3/16"	38 1/2"	6322.21"	44,311
	1-H	P56-8	129'-6"				C	141'-3"	193'-0"	219'-0"	D	270'-9"	3	273'-0"	3'-10 3/16"			
	1-I	P56-8	129'-6"				E	275'-3"	327'-0"	353'-0"	F	404'-9"	4	407'-0"	3'-10 3/4"			
4A	1-J	P56-8	129'-6"	1	5'-0"	3'-10 3/4"	A	7'-3"	59'-0"	85'-0"	B	136'-9"	2	139'-0"	3'-10 3/16"	38 1/2"	6319.57"	44,311
	1-K	P56-8	129'-6"				C	141'-3"	193'-0"	219'-0"	D	270'-9"	3	273'-0"	3'-10 3/4"			
5A	1-L	P56-8	129'-6"	1	5'-0"	3'-10 3/4"	A	7'-3"	59'-0"	85'-0"	B	136'-9"	2	139'-0"	3'-10 3/16"	38 1/2"	6319.57"	44,311
	1-M	P56-8	129'-6"				C	141'-3"	193'-0"	219'-0"	D	270'-9"	3	273'-0"	3'-10 3/4"			

Table of Dimensions - Bed 39 & 40

Set Up No.	Beam Mark	Strand Pattern	Cast Length	Stationing For Stressing Bed Layout												Bed Elongation For D/S	**39 & 40** Bed Length D/S	Stressing Data Gauge Reading D/S
				Hold Up		Beam Start		Hold Down		Beam End		Hold Up						
					Station	Height							Station	Height				
1B	1-A	P56-8	129'-6"	1	5'-0"	3'-10 3/4"	A	7'-3"	59'-0"	85'-0"	B	136'-9"	2	139'-0"	3'-10 3/16"	33 7/16"	5490.71"	44,367
	1-B	P56-8	129'-6"				C	141'-3"	193'-0"	219'-0"	D	270'-9"	3	273'-0"	3'-10 3/16"			
	1-C	P56-8	129'-6"				E	275'-3"	327'-0"	353'-0"	F	404'-9"	4	407'-0"	3'-10 3/4"			
2B	1-D	P56-8	129'-6"	1	5'-0"	3'-10 3/4"	A	7'-3"	59'-0"	85'-0"	B	136'-9"	2	139'-0"	3'-10 3/16"	33 7/16"	5490.71"	44,367
	1-E	P56-8	129'-6"				C	141'-3"	193'-0"	219'-0"	D	270'-9"	3	273'-0"	3'-10 3/16"			
	1-F	P56-8	129'-6"				E	275'-3"	327'-0"	353'-0"	F	404'-9"	4	407'-0"	3'-10 3/4"			
3B	1-G	P56-8	129'-6"	1	5'-0"	3'-10 3/4"	A	7'-3"	59'-0"	85'-0"	B	136'-9"	2	139'-0"	3'-10 3/16"	33 7/16"	5490.71"	44,367
	1-H	P56-8	129'-6"				C	141'-3"	193'-0"	219'-0"	D	270'-9"	3	273'-0"	3'-10 3/16"			
	1-I	P56-8	129'-6"				E	275'-3"	327'-0"	353'-0"	F	404'-9"	4	407'-0"	3'-10 3/4"			
4B	1-J	P56-8	129'-6"	1	5'-0"	3'-10 3/4"	A	7'-3"	59'-0"	85'-0"	B	136'-9"	2	139'-0"	3'-10 3/16"	33 7/16"	5488.07"	44,367
	1-K	P56-8	129'-6"				C	141'-3"	193'-0"	219'-0"	D	270'-9"	3	273'-0"	3'-10 3/4"			
5B	1-L	P56-8	129'-6"	1	5'-0"	3'-10 3/4"	A	7'-3"	59'-0"	85'-0"	B	136'-9"	2	139'-0"	3'-10 3/16"	33 7/16"	5488.07"	44,367
	1-M	P56-8	129'-6"				C	141'-3"	193'-0"	219'-0"	D	270'-9"	3	273'-0"	3'-10 3/4"			

Approved for Fabrication
4-10-2014

NOTE
BEAM LENGTHS SHOWN ARE MEASURED ALONG CENTERLINE OF BEAM. LENGTHS SHOWN DO NOT INCLUDE AN ALLOWANCE FOR ELASTIC SHORTENING.

Revision Legend

Mark	Date	Description	By
2	4/2/14	adj. beam length on all tables of dimensions	bc

Contractor
Johnson Bros. Corp.
Lithia, Florida

Engineer
State of Louisiana
Department of Transportation
& Development

I-210 Over Cove Lane
State Project No. H.010151
Calcasieu Parish, Louisiana
Table of Dimensions ~ LG-54 Beams

LDOTD

Job Number: 13-81
Drawing: 1381-Table
Sheet Number: 8 of 8
Date: 3/6/2014
Drawn By: dl
Checked: bec

GULF COAST PRE-STRESS

09/19/2014

CYLINDER BREAK/POUR SUMMARY

1:40 pm

JOB NUMBER: 13-81 **PROJECT:** I-210: COVE LANE INTERCHANGE
PRODUCT: LG-54 GIRDERS H.010151.6

POUR NO	AGE	AIR	SLUMP	DESIGN	CAST DATE	CYLINDER MARK	CYL. BREAK	BREAK DATE	AGE
1	69	3.80	7.75	10000 psi	07/12/14	A	8834 psi	08/11/14	30
						B	8896 psi	09/08/14	58
						G	7279 psi	07/14/14	2
						H	7039 psi	07/16/14	4
						I	9686 psi	09/08/14	58
						J	8982 psi	08/11/14	30
						K	7431 psi	07/15/14	3
						L	8572 psi	08/11/14	30
						O	8260 psi	07/16/14	4
						R	7666 psi	07/15/14	3
						T	8959 psi	09/08/14	58
						U	7860 psi	07/16/14	4
						W	7305 psi	07/14/14	2
2	73	4.80	9.25	10000 psi	07/08/14	A	10362 psi	07/22/14	14
						B	10138 psi	08/05/14	28
						F	10670 psi	09/03/14	57
						H	8963 psi	07/09/14	1
						J	8534 psi	07/09/14	1
						L	10150 psi	09/03/14	57
						M	10099 psi	08/05/14	28
						N	9475 psi	07/22/14	14
						R	10566 psi	09/04/14	58
						V	10088 psi	08/05/14	28
						X	8906 psi	07/09/14	1
3	62	3.30	7.25	10000 psi	07/19/14	1-G 1	10397 psi	09/18/14	61
						1-G 2	10006 psi	09/18/14	61
						1-J 1	10165 psi	09/18/14	61
						1-J 2	10573 psi	09/18/14	61
						1-K 1	10090 psi	09/18/14	61
						1-K 2	10520 psi	09/18/14	61
						C	9514 psi	09/13/14	56
						E	9536 psi	08/18/14	30
						H	8914 psi	07/21/14	2
						N	9846 psi	09/13/14	56
						O	8861 psi	07/21/14	2
						Q	9885 psi	09/13/14	56
						X	8664 psi	07/21/14	2
4	59	1.50	6.50	10000 psi	07/22/14	F	9381 psi	09/16/14	56
						G	8771 psi	08/19/14	28
						H	7529 psi	07/23/14	1
						N	10381 psi	09/16/14	56

From: Quality Control Fax: +1 (228) 202-1065 To: Bryan Carver Fax: +1 (228) 462-9495 Page 3 of 4 09/19/2014 1:58

MATT MENU SELECTION - 30

1381

DOTD 03-22-073
Metric / English
Rev. 07/98

LOUISIANA DEPARTMENT OF TRANSPORTATION AND DEVELOPMENT
PORTLAND CEMENT CONCRETE MIX DESIGN

Metric / English [E] *(M / E) Located on MATT Menu*

Project No. [H.010151.6] Material Use [S] *P = Pavement S = Structural* Plant Code [0110] Material Code [624]

Type / Class P / P(M) Plant Name GULF COAST PRE-STRESS INC. Mix Design No. [244] Slip Form Paving [N] *Y = Yes N = No*

Mixing Method [2] *1 = Truck Mixer, 2 = Central Mixer, 3 = Site Mixer* Parish Calcasieu Proj. Name I-120 Cove lane Interchange F. A. P.

Materials

	Source Code	Company Name	Location	Mat. Code	Alk. React. *Y = Yes N = No*	Spec. Grav.	Absorp. Factor	Product Name
Cement	0754	HOLCIM, INC. (T/III)	THEODORE, AL.	058		3.15		
Fly Ash								
Slag								
Fine Aggregate	AY03	LAFARGE	HONEY ISLAND, LA.	870	N	2.62	0.5	
Coarse Aggr. 1	AY03	LAFARGE	HONEY ISLAND, LA.	885	N	2.51	2.5	
Coarse Aggr. 2								
Water Reducer	58DP	BASF ADMIXTURES	Normal Set [N] *Y = Yes N = No*		Set Retarder [Y] *Y = Yes N = No*			POZZOLITH 100XR
Air Entrainer								
Set Accelerator			Chloride [ ] *Y = Yes N = No*		Non-Chloride [ ] *Y = Yes N = No*			
Superplasticizer	58FD	BASF ADMIXTURES						GLENIUM 7700
Special Additive A								
Special Additive B								
Special Additive C								

Mixing Water: [1] *1 = City, 2 = Well, 3 = Othe*

Mix Proportions For One Cubic Meter (Cubic Yard) of Concrete

			UNIT
Cement	705	kg (lb)	
Fly Ash		kg (lb)	
Slag		kg (lb)	
Fine Aggregate (SSD)	1435	kg (lb)	
Coarse Aggregate 1 (SSD)	1675	kg (lb)	
Coarse Aggregate 2 (SSD)		kg (lb)	
Water	29.5	L (gal)	
Water Reducer	10.00	mL (oz)	kg, L, mL
Air Entrainer		mL (oz)	(lg, gal, oz)
Set Accelerator		mL (oz)	
Superplasticizer	35.00	mL (oz)	
Special Additive A			
Special Additive B			
Special Additive C			

Contractor Johnson Bros.Corp.

Certified Concrete Technician LARRY NICELEY [1294] Code

Date Submitted [12-17-13]

Departmental Use

Yield		m^3 (ft^3)
Cement Factor		kg / m^3 (bag / yd^3)
Fly Ash		% by Mass (Wt.)
Slag		% by Mass (Wt.)
Water-Cement Ratio		L / m^3 (gal / bag)
Water-Cement Ratio		By Mass (Wt.)
Cement with 0.6% or less Alkalies required		*Y = Yes N = No*

Date Received [- -] ACCEPTED [ ] REJECTED [ ]

District Laboratory Engineer Code Date

Acceptance based on mix proposal meeting spec. requirements for yield, cement factor, water-cement ratio, materials sources, cement type, admixture types, special additive, MATT codes, & results of trial batches

Remarks [GRADE P ((S)ZE 67)]

Page 2 of 4 09/19/2014 1:58
Fax: +1 (228) 452-9495
To: Bryan Carver
Fax: +1 (228) 202-1000
From: Wendy Cotton

APPENDIX B. INSTRUMENTATION PLAN

This appendix includes details regarding the location of different sensors along each girder's length and at the different cross-sections. Data sheets on the various gages as well as the data acquisition system are also provided.

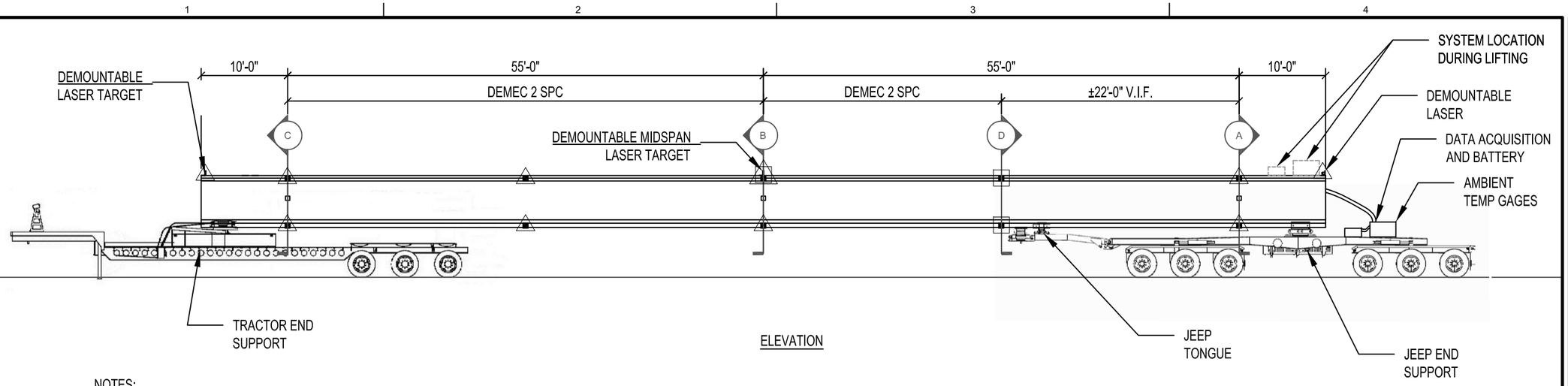

ELEVATION

NOTES:

1. STRAIN GAGES: ALL INTERNAL GAGES TO BE MICROMEASUREMENTS EGP-5-250. GAGES NEED TO BE INSTALLED PRIOR TO CASTING. ESTIMATED TIME TO MOUNT IS 15 MIN/GAGE.
2. DEMEC (DEMOUNTABLE MECHANICAL STRAIN GAGE) SHALL BE MOUNTED AFTER FORMS ARE STRIPPED, BUT PRIOR TO RELEASE.
3. ALL WIRES WILL RUN ALONG TOP OF GIRDER TO SECTION A.

SYMBOL LEGEND:	INSTRUMENTATION PHASE:
DEMEC	PHASE 1 SYMBOLS
TEMP	PHASE 2 SYMBOLS
STRAIN	PHASE 3 SYMBOLS
BDI	

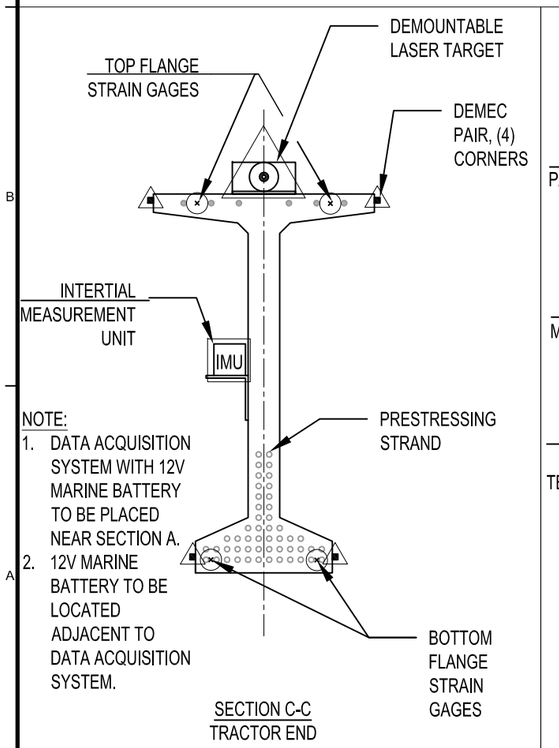

NOTE:

1. DATA ACQUISITION SYSTEM WITH 12V MARINE BATTERY TO BE PLACED NEAR SECTION A.
2. 12V MARINE BATTERY TO BE LOCATED ADJACENT TO DATA ACQUISITION SYSTEM.

SECTION C-C
TRACTOR END

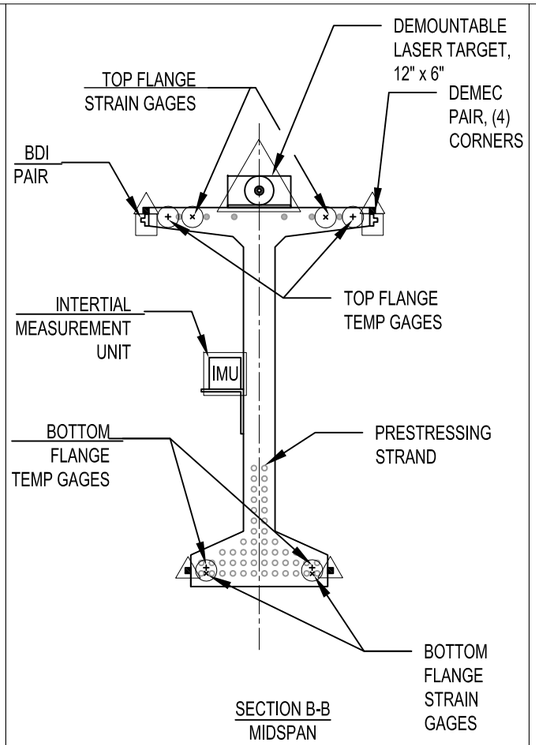

SECTION B-B
MIDSPAN

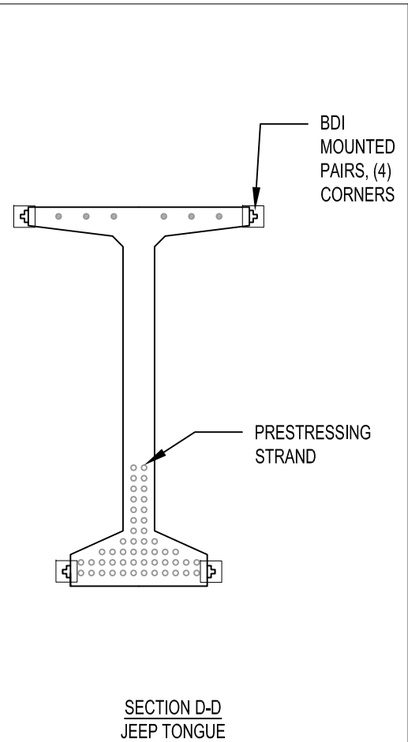

SECTION D-D
JEEP TONGUE

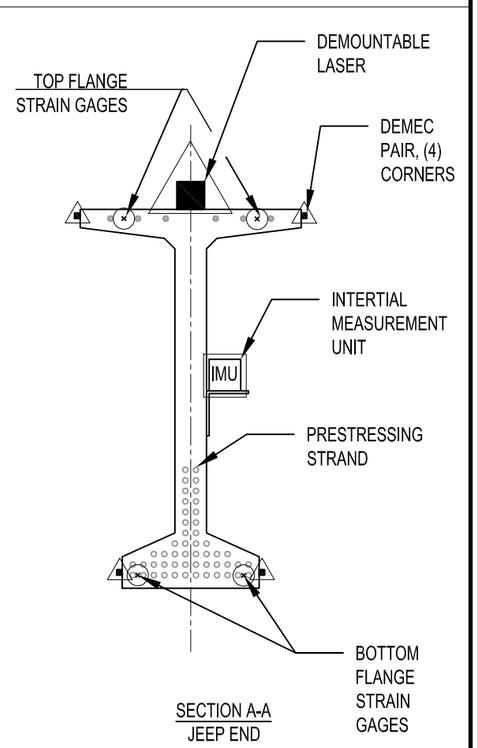

SECTION A-A
JEEP END

© Copyright 2016. All rights reserved. No part of this document may be reproduced in any form or by any means without permission from Wiss, Janney, Elstner Associates, Inc. (WJE). WJE disclaims any responsibility for its unauthorized use.

WJE ENGINEERS ARCHITECTS MATERIALS SCIENTISTS

Wiss, Janney, Elstner Associates, Inc.
330 Pfingsten Road
Northbrook, Illinois 60062
847.272.7400 tel | 847.291.5189 fax
www.wje.com

Headquarters & Laboratories: Northbrook, Illinois
Atlanta | Austin | Boston | Chicago | Cleveland | Dallas | Denver | Detroit
Honolulu | Houston | Los Angeles | Minneapolis | New Haven | New York
Princeton | San Francisco | Seattle | Washington, D.C.

Seal

Consultant

Project

LTRC 10-5ST
DEVELOPMENT OF GUIDELINES FOR TRANSPORTATION OF PRESTRESSED GIRDERS

Client

LOUISIANA DOTD

Mark	Date	Description

Project No.	2010.5518
Date	10/25/2011
Drawn	EJK
Checked	REL
Scale	NTS

INSTRUMENTATION PLAN
BT72

Sheet Title: BT72

Sheet No.: **I-1**

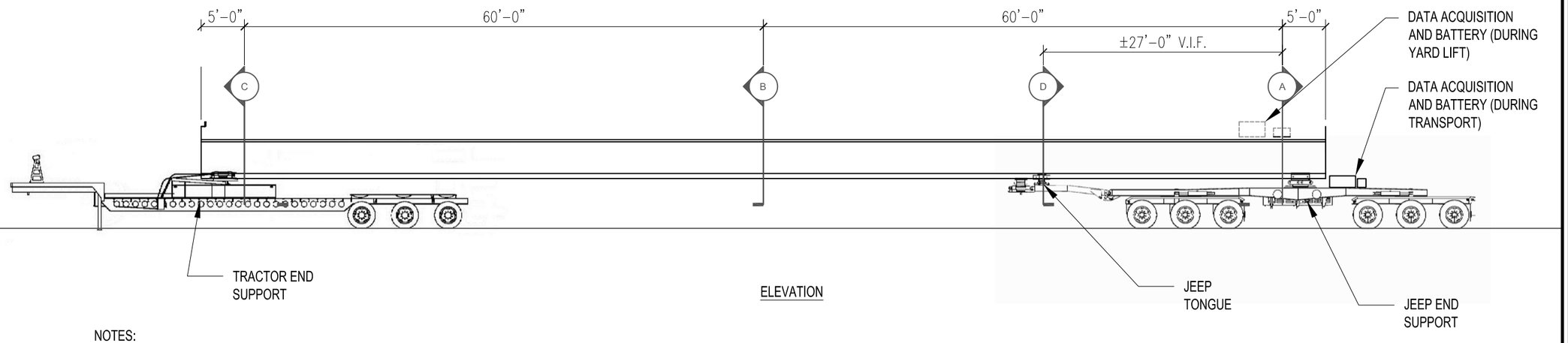

ELEVATION

NOTES:

1. STRAIN GAGES: ALL STRAIN GAGES TO BE BDI ST-350 STRAIN TRANSDUCERS, UNO.
2. ALL WIRES WILL RUN ALONG TOP OF GIRDER TO SECTION C.
3. STRAIN GAGES/ TRANSDUCERS TO BE PLACED AT APPROXIMATE ELEVATION OF STEEL REINFORCEMENT.

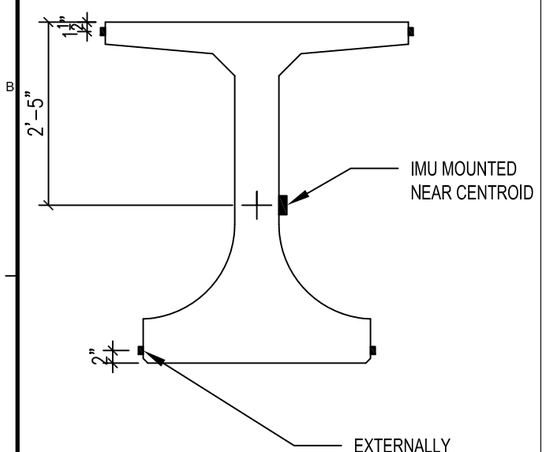

SECTION C-C
TRACTOR END

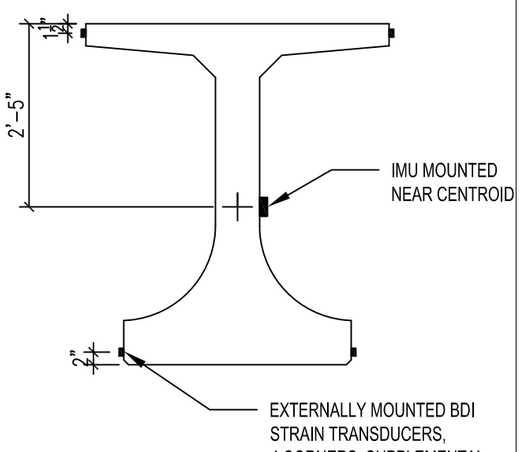

SECTION B-B
MIDSPAN

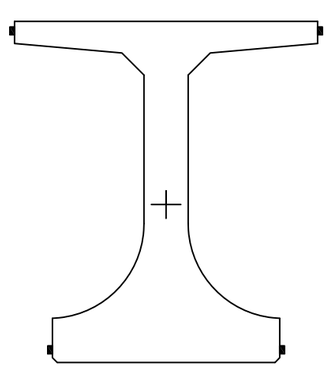

SECTION D-D
JEEP TONGUE

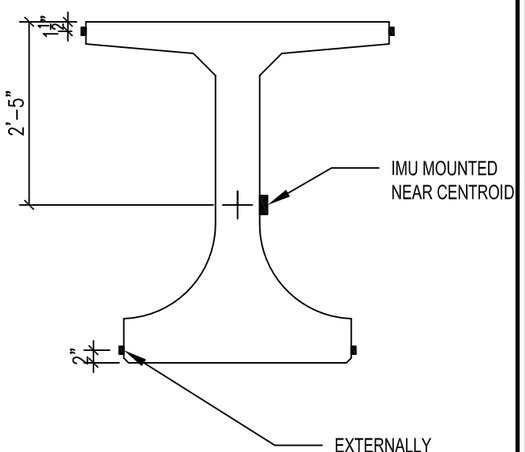

SECTION A-A
JEEP END

© Copyright 2016. All rights reserved. No part of this document may be reproduced in any form or by any means without permission from Wiss, Janney, Elstner Associates, Inc. (WJE). WJE disclaims any responsibility for its unauthorized use.

WJE ENGINEERS ARCHITECTS MATERIALS SCIENTISTS

Wiss, Janney, Elstner Associates, Inc.
330 Pfingsten Road
Northbrook, Illinois 60062
847.272.7400 tel | 847.291.5189 fax
www.wje.com

Headquarters & Laboratories: Northbrook, Illinois
Atlanta | Austin | Boston | Chicago | Cleveland | Dallas | Denver | Detroit
Honolulu | Houston | Los Angeles | Minneapolis | New Haven | New York
Princeton | San Francisco | Seattle | Washington, D.C.

Seal

Consultant

Project
LTRC 10-5ST
DEVELOPMENT OF GUIDELINES FOR TRANSPORTATION OF PRESTRESSED GIRDERS

Client
LOUISIANA DOTD

Mark	Date	Description

Project No.	2010.5518
Date	2/12/2016
Drawn	REL
Checked	REL
Scale	NTS

INSTRUMENTATION PLAN
130 FT LG54 GIRDER

Sheet Title

Sheet No. **I-1**

Special Use Sensors - Concrete Embedment Strain Gages

The EGP-Series Embedment Strain Gage is specially designed for measuring mechanical strains inside concrete structures. The sensing grid, constructed of a nickel-chromium alloy (similar to Karma), has an active gage length of 4 in [100 mm] for averaging strains in aggregate materials. A rugged 5 in [130 mm] outer body of proprietary polymer concrete resists mechanical damage during pouring, minimizes reinforcement of the structure, and provides protection from moisture and corrosive attack. The grid, cast within the polymer concrete to ensure maximum strain sensitivity, is self-temperature-compensated to minimize thermal output when installed in concrete structures. Each gage incorporates a heavy-duty 10 ft [3 m] cable with 22-AWG [0.643 mm dia.] leadwires; a three-wire construction to the sensing grid helps minimize temperature effects in the instrumentation leads. Special lengths of preattached cable will be quoted upon request. Micro-Measurements M-LINE accessory cable 322-DJV is available for adding cable length in the field.

Rugged and reliable, EGP-Series Strain Gages are available in both 120-ohm (EGP-5-120) and 350-ohm (EGP-5-350) resistances.

SPECIFICATIONS

- Construction. Strain sensing grid cast in a sturdy, water-resistant material.
- Sensing Grid. Nickel-chromium alloy on polyimide backing. Active gage length of 4 in [100 mm] nominal. Grid resistance of 120 or 350 ohms, ±0.8%.
- Outer Body. Proprietary polymer concrete. 5 x 0.7 x 0.4 in [130 x 17 x 10 mm] nominal.
- Cable. Three 10 ft [3 m] leads of 22-AWG [0.643 mm dia.] stranded tinned copper in 0.015 in [0.4 mm] thick PVC insulation. Nominal cable diameter of 0.2 in [5 mm]. (Other lengths quoted upon request.)
- Temperature Range. The normal usage range is +25° to +125°F [–5° to +50°C]. Extended range is –25° to +150°F [–30° to +60°C].

EMBEDMENT GAGE SELECTION

GAGE DESIGNATION (Pb-free RoHS COMPLIANT)	RES. IN OHMS	DIMENSIONS (inch / millimeter)			
		ACTIVE GAGE LENGTH	OUTER BODY WIDTH	OUTER BODY LENGTH	OUTER BODY THICKNESS
EGP-5-120	120 ± 0.8%	4	0.7	5	0.4
		100	17	130	10
EGP-5-350	350 ± 0.8%	4	0.7	5	0.4
		100	17	130	10

Disclaimer

All product specifications and data are subject to change without notice.

Vishay Precision Group, Inc., its affiliates, agents, and employees, and all persons acting on its or their behalf (collectively, “Vishay Precision Group”), disclaim any and all liability for any errors, inaccuracies or incompleteness contained herein or in any other disclosure relating to any product.

Vishay Precision Group disclaims any and all liability arising out of the use or application of any product described herein or of any information provided herein to the maximum extent permitted by law. The product specifications do not expand or otherwise modify Vishay Precision Group’s terms and conditions of purchase, including but not limited to the warranty expressed therein, which apply to these products.

No license, express or implied, by estoppel or otherwise, to any intellectual property rights is granted by this document or by any conduct of Vishay Precision Group.

The products shown herein are not designed for use in medical, life-saving, or life-sustaining applications unless otherwise expressly indicated. Customers using or selling Vishay Precision Group products not expressly indicated for use in such applications do so entirely at their own risk and agree to fully indemnify Vishay Precision Group for any damages arising or resulting from such use or sale. Please contact authorized Vishay Precision Group personnel to obtain written terms and conditions regarding products designed for such applications.

Product names and markings noted herein may be trademarks of their respective owners.

BDI
Bridge Diagnostics Inc

- Bridge Testing & Rating Services
- Structural Testing Equipment
- Long-Term Monitoring
- Fatigue Monitoring Systems

BDI Strain Transducer ST-350

The most direct approach to quantifying live-load stresses in a structural member is to record the induced strains. However, it can be tedious work to install foil strain gages since careful surface preparation and soldering is often required. Now, many traditional strain gage installations can be replaced with the highly accurate BDI Strain Transducer. These units are rugged and can be installed in any weather. Since they are pre-wired and easy to mount, BDI Strain Transducers will drastically reduce your testing time!

Highlights

- Very cost effective
- Install in 5 minutes or less
- Completely reusable - never wears out!
- Water and weather resistant
- Custom cable types and lengths available
- Compatible with most data acquisition systems
- The BDI Strain Transducer was one of ***Sensors*** **Magazine's 50 Top Products of 2006**!

BDI Intelliducer

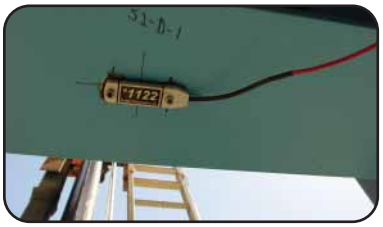

Girders

Reinforced Concrete

Trusses

Many Applications

Measure strains on highway bridges, railroad bridges, navigation lock gates, amusement park rides, and other structures in which a short-term live-load can be easily applied. Also excellent for many laboratory tests and manufacturing processes. The BDI Strain Transducers have been successfully used for measurements on:

- **Steel Structures**
- **Post-tensioned and pre-stressed concrete structures**
- **Reinforced concrete structures**
- **Timber structures**
- **Fiber reinforced polymer structures**

Key Features

- **Easy Installation:** Attaches to all types of structural members in about five minutes each. Instrument and test with 64 strain channels in one day!
- **High Output:** Provides approximately 3 times the output as a typical quarter-arm foil gage installation. This improved signal-to-noise ratio means higher-resolution measurements.
- **Excellent Compatibility:** The BDI Strain Transducers can be used with most data acquisition systems that support full-bridge type sensors, or with our specially-designed BDI Structural Testing System (BDI-STS).
- **Very Cost-Effective:** Due to their complete re-usability and the extensive reduction in installation time, the BDI Strain Transducers will pay for themselves with just a few uses.
- **Field Proven:** These sensors have been used over the last two decades for recording millions of strain measurements on all types of structures, often in harsh field conditions.

Bridge Diagnostics, Incorporated
1965 57th Court North, Suite 106
Boulder, CO 80301-2826 USA
www.bridgetest.com
303.494.3230

Bridge Diagnostics Inc
"We stand below our work"

BDI Strain Transducer ST-350

Options and Accessories

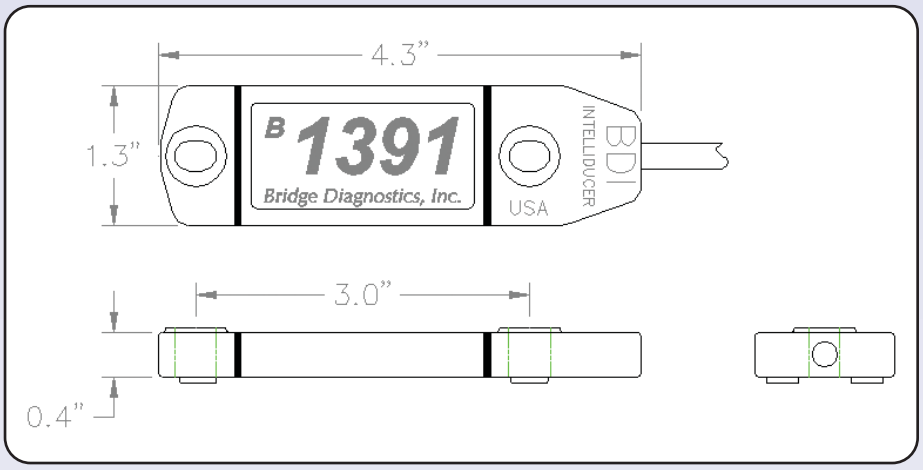

BDI transducers have a 3" gage length

Strain transducers are supplied as standard equipment with BDI Structural Testing Systems

Gage extensions for measuring "averaged" strains on reinforced concrete members

Rugged aluminum covers protect transducers for long-term monitoring

Technical Specifications	
Effective gage length	3.0 in (76.2 mm). Extensions available for use on R/C structures
Overall Size	4.375 in x 1.25 in x 0.5 in (111 mm x 32 mm x 13 mm)
Cable Length	10 ft (3 m) standard, any length available
Material	Aluminum
Circuit	Full wheatstone bridge with 4 active 350W foil gages, 4-wire hookup
Accuracy	± 2%, individually calibrated to NIST standards
Strain Range	Aluminum: ±4000 με
Force required for 1000 με:	Approximately 17 lbs. (76 N)
Sensitivity	Approximately 500 με/mV/V
Weight	Approximately 3 oz. (85 g)
Environmental	Built-in protective cover, also water resistant
Temperature Range	-60°F to 250°F (-50°C to 120°C) operation range
Cable	BDI RC-187: 22 gage, two individually-shielded pairs w/drain
Attachment Methods	Mounting tabs & adhesive, C-Clamps, masonry or wood screws

Mounting tabs and tab jig

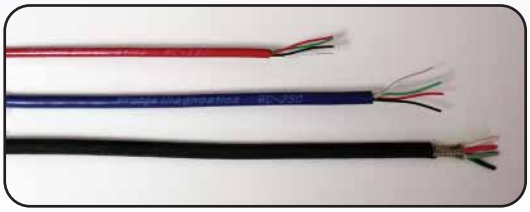

BDI Strain Transducer cable options

Model 801 Tuff Tilt

Uniaxial Tiltmeter

The Model 801 Tuff Tilt Uniaxial Tiltmeter combines precision and durability in an economical instrument. It incorporates a gravity-referenced electrolytic tilt transducer as the internal sensing element, delivering high dynamic range and long-term stability. Housed in a rugged weatherproof enclosure, this analog output tiltmeter may be used outdoors and in other wet environments.

TUFF TILT APPLICATIONS INCLUDE:

- Antenna leveling and tracking (Model 801-H)
- Monitoring of bridges and structures (Model 801-S)
- Rotary position of dam gates and other machinery (Model 801-W)

APPLIED GEOMECHANICS

1+415-364-3200 ● Geomechanics.com

	MODEL 801-H HIGH-GAIN VERSION	MODEL 801-S STANDARD VERSION	MODEL 801-W WIDE-ANGLE VERSION
ANGULAR RANGE	±0.5 degrees	±3 degrees	±50 degrees*
SCALE FACTOR†	0.1°/ volt (single-ended)	0.6°/ volt (single-ended)	10°/ volt (single-ended)
RESOLUTION	<0.0001 degree (<1.75 µradians)	0.0006 degree (10.5 µradians)	0.01 degree
REPEATABILITY	<0.0002 degree	0.001 degree	0.02 degree
LINEARITY	1% of full span typical	<2% of full span typical	0.5% of full span typical
TEMPERATURE COEF.	Scale factor: KS < 0.02%/°C typ. Zero shift: KZ = ±0.0002 degree/°C	KS < 0.02%/°C typ. KZ = ±0.0002 degree/°C typ.	KS < 0.02%/°C typ. KZ = ±0.002 degree/°C typ.
TIME CONSTANT, T	0.35 second (settling time: 1.75 seconds) 2-pole Butterworth low-pass filter, faster response available		0.03 second (settling time: 0.15 second)
TILT OUTPUT	± 5 VDC single-ended, ±10 VDC differential (both provided)		
TEMPERATURE OUTPUT	0.1°C/mV (single-ended), –40° to +100°C, ±0.75°C accuracy, 0°C = 0 mV		
OUTPUT IMPEDANCE	270 Ohms, short circuit and surge protected		
POWER REQ'TS.	+8 to +18 VDC @ 8 mA, 250 mV peak-to-peak ripple max., reverse polarity protected		
ENVIRONMENTAL	–25° to +70° C operating, –30° to +100° C storage; NEMA 4X (IP-65) (wet conditions, nonsubmersible)		
ENCLOSURE & MOUNTING	Painted, die-cast aluminum box, 120 x 80 x 60 mm. Four 4.4 mm dia. mounting holes on 107 x 67 mm (4.21 x 2.64 in) centers		
CABLE	3m (10 ft), 6-conductor + one overall shield, PVC jacket, tinned ends		
WEIGHT	0.6 kg (1.5 lb)		

* greater range available † Divide by 2 for differential scale factor.

CONNECTOR PIN	FUNCTION	WIRE COLOR
A	+12 VDC	Red
B	Signal Ground	White
C	Power Ground	Black
D	+Tilt Out	Green
E	-Tilt Out	Blue
F	Temperature Out	Yellow

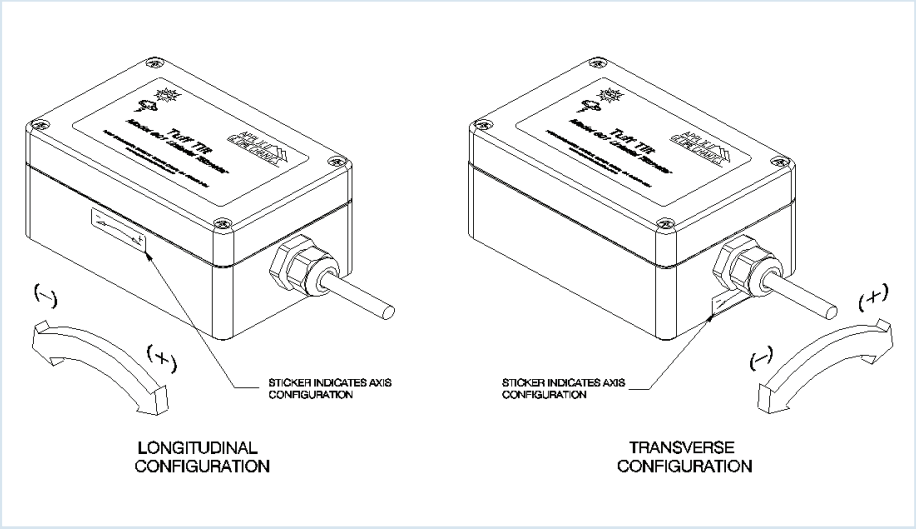

ORDER CODES:

Model A801– □□

- **L**ongitudinal
- **T**ransverse
- **H**igh gain
- **S**tandard gain
- **W**ide angle

USEFUL ACCESSORIES:

70369	Additional cable, please specify length
62204	6-pin male receptacle (connector) for tiltmeter cable
62202	6-socket female plug (mates to P/N 62204)
81439	Mounting bracket for vertical surfaces, with mounting hardware
84051	Horizontal mounting plate (speeds installation) with mounting hardware
Model 870	Readout module for digital display (requires P/N 62204 & multimeter)
ADVisor	Handheld readout unit & datalogger

APPLIED GEOMECHANICS , INC.
140 Chestnut St.
San Francisco, CA 94111
T: +1-415-364-3200
F: +1-415-861-1448
geomechanics.com
A CARBO Company

APPLIED GEOMECHANICS®

©2009 Applied Geomechanics, Inc. All Rights Reserved. 09.09/X

MEMSIC *Powerful Sensing Solutions for a Better Life*

VG350
VERTICAL GYRO SYSTEM

The MEMSIC VG350 is a robust entry-level Vertical Gyro System that utilizes MEMS-based inertial sensors and Extended Kalman Filter algorithms to provide unmatched value in terms of both price and performance. The VG350 is widely accepted in dynamic control and land navigation systems with over 1500 systems currently in service.

Antenna Stabilization

Precision Agriculture

This rugged low-cost inertial system meets the demanding environmental requirements for operation in a wide variety of land vehicle and marine platform systems, and it is ideally suited for cost-sensitive high-volume OEM applications.

Features

- Angle, Rate and Accel Data at 100Hz
- High Reliability MEMS Sensors
- Enhanced Performance Kalman Filter Algorithm
- Wide Temp Range (-40°C to +70°C)
- Wide Input Power Range (9-30V)
- Low Profile <1.5"
- Lightweight <0.5lbs

Applications

- Antenna Stabilization
- Ground Vehicle Navigation
- Precision Agriculture

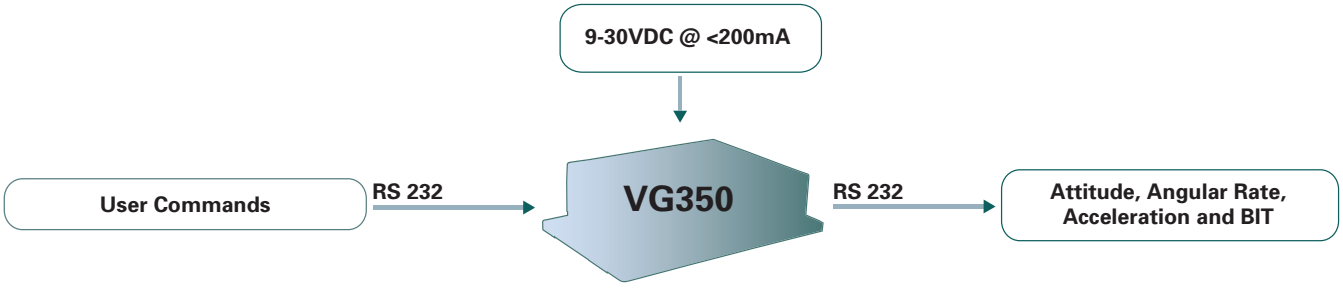

Phone: 408.964.9700 | Fax: 408.854.7702 | E-mail: infoca@memsic.com | www.memsic.com

VG350
VERTICAL GYRO SYSTEM

Performance

Performance	VG350
Attitude	
Range: Roll, Pitch (°)	± 180, ± 90
Dynamic Accuracy[1] (°)	< 0.75
Resolution (°)	< 0.1
Angular Rate	
Range: Roll, Pitch, Yaw (°/sec)	± 300
Bias Stability In-Run[2] (°/hr)	< 12
Bias Stability Over Temp (°/sec)	< ± 0.5
Scale Factor Accuracy (%)	< 1
Non Linearity (%FS)	< 1
Resolution (°/sec)	< 0.02
Angle Random Walk (°/sq-rt hr)	< 3
Bandwidth (Hz)	50
Acceleration	
Input Range: X/Y/Z (g)	± 3
Bias Stability In-Run[2] (mg)	< 1
Bias Stability Over Temp (g)	< ± 0.015
Scale Factor Accuracy (%)	< 1
Non Linearity (%FS)	< 1
Resolution (mg)	< 0.5
Velocity Random Walk (m/s/sq-rt hr)	< 1
Bandwidth (Hz)	50

Specifications

Environment		
Operating Temperature (°C)		-40 to +70
Non-Operating Temperature (°C)		-55 to +70
Electrical		
Input Voltage (VDC)		9 to 30
Power Consumption (W)		< 3
Digital Interface		RS-232
Physical		
Size	(in)	2.50 x 2.50 x 1.50 (excl. flanges)
	(cm)	6.35 x 6.35 x 3.81 (excl. flanges)
Weight	(lbs)	< 0.5
	(kg)	< 0.23
Connector		DSub-9, Male
Reliability		
MTBF (hours)		>35,000

Ordering Information

Model	Description
VG350CA-300	Vertical Gyroscope

This product has been developed exclusively for commercial applications. It has not been tested for, and makes no representation or warranty as to conformance with, any military specifications or its suitability for any military application or end-use. Additionally, any use of this product for nuclear, chemical or biological weapons, or weapons research, or for any use in missiles, rockets, and/or UAV's of 300km or greater range, or any other activity prohibited by the Export Administration Regulations, is expressly prohibited without the written consent and without obtaining appropriate US export license(s) when required by US law. Diversion contrary to U.S. law is prohibited. Specifications are subject to change without notice. Notes: [1] 1-sigma, MEMSIC aggressive drive test. [2] 1-sigma, constant temperature, Allan Variance curve.

NAV-VIEW 3.0 Configuration & Display Software

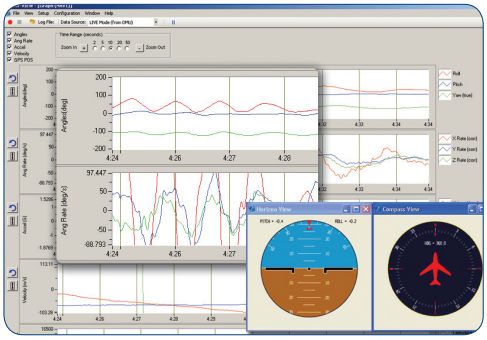

NAV-VIEW 3.0 provides an easy to use graphical interface to display, record and analyze all of the VG350 measurement parameters.

Other Components

Each VG350 is shipped with an interface cable, MEMSIC's User's Manual and NAV-VIEW 3.0 configuration and display software.

Support

For more detailed technical information please refer to the 350-Series User's Manual available online at: www.memsic.com/Support

Technical Sales
United States
(866) 531-6285
info@ni.com

Last Revised: 2011-04-14 16:59:41.0

Real-Time Controller with 256 MB DRAM, 2 GB Storage

NI cRIO-9022

- Small and rugged real-time embedded controller
- Execution target for LabVIEW Real-Time applications
- Reliable and deterministic operation for stand-alone control, monitoring, and logging
- 533 MHz Freescale MPC8347 real-time processor
- Dual Ethernet ports for deterministic expansion I/O
- -20 to 55 °C operating temperature range
- RS232 serial port for connection to peripherals; dual 9 to 35 VDC supply inputs
- Hi-Speed USB host port for connection to USB flash and memory devices

Overview

The NI cRIO-9022 embedded real-time controller is part of the high-performance CompactRIO programmable automation controller (PAC) platform. It features an industrial 533 MHz Freescale MPC8347 real-time processor for deterministic, reliable real-time applications and contains 256 MB of DDR2 RAM and 2 GB of nonvolatile storage for holding programs and logging data.

Back to Top

Requirements and Compatibility

OS Information

- VxWorks

Driver Information

- NI-RIO

Software Compatibility

- LabVIEW
- LabVIEW FPGA Module
- LabVIEW Professional Development System
- LabVIEW Real-Time Module

Back to Top

Application and Technology

System Configuration

The NI cRIO-9022 controller features an industrial 533 MHz Freescale MPC8347 real-time processor for deterministic and reliable real-time applications. This embedded controller is designed for extreme ruggedness, reliability, and low power consumption with dual 9 to 35 VDC supply inputs that deliver isolated power to the CompactRIO chassis and a -20 to 55 °C operating temperature range. The cRIO-9022 accepts 9 to 35 VDC power supply inputs on power-up and 6 to 35 VDC power supply inputs during operation, so it can function for long periods of time in remote applications using a battery or solar power. With the 10/100 Mbits/s and 10/100/1000 Mbits/s Ethernet and serial ports, you can communicate via TCP/IP, UDP, Modbus/TCP, and serial protocols. The cRIO-9022 also features built-in Web (HTTP) and file (FTP) servers and a Hi-Speed USB host port to which you can connect external USB-based storage media (flash drives and hard drives) for embedded logging applications requiring more data storage. In addition, the cRIO-9022 incorporates a fault-tolerant file system that provides increased reliability for data logging. CompactRIO real-time controllers connect to any four- or eight-slot NI cRIO-911x reconfigurable chassis. The embedded field-programmable gate array (FPGA) in the chassis controls each I/O module and passes data to the controller through a local PCI bus using built-in communications functions.

The CompactRIO real-time controller connects to any four- or eight-slot CompactRIO reconfigurable chassis. The user-defined FPGA circuitry in the chassis controls each I/O module and passes data to the controller through a local PCI bus, using built-in communication functions.

Embedded Software

The cRIO-9022 runs NI LabVIEW Real-Time Module software on the Wind River VxWorks real-time operating system (RTOS) for extreme reliability and determinism. You can now use leading VxWorks RTOS technology and LabVIEW graphical programming tools to quickly design, prototype, and deploy a customizable, commercial off-the-shelf embedded system.

You can synchronize embedded code execution to an FPGA-generated interrupt request (IRQ) or an internal millisecond real-time clock source. The LabVIEW Real-Time ETS OS provides reliability and simplifies the development of complete embedded applications that include time-critical control and acquisition loops in addition to lower-priority loops for postprocessing, data logging, and Ethernet/serial communication. Built-in elemental I/O functions such as the FPGA Read/Write function provide a communication interface to the highly optimized reconfigurable FPGA circuitry. Data values are read from the FPGA in integer format and then converted to scaled engineering units in the controller.

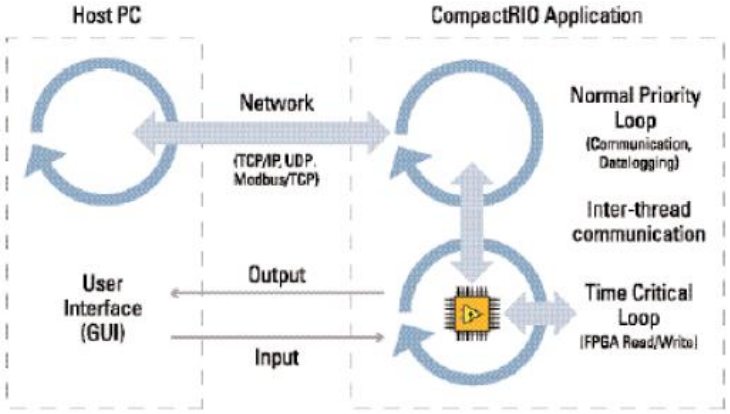

Figure 1. CompactRIO Software Architecture

Built-In Servers

In addition to programmatic communication via TCP/IP, UDP, Modbus/TCP, IrDA, and serial protocols, the CompactRIO controllers include built-in servers for Virtual Instrument Software Architecture (VISA), HTTP, and FTP. The VISA server provides remote download and communication access to the reconfigurable I/O (RIO) FPGA over Ethernet. The HTTP server provides a Web browser user interface to HTML pages, files, and the user interface of embedded LabVIEW applications through a Web browser plug-in. The FTP server provides access to logged data or configuration files.

Back to Top

Ordering Information

For a complete list of accessories, visit the product page on ni.com.

Products	Part Number	Recommended Accessories	Part Number
NI cRIO-9022			
cRIO-9022, Real-Time PowerPC Controller for cRIO, 533 MHz Requires:	780718-01	**Connector Block:** Not Applicable - NI 9978 4-pos screw terminal power supply plugs (quantity 5)	196938-01
		Connector Block: Not Applicable - NI 9979 Strain relief kit for 4-pos power connector	196939-01

Back to Top

Software Recommendations

LabVIEW Professional Development System for Windows

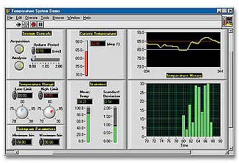

- Advanced software tools for large project development
- Automatic code generation using DAQ Assistant and Instrument I/O Assistant
- Tight integration with a wide range of hardware
- Advanced measurement analysis and digital signal processing
- Open connectivity with DLLs, ActiveX, and .NET objects
- Capability to build DLLs, executables, and MSI installers

NI LabVIEW FPGA Module

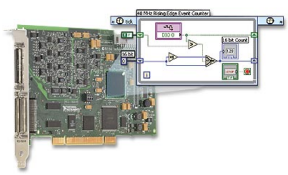

- Create your own I/O hardware without VHDL coding or board design
- Graphically configure FPGAs on NI reconfigurable I/O (RIO) hardware targets
- Define your own control algorithms with loop rates up to 200 MHz
- Execute multiple tasks simultaneously and deterministically
- Implement custom timing and triggering logic, digital protocols, and DSP algorithms
- Incorporate existing HDL code and third-party IP including Xilinx CORE Generator functions

NI LabVIEW Real-Time Module

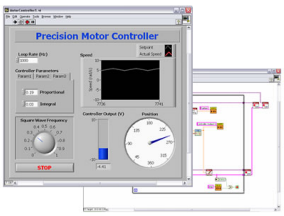

- Design deterministic real-time applications with LabVIEW graphical programming
- Download to dedicated NI or third-party hardware for reliable execution and a wide selection of I/O
- Take advantage of built-in PID control, signal processing, and analysis functions
- Automatically take advantage of multicore CPUs or set processor affinity manually
- Includes real-time operating system (RTOS), development and debugging support, and board support
- Purchase individually or as part of an NI Developer Suite bundle

Back to Top

Support and Services

System Assurance Programs

NI system assurance programs are designed to make it even easier for you to own an NI system. These programs include configuration and deployment services for your NI PXI, CompactRIO, or Compact FieldPoint system. The NI Basic System Assurance Program provides a simple integration test and ensures that your system is delivered completely assembled in one box. When you configure your system with the NI Standard System Assurance Program, you can select from available NI system driver sets and application development environments to create customized, reorderable software configurations. Your system arrives fully assembled and tested in one box with your software preinstalled. When you order your system with the standard program, you also receive system-specific documentation including a bill of materials, an integration test report, a recommended maintenance plan, and frequently asked question documents. Finally, the standard program reduces the total cost of owning an NI system by providing three years of warranty coverage and calibration service. Use the online product advisors at ni.com/advisor to find a system assurance program to meet your needs.

Calibration

NI measurement hardware is calibrated to ensure measurement accuracy and verify that the device meets its published specifications. NI offers a number of calibration services to help maintain the ongoing accuracy of your measurement hardware. These services allow you to be completely confident in your measurements, and help you maintain compliance to standards like ISO 9001, ANSI/NCSL Z540-1 and ISO/IEC 17025. To learn more about NI calibration services or to locate a qualified service center near you, contact your local sales office or visit ni.com/calibration.

Technical Support

Get answers to your technical questions using the following National Instruments resources.

- **Support** - Visit ni.com/support to access the NI KnowledgeBase, example programs, and tutorials or to contact our applications engineers who are located in NI sales offices around the world and speak the local language.
- **Discussion Forums** - Visit forums.ni.com for a diverse set of discussion boards on topics you care about.
- **Online Community** - Visit community.ni.com to find, contribute, or collaborate on customer-contributed technical content with users like you.

Repair

While you may never need your hardware repaired, NI understands that unexpected events may lead to necessary repairs. NI offers repair services performed by highly trained technicians who quickly return your device with the guarantee that it will perform to factory specifications. For more information, visit ni.com/repair.

Training and Certifications

The NI training and certification program delivers the fastest, most certain route to increased proficiency and productivity using NI software and hardware. Training builds the skills to more efficiently develop robust, maintainable applications, while certification validates your knowledge and ability.

- **Classroom training in cities worldwide** - the most comprehensive hands-on training taught by engineers.
- **On-site training at your facility** - an excellent option to train multiple employees at the same time.
- **Online instructor-led training** - lower-cost, remote training if classroom or on-site courses are not possible.
- **Course kits** - lowest-cost, self-paced training that you can use as reference guides.
- **Training memberships** and training credits - to buy now and schedule training later.

Visit ni.com/training for more information.

Extended Warranty

NI offers options for extending the standard product warranty to meet the life-cycle requirements of your project. In addition, because NI understands that your requirements may change, the extended warranty is flexible in length and easily renewed. For more information, visit ni.com/warranty.

OEM

NI offers design-in consulting and product integration assistance if you need NI products for OEM applications. For information about special pricing and services for OEM customers, visit ni.com/oem.

Alliance

Our Professional Services Team is comprised of NI applications engineers, NI Consulting Services, and a worldwide National Instruments Alliance Partner program of more than 600 independent consultants and integrators. Services range from start-up assistance to turnkey system integration. Visit ni.com/alliance.

Detailed Specifications

The following specifications are typical for the entire operating temperature range, – 20 to 55 °C, unless otherwise noted.

Network	
Network interface	
Ethernet port 1	10BaseT, 100BaseTX, and 1000BaseTX Ethernet
Ethernet port 2	10BaseT and 100BaseTX Ethernet
Compatibility	IEEE 802.3
Communication rates	
Ethernet port 1	10 Mbps, 100 Mbps, and 1000 Mbps, auto-negotiated
Ethernet port 2	10 Mbps, 100 Mbps, auto-negotiated
Maximum cabling distance	100 m/segment
RS-232 DTE Serial Port	
Baud rate	300–230,400 bps
Data bits	5, 6, 7, 8
Stop bits	1, 1.5, 2
Parity	Odd, even, mark, space, none
Flow control	RTS/CTS, XON/XOFF, DTR/DSR, none
USB Port	
Maximum data rate	480 Mb/s
Maximum current	500 mA
Memory	
Nonvolatile	2 GB
For information about the life span of the nonvolatile memory and about best practices for using nonvolatile memory, go to ni.com/info and enter the info code SSDBP.	
DRAM	256 MB
Internal Real-Time Clock	
Accuracy	200 ppm; 35 ppm at 25 °C
Integrated Voltage Input Monitor	
The integrated voltage input monitor underreports the voltage at the power connector by up to 400 mV because of voltage drops across internal circuits.	
Power Requirements	
Caution You must use a National Electric Code (NEC) UL Listed Class 2 power supply with the cRIO-9022.	
Recommended power supply	55 W secondary, 35 VDC max
Power consumption with controller supplying power to eight CompactRIO modules	35 W
Voltage requirement	
On powerup	9 to 35 V
After powerup	6 to 35 V
Note The cRIO-9022 is guaranteed to power up when 9 V is applied to V and C. After powerup, it can operate on as little as 6 V.	
Physical Characteristics	
If you need to clean the controller, wipe it with a dry towel.	
Screw-terminal wiring	12–18 AWG copper conductor wire with 10 mm (0.39 in.) of insulation stripped from the end
Torque for screw terminals	0.5 to 0.6 N · m (4.4 to 5.3 lb · in.)

Weight	Approx. 609 g (21.5 oz)

Environmental

The cRIO-9022 is intended for indoor use only. For outdoor use, mount the CompactRIO system in a suitably rated enclosure.

Operating temperature (IEC 60068-2-1, IEC 60068-2-2)	– 20 to 55 °C

Caution For information about how mounting configuration can affect the accuracy of C Series modules, go to ni.com/info and enter the info code rdcriotemp.

Storage temperature (IEC 60068-2-1, IEC 60068-2-2)	– 40 to 85 °C
Ingress protection	IP 40
Operating humidity (IEC 60068-2-56)	10 to 90% RH, noncondensing
Storage humidity (IEC 60068-2-56)	5 to 95% RH, noncondensing
Maximum altitude	2,000 m
Pollution Degree (IEC 60664)	2

Shock and Vibration

To meet these specifications for shock and vibration, you must panel mount or wall mount the CompactRIO system, affix ferrules to the ends of all terminal wires, install a strain relief on the power cable, and install tie wraps on the Ethernet and power cables. You can order the NI 9979, a strain-relief kit for the power cable, from National Instruments. The kit is NI part number 196939-01. For information about using the USB port in high shock and vibration environments, contact National Instruments.

Operating vibration	
Random (IEC 60068-2-64)	5 g_{rms}, 10 to 500 Hz
Sinusoidal (IEC 60068-2-6)	5 g, 10 to 500 Hz
Operating shock (IEC 60068-2-27)	30 g, 11 ms half sine, 50 g, 3 ms half sine, 18 shocks at 6 orientations

Safety

Safety Voltages

Connect only voltages that are within these limits.

V-to-C	35 V max, Measurement Category I

Measurement Category I is for measurements performed on circuits not directly connected to the electrical distribution system referred to as MAINS voltage. MAINS is a hazardous live electrical supply system that powers equipment. This category is for measurements of voltages from specially protected secondary circuits. Such voltage measurements include signal levels, special equipment, limited-energy parts of equipment, circuits powered by regulated low-voltage sources, and electronics.

Caution Do not connect to signals or use for measurements within Measurement Categories II, III, or IV.

Safety Standards

This product is designed to meet the requirements of the following standards of safety for electrical equipment for measurement, control, and laboratory use:

- IEC 61010-1, EN 61010-1
- UL 61010-1, CSA 61010-1

Note For UL and other safety certifications, refer to the product label or the *Online Product Certification* section.

Hazardous Locations

U.S. (UL)	Class I, Division 2, Groups A, B, C, D, T4; Class I, Zone 2, AEx nA IIC T4
Canada (C-UL)	Class I, Division 2, Groups A, B, C, D, T4; Class I, Zone 2, Ex nA IIC T4
Europe (DEMKO)	Ex nA IIC T4

Electromagnetic Compatibility

This product meets the requirements of the following EMC standards for electrical equipment for measurement, control, and laboratory use:

- EN 61326 (IEC 61326): Class A emissions; Industrial Immunity
- EN 55011 (CISPR 11): Group 1, Class A emissions
- AS/NZS CISPR 11: Group 1, Class A emissions
- FCC 47 CFR Part 15B: Class A emissions
- ICES-001: Class A emissions

Note For the standards applied to assess the EMC of this product, refer to the *Online Product Certification* section.

Note For EMC compliance, operate this product according to the documentation.

CE Compliance CE

This product meets the essential requirements of applicable European Directives, as amended for CE marking, as follows:

- 2006/95/EC; Low-Voltage Directive (safety)
- 2004/108/EC; Electromagnetic Compatibility Directive (EMC)

Online Product Certification

Refer to the product Declaration of Conformity (DoC) for additional regulatory compliance information. To obtain product certifications and the DoC for this product, visit ni.com/certification, search by module number or product line, and click the appropriate link in the Certification column.

Environmental Management

National Instruments is committed to designing and manufacturing products in an environmentally responsible manner. NI recognizes that eliminating certain hazardous substances from our products is beneficial not only to the environment but also to NI customers.

For additional environmental information, refer to the *NI and the Environment* Web page at ni.com/environment. This page contains the environmental regulations and directives with which NI complies, as well as other environmental information not included in this document.

Waste Electrical and Electronic Equipment (WEEE)

EU Customers At the end of the product life cycle, all products *must* be sent to a WEEE recycling center. For more information about WEEE recycling centers, National Instruments WEEE initiatives, and compliance with WEEE Directive 2002/96/EC on Waste Electrical and Electronic Equipment, visit ni.com/environment/weee.htm.

电子信息产品污染控制管理办法 （中国 RoHS）

中国客户 National Instruments 符合中国电子信息产品中限制使用某些有害物质指令 (RoHS)。
关于 National Instruments 中国 RoHS 合规性信息，请登录 ni.com/environment/rohs_china。
(For information about China RoHS compliance, go to ni.com/environment/rohs_china.)

Cabling

The following table shows the standard Ethernet cable wiring connections.

Ethernet Cable Wiring Connections		
Pin	**Connector 1**	**Connector 2**
1	white/orange	white/orange
2	orange	orange
3	white/green	white/green
4	blue	blue
5	white/blue	white/blue
6	green	green
7	white/brown	white/brown
8	brown	brown

Back to Top

Pinouts/Front Panel Connections

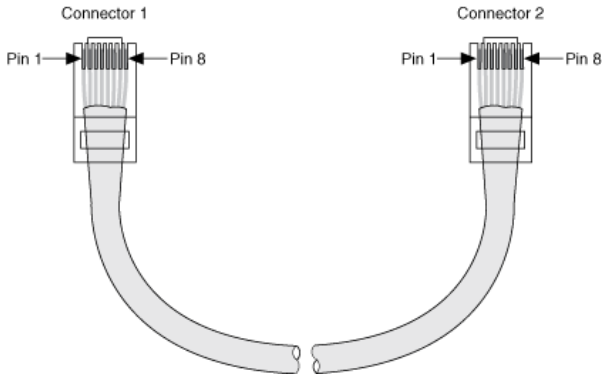

Internet Connector Pinout

Back to Top

©2010 National Instruments. All rights reserved. CompactRIO, FieldPoint, LabVIEW, National Instruments, National Instruments Alliance Partner, NI, and ni.com are trademarks of National Instruments. Other product and company names listed are trademarks or trade names of their respective companies. A National Instruments Alliance Partner is a business entity independent from National Instruments and has no agency, partnership, or joint-venture relationship with National Instruments.

My Profile | RSS | Privacy | Legal | Contact NI © 2011 National Instruments Corporation. All rights reserved.

Technical Sales
United States
(866) 531-6285
info@ni.com

Last Revised: 2011-02-14 16:44:07.0

NI 9870, NI 9871

- 4 RS232 (TIA/EIA-232) or 4 RS485/RS422 serial ports for CompactRIO
- Baud rates from 14 bit/s to 921.6 kbit/s
- Individual 64 B UART FIFO buffers per port
- Data bits: 5, 6, 7, 8; Stop bits: 1, 1.5, 2; Flow control: XON/OFF, RTS/CTS, None
- 8 to 28 VDC externally powered; PC-MF4-PT cable included
- -40 to 70 °C operating range

Overview

The NI 9870 and NI 9871 C Series serial modules add four RS232 or RS485/RS422 serial ports, respectively, to NI CompactRIO systems. Using an NI LabVIEW FPGA API, you can access the four ports directly from the CompactRIO field-programmable gate array (FPGA) to achieve flexibility in communicating with serial devices. The modules have individual 64 B buffers on every port that save CompactRIO FPGA space and simplify programming. These C Series modules support standard start bit, stop bit, and handshaking settings and feature baud rates up to 921.6 kbit/s per port. You can pass up to 2 Mbit/s of data between these modules and CompactRIO.

Back to Top

Requirements and Compatibility

OS Information

- Linux®
- Mac OS X
- Windows
- Windows 7
- Windows Vista
- Windows XP

Driver Information

- C-Series Serial
- NI-RIO

Software Compatibility

- LabVIEW Development System
- LabVIEW FPGA Module
- Visual C#
- Visual C++

Back to Top

Application and Technology

NI C Series Chassis

NI CompactDAQ Platform

NI CompactDAQ delivers the simplicity of USB to sensor and electrical measurements on the benchtop, in the field, and on the production line. By combining the ease of use and low cost of a data logger with the performance and flexibility of modular instrumentation, NI CompactDAQ offers fast, accurate measurements in a small, simple, and affordable system. Flexible software options make it easy to use NI CompactDAQ to log data for simple experiments or to develop a fully automated test or control system. The modular design can measure up to 256 channels of electrical, physical, mechanical, or acoustical signals in a single system. In addition, per-channel ADCs and individually isolated modules ensure fast, accurate, and safe measurements.

Figure 1. NI CompactDAQ Platform

NI CompactRIO Platform

When used with the small, rugged CompactRIO embedded control and data acquisition system, C Series analog input modules connect directly to reconfigurable I/O (RIO) field-programmable gate array (FPGA) hardware to create high-performance embedded systems. The reconfigurable FPGA hardware within CompactRIO provides a variety of options for custom timing, triggering, synchronization, filtering, signal processing, and high-speed decision making for all C Series analog input modules. For instance, with CompactRIO, you can implement custom triggering for any analog sensor type on a per-channel basis using the flexibility and performance of the FPGA and the numerous arithmetic and comparison function blocks built into the NI LabVIEW FPGA Module.

Figure 2. NI CompactRIO Platform

Back to Top

Ordering Information

For a complete list of accessories, visit the product page on ni.com.

Products	Part Number	Recommended Accessories	Part Number
NI 9870 Serial Module			
NI 9870 4-Port RS232 Serial Module	779891-02	No accessories required.	
NI 9871 Serial Module			
NI 9871 4-Port RS485 Serial Module	779892-02	No accessories required.	

Back to Top

Software Recommendations

NI LabVIEW Full Development System for Windows

- Easy-to-use graphical development environment
- Tight integration with a wide range of measurement hardware
- Rapid user interface development for displaying live data
- Extensive signal processing, analysis, and math functionality
- Multiple communication options (TCP/IP, UDP, serial, and more)
- Support for Windows XP/Vista/7 (32-bit) and Windows Vista/7 (64-bit)

NI LabVIEW FPGA Module

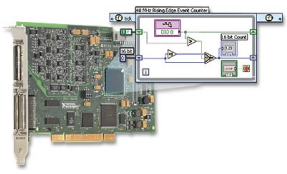

- Create your own I/O hardware without VHDL coding or board design
- Graphically configure FPGAs on NI reconfigurable I/O (RIO) hardware targets
- Define your own control algorithms with loop rates up to 200 MHz
- Execute multiple tasks simultaneously and deterministically
- Implement custom timing and triggering logic, digital protocols, and DSP algorithms
- Incorporate existing HDL code and third-party IP including Xilinx CORE Generator functions

Back to Top

Support and Services

System Assurance Programs

NI system assurance programs are designed to make it even easier for you to own an NI system. These programs include configuration and deployment services for your NI PXI, CompactRIO, or Compact FieldPoint system. The NI Basic System Assurance Program provides a simple integration test and ensures that your system is delivered completely assembled in one box. When you configure your system with the NI Standard System Assurance Program, you can select from available NI system driver sets and application development environments to create customized, reorderable software configurations. Your system arrives fully assembled and tested in one box with your software preinstalled. When you order your system with the standard program, you also receive system-specific documentation including a bill of materials, an integration test report, a recommended maintenance plan, and frequently asked question documents. Finally, the standard program reduces the total cost of owning an NI system by providing three years of warranty coverage and calibration service. Use the online product advisors at ni.com/advisor to find a system assurance program to meet your needs.

Technical Support

Get answers to your technical questions using the following National Instruments resources.

- **Support** - Visit ni.com/support to access the NI KnowledgeBase, example programs, and tutorials or to contact our applications engineers who are located in NI sales offices around the world and speak the local language.
- **Discussion Forums** - Visit forums.ni.com for a diverse set of discussion boards on topics you care about.
- **Online Community** - Visit community.ni.com to find, contribute, or collaborate on customer-contributed technical content with users like you.

Repair

While you may never need your hardware repaired, NI understands that unexpected events may lead to necessary repairs. NI offers repair services performed by highly trained technicians who quickly return your device with the guarantee that it will perform to factory specifications. For more information, visit ni.com/repair.

Training and Certifications

The NI training and certification program delivers the fastest, most certain route to increased proficiency and productivity using NI software and hardware. Training builds the skills to more efficiently develop robust, maintainable applications, while certification validates your knowledge and ability.

- **Classroom training in cities worldwide** - the most comprehensive hands-on training taught by engineers.
- **On-site training at your facility** - an excellent option to train multiple employees at the same time.
- **Online instructor-led training** - lower-cost, remote training if classroom or on-site courses are not possible.
- **Course kits** - lowest-cost, self-paced training that you can use as reference guides.
- **Training memberships** and training credits - to buy now and schedule training later.

Visit ni.com/training for more information.

Extended Warranty

NI offers options for extending the standard product warranty to meet the life-cycle requirements of your project. In addition, because NI understands that your requirements may change, the extended warranty is flexible in length and easily renewed. For more information, visit ni.com/warranty.

OEM

NI offers design-in consulting and product integration assistance if you need NI products for OEM applications. For information about special pricing and services for OEM customers, visit ni.com/oem.

Alliance

Our Professional Services Team is comprised of NI applications engineers, NI Consulting Services, and a worldwide National Instruments Alliance Partner program of more than 600 independent consultants and integrators. Services range from start-up assistance to turnkey system integration. Visit ni.com/alliance.

Back to Top

Detailed Specifications

The following specifications are typical for the range –40 to 70 °C unless otherwise noted.

NI 9870	
Maximum baud rate	921.6 kbps
Maximum cable length	250 pF equivalent
Note Cable capacitance greater than 250 pF may adversely affect the maximum baud rate and thermal dissipation.	
Maximum RS232 Receive signal (RXD, CTS, DSR, DCD, RI) Continuous Voltage	±8 V
Note Continuous RS232 input voltages in excess of ±8 V may cause excessive thermal dissipation.	
Data line ESD protection (human body model)	±15 kV
MTBF	448,008 hours at 25 °C; Bellcore Issue 6, Method 1, Case 3, Limited Part Stress Method

Note Contact NI for Bellcore MTBF specifications at other temperatures or for MIL-HDBK-217F specifications.

NI 9871	
Maximum baud rate	3.6864 Mbps
Maximum cable length	1.2 km (4,000 ft.)
Data line ESD protection (human body model)	±15 kV
MTBF	514,016 hours at 25 °C; Bellcore Issue 6, Method 1, Case 3, Limited Part Stress Method

Note Contact NI for Bellcore MTBF specifications at other temperatures or for MIL-HDBK-217F specifications.

Power Requirements

Power consumption from chassis	
Active mode	0.5 W max
Sleep mode	50 µW max
Thermal dissipation (at 70 °C)	
Active mode	1.5 W max
NI 9870 Sleep mode	0.5 W max
NI 9871 Sleep mode	55 mW max
Required external supply voltage range (V_{SUP})	+8 to +28 VDC
Power supply consumption from external supply V_{SUP}	
NI 9870	
Typical	0.5 W
Maximum	2 W
NI 9871	
Typical	1 W
Maximum	3.5 W

Physical Characteristics

If you need to clean the module, wipe it with a dry towel.	
Weight	Approx. 154 g (5.4 oz)

Safety

NI 9870 Maximum Voltage [1]	
Connect only voltages that are within these limits.	
RS232 Receive Signal-to-COM (RXD, CTS, DSR, DCD, RI)	±25 V max, Measurement Category I
RS232 Transmit Signal-to-COM (TX, RTS, DTR)	±13.2 V max, Measurement Category I
V_{SUP}-to-COM	±28 V max, Measurement Category I
NI 9871 Maximum Voltage [1]	
RS485/RS422 Port-to-COM	–8 to +13 VDC max, Measurement Category I
V_{SUP}-to-COM	±28 V max, Measurement Category I

Measurement Category I is for measurements performed on circuits not directly connected to the electrical distribution system referred to as *MAINS* voltage. MAINS is a hazardous live electrical supply system that powers equipment. This category is for measurements of voltages from specially protected secondary circuits. Such voltage measurements include signal levels, special equipment, limited-energy parts of equipment, circuits powered by regulated low-voltage sources, and electronics.

Caution Do not connect to signals or use for measurements within Measurement Categories II, III, or IV.

Isolation Voltages	
Port-to-earth ground	
Withstand	1000 V_{rms}, verified by a dielectric withstand test, 5 s
Continuous	60 VDC, Measurement Category I
Hazardous Locations	
U.S. (UL)	Class I, Division 2, Groups A, B, C, D, T4; Class I, Zone 2, AEx nA II T4
Canada (C-UL)	Class I, Division 2, Groups A, B, C, D, T4; Class I, Zone 2, Ex nA II T4

Europe (DEMKO)	Ex nA IIC T4

Safety Standards

This product is designed to meet the requirements of the following standards of safety for electrical equipment for measurement, control, and laboratory use:

- IEC 61010-1, EN 61010-1
- UL 61010-1, CSA 61010-1

Note For UL and other safety certifications, refer to the product label or the *Online Product Certification* section.

Electromagnetic Compatibility	
Emissions	EN 55011 Class A at 10 m FCC Part 15A above 1 GHz
Immunity	Industrial levels per EN 61326-1:1997 + A2:2001, Table A.1
EMC/EMI	CE, C-Tick, and FCC Part 15 (Class A) Compliant

Note For the standards applied to assess the EMC of this product, refer to the *Online Product Certification* section.

Note For EMC compliance, operate this device with shielded cabling.

CE Compliance CE

This product meets the essential requirements of applicable European Directives, as amended for CE marking, as follows:

- 2006/95/EC; Low-Voltage Directive (safety)
- 2004/108/EC; Electromagnetic Compatibility Directive (EMC)

Online Product Certification

To obtain product certifications and the DoC for this product, visit ni.com/certification, search by model number or product line, and click the appropriate link in the Certification column.

Shock and Vibration	
To meet these specifications, you must panel mount the CompactRIO system.	
Operating vibration, random (IEC 60068-2-64)	5 g_{rms}, 10 to 500 Hz
Operating shock (IEC 60068-2-27)	30 g, 11 ms half sine, 50 g, 3 ms half sine, 18 shocks at 6 orientations
Operating vibration, sinusoidal (IEC 60068-2-6)	5 g, 10 to 500 Hz

Environmental	
CompactRIO modules are intended for indoor use only. For outdoor use, mount the CompactRIO system in a suitably rated enclosure. Refer to the installation instructions for the chassis you are using for more information about meeting these specifications.	
Operating temperature	–40 to 70 °C
Storage temperature	–40 to 85 °C
Ingress protection	IP 40
Operating humidity	10 to 90% RH, noncondensing
Storage humidity	5 to 95% RH, noncondensing
Maximum altitude	2,000 m
Pollution Degree (IEC 60664)	2

Environmental Management

NI is committed to designing and manufacturing products in an environmentally responsible manner. NI recognizes that eliminating certain hazardous substances from our products is beneficial not only to the environment but also to NI customers.

For additional environmental information, refer to the *NI and the Environment* Web page at ni.com/environment. This page contains the environmental regulations and directives with which NI complies, as well as other environmental information not included in this document.

Waste Electrical and Electronic Equipment (WEEE)

[1] The maximum voltage that can be applied or output without creating a safety hazard.

Back to Top

Pinouts/Front Panel Connections

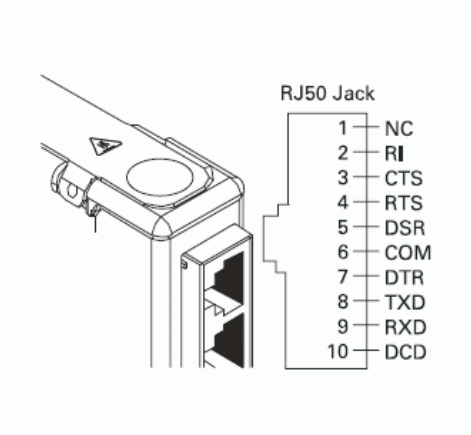

RS232 Port Pinout

RJ-50 Pin	Signal Name*
1	No Connect
2	RI
3	CTS
4	RTS
5	DSR
6	GND
7	DTR
8	TXD
9	RXD
10	DCD
* These signals are shared by all four RJ-50 connectors on the NI 9870.	

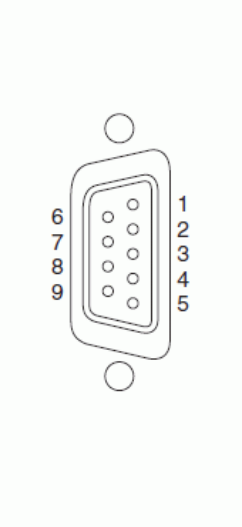

Pin Assignments for RS232 DB-9 Male Connector

Pin	Signal
1	DCD
2	RXD
3	TXD
4	DTR
5	GND
6	DSR
7	RTS
8	CTS
9	RI

Back to Top

©2011 National Instruments. All rights reserved. CompactRIO, FieldPoint, LabVIEW, National Instruments, National Instruments Alliance Partner, NI, ni.com, and NI CompactDAQ are trademarks of National Instruments. Other product and company names listed are trademarks or trade names of their respective companies. A National Instruments Alliance Partner is a business entity independent from National Instruments and has no agency, partnership, or joint-venture relationship with National Instruments.

My Profile | RSS | Privacy | Legal | Contact NI © 2011 National Instruments Corporation. All rights reserved.

Technical Sales
United States
(866) 531-6285
info@ni.com

Last Revised: 2011-09-11 02:25:36.0

16-Channel Thermocouple Module

NI 9213

- Built-in CJC (cold-junction compensation)
- High-speed mode for up to 1,200 S/s (aggregate)
- 250 Vrms channel-to-earth ground safety isolation
- 24-bit ADC for up to 0.02 °C measurement sensitivity
- Autozero channel for offset error compensation
- J, K, T, E, N, B, R, and S types supported
- Included backshell kit (NI 9940) for strain relief

Overview

The NI 9213 is a high-density thermocouple module for NI C Series carriers designed for higher-channel-count systems. With this module, you can add thermocouples to mixed-signal test systems without taking up too many slots.

The NI 9213 is similar to the NI 9211 four-channel thermocouple module except it features four times the channel count and almost 100 times the sample rate.

You can use up to eight NI 9213 modules in an NI CompactDAQ chassis or CompactRIO chassis for 128 thermocouple measurements in a single chassis, or deploy a single module in any of the USB, Ethernet, or Wi-Fi carriers for C Series modules.

Each shipping kit contains:
-NI 9213 module with spring-terminal connectivity
-NI 9940 backshell for cabling and strain relief
-Spring-terminal tool for signal wire insertion

Back to Top

Requirements and Compatibility

OS Information

- Real-Time OS
- Windows

Driver Information

- NI-DAQmx
- NI-RIO

Software Compatibility

- LabVIEW
- LabVIEW SignalExpress
- LabWindows/CVI
- Measurement Studio
- Visual C++
- Visual Studio
- Visual Studio .NET

Back to Top

Comparison Tables

Thermocouple Module	Channels	Sample Rate	Resolution	Feature
NI 9213	16	1,200 S/s	24-bit	Lowest cost/channel
NI 9219	4	50 S/s/ch	24-bit	Channel-to-channel isolation
NI 9211	4	14 S/s	24-bit	Low-channel count

Back to Top

Application and Technology

Channel Density for High-Channel-Count Systems

Temperature measurements can vary greatly over the different components in a machine, the surface of a device, or the volume of a given space. By taking more temperature measurements, you can better quantify the thermal gradients and achieve more accurate test results. The NI 9213 was designed with density in mind to enable a large number of thermocouple channels in a compact space. With up to eight NI 9213 modules installed in an NI CompactRIO or NI CompactDAQ chassis, you can measure up to 128 thermocouples in a system that fits inside a 9 by 9 by 26 cm box. For even more portable temperature measurement systems, you can install the NI 9213 into one of the single module carriers for NI C Series modules to make 16-channel thermocouple measurements over USB, Ethernet, or Wi-Fi (802.11b/g).

CJC and Autozero for a More Accurate Measurement

The NI 9213 has built-in cold-junction compensation (CJC) to eliminate error caused by the physical connection of the sensor to the instrumentation. The contact of two dissimilar metals creating a voltage potential is the principle on which thermocouples are designed, and, as such, the contact of the dissimilar thermocouple metal with the spring terminal must be removed from the calculation. This is done through a process known as cold-junction compensation, with the cold junction being the mating of the sensor to the instrument. All NI instrumentation designed for thermocouple measurement contains CJC circuitry including the NI 9211, NI 9219, and NI 9213. In addition to CJC, the NI 9213 features an extra, internal-only channel known as the autozero channel. By measuring the autozero channel at the beginning of each channel scan, you can eliminate further offset errors to provide a more accurate temperature measurement.

C Series Compatibility

The NI C Series hardware family features more than 50 measurement modules and several chassis and carriers for deployment. With this variety of modules, you can mix and match measurements such as temperature, acceleration, flow, pressure, strain, acoustic, voltage, current, digital, and more to create a custom system. Install the modules in one of several carriers to create a single module USB, Ethernet, or Wi-Fi system, or combine them in chassis such as NI CompactDAQ and CompactRIO to create a mixed-measurement system with synchronized measurements. You can install up to eight modules in a simple, complete NI CompactDAQ USB data acquisition system to synchronize all of the analog output, analog input, and digital I/O from the modules. For a system without a PC, CompactRIO holds up to eight modules and features a built-in processor, RAM, and storage for an embedded data logger or control unit. For higher-speed control, CompactRIO chassis incorporate a field-programmable gate array (FPGA) that you can program with NI LabVIEW software to achieve silicone-speed processing on I/O data from C Series modules.

Back to Top

Ordering Information

For a complete list of accessories, visit the product page on ni.com.

Products	Part Number	Recommended Accessories	Part Number
NI 9213			
NI 9213 CC	780493-02	No accessories required.	
NI 9213			
NI 9213	780493-01	No accessories required.	

Back to Top

Software Recommendations

LabVIEW Professional Development System for Windows

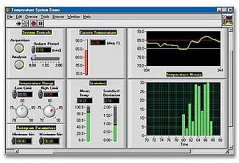

- Advanced software tools for large project development
- Automatic code generation using DAQ Assistant and Instrument I/O Assistant
- Tight integration with a wide range of hardware
- Advanced measurement analysis and digital signal processing
- Open connectivity with DLLs, ActiveX, and .NET objects
- Capability to build DLLs, executables, and MSI installers

Back to Top

Support and Services

System Assurance Programs

NI system assurance programs are designed to make it even easier for you to own an NI system. These programs include configuration and deployment services for your NI PXI,

CompactRIO, or Compact FieldPoint system. The NI Basic System Assurance Program provides a simple integration test and ensures that your system is delivered completely assembled in one box. When you configure your system with the NI Standard System Assurance Program, you can select from available NI system driver sets and application development environments to create customized, reorderable software configurations. Your system arrives fully assembled and tested in one box with your software preinstalled. When you order your system with the standard program, you also receive system-specific documentation including a bill of materials, an integration test report, a recommended maintenance plan, and frequently asked question documents. Finally, the standard program reduces the total cost of owning an NI system by providing three years of warranty coverage and calibration service. Use the online product advisors at ni.com/advisor to find a system assurance program to meet your needs.

Calibration

NI measurement hardware is calibrated to ensure measurement accuracy and verify that the device meets its published specifications. NI offers a number of calibration services to help maintain the ongoing accuracy of your measurement hardware. These services allow you to be completely confident in your measurements, and help you maintain compliance to standards like ISO 9001, ANSI/NCSL Z540-1 and ISO/IEC 17025. To learn more about NI calibration services or to locate a qualified service center near you, contact your local sales office or visit ni.com/calibration.

Technical Support

Get answers to your technical questions using the following National Instruments resources.

- **Support** - Visit ni.com/support to access the NI KnowledgeBase, example programs, and tutorials or to contact our applications engineers who are located in NI sales offices around the world and speak the local language.
- **Discussion Forums** - Visit forums.ni.com for a diverse set of discussion boards on topics you care about.
- **Online Community** - Visit community.ni.com to find, contribute, or collaborate on customer-contributed technical content with users like you.

Repair

While you may never need your hardware repaired, NI understands that unexpected events may lead to necessary repairs. NI offers repair services performed by highly trained technicians who quickly return your device with the guarantee that it will perform to factory specifications. For more information, visit ni.com/repair.

Training and Certifications

The NI training and certification program delivers the fastest, most certain route to increased proficiency and productivity using NI software and hardware. Training builds the skills to more efficiently develop robust, maintainable applications, while certification validates your knowledge and ability.

- **Classroom training in cities worldwide** - the most comprehensive hands-on training taught by engineers.
- **On-site training at your facility** - an excellent option to train multiple employees at the same time.
- **Online instructor-led training** - lower-cost, remote training if classroom or on-site courses are not possible.
- **Course kits** - lowest-cost, self-paced training that you can use as reference guides.
- **Training memberships** and training credits - to buy now and schedule training later.

Visit ni.com/training for more information.

Extended Warranty

NI offers options for extending the standard product warranty to meet the life-cycle requirements of your project. In addition, because NI understands that your requirements may change, the extended warranty is flexible in length and easily renewed. For more information, visit ni.com/warranty.

OEM

NI offers design-in consulting and product integration assistance if you need NI products for OEM applications. For information about special pricing and services for OEM customers, visit ni.com/oem.

Alliance

Our Professional Services Team is comprised of NI applications engineers, NI Consulting Services, and a worldwide National Instruments Alliance Partner program of more than 600 independent consultants and integrators. Services range from start-up assistance to turnkey system integration. Visit ni.com/alliance.

Back to Top

Detailed Specifications

The following specifications are typical for the range – 40 to 70 °C unless otherwise noted.

Warm-up time [1]	15 min
Input Characteristics	
Number of channels	16 thermocouple channels, 1 internal autozero channel, 1 internal cold-junction compensation channel
ADC resolution	24 bits
Type of ADC	Delta-Sigma
Sampling mode	Scanned
Voltage measurement range	±78.125 mV
Temperature measurement ranges	Works over temperature ranges defined by NIST (J, K, T, E, N, B, R, S thermocouple types)

Timing modes		
Timing Mode	**Conversion Time (Per Channel)**	**Sample Rate [2] (All Channels [3])**
High-resolution	55 ms	1 S/s
High-speed	740 μs	75 S/s

Common-mode voltage range	
Channel-to-COM	±1.2 V min
COM-to-earth ground	±250 V
Common-mode rejection ratio	
High-resolution mode (at DC and 50–60 Hz)	
Channel-to-COM	100 dB
COM-to-earth ground	>170 dB
High-speed mode (at 0–60 Hz)	
Channel-to-COM	70 dB
COM-to-earth ground	>150 dB
Input bandwidth	
High-resolution mode	14.4 Hz
High-speed mode	78 Hz
High-resolution noise rejection (at 50 and 60 Hz)	60 dB
Overvoltage protection	±30 V between any two inputs
Differential input impedance	78 MΩ
Input current	50 nA
Input noise	
High-resolution mode	200 nV_{rms}
High-speed mode	7 μV_{rms}
Gain error	
High-resolution mode	0.03% typ at 25 °C, 0.07% typ at – 40 to 70 °C, 0.15% max at – 40 to 70 °C
High-speed mode	0.04% typ at 25 °C, 0.08% typ at – 40 to 70 °C, 0.16% max at – 40 to 70 °C
Offset error	
High-resolution mode	4 μV typ, 6 μV max
High-speed mode	14 μV typ, 17 μV max
Offset error from source impedance	Add 0.05 μV per Ω, when source impedance >50 Ω
Cold-junction compensation accuracy	
0 to 70 °C	0.8 °C typ, 1.7 °C max
– 40 to 70 °C	1.1 °C typ, 2.1 °C max
MTBF	852,407 hours at 25 °C; Bellcore Issue 2, Method 1, Case 3, Limited Part Stress Method

Note Contact NI for Bellcore MTBF specifications at other temperatures or for MIL-HDBK-217F specifications.

Temperature Measurement Accuracy

Measurement sensitivity [4]	
High-resolution mode	
Types J, K, T, E, N	<0.02 °C
Types B, R, S	<0.15 °C
High-speed mode	
Types J, K, T, E	<0.25 °C
Type N	<0.35 °C
Type B	<1.2 °C

Types R, S	<2.8 °C

Figures 6, 7, 8, 9, and 10 show the errors for each thermocouple type when connected to the NI 9213 with the autozero channel on. The figures display the maximum errors over a full temperature range and typical errors at room temperature. The figures account for gain errors, offset errors, differential and integral nonlinearity, quantization errors, noise errors, 50 Ω lead wire resistance, and cold-junction compensation errors. The figures do not account for the accuracy of the thermocouple itself.

Thermocouple Types J and N Errors

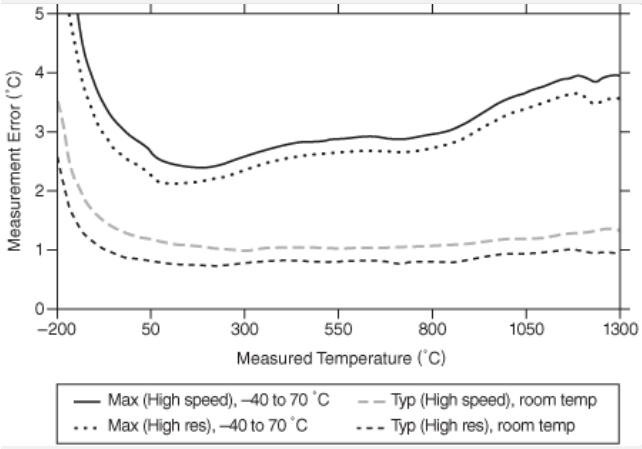

Thermocouple Type K Errors

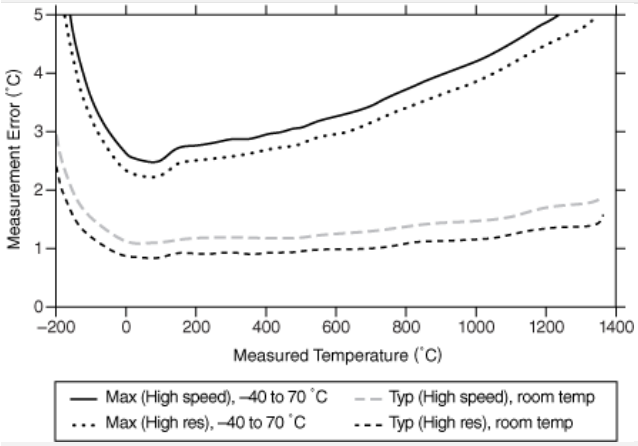

Thermocouple Types T and E Errors

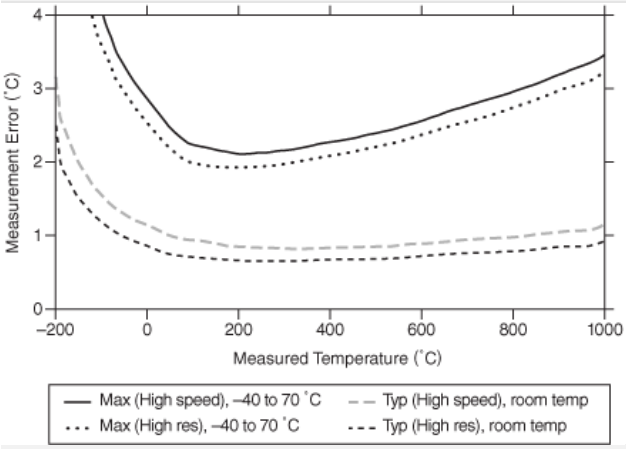

Thermocouple Type B Errors

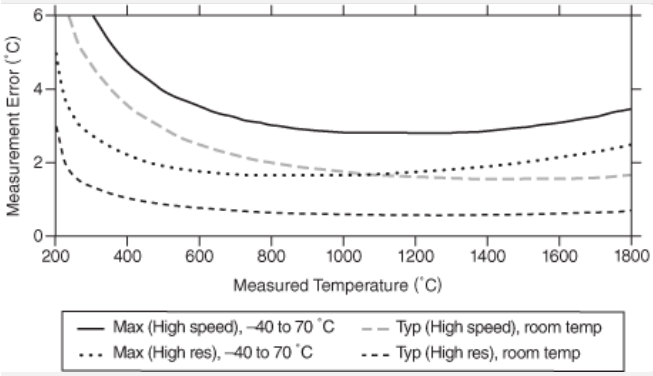

Thermocouple Types R and S Errors

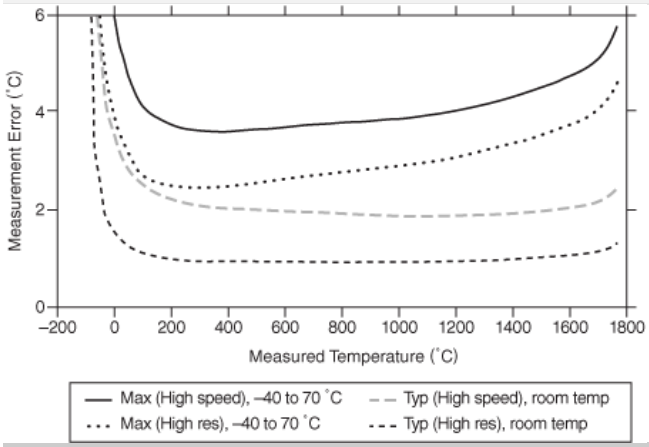

Power Requirements

Power consumption from chassis	
Active mode	490 mW max
Sleep mode	25 µW max
Thermal dissipation (at 70 °C)	
Active mode	840 mW max
Sleep mode	710 mW max

Physical Characteristics

Note For two-dimensional drawings and three-dimensional models of the C Series module and connectors, visit *ni.com/dimensions* and search by module number.

Spring-terminal wiring	18 to 28 AWG copper conductor wire with 7 mm (0.28 in.) of insulation stripped from the end
Weight	159 g (5.61 oz)

If you need to clean the module, wipe it with a dry towel.

Safety

Safety Voltages

Connect only voltages that are within the following limits.

Between any two terminals	±30 V max
Isolation	
Channel-to-channel	None
Channel-to-earth ground	
Continuous	250 V_{rms}, Measurement Category II
Withstand	2,300 V_{rms}, verified by a 5 s dielectric withstand test

Measurement Category II is for measurements performed on circuits directly connected to the electrical distribution system (MAINS [5]). This category refers to local-level electrical distribution, such as that provided by a standard wall outlet (for example, 115 AC voltage for U.S. or 230 AC voltage for Europe). Examples of Measurement Category II are measurements performed on household appliances, portable tools, and similar hardware.

Caution Do *not* connect the NI 9213 to signals or use for measurements within Measurement Categories III or IV.

Safety Standards

This product is designed to meet the requirements of the following standards of safety for electrical equipment for measurement, control, and laboratory use:

- IEC 61010-1, EN 61010-1
- UL 61010-1, CSA 61010-1

Note For UL and other safety certifications, refer to the product label or the *Online Product Certification* section.

Hazardous Locations

U.S. (UL)	Class I, Division 2, Groups A, B, C, D, T4; Class I, Zone 2, AEx nA IIC T4
Canada (C-UL)	Class I, Division 2, Groups A, B, C, D, T4; Class I, Zone 2, Ex nA IIC T4
Europe (DEMKO)	Ex nA IIC T4

Environmental

National Instruments C Series modules are intended for indoor use only but may be used outdoors if installed in a suitable enclosure. Refer to the manual for the chassis you are

using for more information about meeting these specifications.

Operating temperature (IEC 60068-2-1, IEC 60068-2-2)	– 40 to 70 °C
Storage temperature (IEC 60068-2-1, IEC 60068-2-2)	– 40 to 85 °C
Ingress protection	IP 40
Operating humidity (IEC 60068-2-56)	10 to 90% RH, noncondensing
Storage humidity (IEC 60068-2-56)	5 to 95% RH, noncondensing
Maximum altitude	2,000 m
Pollution degree	2

Shock and Vibration

To meet these specifications, you must panel mount the system and use the NI 9940 backshell kit to protect the connections.

Operating vibration	
Random (IEC 60068-2-64)	5 g_{rms}, 10 to 500 Hz
Sinusoidal (IEC 60068-2-6)	5 g, 10 to 500 Hz
Operating shock (IEC 60068-2-27)	30 g, 11 ms half sine, 50 g, 3 ms half sine, 18 shocks at 6 orientations

Electromagnetic Compatibility

This product is designed to meet the requirements of the following standards of EMC for electrical equipment for measurement, control, and laboratory use:

- EN 61326 (IEC 61326): Class A emissions; Industrial immunity
- EN 55011 (CISPR 11): Group 1, Class A emissions
- AS/NZS CISPR 11: Group 1, Class A emissions
- FCC 47 CFR Part 15B: Class A emissions
- ICES-001: Class A emissions

Note For the standards applied to assess the EMC of this product, refer to the *Online Product Certification* section.

Note For EMC compliance, operate this device with double-shielded cables.

CE Compliance

This product meets the essential requirements of applicable European Directives, as amended for CE marking, as follows:

- 2006/95/EC; Low-Voltage Directive (safety)
- 2004/108/EC; Electromagnetic Compatibility Directive (EMC)

Note For the standards applied to assess the EMC of this product, refer to the *Online Product Certification* section.

Online Product Certification

Refer to the product Declaration of Conformity (DoC) for additional regulatory compliance information. To obtain product certifications and the DoC for this product, visit ni.com/certification, search by module number or product line, and click the appropriate link in the Certification column.

Environmental Management

National Instruments is committed to designing and manufacturing products in an environmentally responsible manner. NI recognizes that eliminating certain hazardous substances from our products is beneficial not only to the environment but also to NI customers.

For additional environmental information, refer to the *NI and the Environment* Web page at ni.com/environment. This page contains the environmental regulations and directives with which NI complies, as well as other environmental information not included in this document.

Waste Electrical and Electronic Equipment (WEEE)

EU Customers At the end of their life cycle, all products *must* be sent to a WEEE recycling center. For more information about WEEE recycling centers and National Instruments WEEE initiatives, visit ni.com/environment/weee.htm.

电子信息产品污染控制管理办法 （中国 RoHS）

中国客户 National Instruments 符合中国电子信息产品中限制使用某些有害物质指令 (RoHS)。
关于 National Instruments 中国 RoHS 合规性信息，请登录 ni.com/environment/rohs_china。
(For information about China RoHS compliance, go to ni.com/environment/rohs_china.)

Calibration

You can obtain the calibration certificate for this device at ni.com/calibration.

Calibration interval	1 year

Safety Information

The following section contains important safety information that you must follow when installing and using the hardware.

Do not operate the hardware in a manner not specified in this document and in the user documentation. Misuse of the hardware can result in a hazard. You can compromise the

safety protection if the hardware is damaged in any way. If the hardware is damaged, return it to National Instruments for repair.

Clean the hardware with a soft, nonmetallic brush. Make sure that the hardware is completely dry and free from contaminants before returning it to service.

Do not substitute parts or modify the hardware except as described in this document. Use the hardware only with the chassis, modules, accessories, and cables specified in the installation instructions or specifications. You must have all covers and filler panels installed during operation of the hardware.

Do not operate the hardware in an explosive atmosphere or where there may be flammable gases or fumes unless the hardware is UL (U.S.) or Ex (EU) Certified and marked for hazardous locations. The hardware must be in a suitably rated IP 54 minimum enclosure for hazardous locations. Refer to the hardware's user documentation for more information.

You must insulate signal connections for the maximum voltage for which the hardware is rated. Do not exceed the maximum ratings for the hardware. Do not install wiring while the hardware is live with electrical signals. Do not remove or add connector blocks when power is connected to the system. Avoid contact between your body and the connector block signal when hot swapping hardware. Remove power from signal lines before connecting them to or disconnecting them from the hardware.

Operate the hardware only at or below Pollution Degree 2. Pollution is foreign matter in a solid, liquid, or gaseous state that can reduce dielectric strength or surface resistivity. The following is a description of pollution degrees:

- Pollution Degree 1 means no pollution or only dry, nonconductive pollution occurs. The pollution has no influence. Typical level for sealed components or coated PCBs.
- Pollution Degree 2 means that only nonconductive pollution occurs in most cases. Occasionally, however, a temporary conductivity caused by condensation must be expected. Typical level for most products.
- Pollution Degree 3 means that conductive pollution occurs, or dry, nonconductive pollution occurs that becomes conductive due to condensation.

Operate the hardware at or below the measurement category [6] marked on the hardware label. Measurement circuits are subjected to working voltages [7] and transient stresses (overvoltage) from the circuit to which they are connected during measurement or test. Measurement categories establish standard impulse withstand voltage levels that commonly occur in electrical distribution systems. The following is a description of measurement categories:

- Measurement Category I is for measurements performed on circuits not directly connected to the electrical distribution system referred to as MAINS [8] voltage. This category is for measurements of voltages from specially protected secondary circuits. Such voltage measurements include signal levels, special hardware, limited-energy parts of hardware, circuits powered by regulated low-voltage sources, and electronics.
- Measurement Category II is for measurements performed on circuits directly connected to the electrical distribution system (MAINS [9]). This category refers to local-level electrical distribution, such as that provided by a standard wall outlet (for example, 115 AC voltage for U.S. or 230 AC voltage for Europe). Examples of Measurement Category II are measurements performed on household appliances, portable tools, and similar hardware.
- Measurement Category III is for measurements performed in the building installation at the distribution level. This category refers to measurements on hard-wired hardware such as hardware in fixed installations, distribution boards, and circuit breakers. Other examples are wiring, including cables, bus bars, junction boxes, switches, socket outlets in the fixed installation, and stationary motors with permanent connections to fixed installations.
- Measurement Category IV is for measurements performed at the primary electrical supply installation typically outside buildings. Examples include electricity meters and measurements on primary overcurrent protection devices and on ripple control units.

To obtain the safety certification(s) for this product, visit ni.com/certification, search by model number or product line, and click the appropriate link in the Certification column.

[1] The warm-up time assumes the module is not in sleep mode, is facing forward or upward, and is in a constant ambient temperature. National Instruments recommends allowing the full warm-up time.

[2] If you are using fewer than all channels, the sample rate might be faster. The maximum sample rate = 1/(*Conversion Time* × *Number of Channels*), or 100 S/s, whichever is smaller. Sampling faster than the maximum sample rate may result in the degradation of accuracy.

[3] Including the autozero and cold-junction channels.

[4] Measurement sensitivity represents the smallest change in temperature that a sensor can detect. It is a function of noise. The values assume the full measurement range of the standard thermocouple sensor according to ASTM E230-87.

[5] MAINS is defined as a hazardous live electrical supply system that powers hardware. Suitably rated measuring circuits may be connected to the MAINS for measuring purposes.

[6] Measurement categories, also referred to as overvoltage or installation categories, are defined in electrical safety standard IEC 61010-1 and IEC 60664-1.

[7] Working voltage is the highest rms value of an AC or DC voltage that can occur across any particular insulation.

[8] MAINS is defined as a hazardous live electrical supply system that powers hardware. Suitably rated measuring circuits may be connected to the MAINS for measuring purposes.

[9] MAINS is defined as a hazardous live electrical supply system that powers hardware. Suitably rated measuring circuits may be connected to the MAINS for measuring purposes.

Back to Top

My Profile | RSS | Privacy | Legal | Contact NI © 2011 National Instruments Corporation. All rights reserved.

Technical Sales
United States
(866) 531-6285
info@ni.com

Last Revised: 2010-01-28 13:39:15.0

High-Speed Bridge Module for Load/Pressure/Strain/Torque Measurements

NI 9237

- Built-in full- and half-bridge measurements
- 120 and 350 Ω quarter-bridge completion via NI 9944/45 accessory kits
- 24-bit resolution on four simultaneous inputs sampled at up to 50 kS/s/ch
- Compatible with TEDS sensors
- Up to 10 V programmable excitation
- Connection for external excitation supply for specific levels
- 1,000 Vrms transient isolation for safety
- RJ50 (10P10C) or D-Sub connector options

Overview

The NI 9237 simultaneous bridge module for NI C Series devices contains all the signal conditioning required to power and measure up to four bridge-based sensors simultaneously. It can perform offset/null as well as shunt calibration and remote sense, all of which increase the accuracy of strain and bridge measurements.

For connectivity, you can select from two versions of the module: RJ50 or a 37-pin D-Sub. The RJ50 version, also known as 10P10C, offers quick sensor connection because you can use it for sensor termination. When you need a custom quarter-bridge design, choose the D-Sub version, which does not have an accessory for quarter-bridge completion. You also can use it with standard NI or other D-Sub accessories when you need only full- or half-bridge measurements.

The NI 9944 and NI 9945 accessories with quarter-bridge sensors have a female RJ50 connector on one end and screw terminals on the other end. You can purchase these accessories with a kit of RJ50 cables (quantity 4).

For screw terminals without the quarter-bridge completion, purchase the NI 9949 and a kit of RJ50 cables (quantity 4). This setup exposes all 10 pins for each channel as screw terminals.

Back to Top

Requirements and Compatibility

OS Information

- Real-Time OS
- Windows

Driver Information

- NI-DAQmx
- NI-RIO

Software Compatibility

- ANSI C/C++
- LabVIEW
- LabVIEW SignalExpress
- LabWindows/CVI
- Measurement Studio
- Visual Basic
- Visual Studio
- Visual Studio .NET

Back to Top

Comparison Tables

Module	Channels	Max Sample Rate (kS/s/ch)	Resolution (bits)	Quarter-Bridge	Half and Full	Simultaneous
NI 9237	4	50	24	yes (120/350 Ω)	yes	yes
NI 9237 D-Sub	4	50	24	no	yes	yes
NI 9235	8	10	24	120 Ω	no	yes
NI 9236	8	10	24	350 Ω	no	yes

Back to Top

Application and Technology

High-Speed Simultaneous Sampling

Mechanical test applications that involve impact testing, high-speed machinery, or moving vehicles often require high-speed sample rates to capture the event at full speed. You need to separate analog-to-digital converter (ADC) circuitry to perform a time-synchronous measurement as the strain event propagates through the structure. When you use multiple NI 9237 modules in either an NI CompactDAQ or CompactRIO chassis, all modules and channels are synchronized through a single set of clocked signals in the chassis.

Programmable Excitation

The NI 9237 can output voltage excitation up to 10 V. For more specific excitation requirements, the NI 9237 has inputs for external excitation. See the product manual for more information on excitation.

TEDS Compatibility

IEEE 1451.4, also known as TEDS (transducer electronic data sheet), technology consists of a standardized set of templates for specific sensors that store information such as manufacturer, manufacture date, calibration data, sensor-specific setup data, and more. TEDS is typically implemented on the sensor side via an onboard EEPROM. With this, the sensor has all of the information needed for setup and calibration stored locally, so you no longer have to keep up with paper data sheets. On the instrumentation side, the measurement system must have the capability to read and understand the TEDS data from the sensor. The NI 9237 has the capability to read TEDS information for TEDS-enabled sensors.

C Series Compatibility

The NI C Series hardware family features more than 50 measurement modules and several chassis and carriers for deployment. With this variety of modules, you can mix and match measurements such as temperature, acceleration, flow, pressure, strain, acoustic, voltage, current, digital, and more to create a custom system. Install the modules in one of several carriers to create a single module USB, Ethernet, or Wi-Fi system, or combine them in chassis such as NI CompactDAQ and CompactRIO to create a mixed-measurement system with synchronized measurements. You can install up to eight modules in a simple, complete NI CompactDAQ USB data acquisition system to synchronize all of the analog output, analog input, and digital I/O from the modules. For a system without a PC, CompactRIO holds up to eight modules and features a built-in processor, RAM, and storage for an embedded data logger or control unit. For higher-speed control, CompactRIO chassis incorporate a field-programmable gate array (FPGA) that you can program with NI LabVIEW software to achieve silicone-speed processing on I/O data from C Series modules.

Back to Top

Ordering Information

For a complete list of accessories, visit the product page on ni.com.

Products	Part Number	Recommended Accessories	Part Number
NI 9237 Module Kits			
NI 9237 D-Sub	780264-01	No accessories required.	
NI 9237 (RJ50)	779521-01	No accessories required.	
RJ50 Cables for Use with NI 9237			
RJ50 to "pigtail wires" or "flying leads" (10 m, qty 1)	195950-10	No accessories required.	
RJ50 to "pigtail wires" or "flying leads" (2 m, qty 4)	195950-02	No accessories required.	
RJ50 to RJ50 cable (10 m, qty 1)	194612-10	No accessories required.	
RJ50 to RJ50 cable kit (2 m, qty 4)	194612-02	No accessories required.	
D-Sub Cables for Use with NI 9237 D-Sub			
NI SH37F-Tajimi 37-pin D-Sub cable to connect to 7-pin male Tajimi connector (10 m, qty.1)	199254-10	No accessories required.	
NI SH37F-Tajimi 37-pin D-Sub cable to connect to 7-pin male Tajimi connector (1 m, qty. 1)	199254-01	No accessories required.	
37-pin D-Sub (M-F) shielded cable	778621-01	No accessories required.	
External Excitation Connector			
Spare/replacement 4-position connector for external excitation on the NI 9237 (RJ50)	194611-01	No accessories required.	
D-Sub Terminal Blocks			
37-pin D-Sub to screw terminal connector block with vertical DIN-rail mount	778672-01	No accessories required.	
37-pin D-Sub to screw terminal connector block with horizontal DIN-rail mount	778673-01	No accessories required.	
NI CB-37F-LP unshielded I/O connector block	779353-01	No accessories required.	
RJ50 Connectivity Accessories			

NI 9945 - Quarter-bridge completion accessory (350 Ohm, qty. 4) purchase with cable kit	194739-01	No accessories required.
NI 9944 - Quarter-bridge completion accessory (120 Ohm, qty. 4) purchase with cable kit	194738-01	No accessories required.
NI 9949 - RJ50 to screw terminal adaptor (qty. 4) purchase with cable kit.	196809-01	No accessories required.
D-Sub Connector Kit		
NI 9933 - creates custom cable for NI 9237 using D-Sub to screw terminal connection	779103-01	No accessories required.

Back to Top

Software Recommendations

LabVIEW Professional Development System for Windows

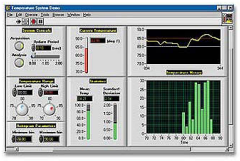

- Advanced software tools for large project development
- Automatic code generation using DAQ Assistant and Instrument I/O Assistant
- Tight integration with a wide range of hardware
- Advanced measurement analysis and digital signal processing
- Open connectivity with DLLs, ActiveX, and .NET objects
- Capability to build DLLs, executables, and MSI installers

Back to Top

Support and Services

System Assurance Programs

NI system assurance programs are designed to make it even easier for you to own an NI system. These programs include configuration and deployment services for your NI PXI, CompactRIO, or Compact FieldPoint system. The NI Basic System Assurance Program provides a simple integration test and ensures that your system is delivered completely assembled in one box. When you configure your system with the NI Standard System Assurance Program, you can select from available NI system driver sets and application development environments to create customized, reorderable software configurations. Your system arrives fully assembled and tested in one box with your software preinstalled. When you order your system with the standard program, you also receive system-specific documentation including a bill of materials, an integration test report, a recommended maintenance plan, and frequently asked question documents. Finally, the standard program reduces the total cost of owning an NI system by providing three years of warranty coverage and calibration service. Use the online product advisors at ni.com/advisor to find a system assurance program to meet your needs.

Calibration

NI measurement hardware is calibrated to ensure measurement accuracy and verify that the device meets its published specifications. NI offers a number of calibration services to help maintain the ongoing accuracy of your measurement hardware. These services allow you to be completely confident in your measurements, and help you maintain compliance to standards like ISO 9001, ANSI/NCSL Z540-1 and ISO/IEC 17025. To learn more about NI calibration services or to locate a qualified service center near you, contact your local sales office or visit ni.com/calibration.

Technical Support

Get answers to your technical questions using the following National Instruments resources.

- **Support** - Visit ni.com/support to access the NI KnowledgeBase, example programs, and tutorials or to contact our applications engineers who are located in NI sales offices around the world and speak the local language.
- **Discussion Forums** - Visit forums.ni.com for a diverse set of discussion boards on topics you care about.
- **Online Community** - Visit community.ni.com to find, contribute, or collaborate on customer-contributed technical content with users like you.

Repair

While you may never need your hardware repaired, NI understands that unexpected events may lead to necessary repairs. NI offers repair services performed by highly trained technicians who quickly return your device with the guarantee that it will perform to factory specifications. For more information, visit ni.com/repair.

Training and Certifications

The NI training and certification program delivers the fastest, most certain route to increased proficiency and productivity using NI software and hardware. Training builds the skills to more efficiently develop robust, maintainable applications, while certification validates your knowledge and ability.

- **Classroom training in cities worldwide** - the most comprehensive hands-on training taught by engineers.
- **On-site training at your facility** - an excellent option to train multiple employees at the same time.
- **Online instructor-led training** - lower-cost, remote training if classroom or on-site courses are not possible.
- **Course kits** - lowest-cost, self-paced training that you can use as reference guides.
- **Training memberships** and training credits - to buy now and schedule training later.

Visit ni.com/training for more information.

Extended Warranty

NI offers options for extending the standard product warranty to meet the life-cycle requirements of your project. In addition, because NI understands that your requirements may change, the extended warranty is flexible in length and easily renewed. For more information, visit ni.com/warranty.

OEM

NI offers design-in consulting and product integration assistance if you need NI products for OEM applications. For information about special pricing and services for OEM customers, visit ni.com/oem.

Alliance

Our Professional Services Team is comprised of NI applications engineers, NI Consulting Services, and a worldwide National Instruments Alliance Partner program of more than 600 independent consultants and integrators. Services range from start-up assistance to turnkey system integration. Visit ni.com/alliance.

Back to Top

Detailed Specifications

The following specifications are typical for the range –40 to 70 °C unless otherwise noted.

Input Characteristics	
Number of channels	4 analog input channels
Bridge completion	
Half and Full	Internal
Quarter	External
ADC resolution	24 bits
Type of ADC	Delta-Sigma (with analog prefiltering)
Sampling mode	Simultaneous
Internal master timebase (f_M)	
Frequency	12.8 MHz
Accuracy	±100 ppm max
Data rate range (f_s) using internal master timebase	
Minimum	1.613 kS/s
Maximum	50 kS/s
Data rate range (f_s) using external master timebase	
Minimum	390.625 S/s
Maximum	51.3 kS/s
Data rates [1]	$\frac{f_M \div 256}{n}, n = 1, 2, \ldots, 31$
Typical input range	± 25 mV/V
Scaling coefficient	2.9802 nV/V per LSB
Overvoltage protection between any two pins	±30 V

Accuracy		
Measurement Conditions [2]	**Percent of Reading (Gain Error)**	**Percent of Range** [3] **(Offset Error)**
Calibrated typ (25 °C, ±5 °C)	0.05%	0.05%
Calibrated max (– 40 to 70 °C)	0.20%	0.25%
Uncalibrated typ (25 °C, ±5 °C)	0.20%	0.1%
Uncalibrated max (– 40 to 70 °C)	0.60%	0.35%

Gain drift	10 ppm/°C max
Offset drift	
2.5 V excitation	0.6 µV/V per °C
3.3 V excitation	0.5 µV/V per °C
5 V excitation	0.3 µV/V per °C
10 V excitation	0.2 µV/V per °C

Channel-to-channel matching (calibrated)			
Input Signal Frequency (f_{in})	Gain		Phase
	Typical	Maximum	Maximum
0 to 1 kHz	0.15%	0.3%	0.125°/kHz · f_{in}
1 to 20 kHz	0.4%	1.1%	

Phase nonlinearity	
f_{in} = 0 to 1 kHz	<0.001°
f_{in} = 0 to 20 kHz	±0.1°
Input delay	38.4/f_s + 4.8 µs
Passband	
Frequency	0.45 · f_s
Flatness	0.1 dB max
Stopband	
Frequency	0.55 · f_s
Rejection	100 dB
Alias-free bandwidth	0.45 · f_s
Oversample rate	64 · f_s
Rejection at oversample rate [4]	
f_s = 10 kS/s	60 dB @ 640 kHz
f_s = 50 kS/s	90 dB @ 3.2 MHz
Common-mode voltage, all signals to earth ground	±60 VDC
CMRR	
Relative to earth ground [5] (f_{in} = 0 to 60 Hz)	140 dB
Relative to EX– (f_{in} = 0 to 1 kHz)	85 dB
SFDR (1 kHz, –60 dBFS)	106 dB
Total Harmonic Distortion (THD)	
1 kHz, –20 dBFS	100 dB
8 kHz, –20 dBFS	90 dB

Input noise			
Excitation Voltage	Density (nV/V_{rms} per $\sqrt{1}$ Hz)	Total f_{in} = 0 to 25 kHz ($\mu V/V_{rms}$)	Total f_{in} = 0 to 1 kHz (nV/V_{rms})
2.5 V	8	1.3	250
3.3 V	6	1.0	190
5 V	4	0.6	130
10 V	2	0.3	65

Excitation noise	0.1 mV/V_{rms}
Crosstalk	
f_{in} = 1 kHz	110 dB
f_{in} = 10 kHz	100 dB
Excitation	
Internal voltage	2.5 V, 3.3 V, 5.0 V, 10.0 V
Internal power	150 mW max
External voltage	2 V to 10 V
Shunt calibration	

Resistance	100 kΩ
Resistor accuracy	
25°C	±110 Ω
–40 to 70°C	±200 Ω
MTBF	603,359 hours at 25 °C; Bellcore Issue 2, Method 1, Case 3, Limited Part Stress Method

Note Contact NI for Bellcore MTBF specifications at other temperatures or for MIL-HDBK-217F specifications.

Power Requirements

Power consumption from chassis	
Active mode	740 mW max
Sleep mode	25 µW max
Thermal dissipation (at 70 °C)	
Active mode	740 mW max
Sleep mode	25 µW max

Physical Characteristics

Weight	152 g (5.4 oz)

Safety

If you need to clean the module, wipe it with a dry towel.

Safety Voltages

Connect only voltages that are within the following limits.

Between any two pins	±30 V max
Isolation	
Channel-to-channel	None
Channel-to-earth ground	
Continuous	60 VDC, Measurement Category I
Withstand	1,000 V_{rms}, verified by a 5 s dielectric withstand test

Measurement Category I is for measurements performed on circuits not directly connected to the electrical distribution system referred to as MAINS [6] voltage. This category is for measurements of voltages from specially protected secondary circuits. Such voltage measurements include signal levels, special equipment, limited-energy parts of equipment, circuits powered by regulated low-voltage sources, and electronics.

Caution Do *not* connect the NI 9237 to signals or use for measurements within Measurement Categories II, III, or IV.

Safety Standards

This product is designed to meet the requirements of the following standards of safety for electrical equipment for measurement, control, and laboratory use:

- IEC 61010-1, EN 61010-1
- UL 61010-1, CSA 61010-1

Note For UL and other safety certifications, refer to the product label or the *Online Product Certification* section.

Hazardous Locations

U.S. (UL)	Class I, Division 2, Groups A, B, C, D, T4; Class I, Zone 2, AEx nC IIC T4
Canada (C-UL)	Class I, Division 2, Groups A, B, C, D, T4; Class I, Zone 2, Ex nC IIC T4
Europe (DEMKO)	EEx nC IIC T4

Electromagnetic Compatibility

This product meets the requirements of the following EMC standards for electrical equipment for measurement, control, and laboratory use:

- EN 61326 (IEC 61326): Class A emissions; Basic immunity
- EN 55011 (CISPR 11): Group 1, Class A emissions
- AS/NZS CISPR 11: Group 1, Class A emissions
- FCC 47 CFR Part 15B: Class A emissions
- ICES-001: Class A emissions

Note For the standards applied to assess the EMC of this product, refer to the *Online Product Certification* section.

Note For EMC compliance, operate this device with shielded cables.

CE Compliance

This product meets the essential requirements of applicable European Directives, as amended for CE marking, as follows:

- 2006/95/EC; Low-Voltage Directive (safety)
- 2004/108/EC; Electromagnetic Compatibility Directive (EMC)

Note For the standards applied to assess the EMC of this product, refer to the *Online Product Certification* section.

Online Product Certification

Refer to the product Declaration of Conformity (DoC) for additional regulatory compliance information. To obtain product certifications and the DoC for this product, visit ni.com/certification, search by module number or product line, and click the appropriate link in the Certification column.

Shock and Vibration

To meet these specifications, you must panel mount the system.

Operating vibration	
Random (IEC 60068-2-64)	5 g_{rms}, 10 to 500 Hz
Sinusoidal (IEC 60068-2-6)	5 g, 10 to 500 Hz
Operating shock (IEC 60068-2-27)	30 g, 11 ms half sine, 50 g, 3 ms half sine, 18 shocks at 6 orientations

Environmental

National Instruments C Series modules are intended for indoor use only but may be used outdoors if installed in a suitable enclosure. Refer to the manual for the chassis you are using for more information about meeting these specifications.

Operating temperature (IEC 60068-2-1, IEC 60068-2-2)	– 40 to 70 °C
Storage temperature (IEC 60068-2-1, IEC 60068-2-2)	– 40 to 85 °C
Ingress protection	IP 40
Operating humidity (IEC 60068-2-56)	10 to 90% RH, noncondensing
Storage humidity (IEC 60068-2-56)	5 to 95% RH, noncondensing
Maximum altitude	2,000 m
Pollution Degree (IEC 60664)	2

Environmental Management

National Instruments is committed to designing and manufacturing products in an environmentally responsible manner. NI recognizes that eliminating certain hazardous substances from our products is beneficial not only to the environment but also to NI customers.

For additional environmental information, refer to the *NI and the Environment* Web page at ni.com/environment. This page contains the environmental regulations and directives with which NI complies, as well as other environmental information not included in this document.

Waste Electrical and Electronic Equipment (WEEE)

EU Customers At the end of their life cycle, all products *must* be sent to a WEEE recycling center. For more information about WEEE recycling centers and National Instruments WEEE initiatives, visit ni.com/environment/weee.htm.

电子信息产品污染控制管理办法 （中国 RoHS）

中国客户 National Instruments 符合中国电子信息产品中限制使用某些有害物质指令 (RoHS)。
关于 National Instruments 中国 RoHS 合规性信息，请登录 ni.com/environment/rohs_china。
(For information about China RoHS compliance, go to ni.com/environment/rohs_china.)

Calibration

You can obtain the calibration certificate for this device at ni.com/calibration.

Calibration interval	1 year

[1] The data rate must remain within the appropriate data rate range. Refer to the *Understanding Data Rates* section of the *NI 9237 Operating Instructions and Specifications* for more information.

[2] Before offset null or shunt calibration.

[3] Range equals 25 mV/V.

[4] Rejection by analog prefilter of signal frequencies at oversample rate.

[5] Measured with a balanced cable. Shielded cables that are not twisted-pair may be significantly unbalanced. To improve the balance of shielded, twisted-pair cables, NI recommends twisting together the AI+/AI– pair, the RS+/RS– pair, and the EX+/EX– pair.

[6] MAINS is defined as the (hazardous live) electrical supply system to which equipment is designed to be connected for the purpose of powering the equipment. Suitably rated measuring circuits may be connected to the MAINS for measuring purposes.

Back to Top

Pinouts/Front Panel Connections

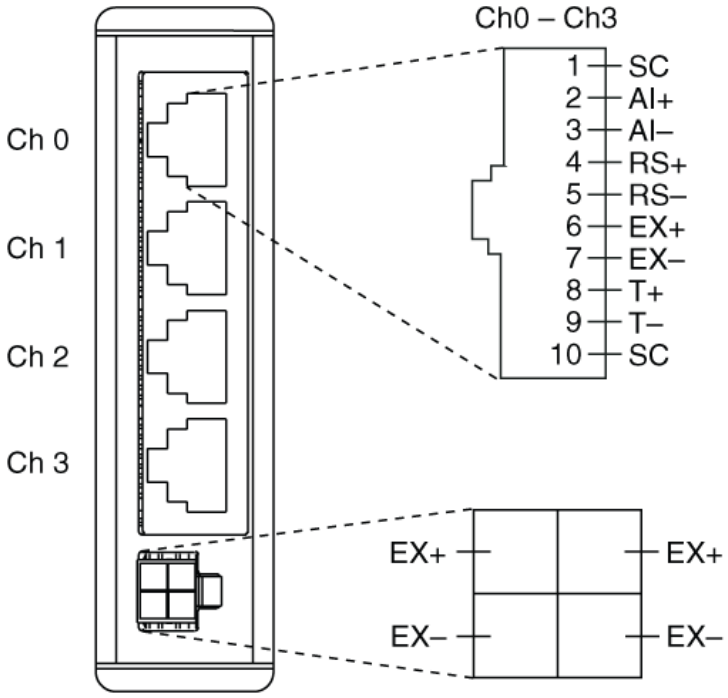

NI 9237 Pin Assignments

Back to Top

©2009 National Instruments. All rights reserved. CompactRIO, CVI, FieldPoint, LabVIEW, Measurement Studio, National Instruments, National Instruments Alliance Partner, NI, ni.com, NI CompactDAQ, and SignalExpress are trademarks of National Instruments. The mark LabWindows is used under a license from Microsoft Corporation. Windows is a registered trademark of Microsoft Corporation in the United States and other countries. Other product and company names listed are trademarks or trade names of their respective companies. A National Instruments Alliance Partner is a business entity independent from National Instruments and has no agency, partnership, or joint-venture relationship with National Instruments.

My Profile | RSS | Privacy | Legal | Contact NI © 2011 National Instruments Corporation. All rights reserved.

Technical Sales
United States
(866) 531-6285
info@ni.com

Last Revised: 2010-03-03 15:06:31.0

24-Bit Universal Analog Input

NI 9219

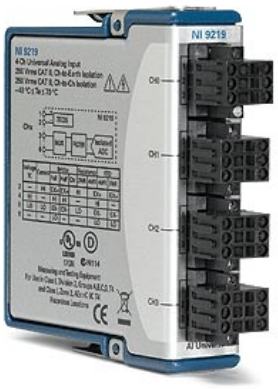

- 250 Vrms channel-to-channel isolation
- Built-in quarter-, half-, and full-bridge support
- Built-in voltage and current excitation
- Thermocouple, RTD, resistance, voltage, and current measurements
- CJC per channel for accurate thermocouple measurement
- 100 S/s/ch simultaneous inputs (50 S/s/ch for thermocouple)

Overview

The NI 9219 is a four-channel universal C Series module designed for multipurpose testing in any NI CompactDAQ or CompactRIO chassis. With the NI 9219, you can measure several signals from sensors such as strain gages, RTDs, thermocouples, load cells, and other powered sensors. The channels are individually selectable, so you can perform a different measurement type on each of the four channels. Measurement ranges differ for each type of measurement and include up to ±60 V for voltage and ±25 mA for current. Please see the manual for detailed specifications and ranges.

Back to Top

Requirements and Compatibility

OS Information

- Real-Time OS
- Windows

Driver Information

- NI-DAQmx
- NI-RIO

Software Compatibility

- LabVIEW
- LabVIEW SignalExpress
- LabWindows/CVI
- Measurement Studio
- Visual C++
- Visual Studio
- Visual Studio .NET

Back to Top

Comparison Tables

Thermocouple Module	Channels	Sample Rate	Resolution	Feature
NI 9213	16	1,200 S/s	24-bit	Lowest cost/channel
NI 9219	4	50 S/s/ch	24-bit	Channel-to-channel isolation
NI 9211	4	14 S/s	24-bit	Low-channel count

Back to Top

Application and Technology

Because of the driver design, the NI 9219 does not limit the overall speed of an NI CompactDAQ system when used with faster sampling modules. With 250 Vrms of channel-to-channel isolation, the NI 9219 protects not only the surrounding modules, chassis, and connected computer system but also the other channels within the same module. In addition to increased safety, channel-to-channel isolation eliminates problems associated with ground loops.

Connectivity Accessories

The NI 9219 uses six-position spring terminal connectors in each channel for direct signal connectivity. You can purchase additional connectors to reduce signal connection time for multiple test units. In addition to extra connectors, a strain relief kit is available to secure the signal wires. NI recommends:

- NI 9972 - strain relief backshells for signal wire security and high-voltage protection (qty 4)
- NI 9973 - extra connectors for six-position connector modules (qty 10)

NI C Series Compatibility

The NI C Series hardware family features more than 50 measurement modules and several chassis and carriers for deployment. With this variety of modules, you can mix and match measurements such as temperature, acceleration, flow, pressure, strain, acoustic, voltage, current, digital, and more to create a custom system. Install the modules in one of several carriers to create a single module USB, Ethernet, or Wi-Fi system, or combine them in chassis such as NI CompactDAQ and CompactRIO to create a mixed-measurement system with synchronized measurements. You can install up to eight modules in a simple, complete NI CompactDAQ USB data acquisition system to synchronize all of the analog output, analog input, and digital I/O from the modules. For a system without a PC, CompactRIO holds up to eight modules and features a built-in processor, RAM, and storage for an embedded data logger or control unit. For higher-speed control, CompactRIO chassis incorporate a field-programmable gate array (FPGA) that you can program with NI LabVIEW software to achieve silicon-speed processing on I/O data from C Series modules.

Advanced Features

When used with CompactRIO, NI C Series analog input modules connect directly to reconfigurable I/O (RIO) FPGA hardware to create high-performance embedded systems. The reconfigurable FPGA hardware within CompactRIO provides a variety of options for custom timing, triggering, synchronization, filtering, signal processing, and high-speed decision making for all C Series analog modules. For instance, with CompactRIO, you can implement custom triggering for any analog sensor type on a per-channel basis using the flexibility and performance of the FPGA and the numerous arithmetic and comparison function blocks built into the LabVIEW FPGA Module.

Key Features

- High-accuracy, high-performance analog measurements for any CompactRIO embedded system, R Series expansion chassis, or NI CompactDAQ chassis
- Screw terminals, BNC, D-Sub, spring terminals, strain relief, high voltage, cable, solder cup backshell, and other connectivity options
- Available channel-to-earth ground double-isolation barrier for safety, noise immunity, and high common-mode voltage range
- CompactRIO Extreme Industrial Certifications and Ratings
- Built-in signal conditioning for direct connection to sensors and industrial devices

Visit ni.com/compactrio or ni.com/compactdaq for up-to-date information on module availability, example programs, application notes, and other developer tools.

Back to Top

Ordering Information

For a complete list of accessories, visit the product page on ni.com.

Products	Part Number	Recommended Accessories	Part Number
NI 9219			
NI 9219	779781-01	No accessories required.	

Back to Top

Software Recommendations

LabVIEW Professional Development System for Windows

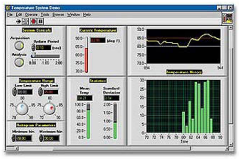

- Advanced software tools for large project development
- Automatic code generation using DAQ Assistant and Instrument I/O Assistant
- Tight integration with a wide range of hardware
- Advanced measurement analysis and digital signal processing
- Open connectivity with DLLs, ActiveX, and .NET objects
- Capability to build DLLs, executables, and MSI installers

Back to Top

Support and Services

System Assurance Programs

NI system assurance programs are designed to make it even easier for you to own an NI system. These programs include configuration and deployment services for your NI PXI, CompactRIO, or Compact FieldPoint system. The NI Basic System Assurance Program provides a simple integration test and ensures that your system is delivered completely assembled in one box. When you configure your system with the NI Standard System Assurance Program, you can select from available NI system driver sets and application development environments to create customized, reorderable software configurations. Your system arrives fully assembled and tested in one box with your software preinstalled. When you order your system with the standard program, you also receive system-specific documentation including a bill of materials, an integration test report, a recommended maintenance plan, and frequently asked question documents. Finally, the standard program reduces the total cost of owning an NI system by providing three years of warranty coverage and calibration service. Use the online product advisors at ni.com/advisor to find a system assurance program to meet your needs.

Calibration

NI measurement hardware is calibrated to ensure measurement accuracy and verify that the device meets its published specifications. NI offers a number of calibration services to help maintain the ongoing accuracy of your measurement hardware. These services allow you to be completely confident in your measurements, and help you maintain compliance to standards like ISO 9001, ANSI/NCSL Z540-1 and ISO/IEC 17025. To learn more about NI calibration services or to locate a qualified service center near you, contact your local sales office or visit ni.com/calibration.

Technical Support

Get answers to your technical questions using the following National Instruments resources.

- **Support** - Visit ni.com/support to access the NI KnowledgeBase, example programs, and tutorials or to contact our applications engineers who are located in NI sales offices around the world and speak the local language.
- **Discussion Forums** - Visit forums.ni.com for a diverse set of discussion boards on topics you care about.
- **Online Community** - Visit community.ni.com to find, contribute, or collaborate on customer-contributed technical content with users like you.

Repair

While you may never need your hardware repaired, NI understands that unexpected events may lead to necessary repairs. NI offers repair services performed by highly trained technicians who quickly return your device with the guarantee that it will perform to factory specifications. For more information, visit ni.com/repair.

Training and Certifications

The NI training and certification program delivers the fastest, most certain route to increased proficiency and productivity using NI software and hardware. Training builds the skills to more efficiently develop robust, maintainable applications, while certification validates your knowledge and ability.

- **Classroom training in cities worldwide** - the most comprehensive hands-on training taught by engineers.
- **On-site training at your facility** - an excellent option to train multiple employees at the same time.
- **Online instructor-led training** - lower-cost, remote training if classroom or on-site courses are not possible.
- **Course kits** - lowest-cost, self-paced training that you can use as reference guides.
- **Training memberships** and training credits - to buy now and schedule training later.

Visit ni.com/training for more information.

Extended Warranty

NI offers options for extending the standard product warranty to meet the life-cycle requirements of your project. In addition, because NI understands that your requirements may change, the extended warranty is flexible in length and easily renewed. For more information, visit ni.com/warranty.

OEM

NI offers design-in consulting and product integration assistance if you need NI products for OEM applications. For information about special pricing and services for OEM customers, visit ni.com/oem.

Alliance

Our Professional Services Team is comprised of NI applications engineers, NI Consulting Services, and a worldwide National Instruments Alliance Partner program of more than 600 independent consultants and integrators. Services range from start-up assistance to turnkey system integration. Visit ni.com/alliance.

Back to Top

Detailed Specifications

The following specifications are typical for the range –40 to 70 °C unless otherwise noted.

Input Characteristics	
Number of channels	4 analog input channels
ADC resolution	24 bits
Type of ADC	Delta-sigma (with analog prefiltering)
Sampling mode	Simultaneous
Type of TEDS supported	IEEE 1451.4 TEDS Class II (Interface)

Mode input ranges		
Mode	**Nominal Range(s)**	**Actual Range(s)**
Voltage	±60 V, ±15 V, ±4 V, ±1 V, ±125 mV	±60 V, ±15 V, ±4 V, ±1 V, ±125 mV
Current	±25 mA	±25 mA
4-Wire and 2-Wire Resistance	10 kΩ, 1 kΩ	10.5 kΩ, 1.05 kΩ
Thermocouple	±125 mV	±125 mV
4-Wire and 3-Wire RTD	Pt 1000, Pt 100	5.05 kΩ, 505 Ω
Quarter-Bridge	350 Ω, 120 Ω	390 Ω, 150 Ω
Half-Bridge	±500 mV/V	±500 mV/V
Full-Bridge	±62.5 mV/V, ±7.8 mV/V	±62.5 mV/V, ±7.8125 mV/V
Digital In	—	0–60 V
Open Contact	—	1.05 kΩ

Conversion time, no channels in TC mode	
High speed	10 ms for all channels
Best 60 Hz rejection	110 ms for all channels
Best 50 Hz rejection	130 ms for all channels
High resolution	500 ms for all channels
Conversion time, one or more channels in TC mode	
High speed	20 ms for all channels
Best 60 Hz rejection	120 ms for all channels
Best 50 Hz rejection	140 ms for all channels
High resolution	510 ms for all channels
Overvoltage protection	
Terminals 1 and 2	±30 V
Terminals 3 through 6, across any combination	±60 V
Input impedance	
Voltage and Digital In modes (±60 V, ±15 V, ±4 V)	1 MΩ
Current mode	<40 Ω
All other modes	>1 GΩ

Accuracy		
Mode, Range	**Gain Error (Percent of Reading)**	**Offset Error (ppm of Range)**
	Typ (25 °C, ±5 °C), Max (–40 to 70 °C)	
Voltage, ±60 V	±0.3, ±0.4	±20, ±50
Voltage, ±15 V	±0.3, ±0.4	±60, ±180
Voltage, ±4 V	±0.3, ±0.4	±240, ±720
Voltage, ±1 V	±0.1, ±0.18	±15, ±45
Voltage/Thermocouple, ±125 mV	±0.1, ±0.18	±120, ±360
Current, ±25 mA	±0.1, ±0.6	±30, ±100
4-Wire and 2-Wire [1] Resistance, 10 kΩ	±0.1, ±0.5	±120, ±320
4-Wire and 2-Wire [1] Resistance, 1 kΩ	±0.1, ±0.5	±1200, ±3200
4-Wire and 3-Wire RTD, Pt 1000	±0.1, ±0.5	±240, ±640
4-Wire and 3-Wire RTD, Pt 100	±0.1, ±0.5	±2400, ±6400
Quarter-Bridge, 350 Ω	±0.1, ±0.5	±2400, ±6400
Quarter-Bridge, 120 Ω	±0.1, ±0.5	±2400, ±6400
Half-Bridge, ±500 mV/V	±0.03, ±0.07	±300, ±450
Full-Bridge, ±62.5 mV/V	±0.03, ±0.08	±300, ±1000
Full-Bridge, ±7.8 mV/V	±0.03, ±0.08	±2200, ±8000

Cold-junction compensation sensor accuracy	±1°C typ

Stability		
Mode, Range	**Gain Drift (ppm of Read-ing/°C)**	**Offset Drift (ppm of Range/°C)**
Voltage, ±60 V	±20	±0.2
Voltage, ±15 V	±20	±0.8
Voltage, ±4 V	±20	±3.2
Voltage, ±1 V	±10	±0.2
Voltage/Thermocouple, ±125 mV	±10	±1.6
Current, ±25 mA	±15	±0.4
4-Wire and 2-Wire Resistance, 10 kΩ	±15	±3
4-Wire and 2-Wire Resistance, 1 kΩ	±15	±30
4-Wire and 3-Wire RTD, Pt 1000	±15	±6
4-Wire and 3-Wire RTD, Pt 100	±15	±60
Quarter-Bridge, 350 Ω	±15	±120
Quarter-Bridge, 120 Ω	±15	±240
Half-Bridge, ±500 mV/V	±3	±20
Full-Bridge, ±62.5 mV/V	±3	±20
Full-Bridge, ±7.8 mV/V	±3	±20

Input noise in ppm of $Range_{rms}$				
Mode, Range	**Conversion Time**			
	High speed	**Best 60 Hz re-jection**	**Best 50 Hz re-jection**	**High resolution**
Voltage, ±60 V	7.6	1.3	1.3	0.5
Voltage, ±15 V	10.8	1.9	1.9	0.7
Voltage, ±4 V	10.8	2.7	2.7	1.3
Voltage, ±1 V	7.6	1.3	1.3	0.5
Voltage/Thermocouple, ±125 mV	10.8	1.9	1.9	1.0
Current, ±25 mA	10.8	1.9	1.9	1.0
4-Wire and 2-Wire Resistance, 10 kΩ	4.1	1.3	0.8	0.3
4-Wire and 2-Wire Resistance, 1 kΩ	7.1	1.8	1.2	0.7
4-Wire and 3-Wire RTD, Pt 1000	7.6	1.7	1.1	0.4
4-Wire and 3-Wire RTD, Pt 100	10.8	1.9	1.9	0.9
Quarter-Bridge, 350 Ω	5.4	1.0	1.0	0.7
Quarter-Bridge, 120 Ω	5.4	1.0	1.0	0.7
Half-Bridge, ±500 mV/V	3.8	0.5	0.5	0.2
Full-Bridge, ±62.5 mV/V	5.4	1.0	1.0	0.8
Full-Bridge, ±7.8 mV/V	30	4.7	4.7	2.3

Input bias current	<1 nA
INL	±15 ppm
CMRR (f_{in} = 60 Hz)	>100 dB
NMRR	
Best 60 Hz rejection	90 dB at 60 Hz
Best 50 Hz rejection	80 dB at 50 Hz
High resolution	65 dB at 50 Hz and 60 Hz

Excitation level for Half-Bridge and Full-Bridge modes		
Mode	**Load Resistance (Ω)**	**Excitation (V)**
Half-Bridge	700	2.5

	240	2.0
Full-Bridge	350	2.7
	120	2.2

Excitation level for Resistance, RTD, and Quarter-Bridge modes	
Load Resistance (Ω)	**Excitation (mV)**
120	50
350	150
1 k	430
10 k	2200

MTBF	384,716 hours at 25 °C; Bellcore Issue 2, Method 1, Case 3, Limited Part Stress Method

Note Contact NI for Bellcore MTBF specifications at other temperatures or for MIL-HDBK-217F specifications.

Power Requirements

Power consumption from chassis	
Active mode	750 mW max
Sleep mode	25 µW max
Thermal dissipation (at 70 °C)	
Active mode	625 mW max
Sleep mode	25 µW max

Physical Characteristics

Note For two-dimensional drawings and three-dimensional models of the C Series module and connectors, visit ni.com/dimensions and search by module number.

Spring-terminal wiring	18 to 28 AWG copper conductor wire with 7 mm (0.28 in.) of insulation stripped from the end
Weight	156 g (5.5 oz)

Safety

If you need to clean the module, wipe it with a dry towel.

Safety Voltages

Connect only voltages that are within the following limits.

Channel-to-channel	
Continuous	250 VAC, Measurement Category II
Withstand	1,390 VAC, verified by a 5 s dielectric withstand test
Channel-to-earth ground	
Continuous	250 VAC, Measurement Category II
Withstand	2,300 VAC, verified by a 5 s dielectric withstand test
Zone 2 hazardous locations applications in Europe channel-to-channel and channel-to-earth ground	60 VDC, Measurement Category I

Measurement Category I is for measurements performed on circuits not directly connected to the electrical distribution system referred to as MAINS [2] voltage. This category is for measurements of voltages from specially protected secondary circuits. Such voltage measurements include signal levels, special equipment, limited-energy parts of equipment, circuits powered by regulated low-voltage sources, and electronics.

Caution Do *not* connect to signals or use for measurements within Measurement Categories II, III, or IV.

Measurement Category II is for measurements performed on circuits directly connected to the electrical distribution system. This category refers to local-level electrical distribution, such as that provided by a standard wall outlet (e.g., 115 V for U.S. or 230 V for Europe). Examples of Measurement Category II are measurements performed on household appliances, portable tools, and similar products.

Caution Do *not* connect to signals or use for measurements within Measurement Categories III or IV.

Hazardous Locations

U.S. (UL)	Class I, Division 2, Groups A, B, C, D, T4; Class I, Zone 2, AEx nA IIC T4
Canada (C-UL)	Class I, Division 2, Groups A, B, C, D, T4; Class I, Zone 2, Ex nA IIC T4
Europe (DEMKO)	Ex nA IIC T4

Safety Standards

This product is designed to meet the requirements of the following standards of safety for electrical equipment for measurement, control, and laboratory use:

- IEC 61010-1, EN 61010-1
- UL 61010-1, CSA 61010-1

Note For UL and other safety certifications, refer to the product label or the *Online Product Certification* section.

Electromagnetic Compatibility

This product meets the requirements of the following EMC standards for electrical equipment for measurement, control, and laboratory use:

- EN 61326 (IEC 61326): Class A emissions; Industrial Immunity
- EN 55011 (CISPR 11): Group 1, Class A emissions
- AS/NZS CISPR 11: Group 1, Class A emissions
- FCC 47 CFR Part 15B: Class A emissions
- ICES-001: Class A emissions

Note For the standards applied to assess the EMC of this product, refer to the *Online Product Certification* section.

Note For EMC compliance, operate this device with shielded cables.

CE Compliance

This product meets the essential requirements of applicable European Directives, as amended for CE marking, as follows:

- 2006/95/EC; Low-Voltage Directive (safety)
- 2004/108/EC; Electromagnetic Compatibility Directive (EMC)

Note For the standards applied to assess the EMC of this product, refer to the *Online Product Certification* section.

Online Product Certification

Refer to the product Declaration of Conformity (DoC) for additional regulatory compliance information. To obtain product certifications and the DoC for this product, visit ni.com/certification, search by module number or product line, and click the appropriate link in the Certification column.

Shock and Vibration

To meet these specifications, you must panel mount the system.

Operating vibration	
Random (IEC 60068-2-64)	5 g_{rms}, 10 to 500 Hz
Sinusoidal (IEC 60068-2-6)	5 g, 10 to 500 Hz
Operating shock (IEC 60068-2-27)	30 g, 11 ms half sine, 50 g, 3 ms half sine, 18 shocks at 6 orientations

Environmental

National Instruments C Series modules are intended for indoor use only but may be used outdoors if installed in a suitable enclosure. Refer to the manual for the chassis you are using for more information about meeting these specifications.

Operating temperature (IEC 60068-2-1, IEC 60068-2-2)	–40 to 70 °C
Storage temperature (IEC 60068-2-1, IEC 60068-2-2)	–40 to 85 °C
Ingress protection	IP 40
Operating humidity (IEC 60068-2-56)	10 to 90% RH, noncondensing
Storage humidity (IEC 60068-2-56)	5 to 95% RH, noncondensing
Maximum altitude	2,000 m
Pollution Degree (IEC 60664)	2

Environmental Management

National Instruments is committed to designing and manufacturing products in an environmentally responsible manner. NI recognizes that eliminating certain hazardous substances from our products is beneficial not only to the environment but also to NI customers.

For additional environmental information, refer to the *NI and the Environment* Web page at ni.com/environment. This page contains the environmental regulations and directives with which NI complies, as well as other environmental information not included in this document.

Waste Electrical and Electronic Equipment (WEEE)

EU Customers At the end of their life cycle, all products *must* be sent to a WEEE recycling center. For more information about WEEE recycling centers and National Instruments WEEE initiatives, visit ni.com/environment/weee.htm.

电子信息产品污染控制管理办法 （中国 RoHS）

中国客户 National Instruments 符合中国电子信息产品中限制使用某些有害物质指令 (RoHS)。
关于 National Instruments 中国 RoHS 合规性信息，请登录 ni.com/environment/rohs_china。
(For information about China RoHS compliance, go to ni.com/environment/rohs_china.)

Calibration

You can obtain the calibration certificate for this device at ni.com/calibration.

Calibration interval	1 year

[1] 2-Wire Resistance mode accuracy depends on the lead wire resistance. This table assumes 0 Ω of lead wire resistance.

[2] MAINS is defined as the (hazardous live) electrical supply system to which equipment is designed to be connected for the purpose of powering the equipment. Suitably rated measuring circuits may be connected to the MAINS for measuring purposes.

Back to Top

Pinouts/Front Panel Connections

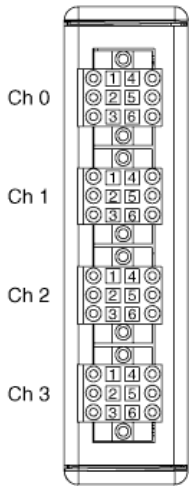

Back to Top

©2010 National Instruments. All rights reserved. CompactRIO, CVI, FieldPoint, LabVIEW, National Instruments, National Instruments Alliance Partner, NI, ni.com, NI CompactDAQ, and SignalExpress are trademarks of National Instruments. The mark LabWindows is used under a license from Microsoft Corporation. Windows is a registered trademark of Microsoft Corporation in the United States and other countries. Other product and company names listed are trademarks or trade names of their respective companies. A National Instruments Alliance Partner is a business entity independent from National Instruments and has no agency, partnership, or joint-venture relationship with National Instruments.

My Profile | RSS | Privacy | Legal | Contact NI © 2011 National Instruments Corporation. All rights reserved.

APPENDIX C. TRANSFERING EMBEDDED STRAINS TO SURFACE STRAINS

In order to obtain the highest strains during transportation, strains measured using embedded strain gage in Girder 1 were transferred to surface strains. The measured strains during girder transportation include the effect of prestressing force, bending moment due to gravity loads (girder own weight), and lateral bending moment due to sweep and girder tilt during transportation. As indicated earlier, the strains were measured at four points: a) bottom strain - left side (ε_{bl}), b) bottom strain - right side (ε_{br}), c) top strain - left side (ε_{tl}), and a) top strain - right side (ε_{tr}). Assuming linear behavior, the strains measured from embedded sensors can be transferred to surface strains using the following equations.

Assume that the left strains has a higher value than the right strains

$$\varepsilon_{bl-E} = \varepsilon_{vertival\ loads} + \varepsilon_{lateral\ loads}$$ Measured embedded strain - bottom left

$$\varepsilon_{br-E} = \varepsilon_{vertival\ loads} - \varepsilon_{lateral\ loads}$$ Measured embedded strain - bottom right

$$\varepsilon_{lateral\ loads} = \frac{\varepsilon_{bl} - \varepsilon_{br}}{2} = \frac{\Delta\varepsilon}{2}$$

Transfer measured strain from embedded gages to surface strains

$$\varepsilon_{bl-S} = \varepsilon_{bl-E} + \left(\frac{\Delta\varepsilon}{2} * \frac{Distnace\ from\ centerline\ to\ extreme\ fiber}{Distnace\ from\ centerline\ to\ strain\ gage} - \frac{\Delta\varepsilon}{2}\right)$$

$$\varepsilon_{br-S} = \varepsilon_{br-E} - \left(\frac{\Delta\varepsilon}{2} * \frac{Distnace\ from\ centerline\ to\ extreme\ fiber}{Distnace\ from\ centerline\ to\ strain\ gage} - \frac{\Delta\varepsilon}{2}\right)$$

For Girder 1: Bottom strains

$$\varepsilon_{bl-S} = \varepsilon_{bl-E} + 0.15\ \Delta\varepsilon$$ Calculated surface strain - bottom left

$$\varepsilon_{br-S} = \varepsilon_{br-E} - 0.15\ \Delta\varepsilon$$ Calculated surface strain - bottom right

Using a similar approach for Girder 1: Top strains

$$\varepsilon_{tl-S} = \varepsilon_{tl-E} + 0.32\ \Delta\varepsilon$$ Calculated surface strain - top left

$$\varepsilon_{tr-S} = \varepsilon_{tr-E} - 0.32\ \Delta\varepsilon$$ Calculated surface strain - top right

APPENDIX D. ESTIMATED ANALYTICAL STRAINS

This appendix includes two Mathcad sheets to show detailed calculations of the predicted strains at transfer at each of the monitored sections. These calculated strains were used to determine the state of strain of Girder 1 section D and in all the sections of Girder 2 prior to transport.

Estimated analytical strains for Girder 1 - BT72

Objective:
Estimate the concrete strains analytically at the different strain gage locations.

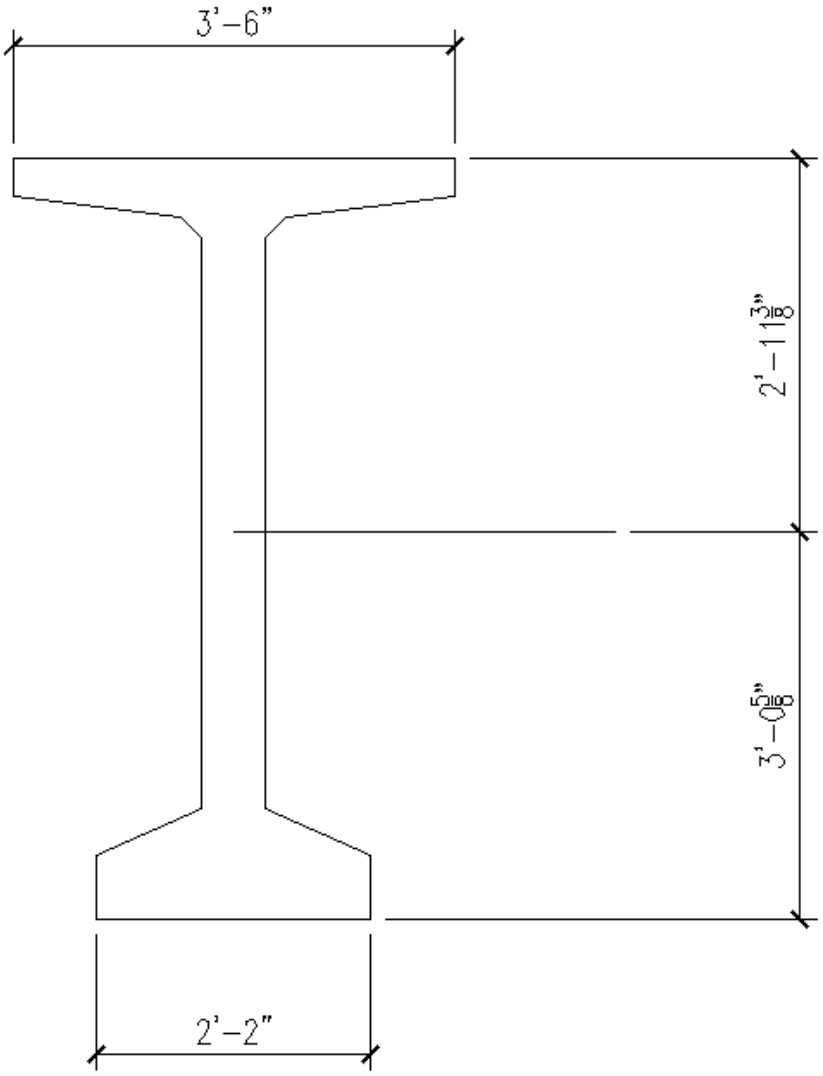

$A_c := 767in^2$ $I_x := 545857 \cdot in^4$ $I_y := 37634in^4$ $r_x := 26.677in$ $\gamma_{conc} := 150 \frac{lbf}{ft^3}$

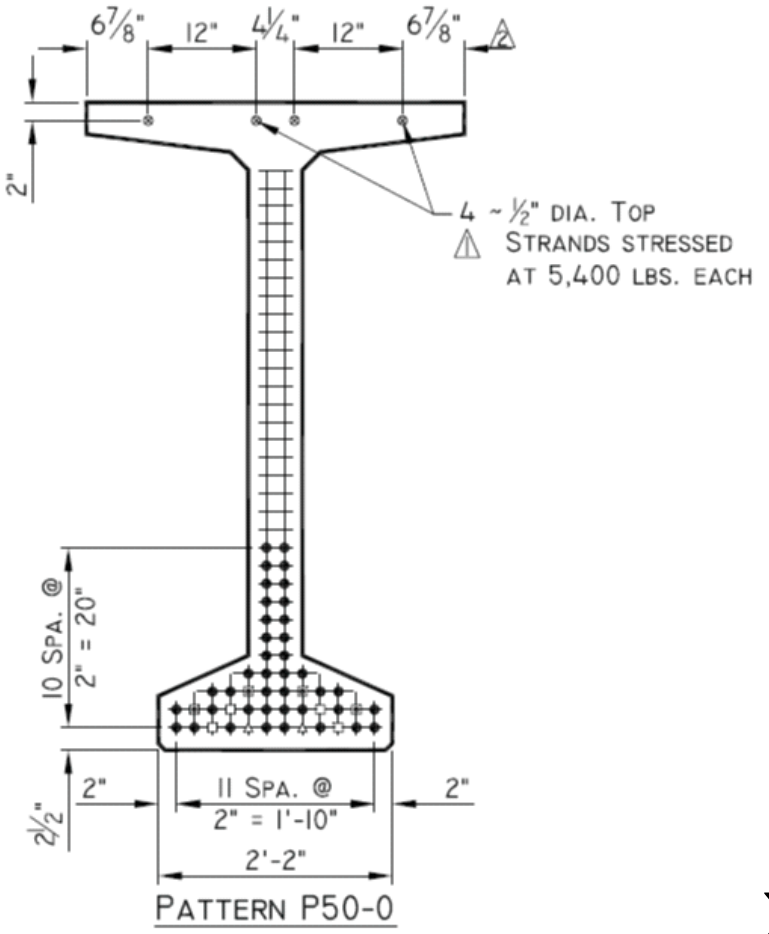

$A_{strand} := 0.153in^2$

Vector of number of 1/2"dia. strands per row, as shown by the diagram

$$strandsPerRow := \begin{pmatrix} 12 \\ 12 \\ 8 \\ 4 \\ 2 \\ 2 \\ 2 \\ 2 \\ 2 \\ 2 \\ 2 \end{pmatrix}$$

$\sum strandsPerRow = 50$

Calculate the CG of the prestressing steel

$$fpsCG := \frac{strandsPerRow_1 \cdot A_{strand} \cdot 2.5in + \sum_{k=2}^{11} \left[strandsPerRow_k \cdot A_{strand} \cdot [2.5in + 2in \cdot (k-1)] \right]}{A_{strand} \cdot \sum strandsPerRow}$$

$fpsCG = 8.02 \cdot in$ *CG of prestressing is 8.02 in up from the bottom*

The total amount of prestressing steel is equal to Aps

$A_{ps} := A_{strand} \cdot \sum strandsPerRow = 7.65 \cdot in^2$

The prestressing steel is assumed to have the following ultimate stress (fpu), modulus of elasticity (Es)

$f_{pu} := 270ksi$

$E_s := 29000ksi$

The concrete has the following material properties

$f_{ci} := 8170psi$

$E_{ci} := 5930ksi$

The modular ratio between the steel and concrete is calculated as n:

$$n := \frac{E_s}{E_{ci}} = 4.9$$

Composite section CG at release

$CG_y := 36.6in$

$$CG_{yi} := \frac{CG_y \cdot A_c + (n-1)A_{ps}\,fpsCG}{A_c + (n-1)A_{ps}} = 35.5 \cdot in$$

$$A_{ci} := A_c + (n-1)A_{ps} = 796.8 \cdot in^2$$

$$I_{xi} := I_x + A_c \cdot (CG_{yi} - CG_y)^2 + (n-1) \cdot A_{ps} \cdot (fpsCG - CG_{yi})^2 = 569258.6 \cdot in^4$$

$e := CG_{yi} - fpsCG = 27.5 \cdot in$

Calculate girder dead load moment at centerline

The moment calculation is based on a length of the girder

$L_{crib} := 129ft$

The weight of the girder based on solid concrete is calculated as

$$w_{dl} := A_c \cdot \gamma_{conc} = 0.8 \cdot \frac{kip}{ft}$$

The dead load of the girder is therefore:

$$M_{dl} := \frac{w_{dl} \cdot L_{crib}^2}{8} = 1661.9 \cdot kip \cdot ft$$

Concrete Strains due only to transfer at release

$f_{si} := 0.75 \cdot f_{pu} = 202.5 \cdot ksi$

$F_{si} := A_{ps} \cdot f_{si} = 1549.1 \cdot kip$

$f_{cgp} := \frac{-F_{si}}{A_{ci}} - \frac{F_{si} \cdot e^2}{I_{xi}} + \frac{M_{dl} \cdot e}{I_{xi}} = -3 \cdot ksi$

$\varepsilon_{cgp} := \frac{f_{cgp}}{E_{ci}} \cdot 1 \times 10^6 = -512.69$

Elastic shortening losses

$f_{ES} := n \cdot f_{cgp} \cdot -1 = 14.9 \cdot ksi$

$F_{se} := \left(f_{si} - f_{ES}\right) \cdot A_{ps} = 1435.4 \cdot kip$

Concrete Strains due only to transfer and dead load after elastic shoretening losses at centerline at strain gages locations (Section B-B)

$y_{botms} := CG_{yi} - 2in = 33.5 \cdot in$

$y_{topms} := 72in - CG_{yi} - 1.5in = 35 \cdot in$

$f_{c.sedl.bot} := \frac{M_{dl} \cdot y_{botms}}{I_{xi}} + \frac{-F_{se}}{A_{ci}} - \frac{F_{se} \cdot e \cdot y_{botms}}{I_{xi}} = -3 \cdot ksi$

$\varepsilon_{c.sedl.bot} := \frac{f_{c.sedl.bot}}{E_{ci}} \cdot 1 \times 10^6 = -497.98$

$f_{c.sedl.top} := -\frac{M_{dl} \cdot y_{topms}}{I_{xi}} + \frac{-F_{se}}{A_{ci}} + \frac{F_{se} \cdot e \cdot y_{topms}}{I_{xi}} = -0.6 \cdot ksi$

$\varepsilon_{c.sedl.top} := \frac{f_{c.sedl.top}}{E_{ci}} \cdot 1 \times 10^6 = -101.31$

Concrete Strains due only to transfer and dead load after elastic shoretening losses at centerline at strain gages locations (Section D-D) Jeep guide 32ft from end

This section has the same properties as the mid span section

$$M_{dldd} := w_{dl} \cdot L_{crib} \cdot 0.5 \cdot 31.5ft - w_{dl} \cdot (31.5ft)^2 \cdot 0.5 = 1226.9 \cdot kip \cdot ft$$

$$f_{c.sedl.botdd} := \frac{M_{dldd} \cdot y_{botms}}{I_{xi}} + \frac{-F_{se}}{A_{ci}} - \frac{F_{se} \cdot e \cdot y_{botms}}{I_{xi}} = -3.3 \cdot ksi$$

$$\varepsilon_{c.sedl.botdd} := \frac{f_{c.sedl.botdd}}{E_{ci}} \cdot 1 \times 10^6 = -549.83$$

$$f_{c.sedl.topdd} := -\frac{M_{dldd} \cdot y_{topms}}{I_{xi}} + \frac{-F_{se}}{A_{ci}} + \frac{F_{se} \cdot e \cdot y_{topms}}{I_{xi}} = -0.28 \cdot ksi$$

$$\varepsilon_{c.sedl.topdd} := \frac{f_{c.sedl.topdd}}{E_{ci}} \cdot 1 \times 10^6 = -47.24$$

Concrete Strains due only to transfer and dead load after elastic shoretening losses 10 ft from the ends at strain gages locations (Section A-A and C-C)

$$strandsPerRowaa := \begin{pmatrix} 8 \\ 10 \\ 8 \\ 4 \\ 2 \\ 2 \\ 2 \\ 2 \\ 2 \\ 2 \\ 2 \end{pmatrix}$$

$$fpsCG_{aa} := \frac{strandsPerRowaa_1 \cdot A_{strand} \cdot 2.5in + \sum_{k=2}^{11} \left[strandsPerRowaa_k \cdot A_{strand} \cdot [2.5in + 2in \cdot (k-1)] \right]}{A_{strand} \cdot \sum strandsPerRow}$$

$$fpsCG_{aa} = 7.6 \cdot in$$

$e_{aa} := CG_{yi} - fpsCG_{aa} = 27.9 \cdot in$

$M_{dlaa} := w_{dl} \cdot L_{crib} \cdot 0.5 \cdot 9.5ft - w_{dl} \cdot (9.5ft)^2 \cdot 0.5 = 453.5 \cdot kip \cdot ft$

$$f_{cgpaa} := \frac{-F_{si}}{A_{ci}} - \frac{F_{si} \cdot e_{aa}^2}{I_{xi}} + \frac{M_{dlaa} \cdot e_{aa}}{I_{xi}} = -3.8 \cdot ksi$$

Elastic shortening losses

$f_{ESaa} := n \cdot f_{cgpaa} \cdot -1 = 18.6 \cdot ksi$

$F_{seaa} := \left(f_{si} - f_{ESaa}\right) \cdot 44 \cdot 0.153in^2 = 1238.3 \cdot kip$

Concrete strains

$y_{botaa} := CG_{yi} - 2in = 33.5 \cdot in$ $\qquad$ $y_{topaa} := 72in - CG_{yi} - 1.5in = 35 \cdot in$

$$f_{c.sedl.botaa} := \frac{M_{dlaa} \cdot y_{botaa}}{I_{xi}} + \frac{-F_{seaa}}{A_{ci}} - \frac{F_{seaa} \cdot e_{aa} \cdot y_{botaa}}{I_{xi}} = -3.3 \cdot ksi$$

$$\varepsilon_{c.sedl.botaa} := \frac{f_{c.sedl.botaa}}{E_{ci}} \cdot 1 \times 10^6 = -551.12$$

$$f_{c.sedl.topaa} := -\frac{M_{dlaa} \cdot y_{topaa}}{I_{xi}} + \frac{-F_{seaa}}{A_{ci}} + \frac{F_{seaa} \cdot e_{aa} \cdot y_{topaa}}{I_{xi}} = 0.23 \cdot ksi$$

$$\varepsilon_{c.sedl.topaa} := \frac{f_{c.sedl.topaa}}{E_{ci}} \cdot 1 \times 10^6 = 39.32$$

Estimated analytical strains for Girder 2 - LG54

Objective:
Estimate the concrete strains analytically at the different strain gage locations.

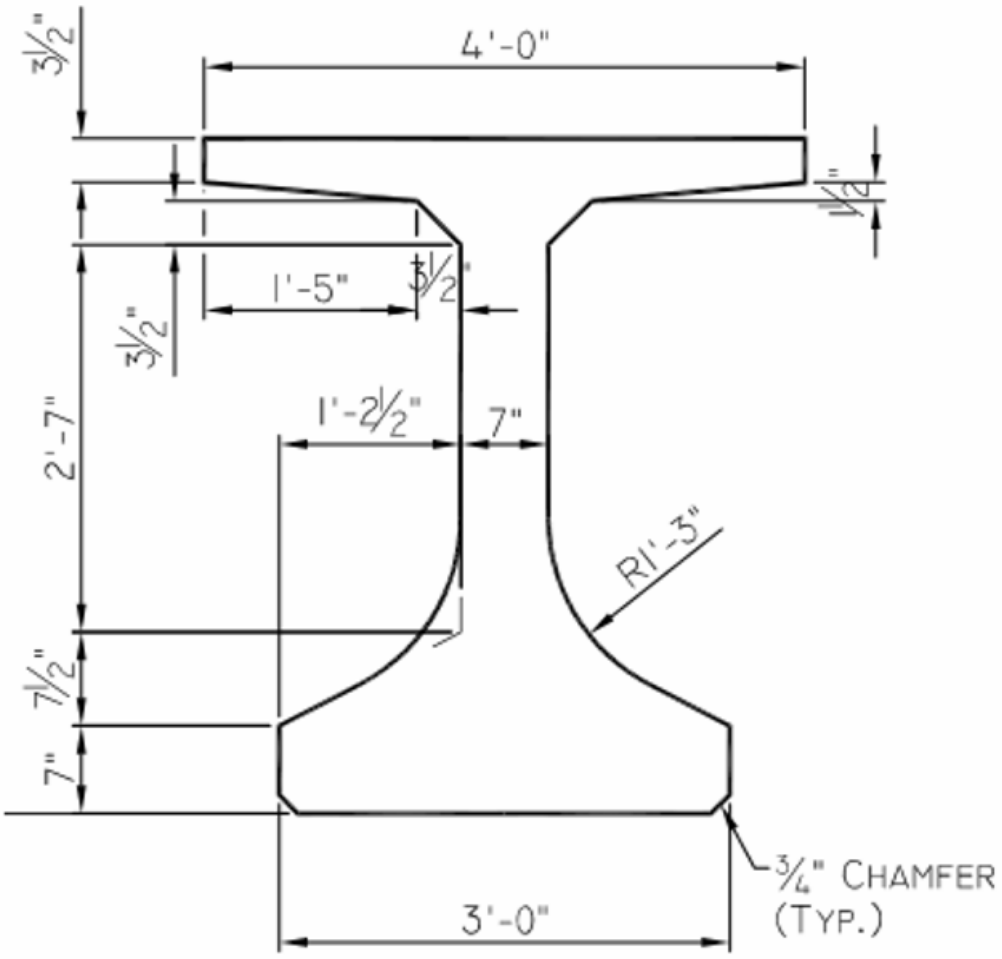

LG-54 BEAM

$A_c := 868\,in^2$ $I_x := 344586 \cdot in^4$ $I_y := 70877 in^4$ $r_x := 19.9in$ $\gamma_{conc} := 150 \frac{lbf}{ft^3}$

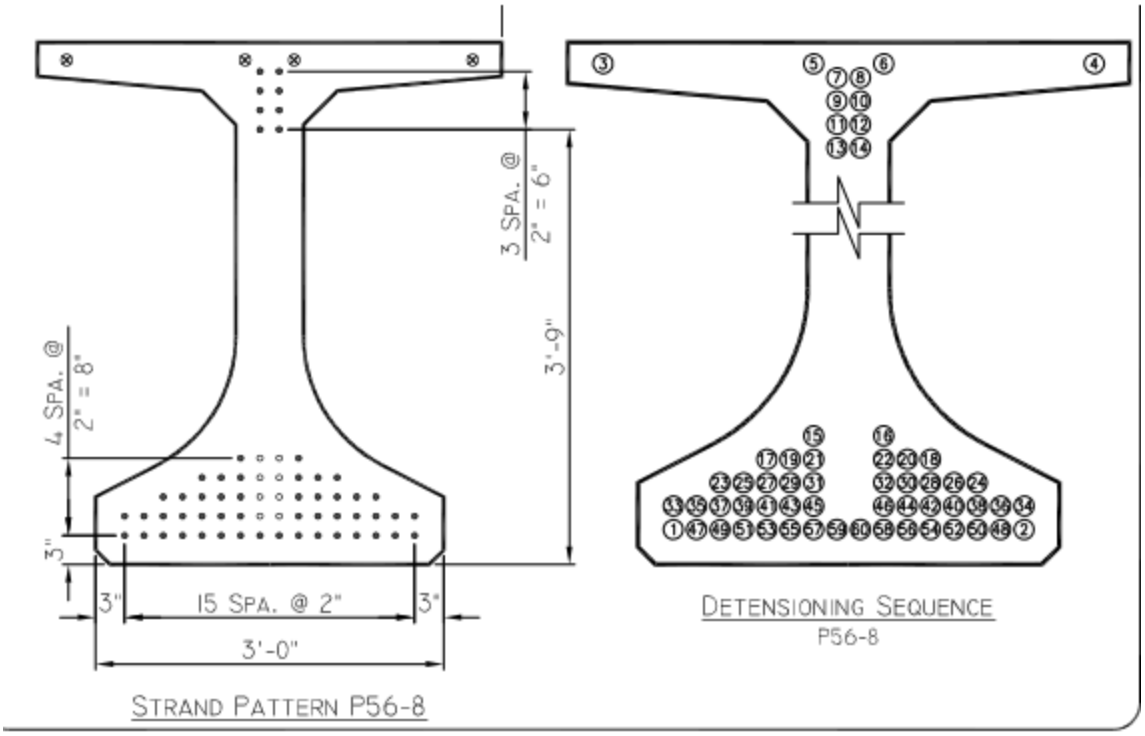

STRAND INFORMATION

- 56 — TOTAL NUMBER OF 0.6"Ø 270K L/R STRANDS STRESSED @ 43,940 LBS. EACH
- 48 — TOTAL NUMBER OF STRAIGHT STRANDS
- 4 — TOTAL NUMBER OF 0.375"Ø TOP STRANDS STRESSED @ 10,000 LBS. EACH
- 8 — TOTAL NUMBER OF DRAPED STRANDS

DRAPED STRAND INFO.

H = 3'-9"
h = 5"

SYMBOL LEGEND

- ● DENOTES FULLY BONDED 0.6"Ø STRANDS STRESSED @ 43,940 LBS. EACH
- ⊗ DENOTES FULLY BONDED 0.375"Ø STRANDS STRESSED @ 10,000 LBS. EACH
- ○ DENOTES DRAPED STRAND @ MID-SPAN

$A_{strand} := 0.217in^2$

Vector of number of 0.6" dia. strands per row at midspan, as shown by the diagram

$$strandsPerRow := \begin{pmatrix} 16 \\ 16 \\ 12 \\ 8 \\ 4 \end{pmatrix}$$

$\sum strandsPerRow = 56$

Calculate the CG of the prestressing steel

$$fpsCG := \frac{strandsPerRow_1 \cdot A_{strand} \cdot 3in + \sum_{k=2}^{5} \left[strandsPerRow_k \cdot A_{strand} \cdot [3in + 2in \cdot (k-1)] \right]}{A_{strand} \cdot \sum strandsPerRow}$$

$fpsCG = 5.86 \cdot in$ *CG of prestressing is 5.86 in up from the bottom*

The total amount of prestressing steel is equal to Aps

$A_{ps} := A_{strand} \cdot \sum strandsPerRow = 12.15 \cdot in^2$

The prestressing steel is assumed to have the following ultimate stress (fpu), modulus of elasticity (Es)

$f_{pu} := 270ksi$

$E_s := 29000ksi$

The concrete has the following material properties

$f_{ci} := 8170psi$

$E_{ci} := 5930ksi$

The modular ratio between the steel and concrete is calculated as n:

$n := \frac{E_s}{E_{ci}} = 4.9$

Composite section CG at release

$CG_y := 25.1in$

$CG_{yi} := \frac{CG_y \cdot A_c + (n-1) A_{ps} fpsCG}{A_c + (n-1) A_{ps}} = 24.1 \cdot in$

$A_{ci} := A_c + (n-1) A_{ps} = 915.8 \cdot in^2$

$I_{xi} := I_x + A_c \cdot (CG_{yi} - CG_y)^2 + (n-1) \cdot A_{ps} \cdot (fpsCG - CG_{yi})^2 = 361188 \cdot in^4$

$e := CG_{yi} - fpsCG = 18.2 \cdot in$

Calculate girder dead load moment at centerline

The moment calculation is based on a length of the girder

$L_{crib} := 129ft$

The weight of the girder based on solid concrete is calculated as

$w_{dl} := A_c \cdot \gamma_{conc} = 0.9 \cdot \frac{kip}{ft}$

The dead load of the girder is therefore:

$M_{dl} := \frac{w_{dl} \cdot L_{crib}^2}{8} = 1881.9 \cdot kip \cdot ft$

Concrete Stresses due only to transfer at release

$f_{si} := 0.75 \cdot f_{pu} = 202.5 \cdot ksi$

$F_{si} := A_{ps} \cdot f_{si} = 2460.8 \cdot kip$

$f_{cgp} := \frac{-F_{si}}{A_{ci}} - \frac{F_{si} \cdot e^2}{I_{xi}} + \frac{M_{dl} \cdot e}{I_{xi}} = -3.8 \cdot ksi$ $\varepsilon_{cgp} := \frac{f_{cgp}}{E_{ci}} \cdot 1 \times 10^6 = -643.36$

Elastic shortening losses

$f_{ES} := n \cdot f_{cgp} \cdot -1 = 18.7 \cdot ksi$ $F_{se} := \left(f_{si} - f_{ES}\right) \cdot A_{ps} = 2234.1 \cdot kip$

Concrete Stresses due only to transfer and dead load after elastic shoretening losses at centerline at strain gages locations (Section B-B)

$y_{botms} := CG_{yi} - 2in = 22.1 \cdot in$ $y_{topms} := 54in - CG_{yi} - 1.5in = 28.4 \cdot in$

$f_{c.sedl.bot} := \frac{M_{dl} \cdot y_{botms}}{I_{xi}} + \frac{-F_{se}}{A_{ci}} - \frac{F_{se} \cdot e \cdot y_{botms}}{I_{xi}} = -3.6 \cdot ksi$

$\varepsilon_{c.sedl.bot} := \frac{f_{c.sedl.bot}}{E_{ci}} \cdot 1 \times 10^6 = -599.11$

$f_{c.sedl.top} := -\frac{M_{dl} \cdot y_{topms}}{I_{xi}} + \frac{-F_{se}}{A_{ci}} + \frac{F_{se} \cdot e \cdot y_{topms}}{I_{xi}} = -1.01 \cdot ksi$

$\varepsilon_{c.sedl.top} := \frac{f_{c.sedl.top}}{E_{ci}} \cdot 1 \times 10^6 = -170.28$

Concrete Stresses due only to transfer and dead load after elastic shoretening losses at centerline at strain gages locations (Section D-D) Jeep guide 32ft from end

$$strandsPerRowdd := \begin{pmatrix} 16 \\ 14 \\ 10 \\ 6 \\ 2 \\ 2 \\ 2 \\ 2 \\ 2 \end{pmatrix}$$

$$T2 := \sum_{k=2}^{5} \left[strandsPerRowdd_k \cdot A_{strand} \cdot [3in + 2in \cdot (k-1)] \right]$$

$$T3 := \sum_{k=6}^{9} \left[strandsPerRowdd_k \cdot A_{strand} \cdot [20in + 2in \cdot (k-6)] \right]$$

$$fpsCG_{dd} := \frac{strandsPerRowdd_1 \cdot A_{strand} \cdot 3in + T2 + T3}{A_{strand} \cdot \sum strandsPerRow}$$

$$fpsCG_{dd} = 8 \cdot in$$

$$CG_{yidd} := \frac{CG_y \cdot A_c + (n-1) A_{ps} fpsCG_{dd}}{A_c + (n-1) A_{ps}} = 24.2 \cdot in$$

$$A_{ci} := A_c + (n-1) A_{ps} = 915.8 \cdot in^2$$

$$I_{xidd} := I_x + A_c \cdot \left(CG_{yidd} - CG_y\right)^2 + (n-1) \cdot A_{ps} \cdot \left(fpsCG_{dd} - CG_{yidd}\right)^2 = 357696.3 \cdot in^4$$

$$e_{dd} := CG_{yidd} - fpsCG_{dd} = 16.2 \cdot in$$

Elastic shortening at Section D-D

$$M_{dldd} := w_{dl} \cdot L_{crib} \cdot 0.5 \cdot 31.5ft - w_{dl} \cdot (31.5ft)^2 \cdot 0.5 = 1389.3 \cdot kip \cdot ft$$

$$f_{c.botdd} := \frac{-F_{si}}{A_{ci}} - \frac{F_{si} \cdot e_{dd}^2}{I_{xidd}} + \frac{M_{dldd} \cdot e_{dd}}{I_{xidd}} = -3.7 \cdot ksi \qquad \varepsilon_{c.botdd} := \frac{f_{c.botdd}}{E_{ci}} \cdot 1 \times 10^6 = -630.79$$

$$f_{ESdd} := n \cdot f_{c.botdd} \cdot -1 = 18.3 \cdot ksi$$

$$F_{sedd} := \left(f_{si} - f_{ESdd}\right) \cdot A_{ps} = 2238.5 \cdot kip$$

Concrete strains

$y_{botdd} := CG_{yidd} - 2in = 22.2 \cdot in$ $y_{topdd} := 54in - CG_{yidd} - 1.5in = 28.3 \cdot in$

$$f_{c.sedl.botdd} := \frac{M_{dldd} \cdot y_{botdd}}{I_{xidd}} + \frac{-F_{sedd}}{A_{ci}} - \frac{F_{sedd} \cdot e_{dd} \cdot y_{botdd}}{I_{xidd}} = -3.7 \cdot ksi$$

$$\varepsilon_{c.sedl.botdd} := \frac{f_{c.sedl.botdd}}{E_{ci}} \cdot 1 \times 10^{6} = -617.82$$

$$f_{c.sedl.topdd} := -\frac{M_{dldd} \cdot y_{topdd}}{I_{xidd}} + \frac{-F_{sedd}}{A_{ci}} + \frac{F_{sedd} \cdot e_{dd} \cdot y_{topdd}}{I_{xidd}} = -0.89 \cdot ksi$$

$$\varepsilon_{c.sedl.topdd} := \frac{f_{c.sedl.topdd}}{E_{ci}} \cdot 1 \times 10^{6} = -150.45$$

Concrete Stresses due only to transfer and dead load after elastic shoretening losses 10 ft from the ends at strain gages locations (Section A-A and C-C)

$$strandsPerRowaa := \begin{pmatrix} 16 \\ 14 \\ 10 \\ 6 \\ 2 \\ 2 \\ 2 \\ 2 \\ 2 \end{pmatrix}$$

$$T2a := \sum_{k=2}^{5} \left[strandsPerRowaa_k \cdot A_{strand} \cdot [3in + 2in \cdot (k-1)] \right]$$

$$T3a := \sum_{k=6}^{9} \left[strandsPerRowaa_k \cdot A_{strand} \cdot [41in + 2in \cdot (k-6)] \right]$$

$$fpsCG_{aa} := \frac{strandsPerRowaa_1 \cdot A_{strand} \cdot 3in + T2a + T3a}{A_{strand} \cdot \sum strandsPerRow}$$

$fpsCG_{aa} = 11 \cdot in$

$$CG_{yiaa} := \frac{CG_y \cdot A_c + (n-1) A_{ps} \, fpsCG_{aa}}{A_c + (n-1) A_{ps}} = 24.4 \cdot in$$

$A_{ci} := A_c + (n-1)A_{ps} = 915.8 \cdot in^2$

$I_{xiaa} := I_x + A_c \cdot (CG_{yiaa} - CG_y)^2 + (n-1) \cdot A_{ps} \cdot (fpsCG_{aa} - CG_{yiaa})^2 = 353499.7 \cdot in^4$

$e_{aa} := CG_{yiaa} - fpsCG_{aa} = 13.4 \cdot in$

Elastic shortening at Section A-A

$M_{dlaa} := w_{dl} \cdot L_{crib} \cdot 0.5 \cdot 4.5ft - w_{dl} \cdot (4.5ft)^2 \cdot 0.5 = 253.4 \cdot kip \cdot ft$

$f_{c.botaa} := \frac{-F_{si}}{A_{ci}} - \frac{F_{si} \cdot e_{aa}^2}{I_{xiaa}} + \frac{M_{dlaa} \cdot e_{aa}}{I_{xiaa}} = -3.8 \cdot ksi$ $\qquad \varepsilon_{c.botaa} := \frac{f_{c.botaa}}{E_{ci}} \cdot 1 \times 10^6 = -643.64$

$f_{ESaa} := n \cdot f_{c.botaa} \cdot -1 = 18.7 \cdot ksi$

$F_{seaa} := (f_{si} - f_{ESaa}) \cdot A_{ps} = 2234 \cdot kip$

Concrete strains

$y_{botaa} := CG_{yiaa} - 2in = 22.4 \cdot in$ $\qquad y_{topaa} := 54in - CG_{yiaa} - 1.5in = 28.1 \cdot in$

$f_{c.sedl.botaa} := \frac{M_{dlaa} \cdot y_{botaa}}{I_{xiaa}} + \frac{-F_{seaa}}{A_{ci}} - \frac{F_{seaa} \cdot e_{aa} \cdot y_{botaa}}{I_{xiaa}} = -4.1 \cdot ksi$

$\varepsilon_{c.sedl.botaa} := \frac{f_{c.sedl.botaa}}{E_{ci}} \cdot 1 \times 10^6 = -697.73$

$f_{c.sedl.topaa} := -\frac{M_{dlaa} \cdot y_{topaa}}{I_{xiaa}} + \frac{-F_{seaa}}{A_{ci}} + \frac{F_{seaa} \cdot e_{aa} \cdot y_{topaa}}{I_{xiaa}} = -0.3 \cdot ksi$

$\varepsilon_{c.sedl.topaa} := \frac{f_{c.sedl.topaa}}{E_{ci}} \cdot 1 \times 10^6 = -51.34$

APPENDIX E. RAW DATA EVENT PLOTS FOR GIRDER 1

This appendix includes plots of raw data for recorded strains, accelerations and rotations as well as temperature of Girder 1 for the transportation record and selected events. BDI gages strain readings are not corrected for temperature changes in these plots. A list of the plots included in this appendix is below.

Appendix E: List of Figures

Figure E. 1 Girder 1 prestress transfer strain 193
Figure E. 2 Girder 1 prestress transfer lift strain 194
Figure E. 3 Girder 1 yard lift strain and acceleration 195
Figure E. 4 Girder 1 yard lift strain and rotation 196
Figure E. 5 View of Girder 1 during yard lift 197
Figure E. 6 Girder 1 transportation record strain and acceleration 198
Figure E. 7 Girder 1 transportation record strain and rotation 199
Figure E. 8 Event G1-A1 strain and acceleration 200
Figure E. 9 View of Girder 1 during Event G1-A1 201
Figure E. 10 Event G1-A2 strain and acceleration 202
Figure E. 11 View of Girder 1 during Event G1-A2 203
Figure E. 12 Event G1-A3 strain and acceleration 204
Figure E. 13 View of Girder 1 during Event G1-A3 205
Figure E. 14 Event G1-A4 strain and acceleration 206
Figure E. 15 Event G1-A4 strain and rotation 207
Figure E. 16 View of Girder 1 during Event G1-A4 208
Figure E. 17 Event G1-A5 strain and acceleration 209
Figure E. 18 View of Girder 1 during Event G1-A5 210
Figure E. 19 Event G1-S1 strain and acceleration 211
Figure E. 20 Event G1-S1 strain and rotation 212
Figure E. 21 View of Girder 1 during Event G1-S1 213
Figure E. 22 Event G1-S2 strain and acceleration 214
Figure E. 23 Event G1-S2 strain and rotation 215
Figure E. 24 View of Girder 1 during Event G1-S2 216
Figure E. 25 Event G1-S3 strain and acceleration 217
Figure E. 26 Event G1-S4 strain and acceleration 218
Figure E. 27 Event G1-S4 strain and rotation 219
Figure E. 28 View of Girder 1 during Event G1-S4 220
Figure E. 29 Event G1-S5 strain 221
Figure E. 30 Temperature effect on strain at midspan section B and tongue location section D 222
Figure E. 31 Girder 1 strain and acceleration during railroad crossing 223
Figure E. 32 View of Girder 1 during railroad crossing 224
Figure E. 33 Girder 1 strain and acceleration during causeway crossing 225
Figure E. 34 View of Girder 1 during causeway crossing 226

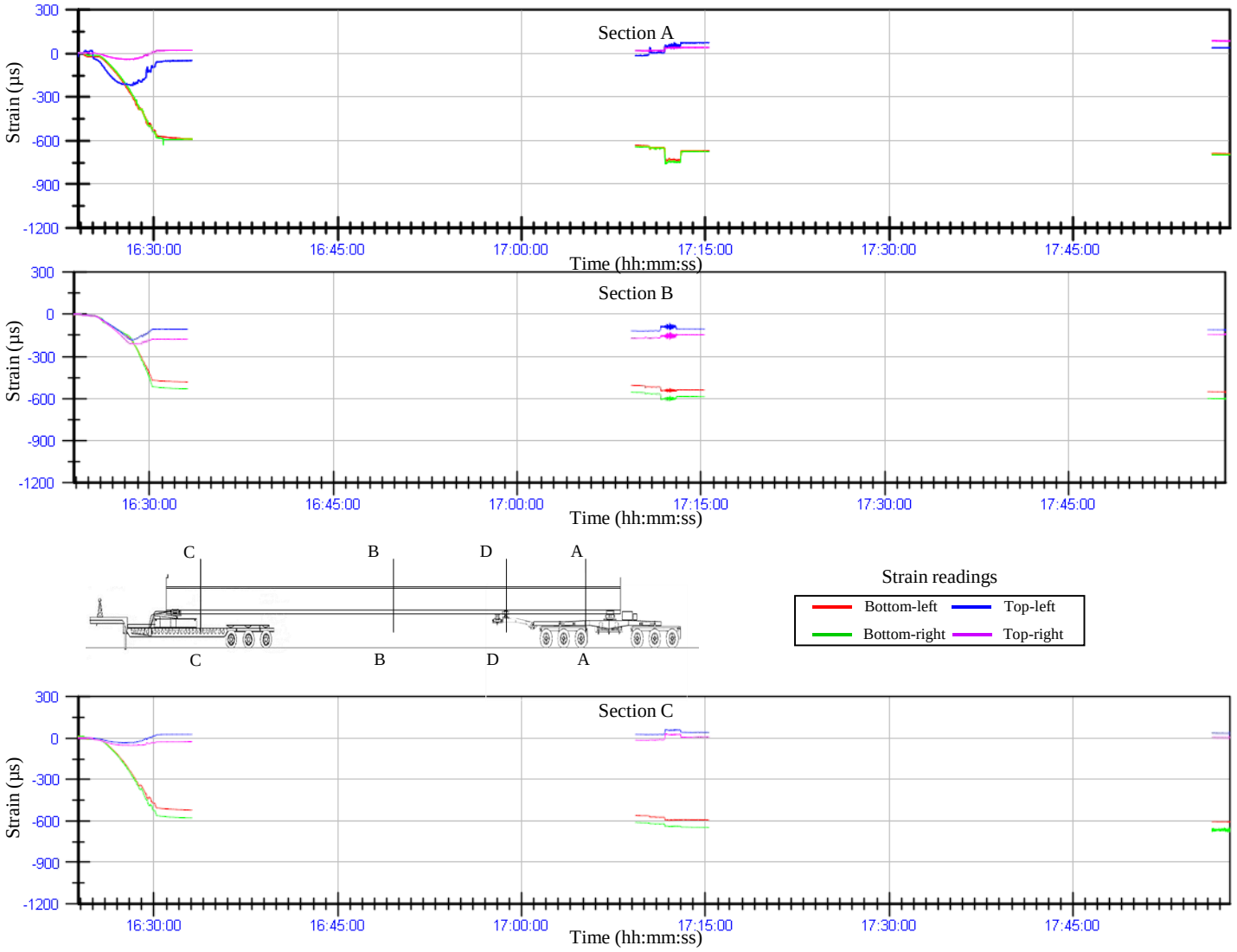

Figure E. 1
Girder 1 prestress transfer strain

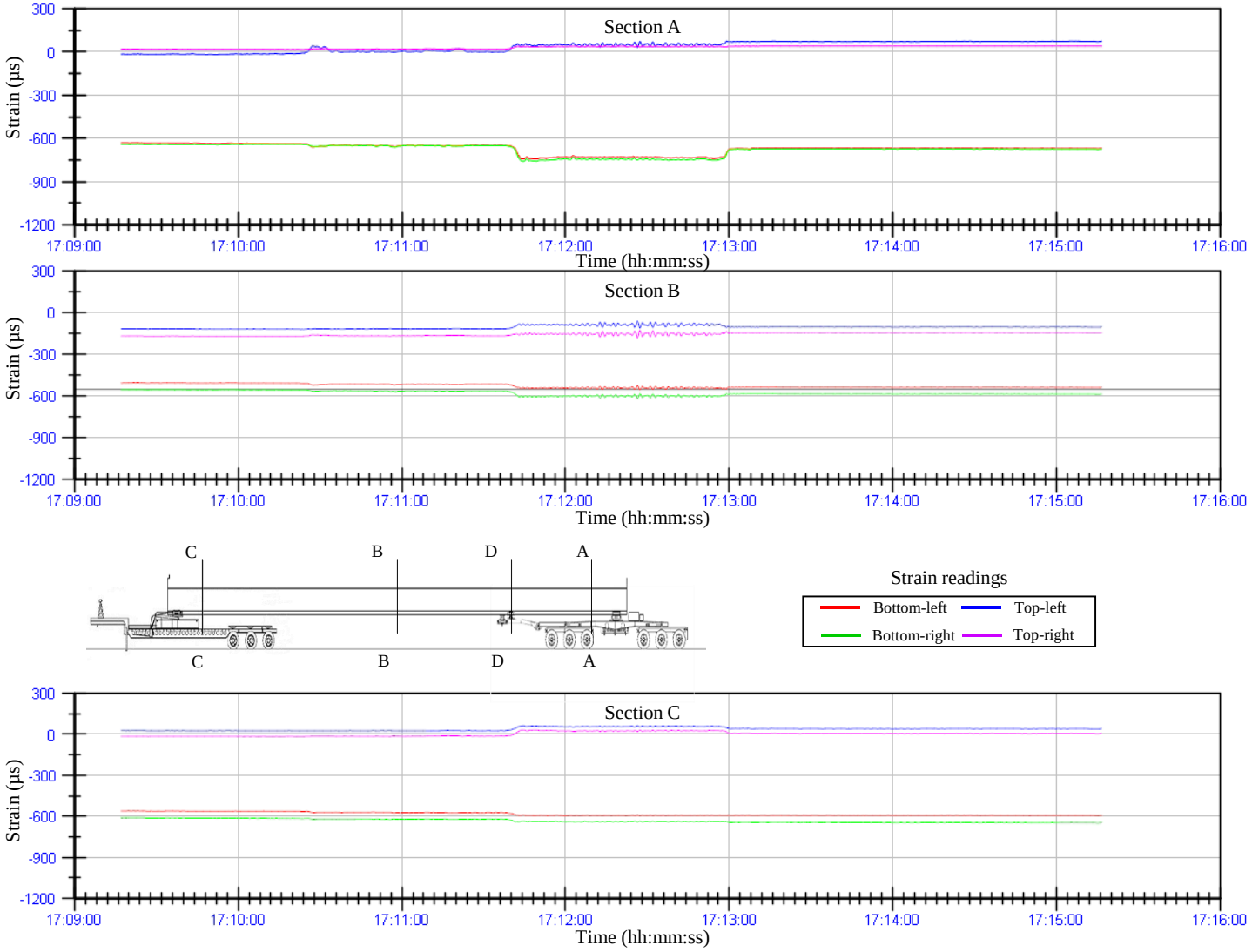

Figure E. 2
Girder 1 prestress transfer lift strain

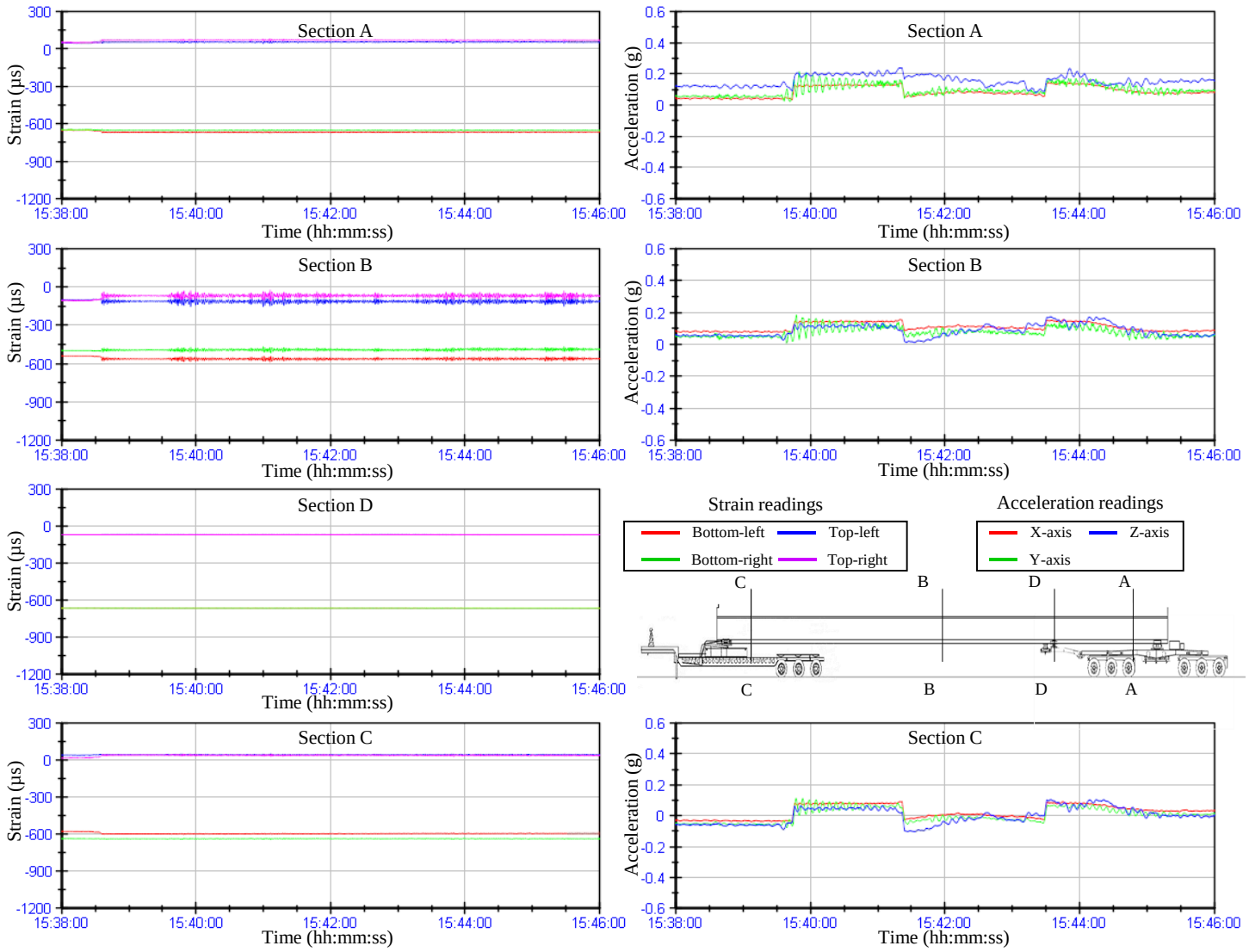

Figure E. 3
Girder 1 yard lift strain and acceleration

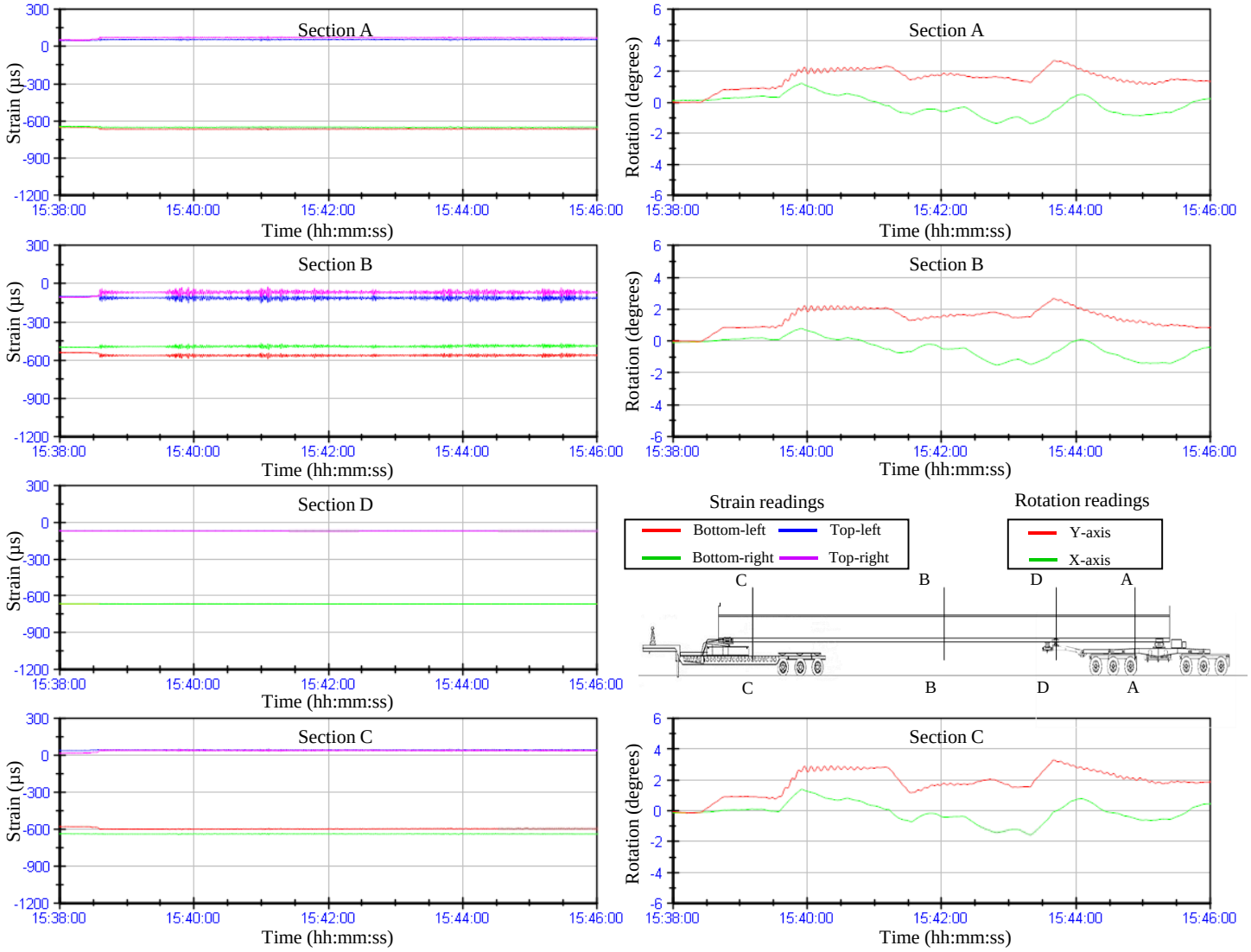

Figure E. 4
Girder 1 yard lift strain and rotation

Figure E. 5
View of Girder 1 during yard lift

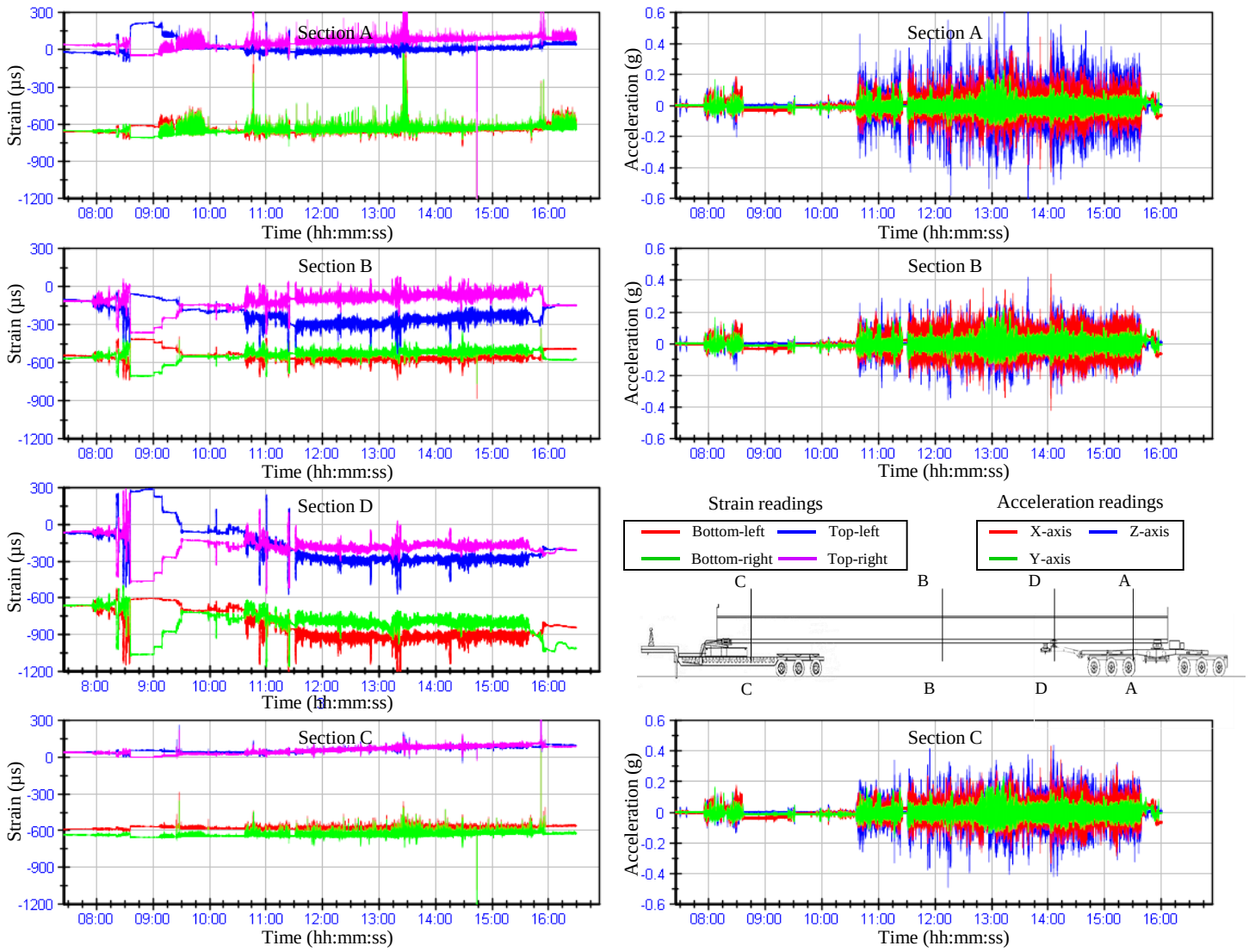

Figure E. 6
Girder 1 transportation record strain and acceleration

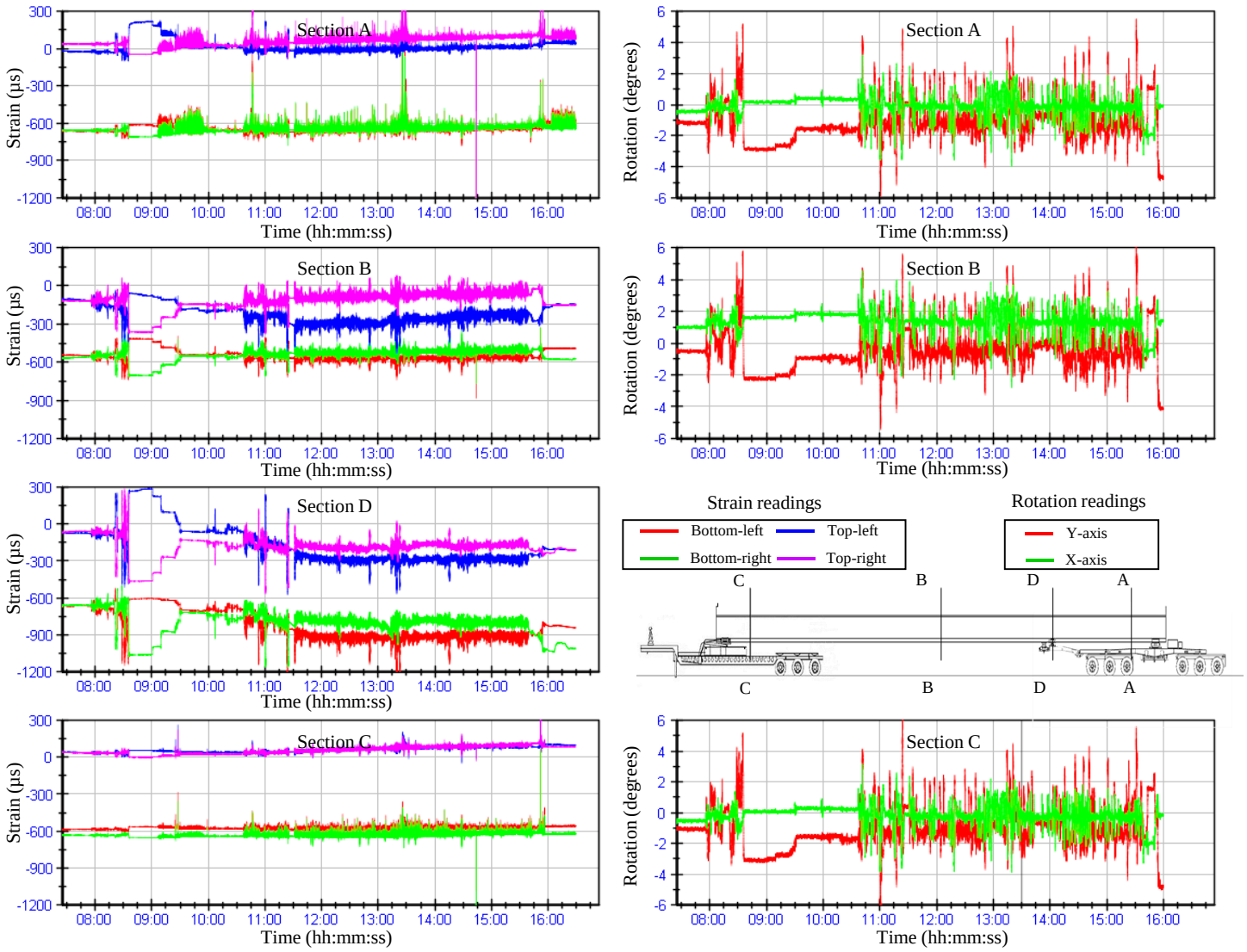

Figure E. 7
Girder 1 transportation record strain and rotation

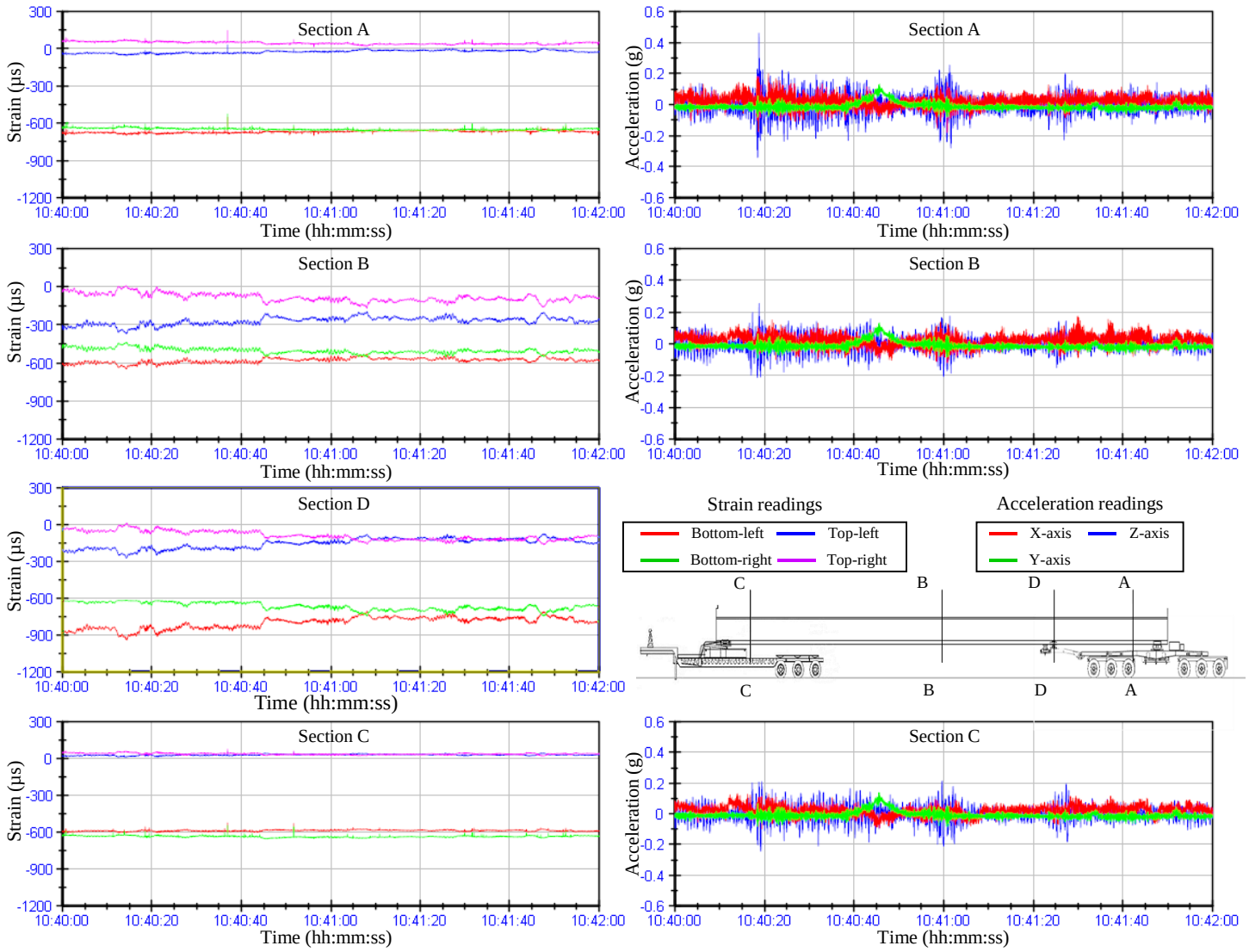

Figure E. 8
Event G1-A1 strain and acceleration

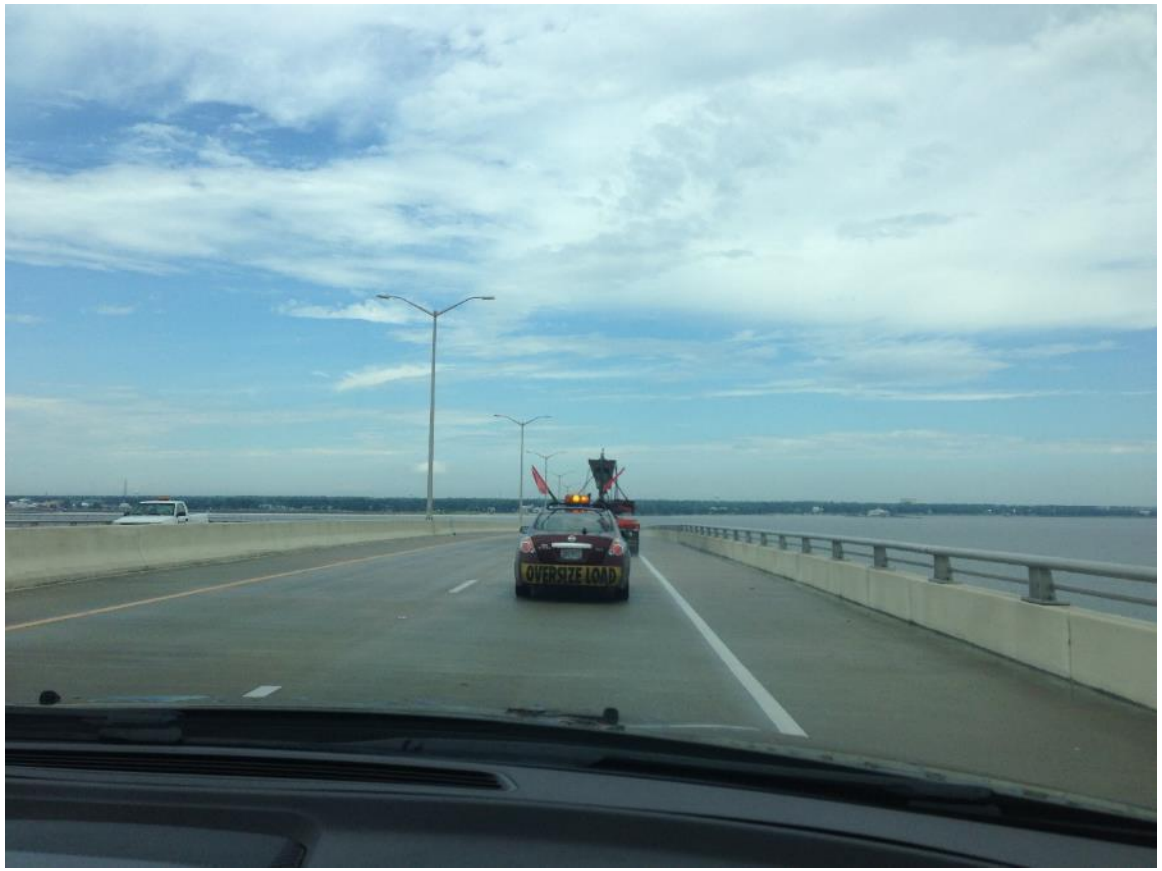

Figure E. 9
View of Girder 1 during Event G1-A1

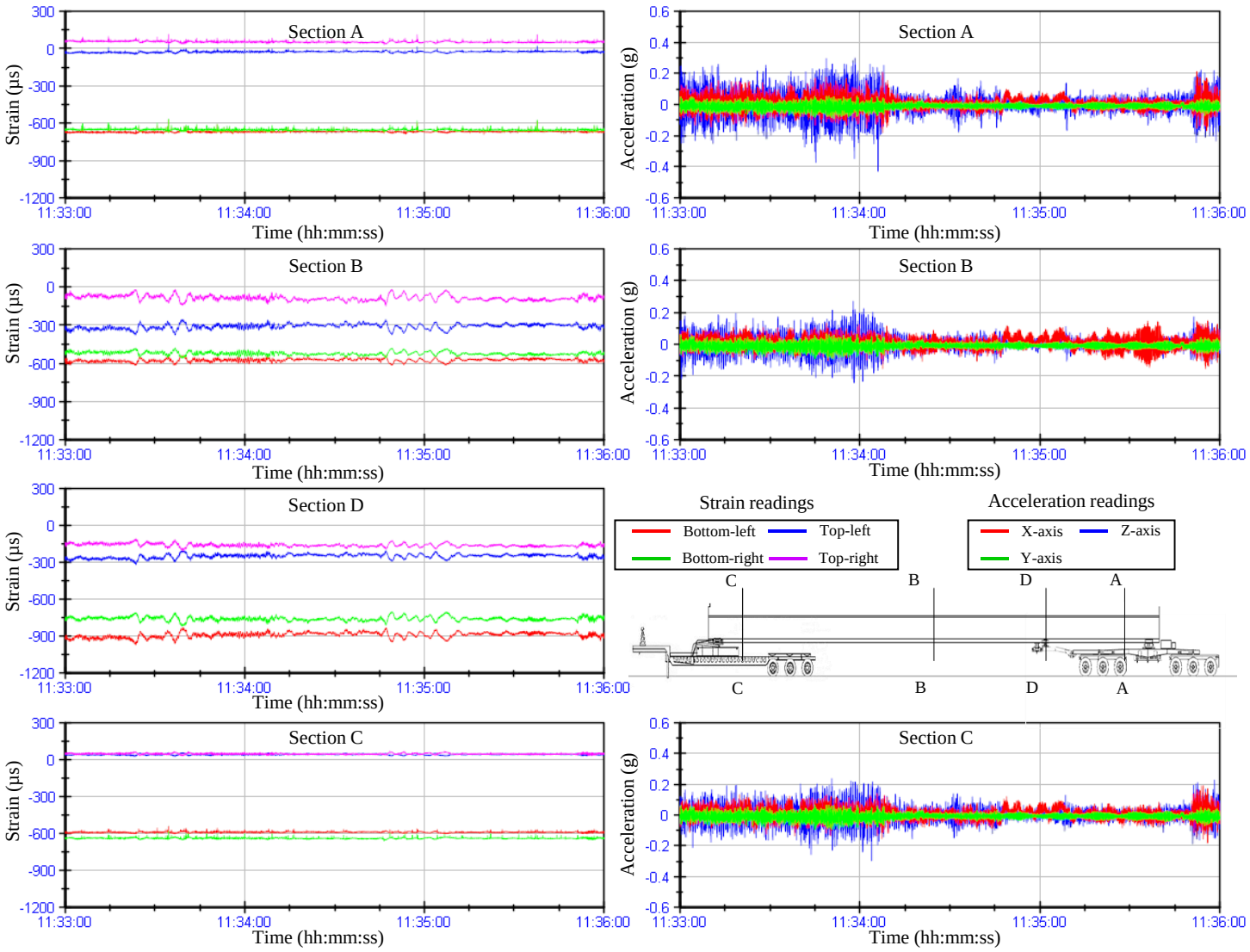

Figure E. 10
Event G1-A2 strain and acceleration

Figure E. 11
View of Girder 1 during Event G1-A2

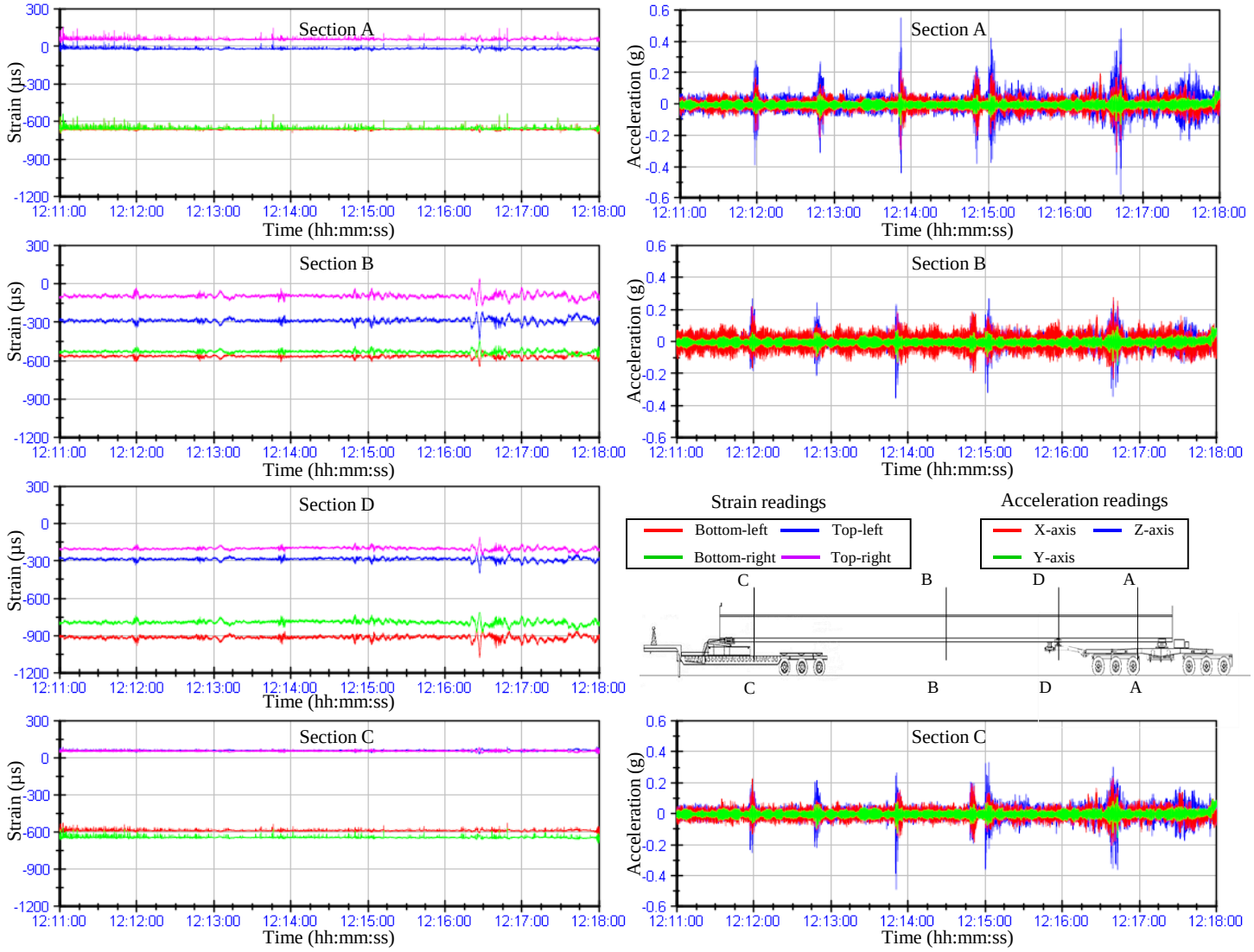

Figure E. 12
Event G1-A3 strain and acceleration

Figure E. 13
View of Girder 1 during Event G1-A3

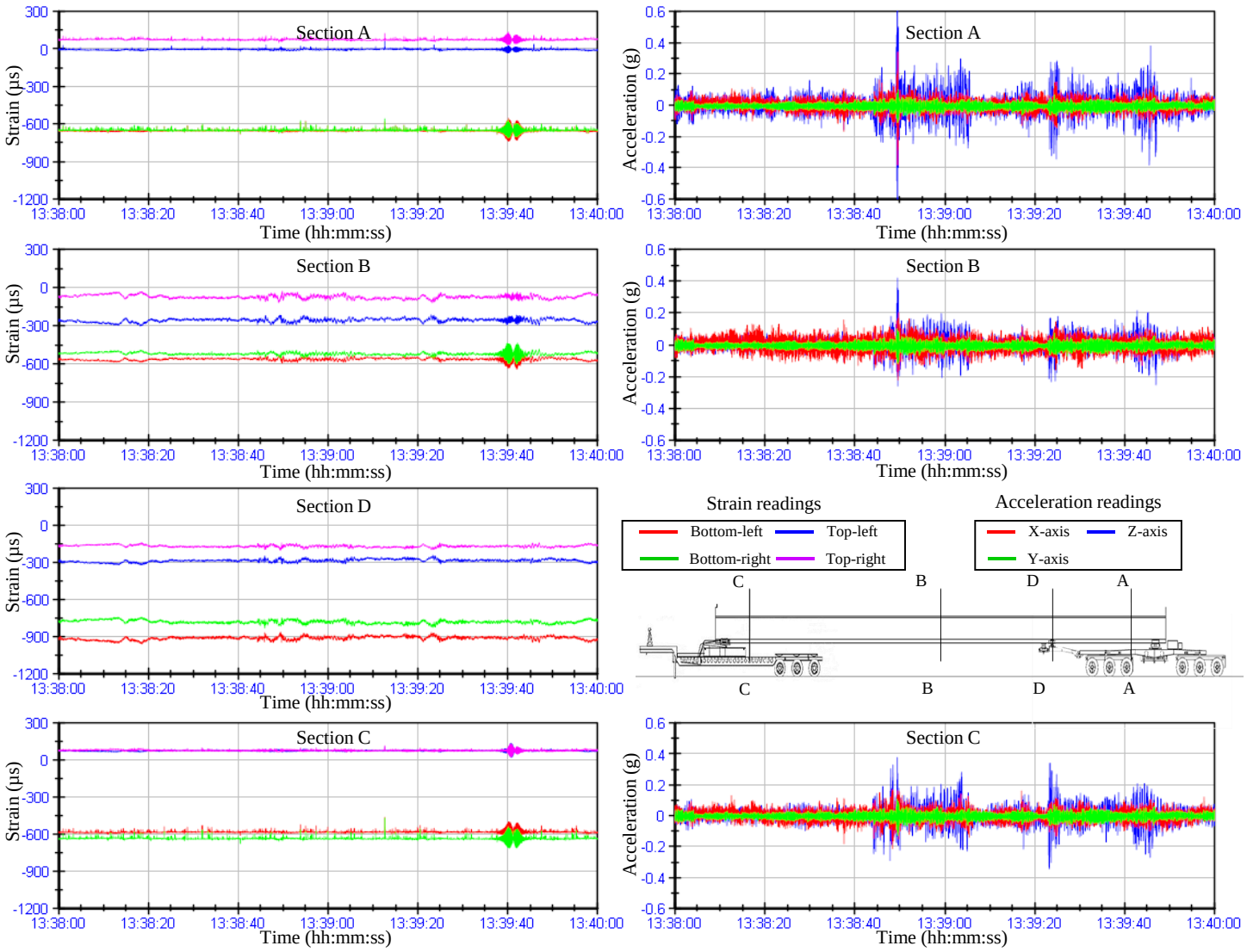

Figure E. 14
Event G1-A4 strain and acceleration

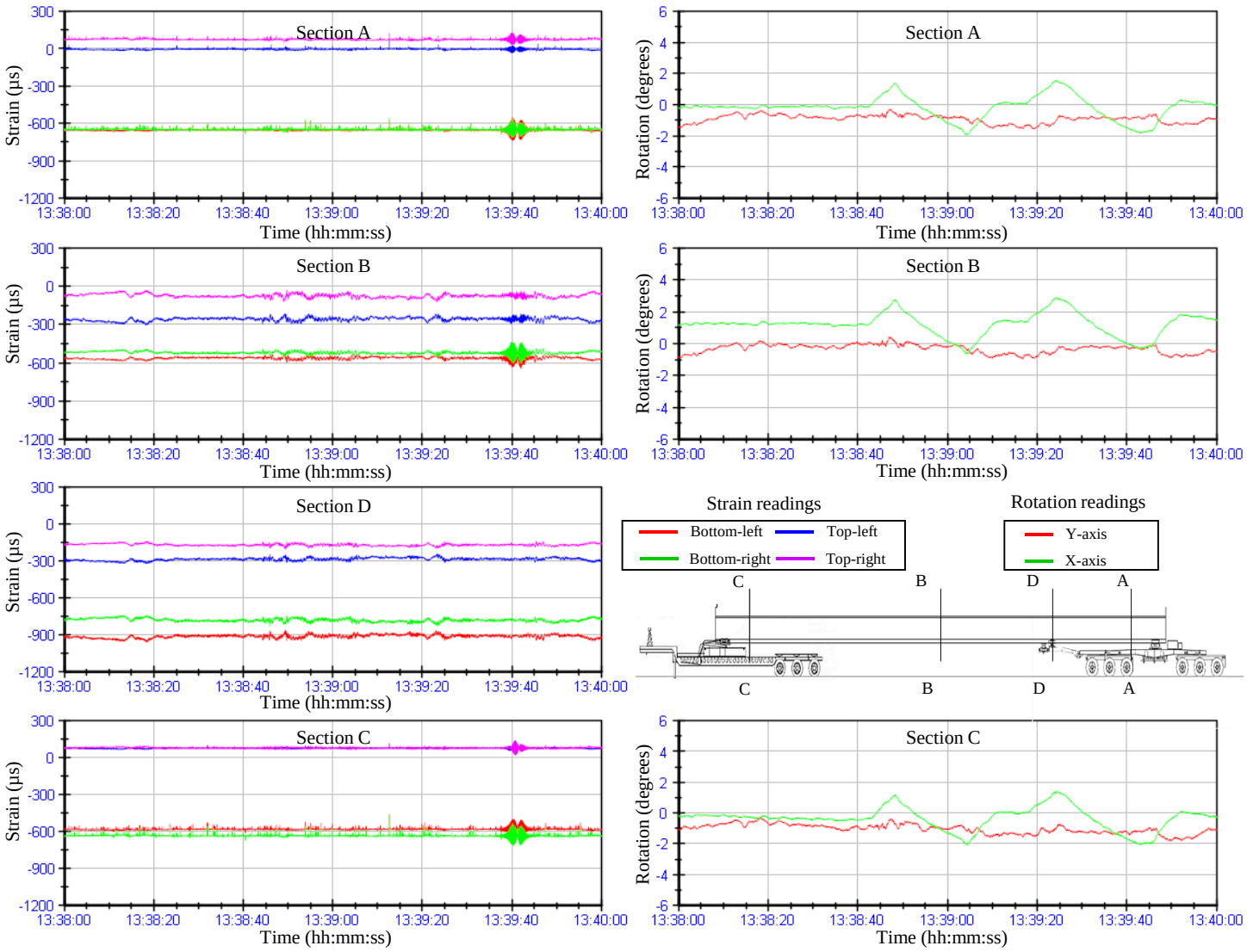

Figure E. 15
Event G1-A4 strain and rotation

Figure E. 16
View of Girder 1 during Event G1-A4

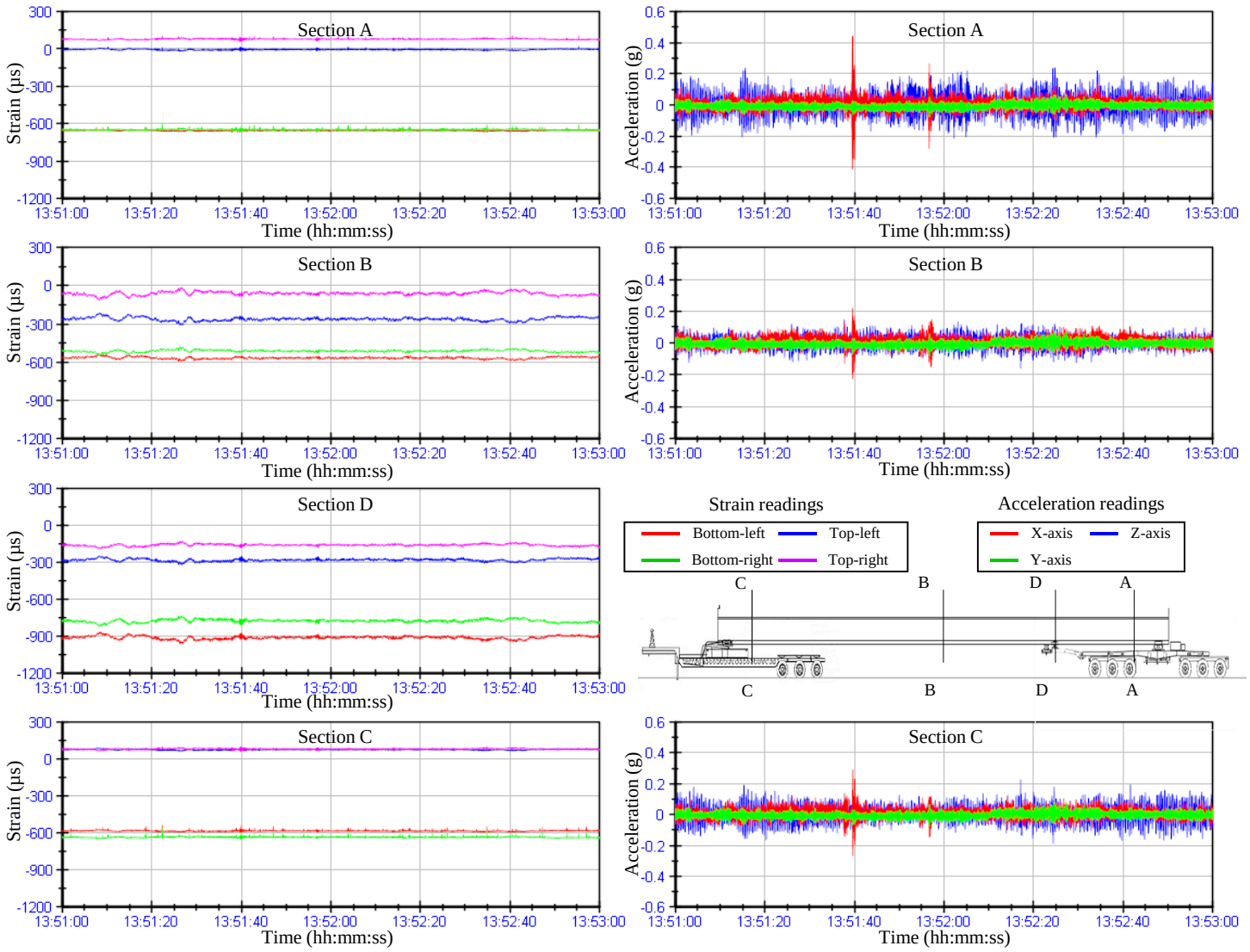

Figure E. 17
Event G1-A5 strain and acceleration

Figure E. 18
View of Girder 1 during Event G1-A5

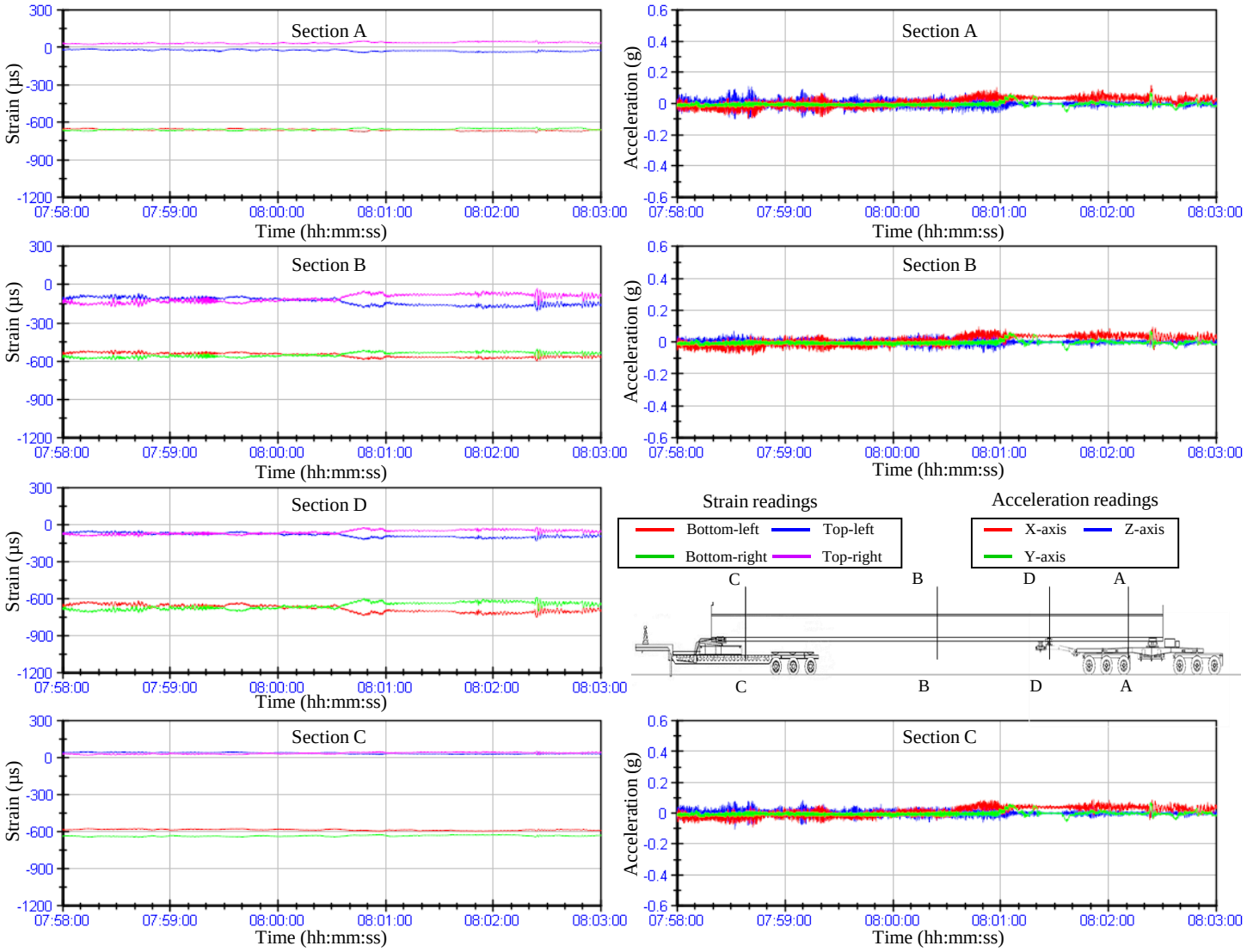

Figure E. 19
Event G1-S1 strain and acceleration

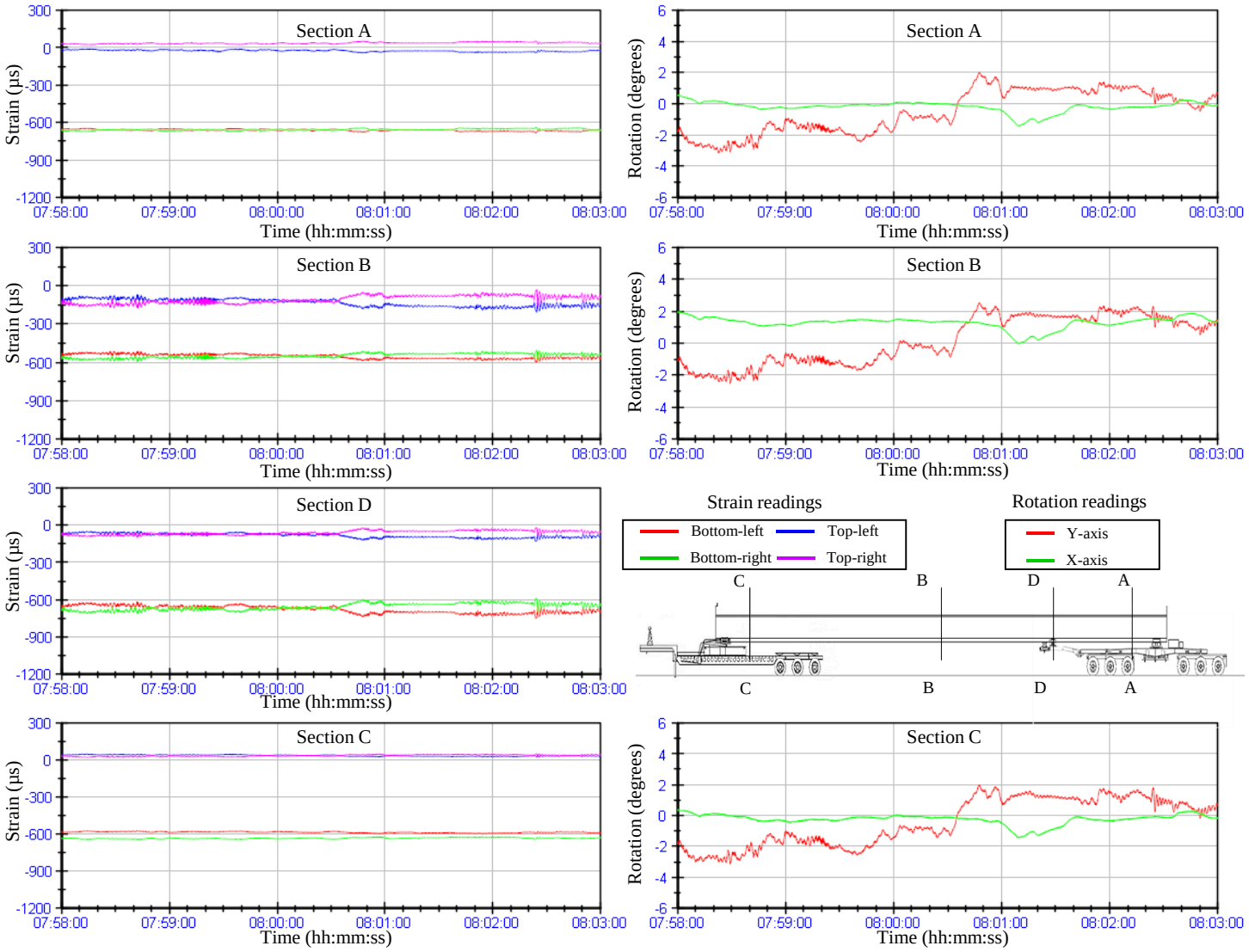

Figure E. 20
Event G1-S1 strain and rotation

Figure E. 21
View of Girder 1 during Event G1-S1

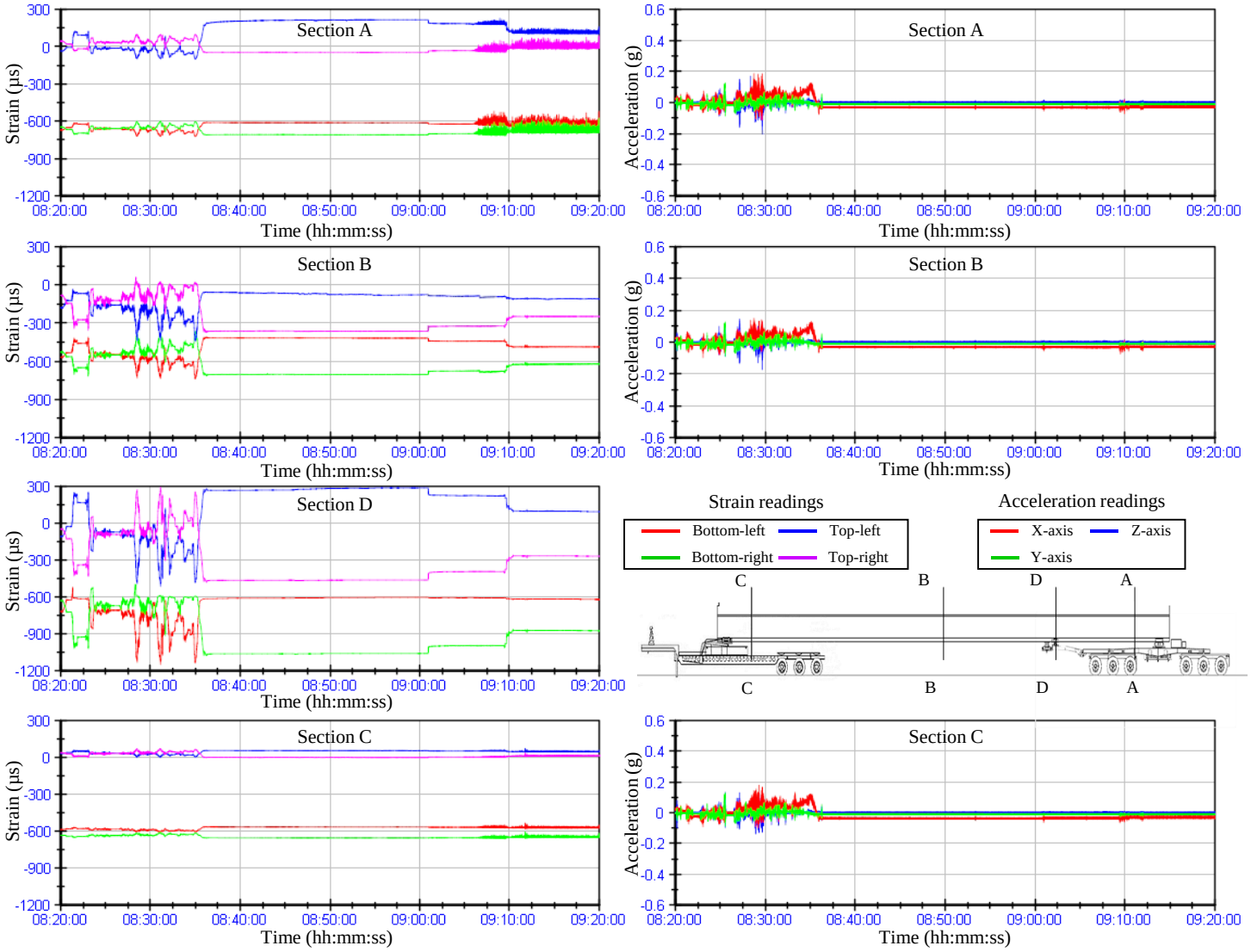

Figure E. 22
Event G1-S2 strain and acceleration

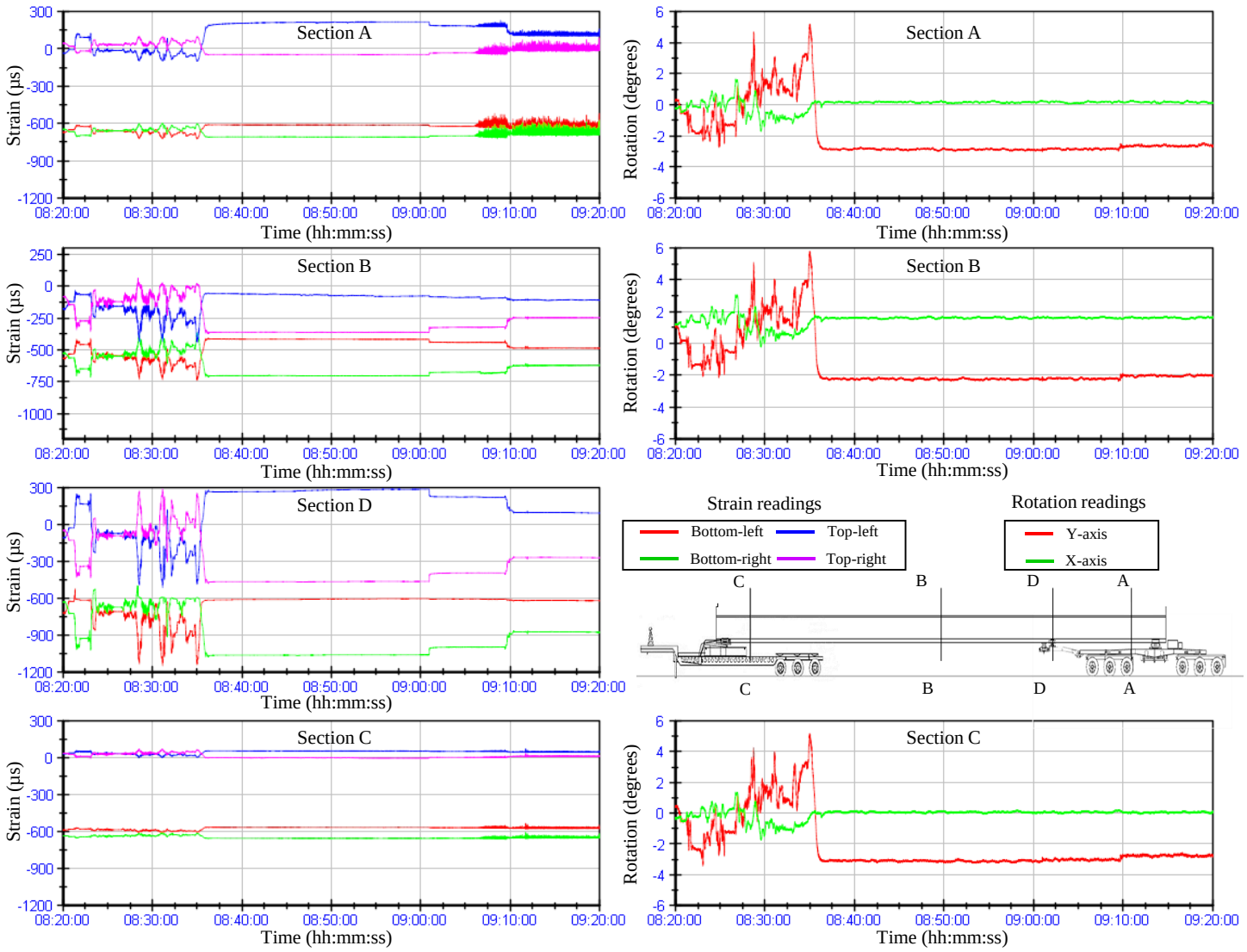

Figure E. 23
Event G1-S2 strain and rotation

Figure E. 24
View of Girder 1 during Event G1-S2

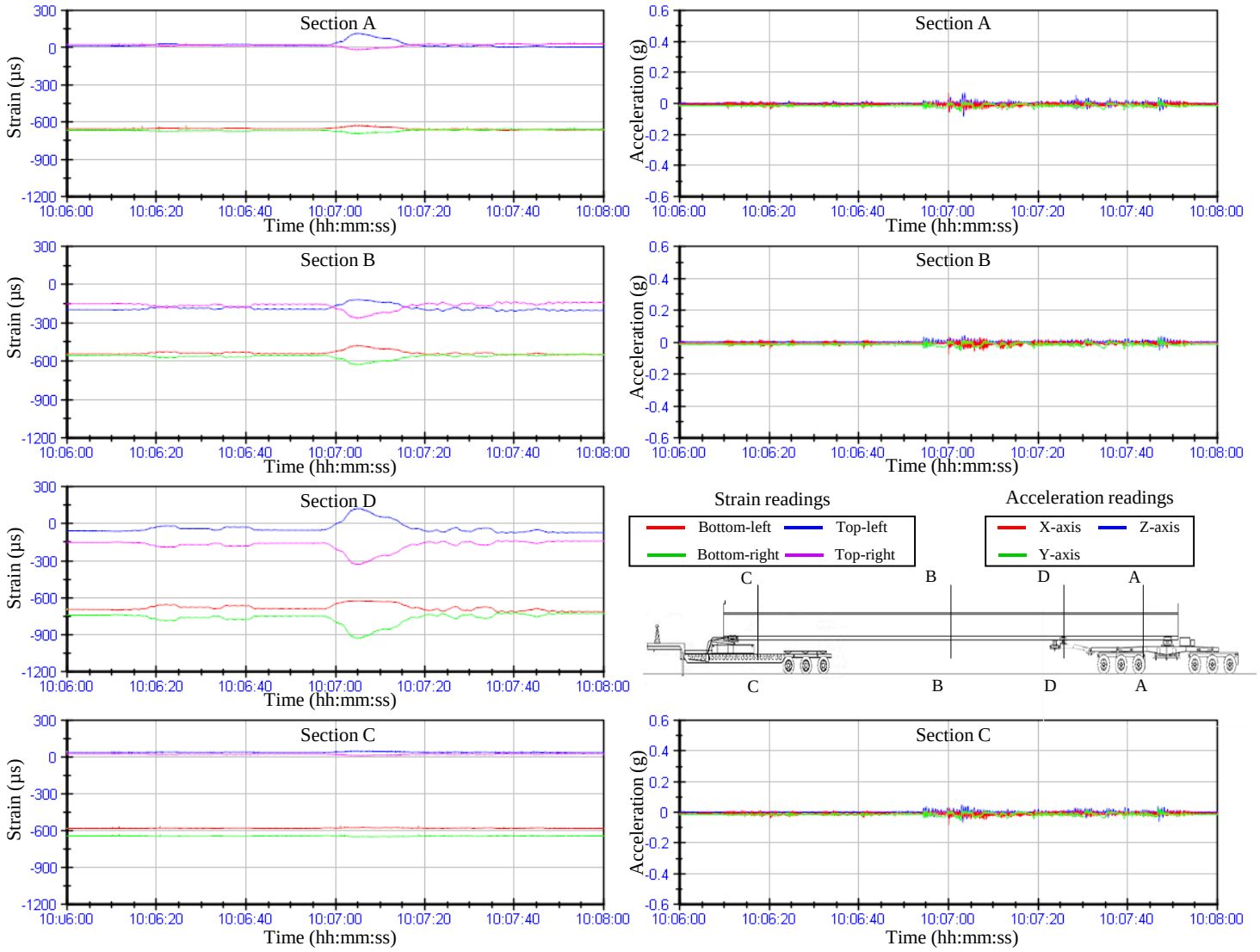

Figure E. 25
Event G1-S3 strain and acceleration

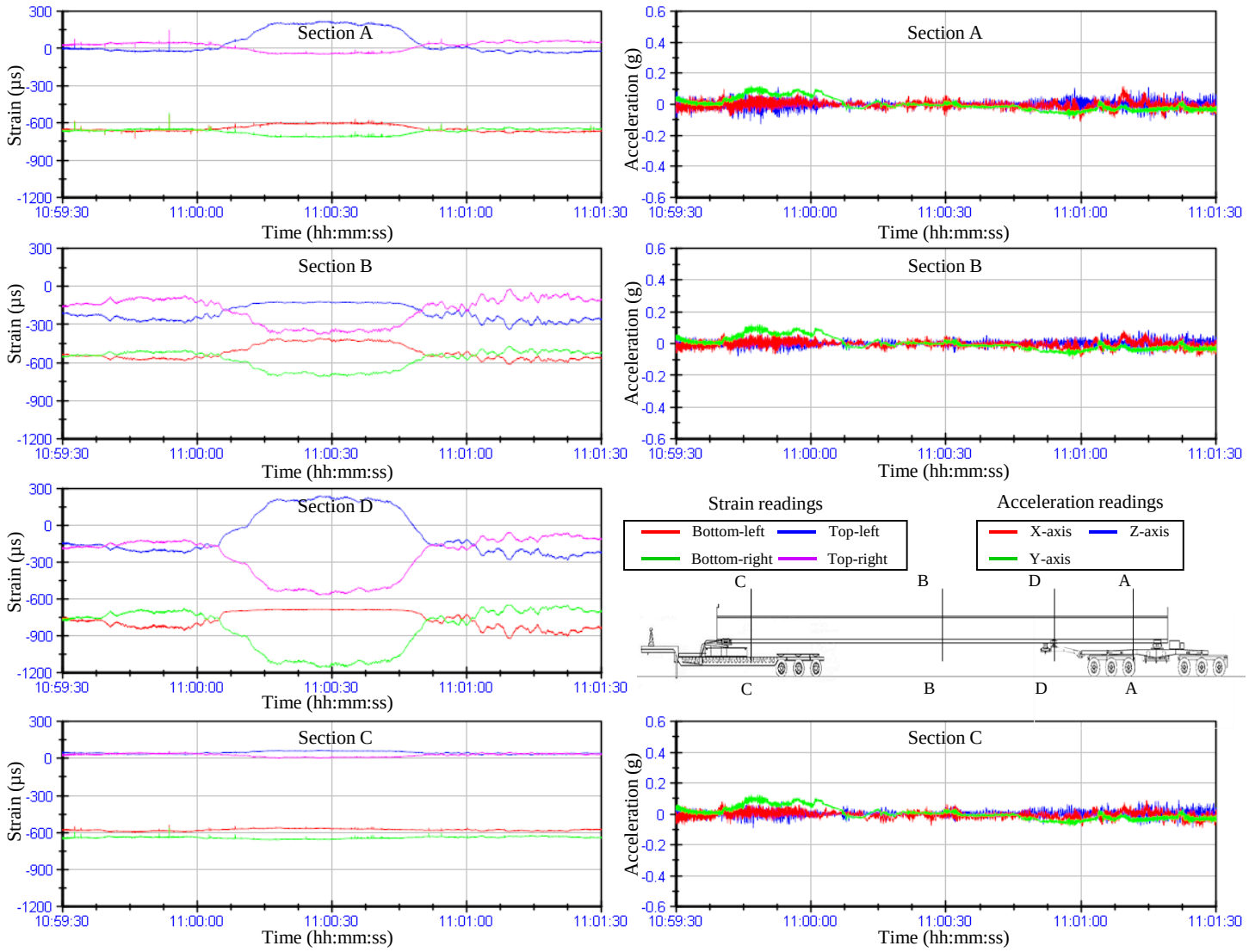

Figure E. 26
Event G1-S4 strain and acceleration

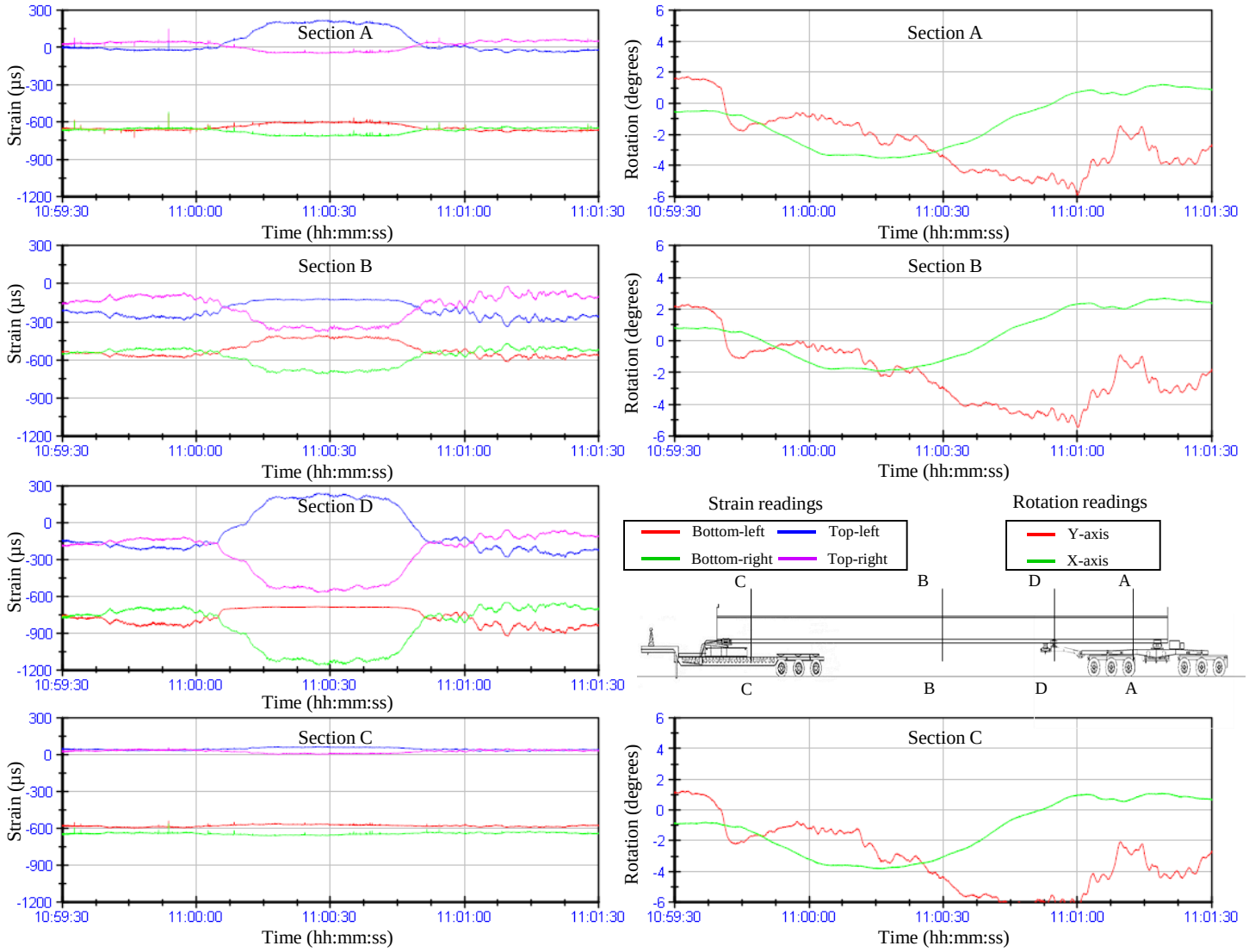

Figure E. 27
Event G1-S4 strain and rotation

Figure E. 28
View of Girder 1 during Event G1-S4

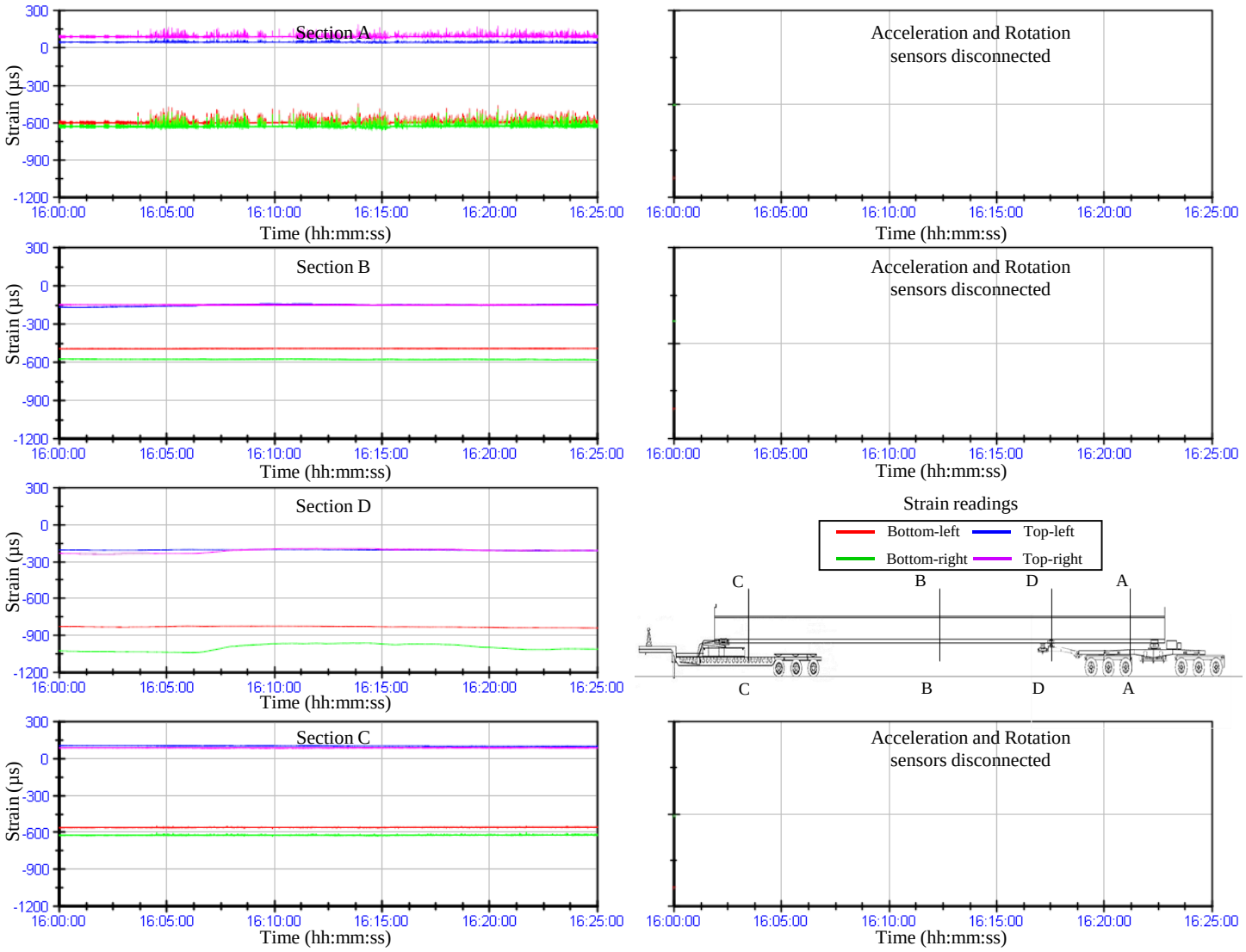

Figure E. 29
Event G1-S5 strain

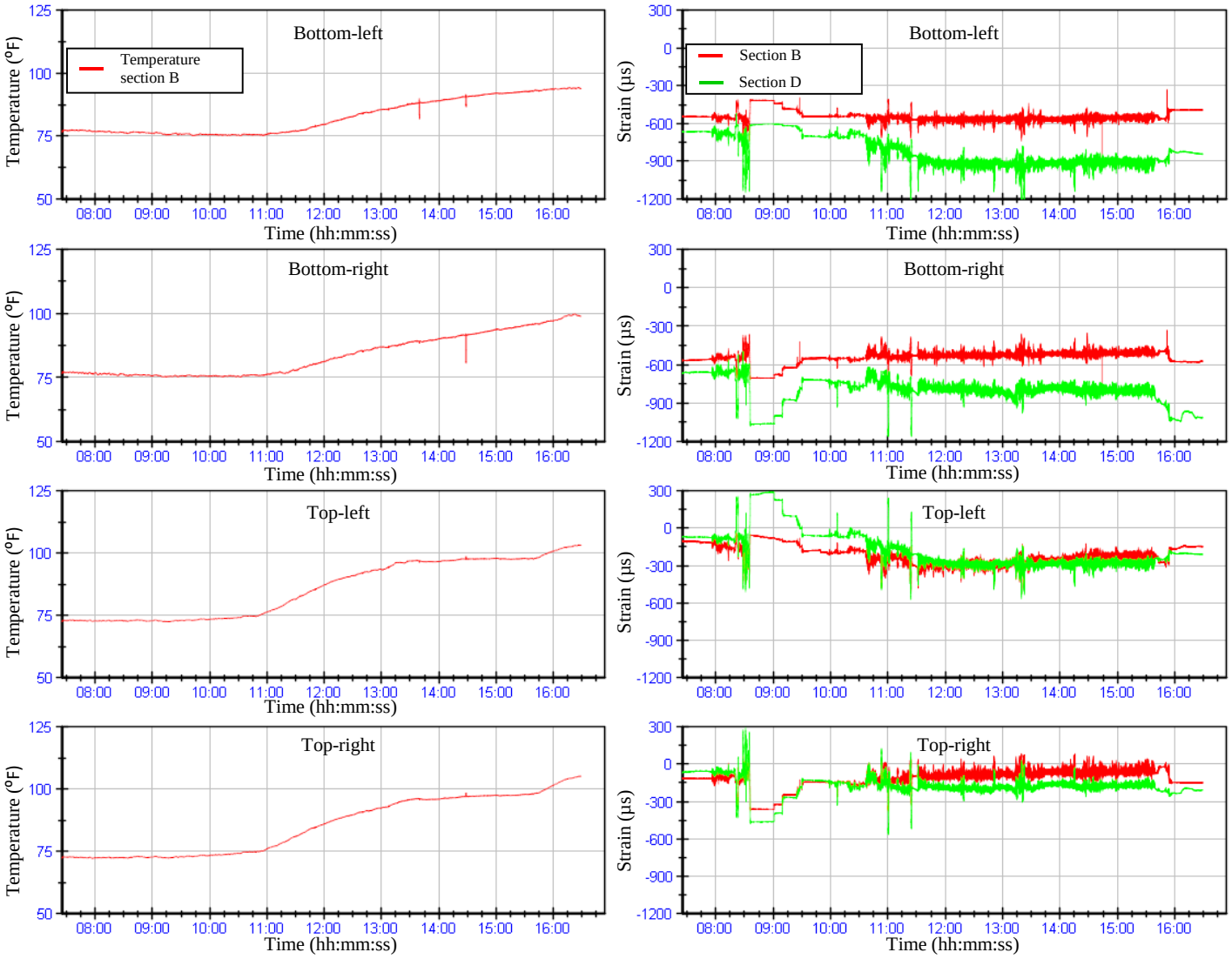

Figure E. 30
Temperature effect on strain at midspan section B and tongue location section D

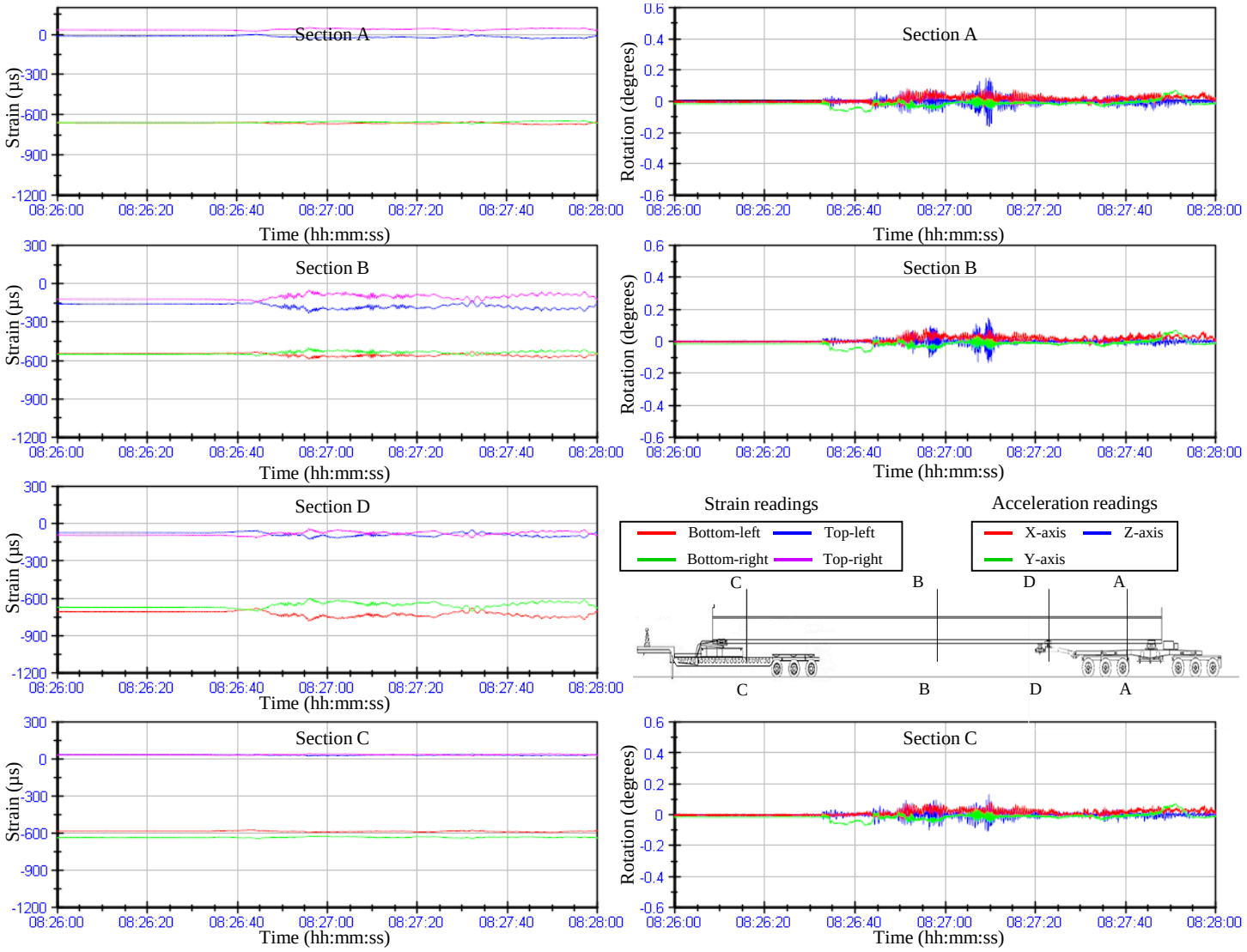

Figure E. 31
Girder 1 strain and acceleration during railroad crossing

Figure E. 32
View of Girder 1 during railroad crossing

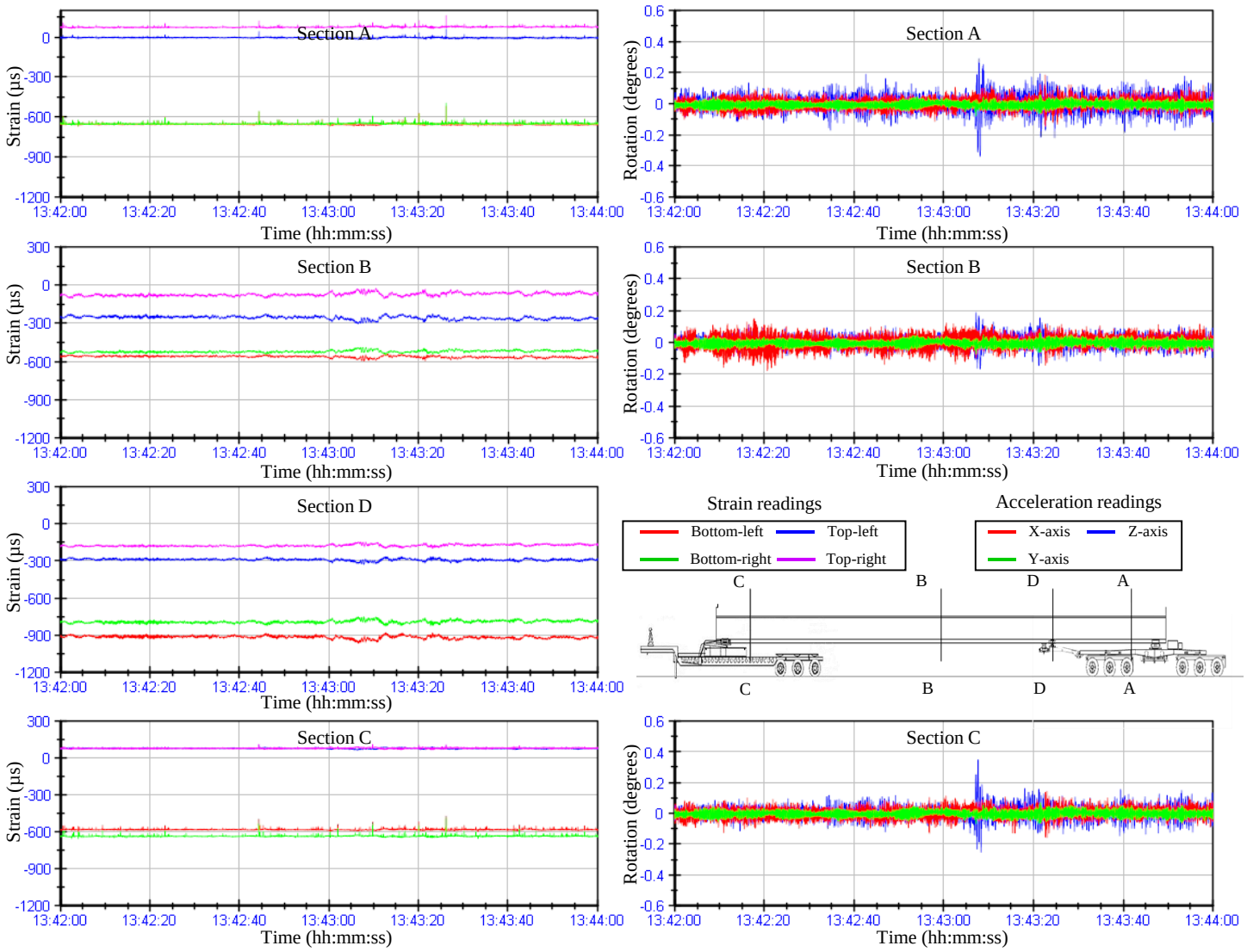

Figure E. 33
Girder 1 strain and acceleration during causeway crossing

Figure E. 34
View of Girder 1 during causeway crossing

APPENDIX F. RAW DATA EVENT PLOTS FOR GIRDER 2

This appendix includes plots of raw data for recorded strains, accelerations and rotations as well as temperature of Girder 2 for the transportation record and selected events. BDI gages strain readings are not corrected for temperature changes in these plots. A list of the plots included in this appendix is below.

Appendix F: List of Figures

Figure F. 1 Girder 2 yard lift strain and acceleration 229
Figure F. 2 Girder 2 yard lift strain and rotation 230
Figure F. 3 View of Girder 2 during yard lift 231
Figure F. 4 Girder 2 transportation record strain and acceleration 232
Figure F. 5 Girder 2 transportation record strain and rotation 233
Figure F. 6 Event G2-A1 strain and acceleration 234
Figure F. 7 View of Girder 2 during Event G2-A1 235
Figure F. 8 Event G2-A2 strain and acceleration 236
Figure F. 9 Event G2-A3 strain and acceleration 237
Figure F. 10 View of Girder 2 during Event G2-A3 238
Figure F. 11 Event G2-A4 strain and acceleration 239
Figure F. 12 Event G2-A5 strain and acceleration 240
Figure F. 13 Event G2-S1 strain and acceleration 241
Figure F. 14 Event G2-S1 strain and rotation 242
Figure F. 15 View of Girder 2 during Event G2-S1 243
Figure F. 16 Event G2-S2 strain and acceleration 244
Figure F. 17 View of Girder 2 during Event G2-S2 245
Figure F. 18 Event G2-S3 strain and acceleration 246
Figure F. 19 Event G2-S3 strain and rotation 247
Figure F. 20 View of Girder 2 during Event G2-S3 248
Figure F. 21 Event G2-S4 strain and acceleration 249
Figure F. 22 Event G2-S4 strain and rotation 250
Figure F. 23 View of Girder 2 during Event G2-S4 251
Figure F. 24 Event G2-S5 strain and acceleration 252
Figure F. 25 Event G2-S5 strain and rotation 253
Figure F. 26 View of Girder 2 during Event G2-S5 254
Figure F. 27 Temperature effect on strain at midspan section B and tongue location section D 255
Figure F. 28 Girder 2 strain and acceleration during railroad crossing 256
Figure F. 29 View of Girder 2 during railroad crossing 257
Figure F. 30 Girder 2 strain and acceleration during causeway crossing 258
Figure F. 31 View of Girder 2 during causeway crossing 259

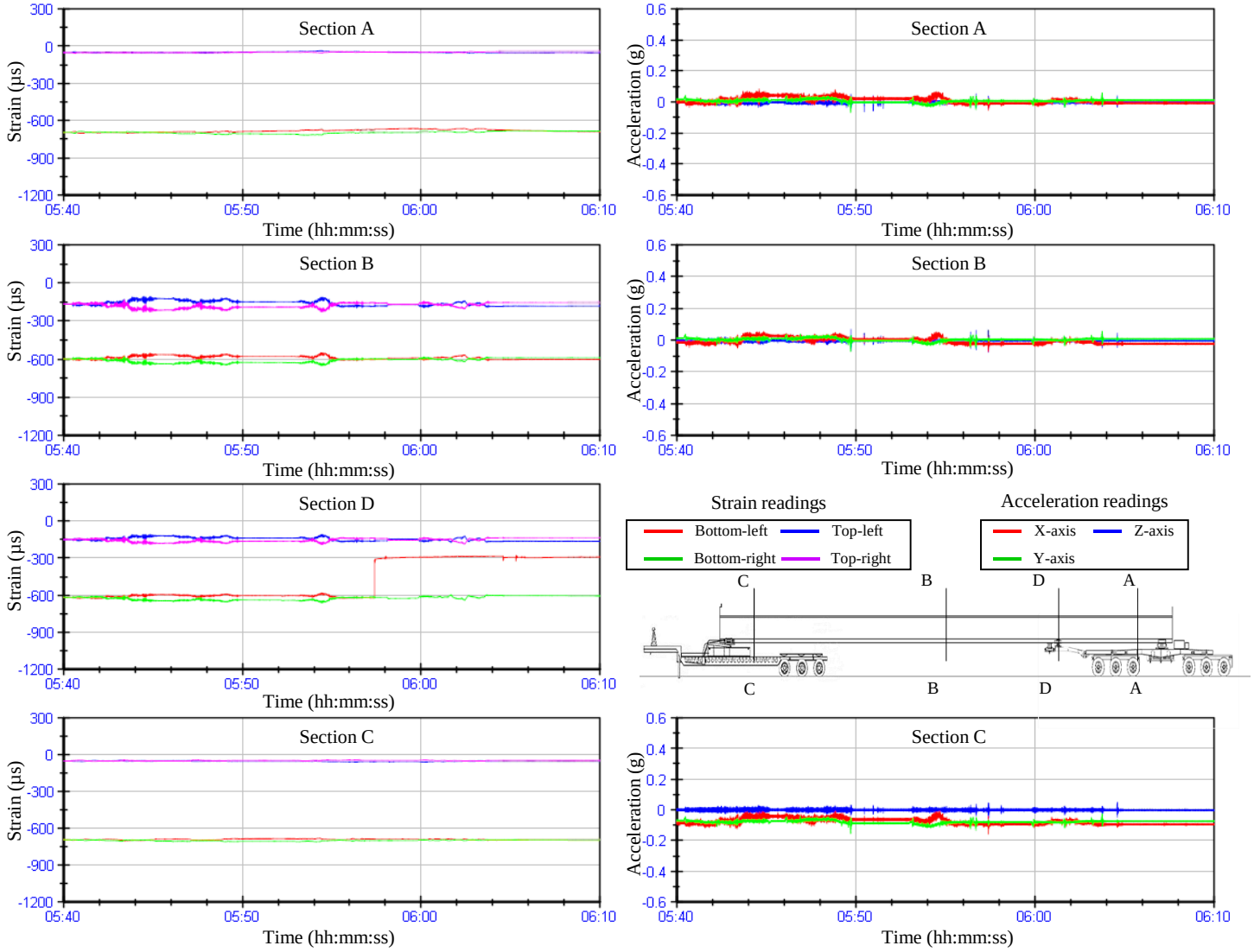

Figure F. 1
Girder 2 yard lift strain and acceleration

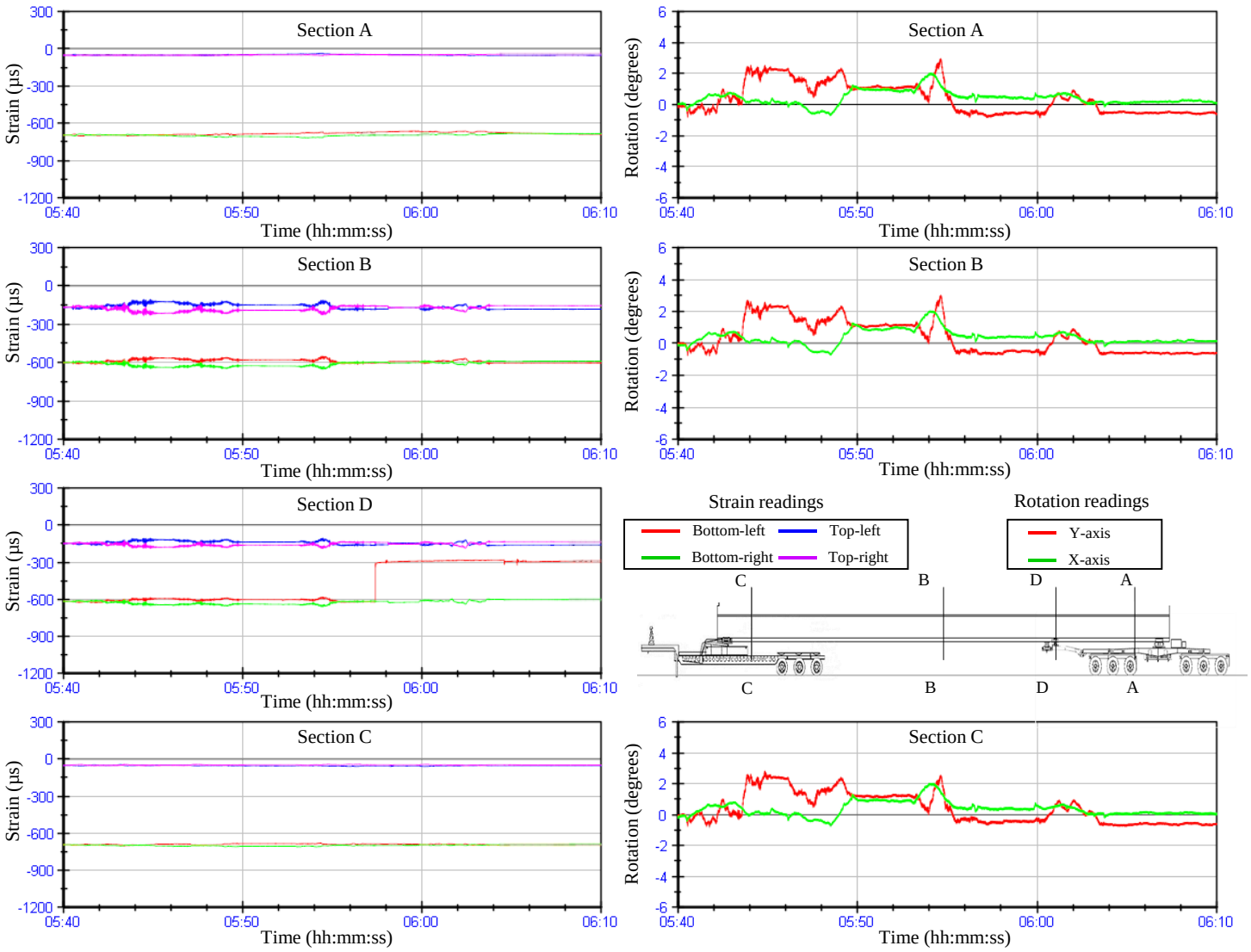

Figure F. 2
Girder 2 yard lift strain and rotation

Figure F. 3
View of Girder 2 during yard lift

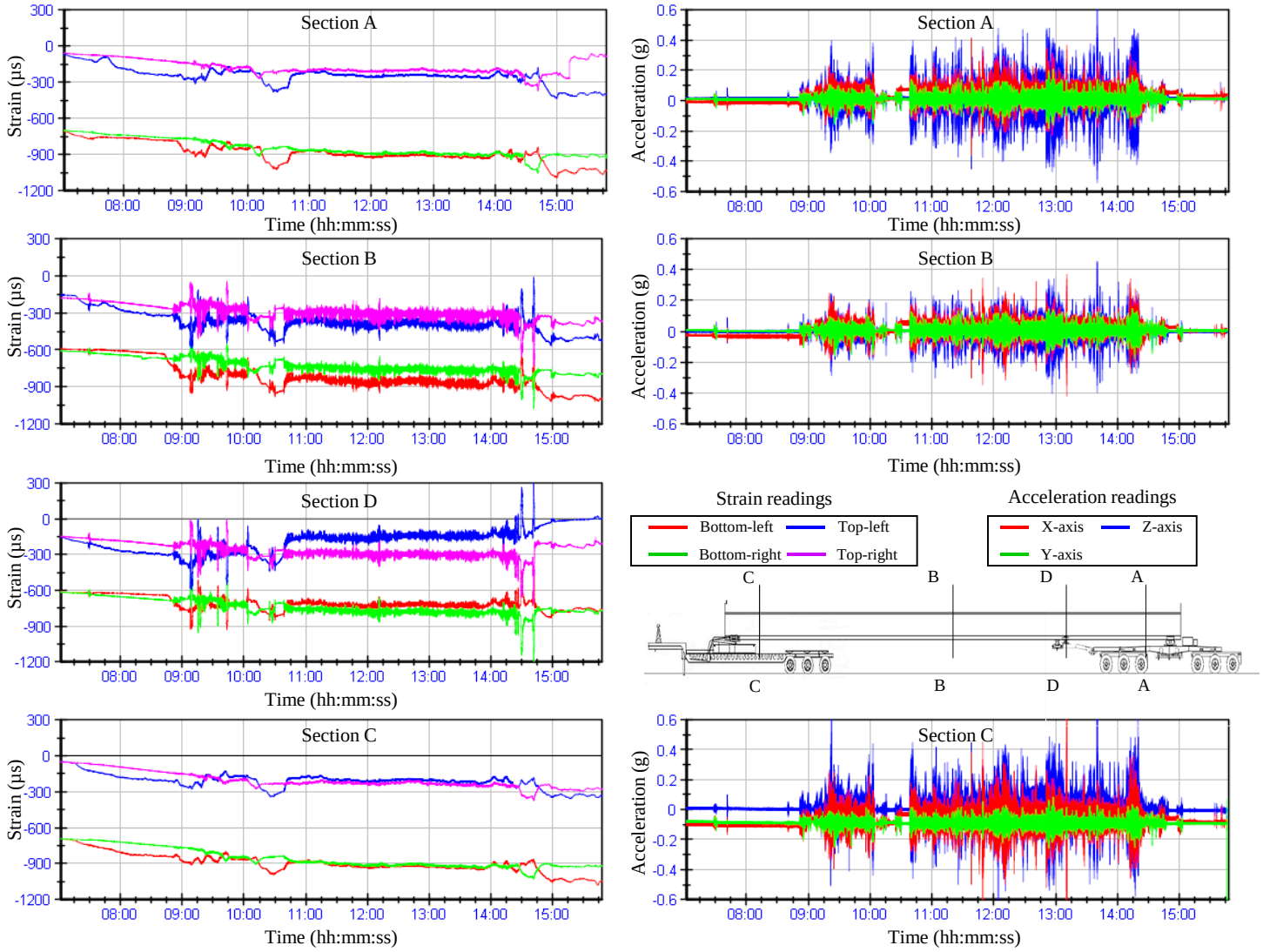

Figure F. 4
Girder 2 transportation record strain and acceleration

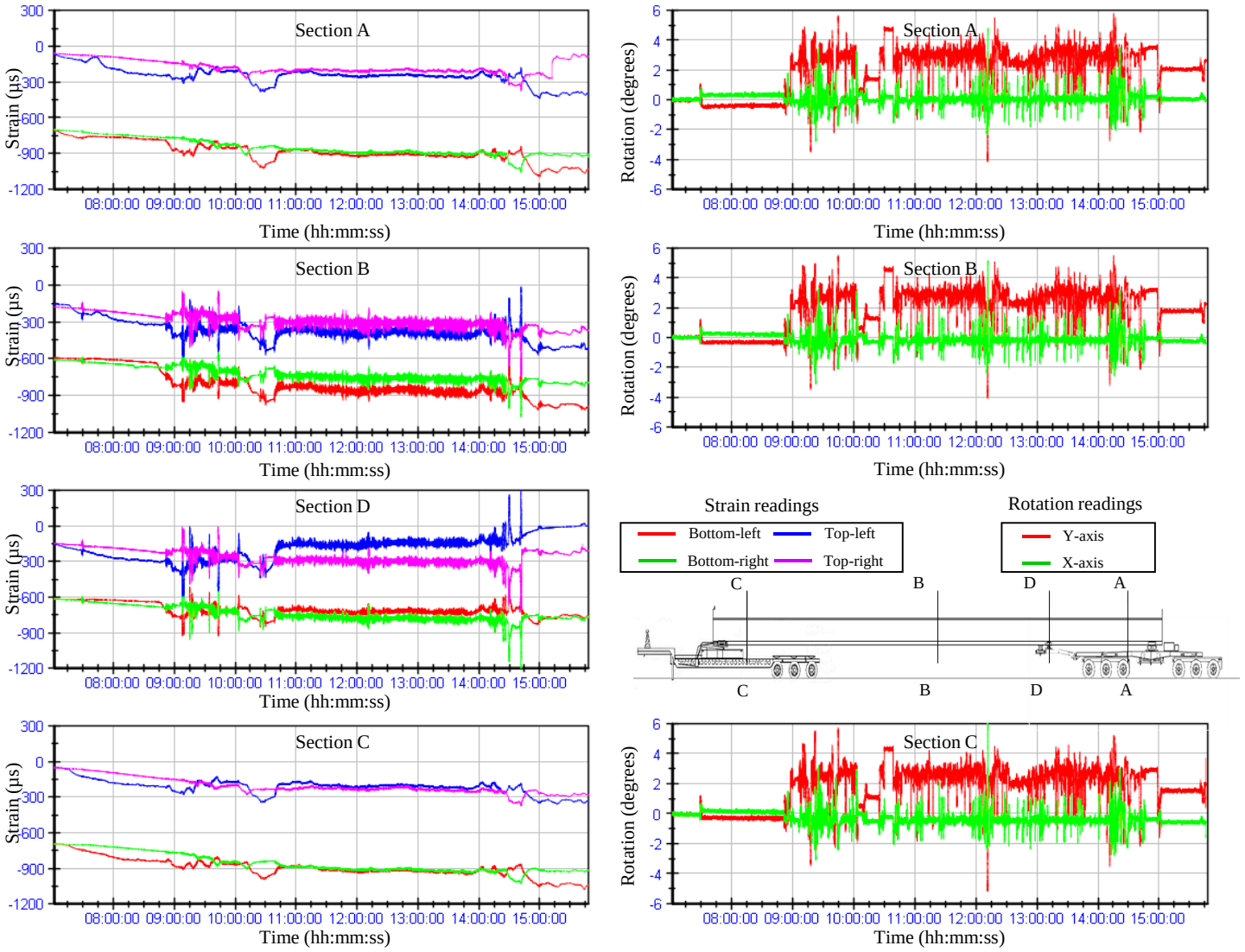

Figure F. 5
Girder 2 transportation record strain and rotation

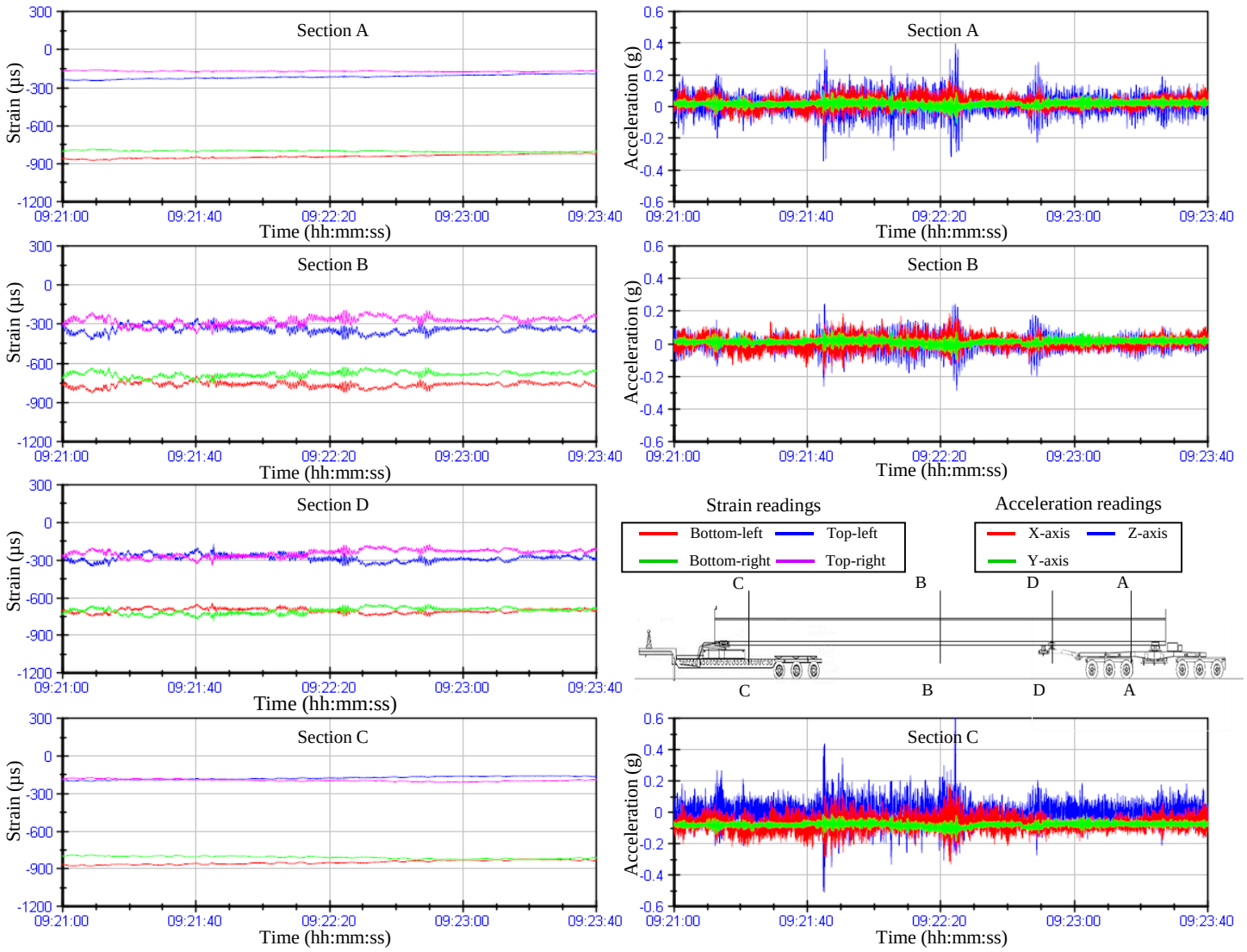

Figure F. 6
Event G2-A1 strain and acceleration

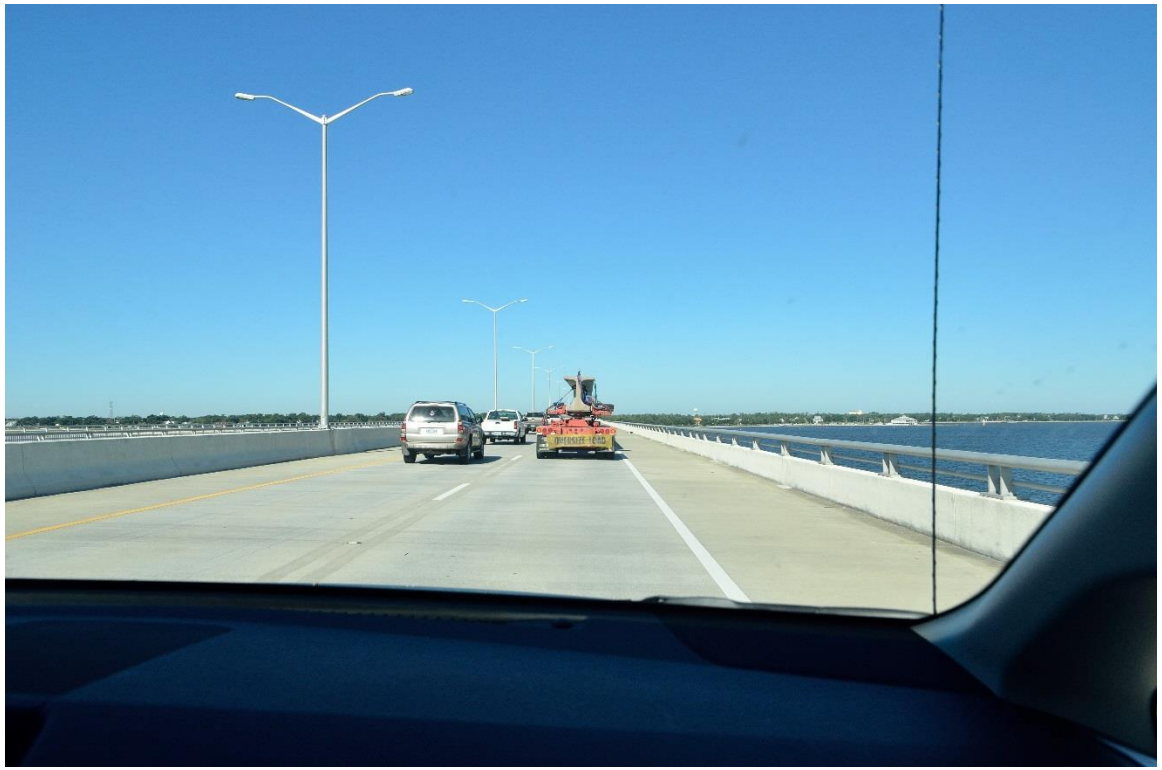

Figure F. 7
View of Girder 2 during Event G2-A1

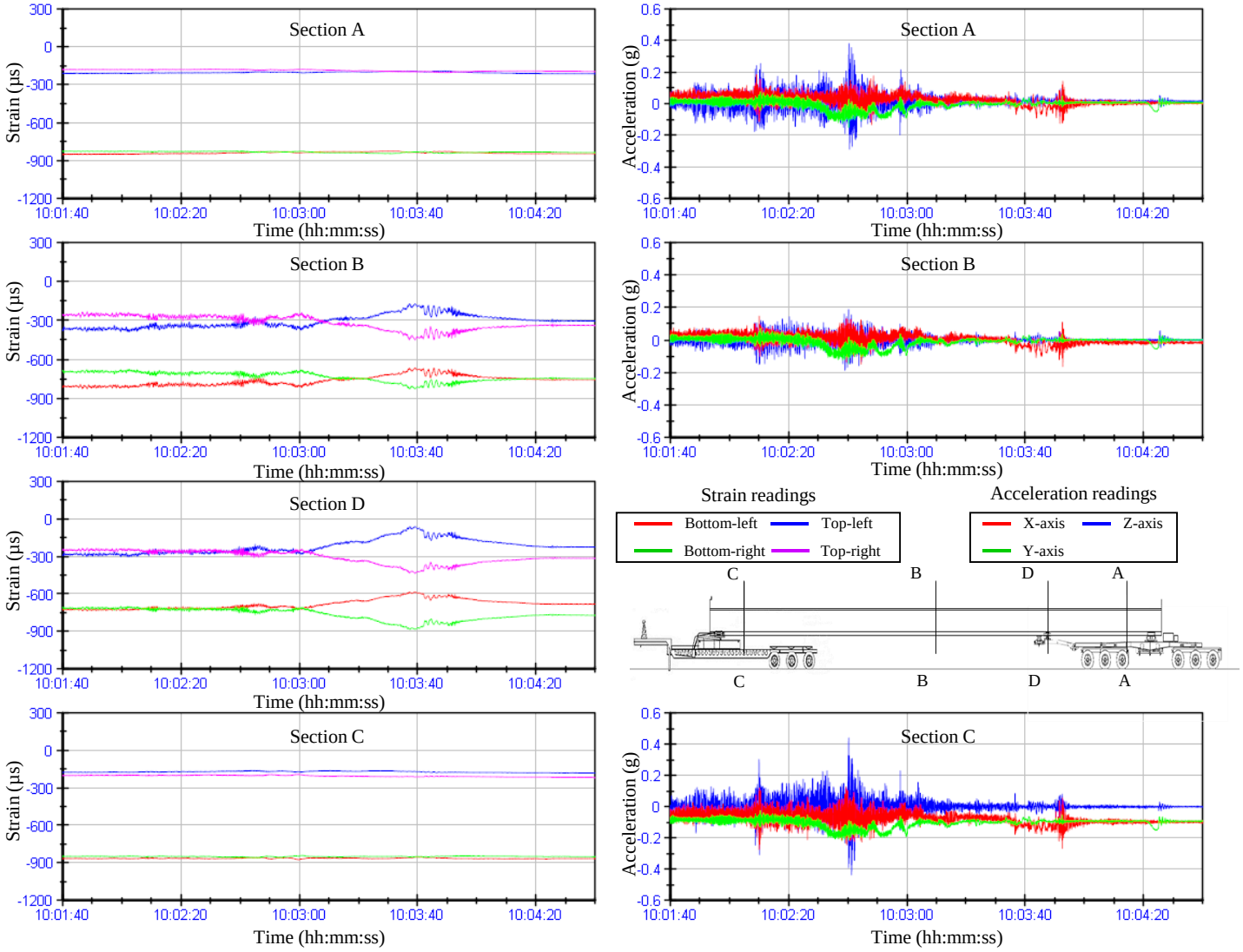

Figure F. 8
Event G2-A2 strain and acceleration

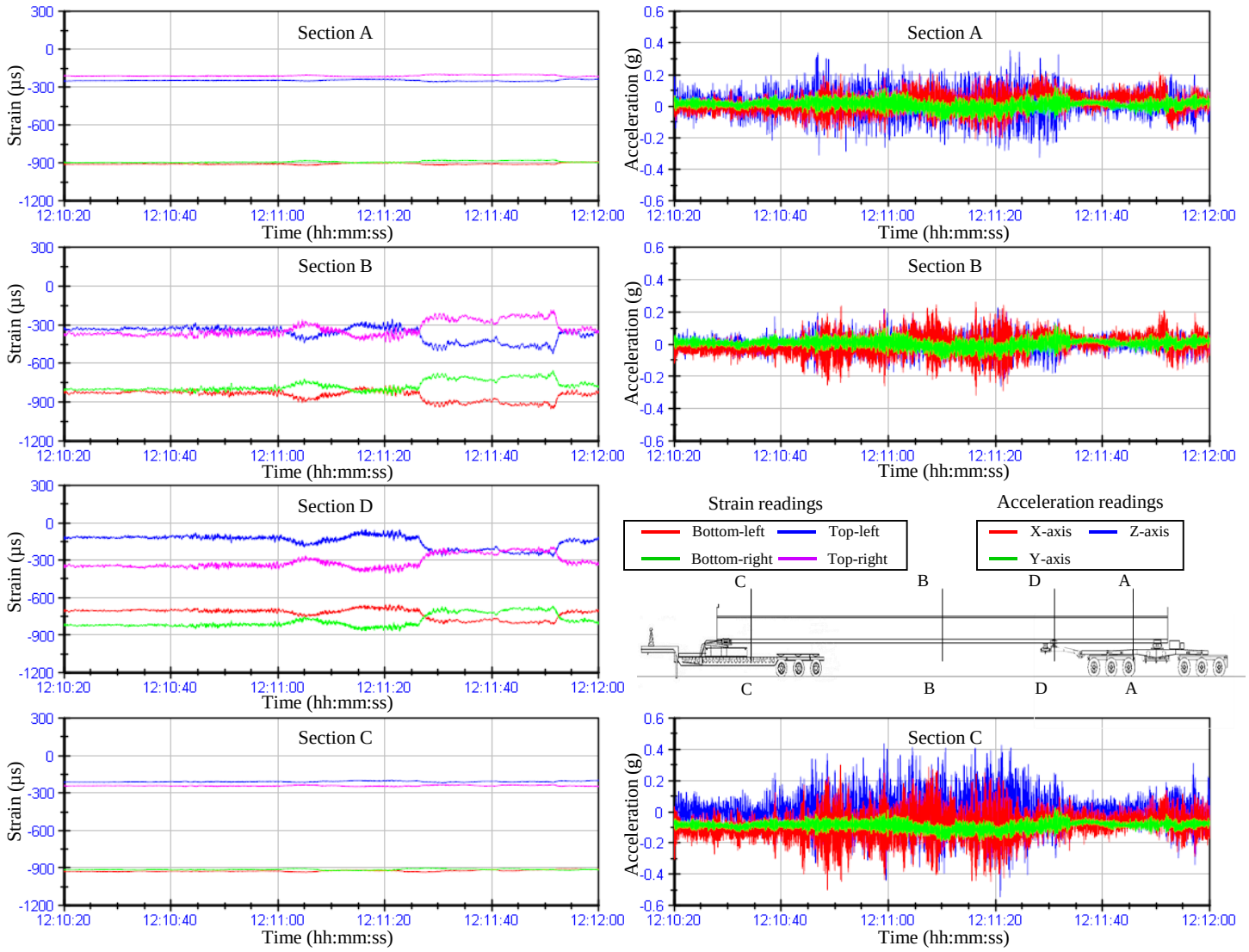

Figure F. 9
Event G2-A3 strain and acceleration

Figure F. 10
View of Girder 2 during Event G2-A3

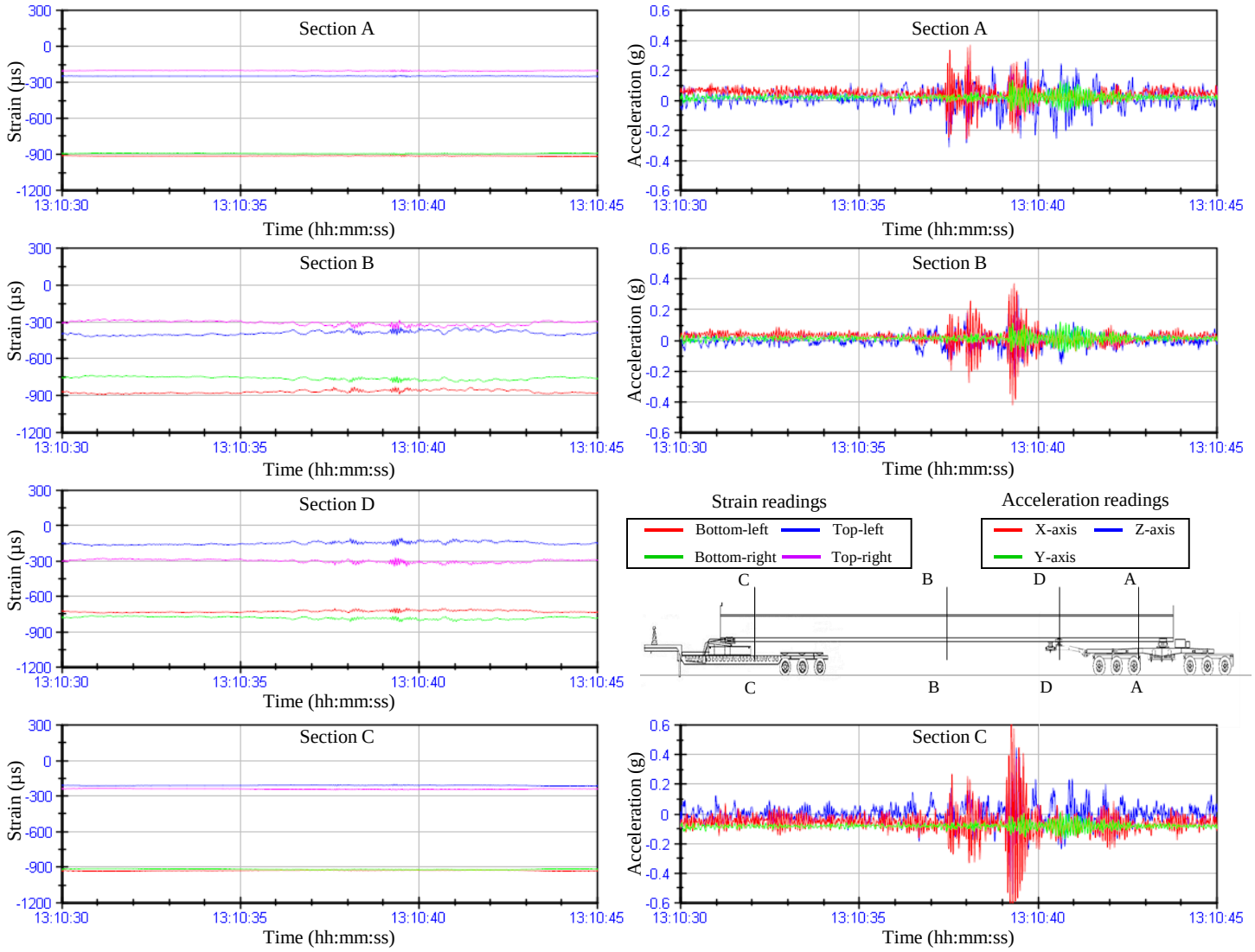

Figure F. 11
Event G2-A4 strain and acceleration

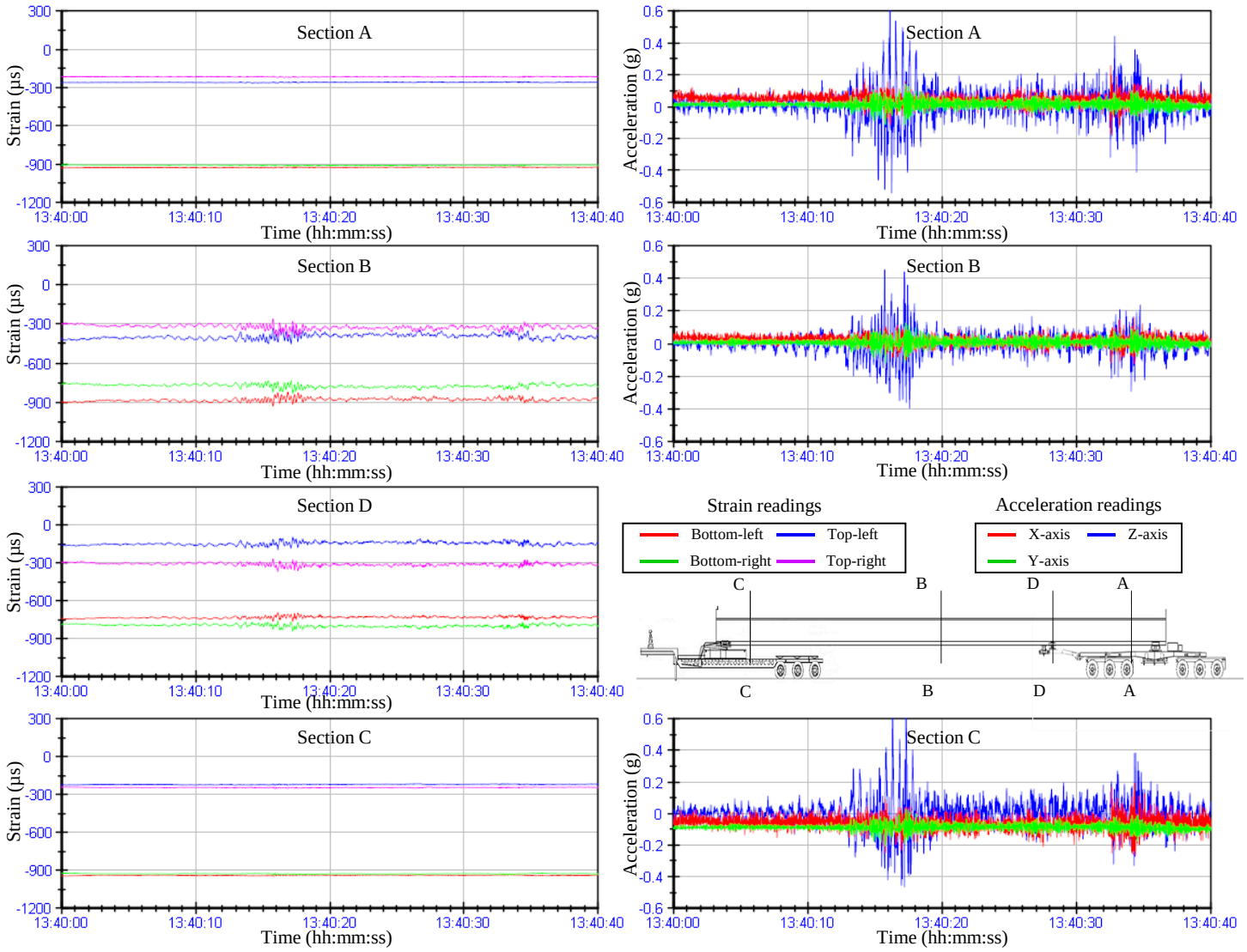

Figure F. 12
Event G2-A5 strain and acceleration

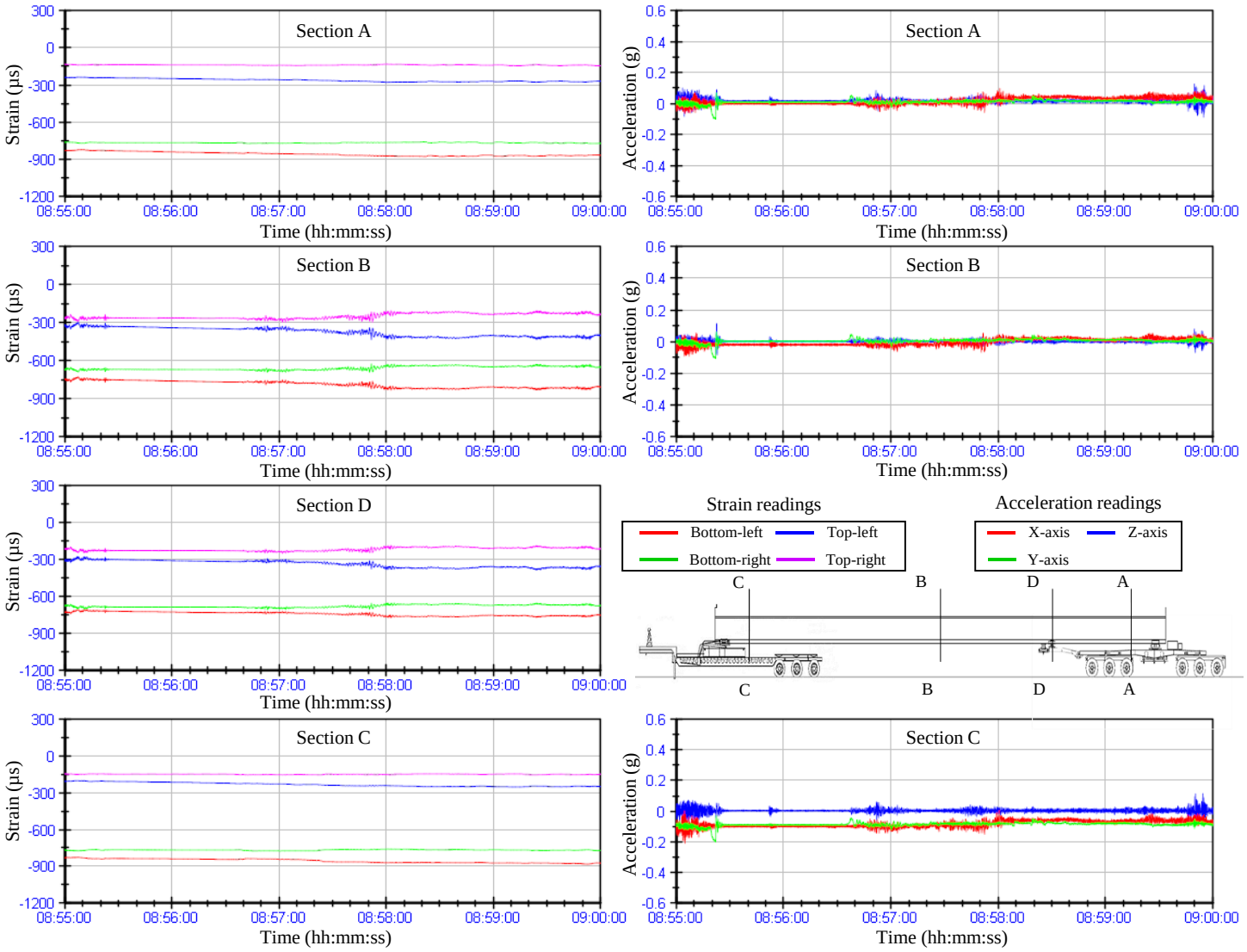

Figure F. 13
Event G2-S1 strain and acceleration

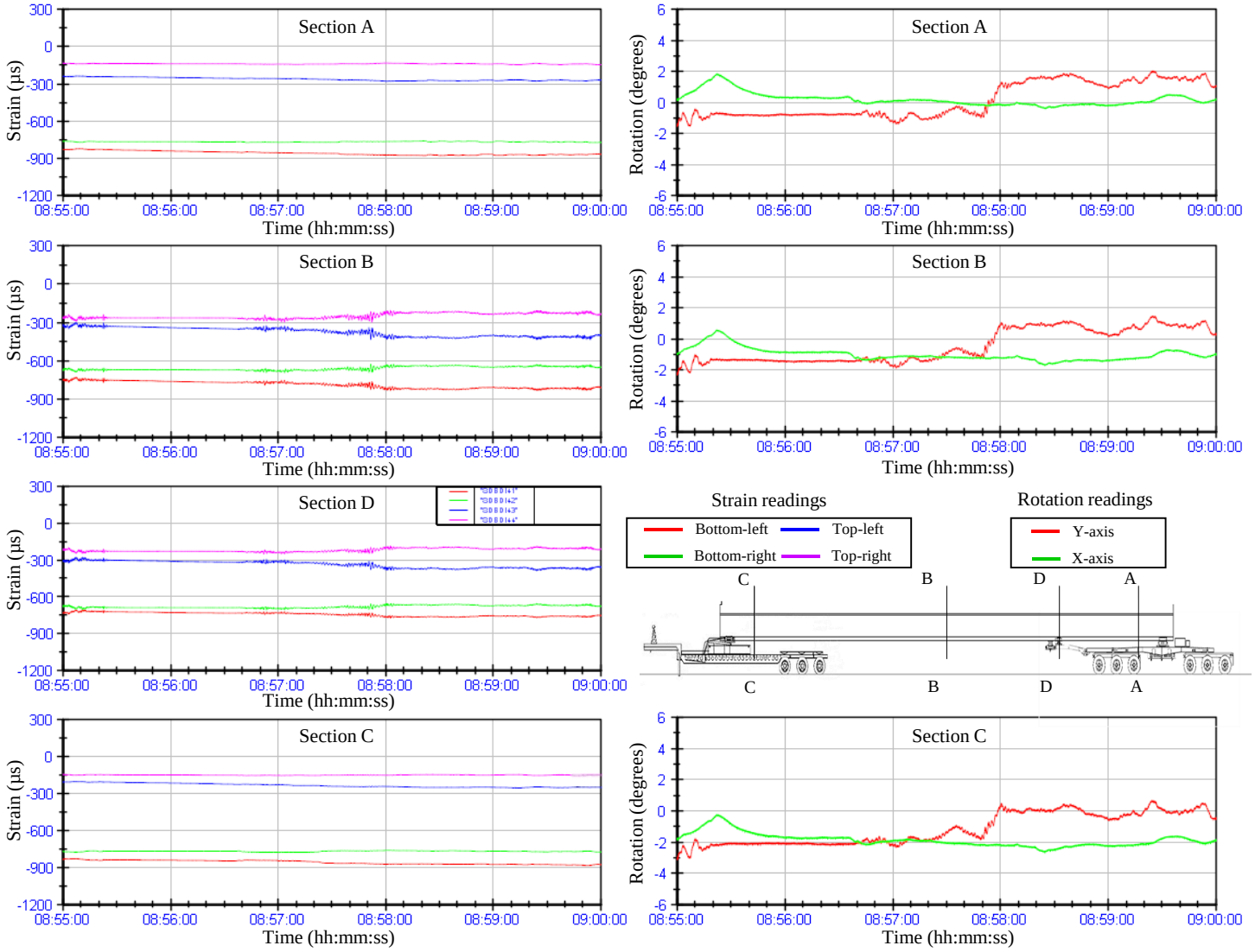

Figure F. 14
Event G2-S1 strain and rotation

Figure F. 15
View of Girder 2 during Event G2-S1

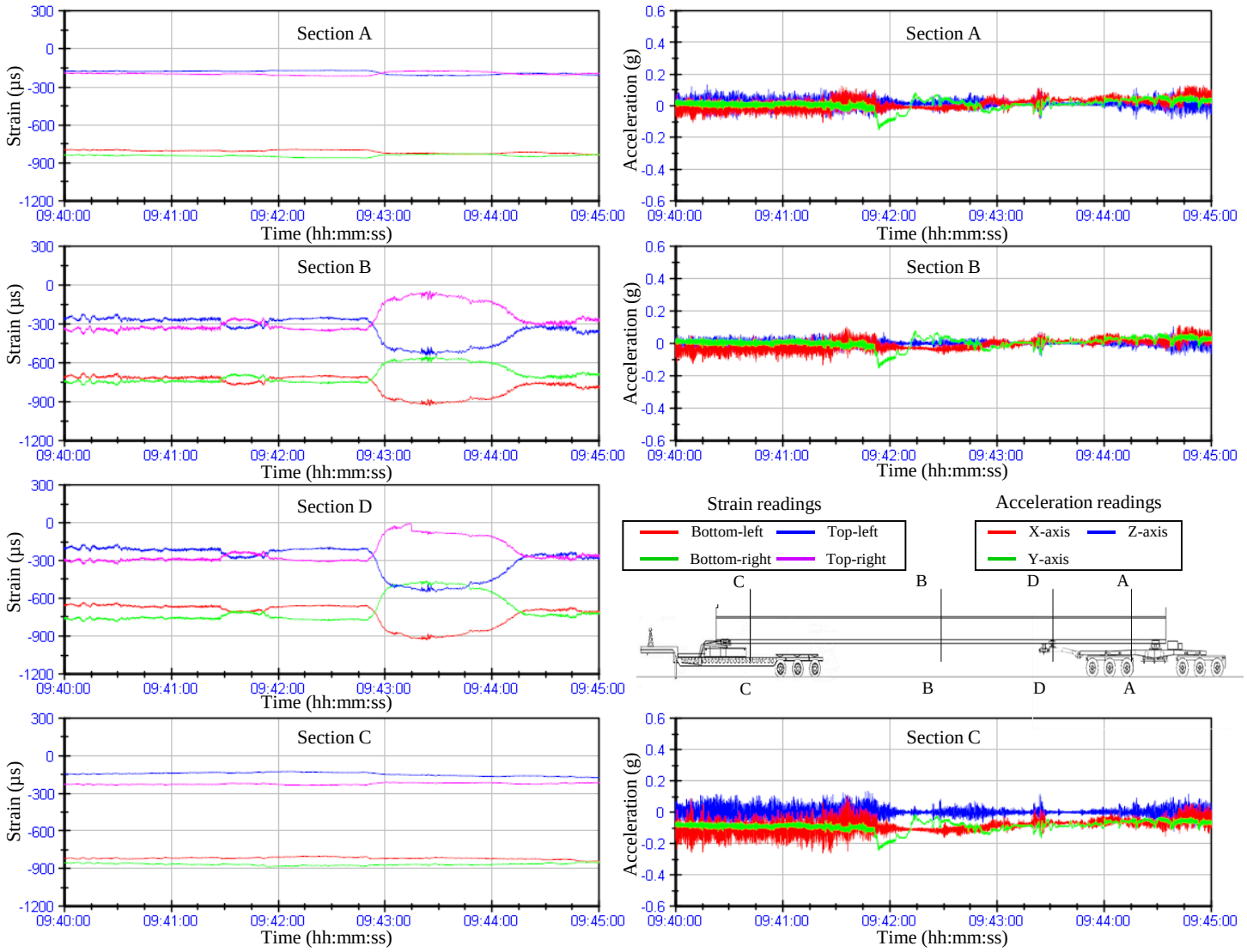

Figure F. 16
Event G2-S2 strain and acceleration

Figure F. 17
View of Girder 2 during Event G2-S2

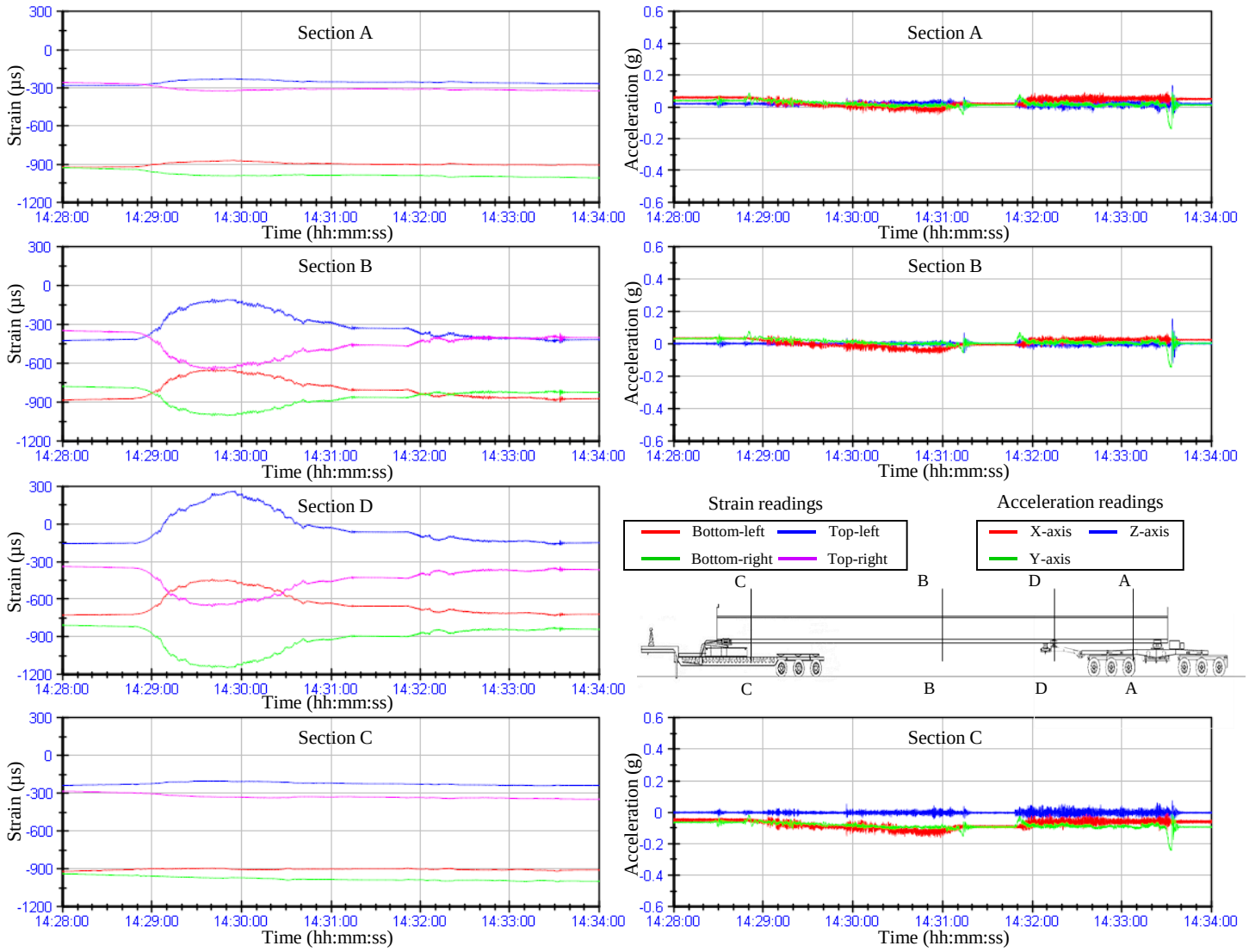

Figure F. 18
Event G2-S3 strain and acceleration

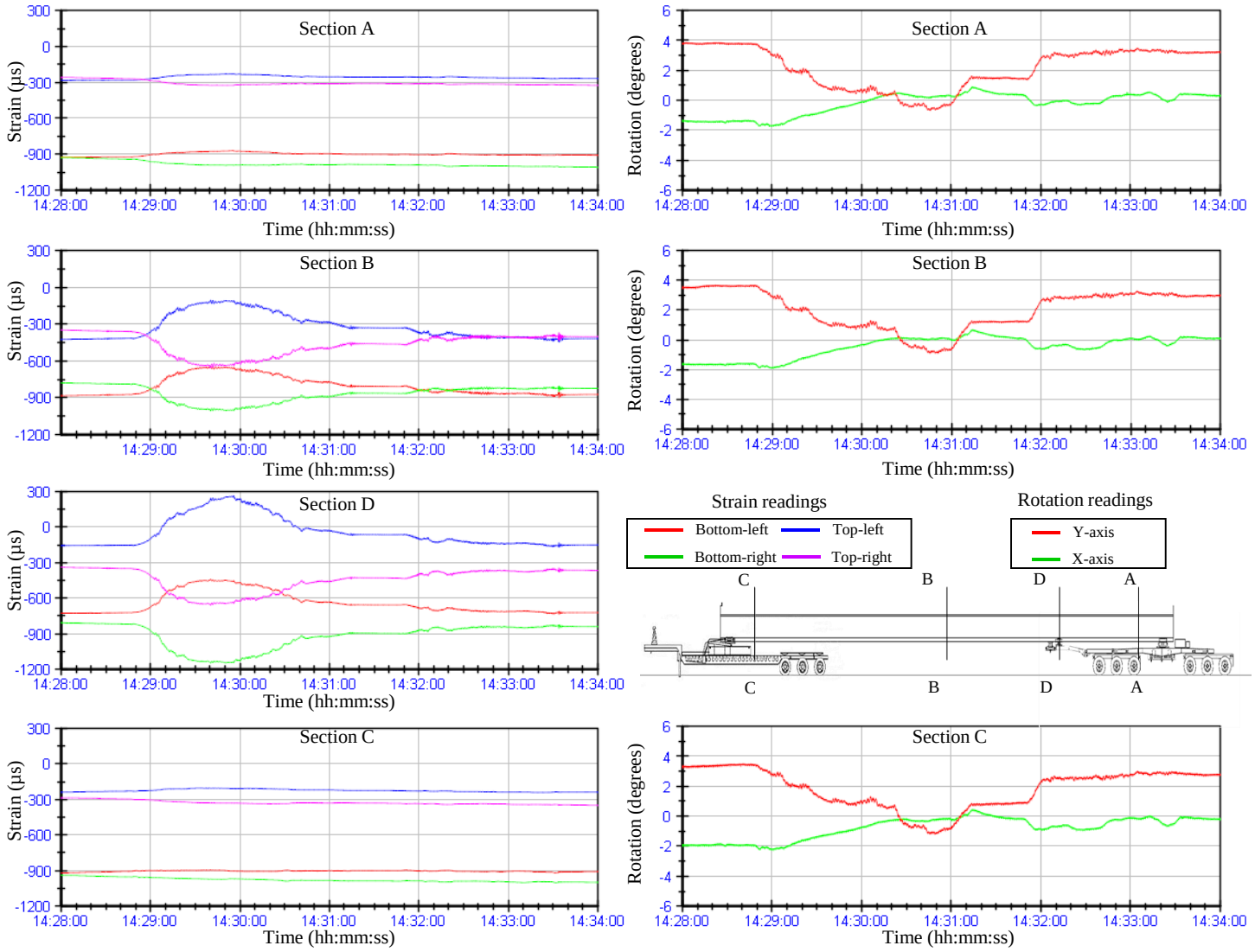

Figure F. 19
Event G2-S3 strain and rotation

Figure F. 20
View of Girder 2 during Event G2-S3

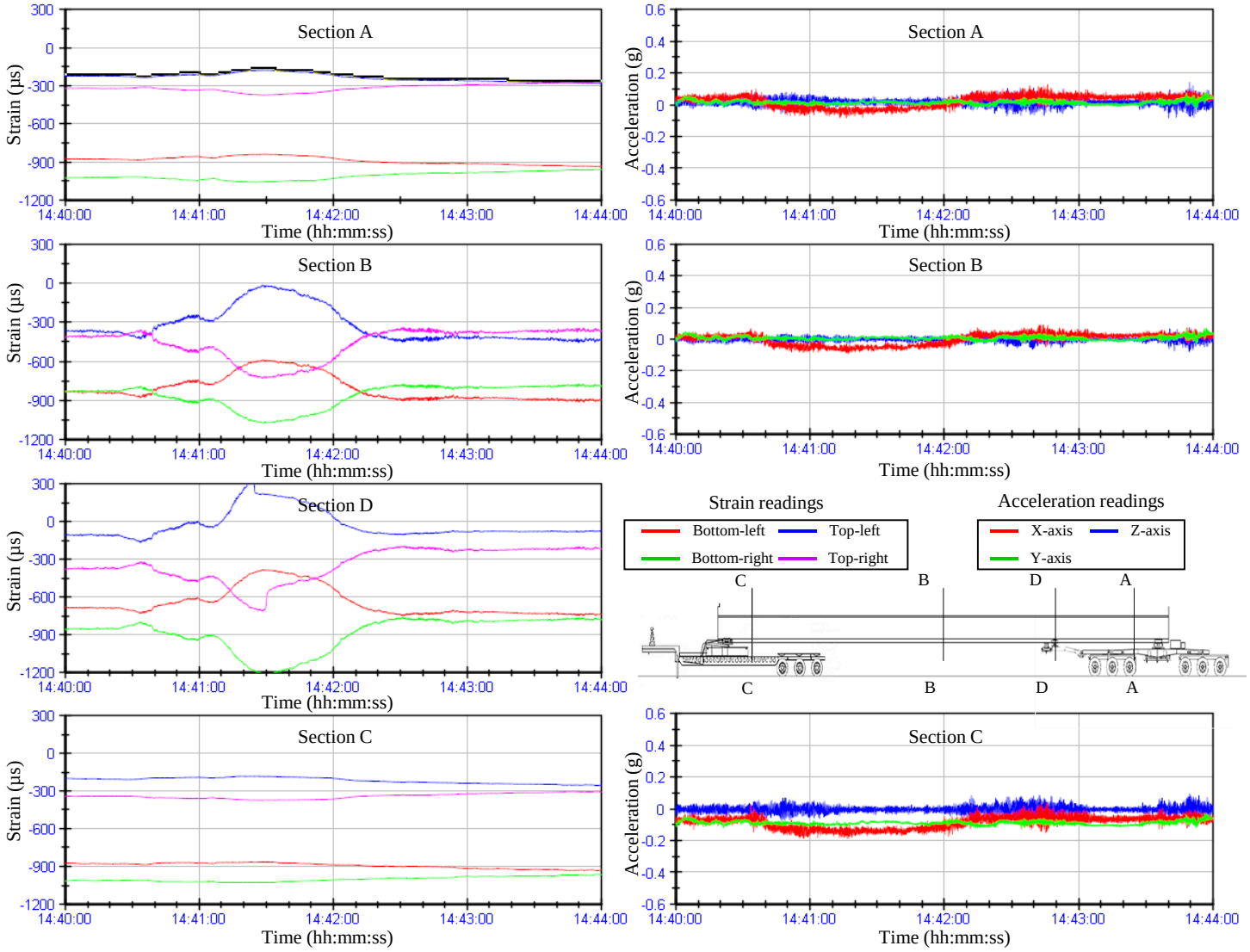

Figure F. 21
Event G2-S4 strain and acceleration

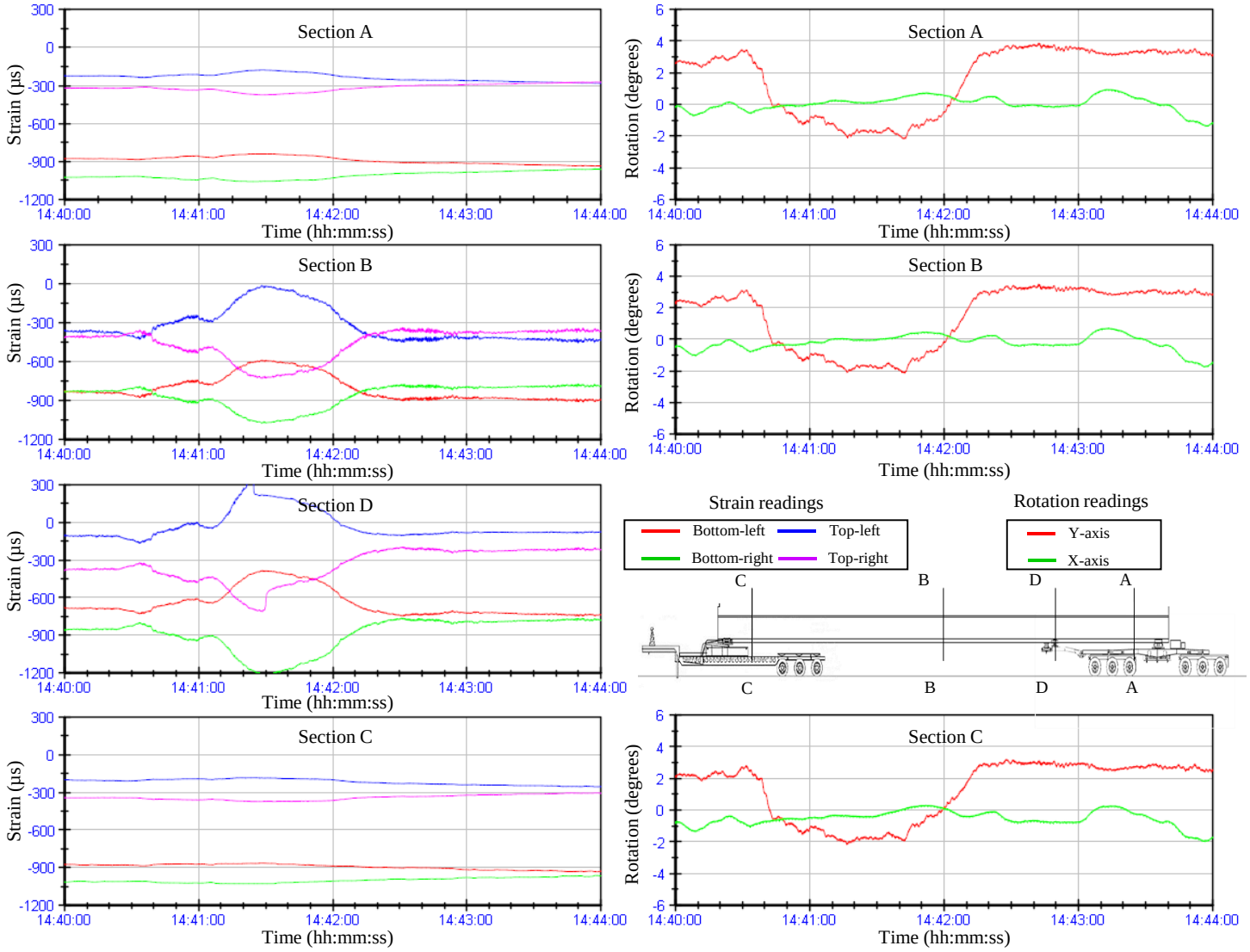

Figure F. 22
Event G2-S4 strain and rotation

Figure F. 23
View of Girder 2 during Event G2-S4

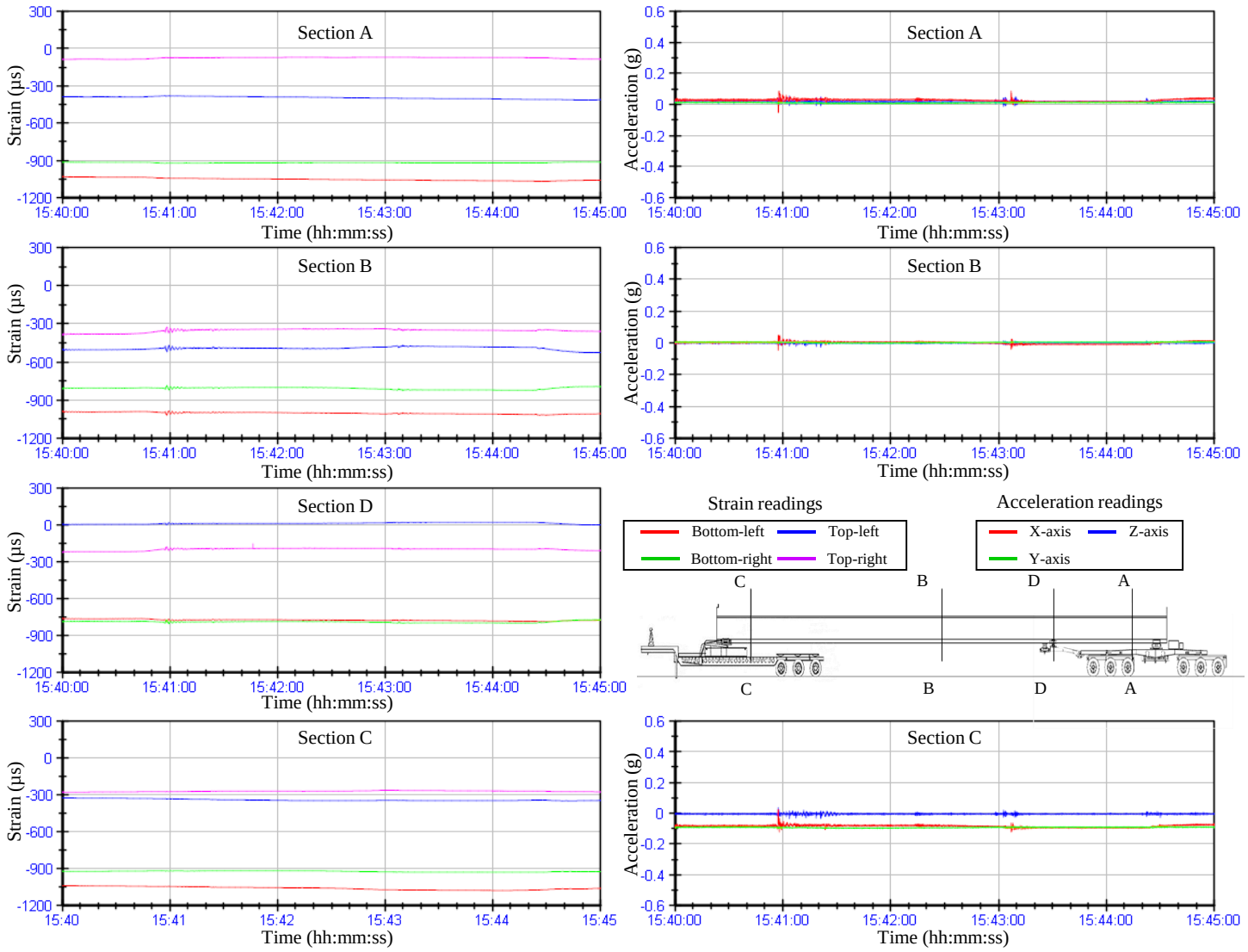

Figure F. 24
Event G2-S5 strain and acceleration

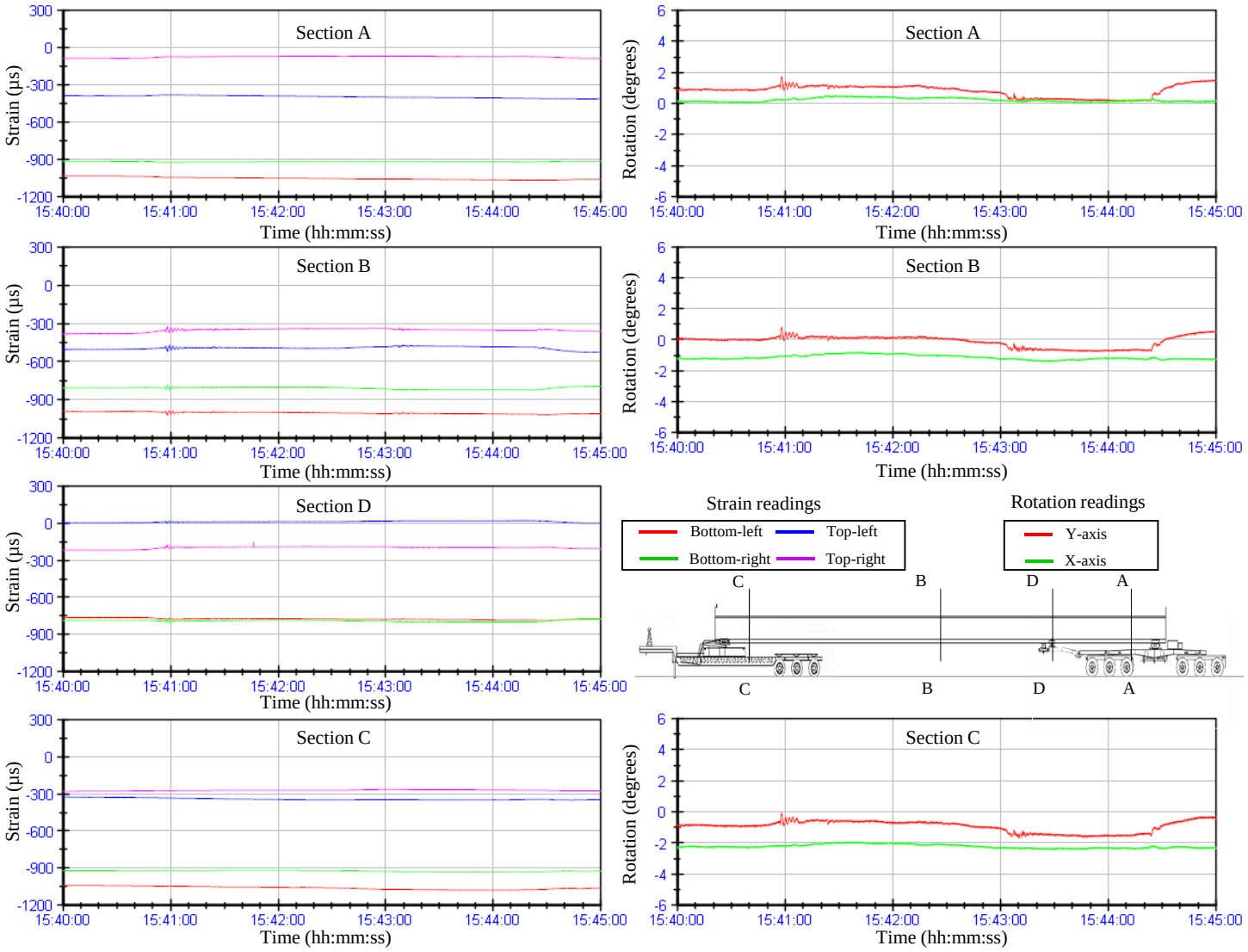

Figure F. 25
Event G2-S5 strain and rotation

Figure F. 26
View of Girder 2 during Event G2-S5

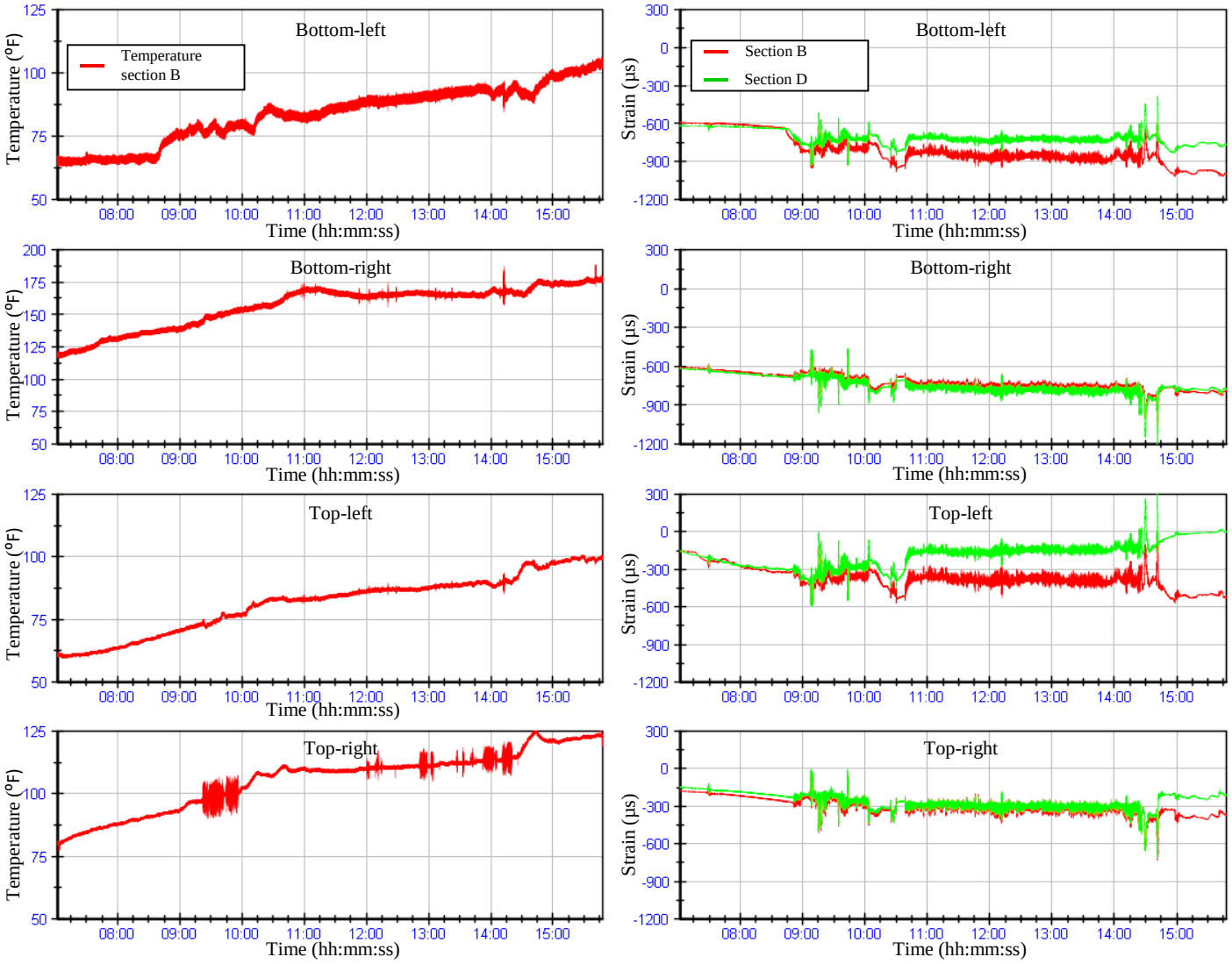

Figure F. 27
Temperature effect on strain at midspan section B and tongue location section D

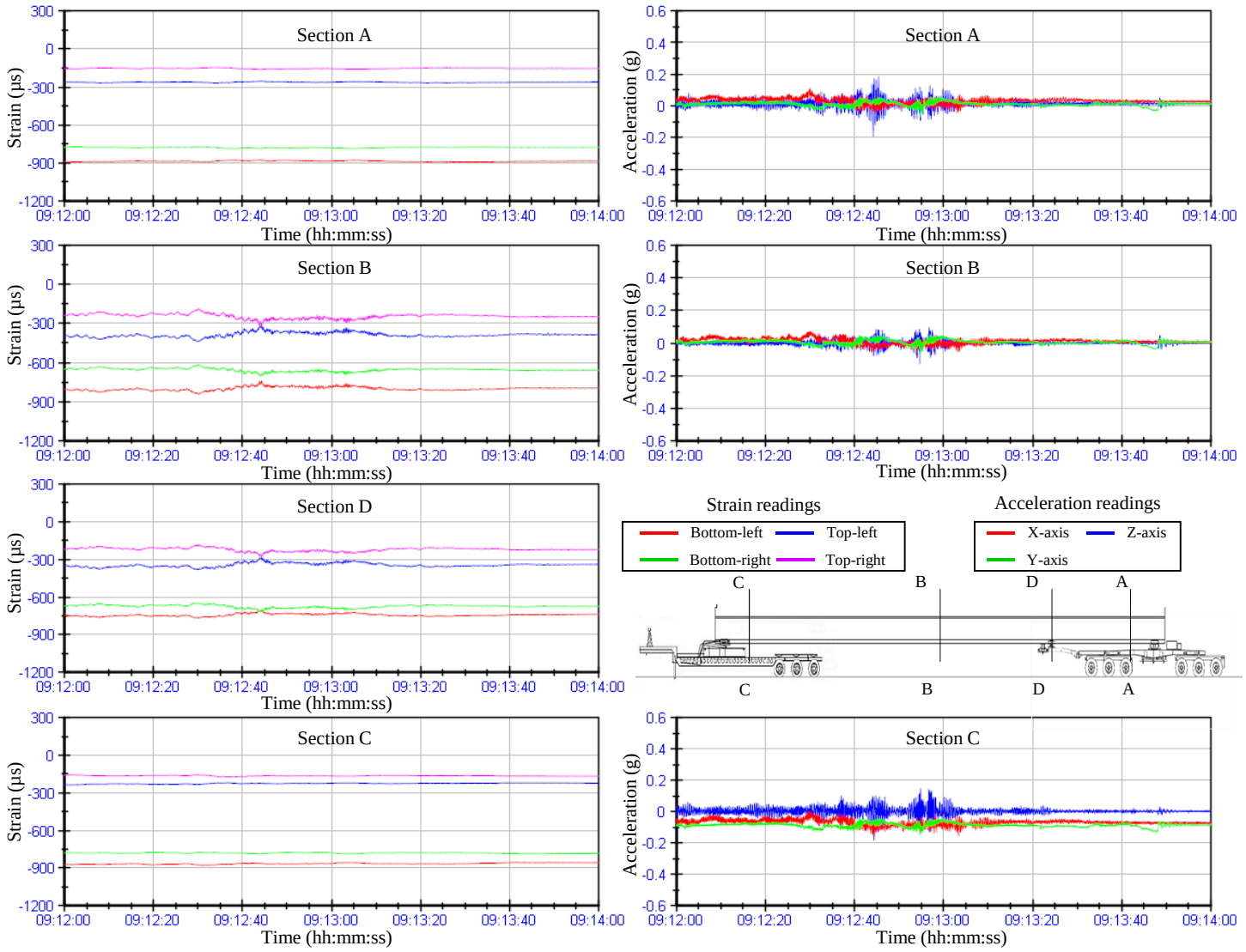

Figure F. 28
Girder 2 strain and acceleration during railroad crossing

Figure F. 29
View of Girder 2 during railroad crossing

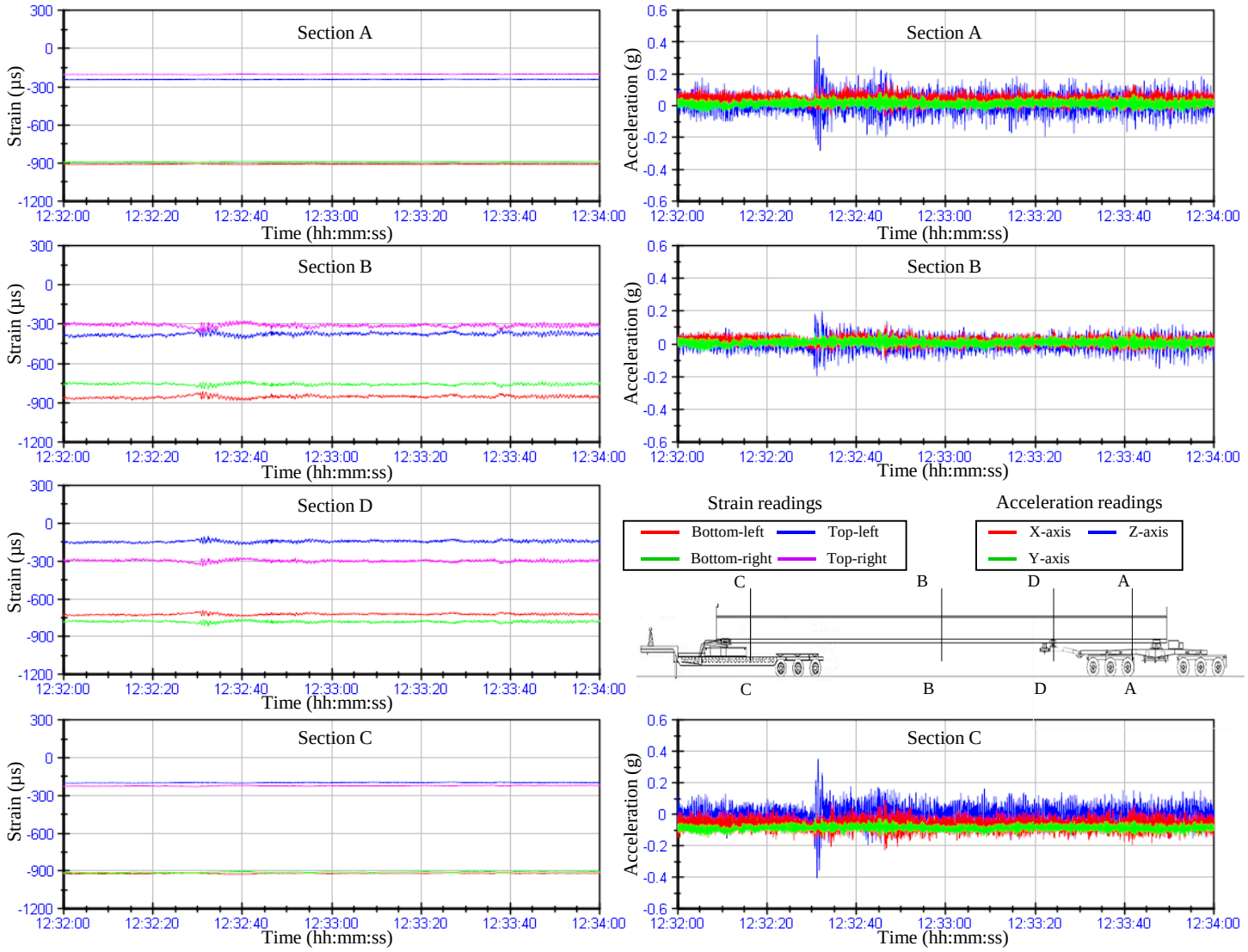

Figure F. 30
Girder 2 strain and acceleration during causeway crossing

Figure F. 31
View of Girder 2 during causeway crossing

APPENDIX G. GIRDERS STABILITY ANALYSIS

Girder 1: Lift and Transpotation Stability Analysis

Objective:
The objective of this sheet is to check the stability of the 130 ft long BT-72 girders during lift and transportation. Long span girders are typically designed with small widths of the web and flanges to reduce the weight during handling and, therefore, they tend to have low minor-axis inertia. The latter in addition to initial imperfections such as sweep tolerance and lifting loop placement causes the girder to tip about the roll axis. Therefore, long span girders are susceptible to lateral buckling and stability problems (rolling). This often results in lateral deflection due to bending about the weak axis which, If not checked properly, may lead to cracking.

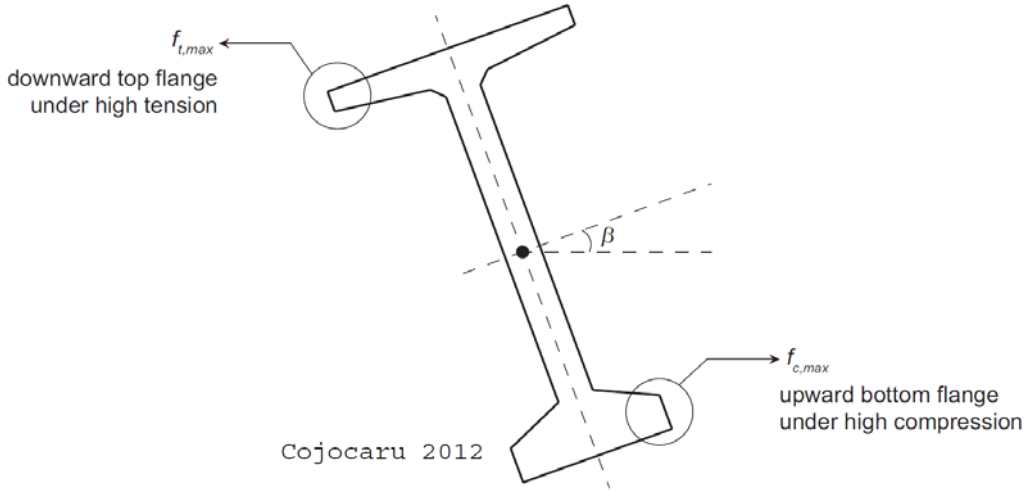

This sheet uses the theories developed by Mast (1989) to evaluate stability of girders during lift and Mast (1993) to evaluate stability of long girders during transportation. This approach is also adopted by the PCI Design Handbook 6th edition.

As discussed in Mast's papers, the main factors that contribute to girder stability are: the elastic stiffness properties of the girder, initial imperfections, location of lifting points, and properties of the support. This sheet follows Mast's approach to acquire maximum safe roll angle and factor of safety for the 130 ft long BT-72 girder.

Refernces:
Cojocaru, R. (2012). "Lifting Analysis of Precast Prestressed Concrete Beams." Thesis, Virginia Polytechnic Institute and State University.
Mast, R. F. (1989). "Lateral stability of long prestressed concrete beams, Part 1." PCI Journal, 34(1), 34-53.
Mast, R. F. (1993). "Lateral stability of long prestressed concrete beams, Part 2." PCI Journal, 38(1), 70-88.
PCI Design Handbook, 6th ed., Prestressed Concrete Institute, Chicago, IL.
PCI Bridge Design Manual (2003), 2nd ed., Prestressed Concrete Institute, Chicago, IL.

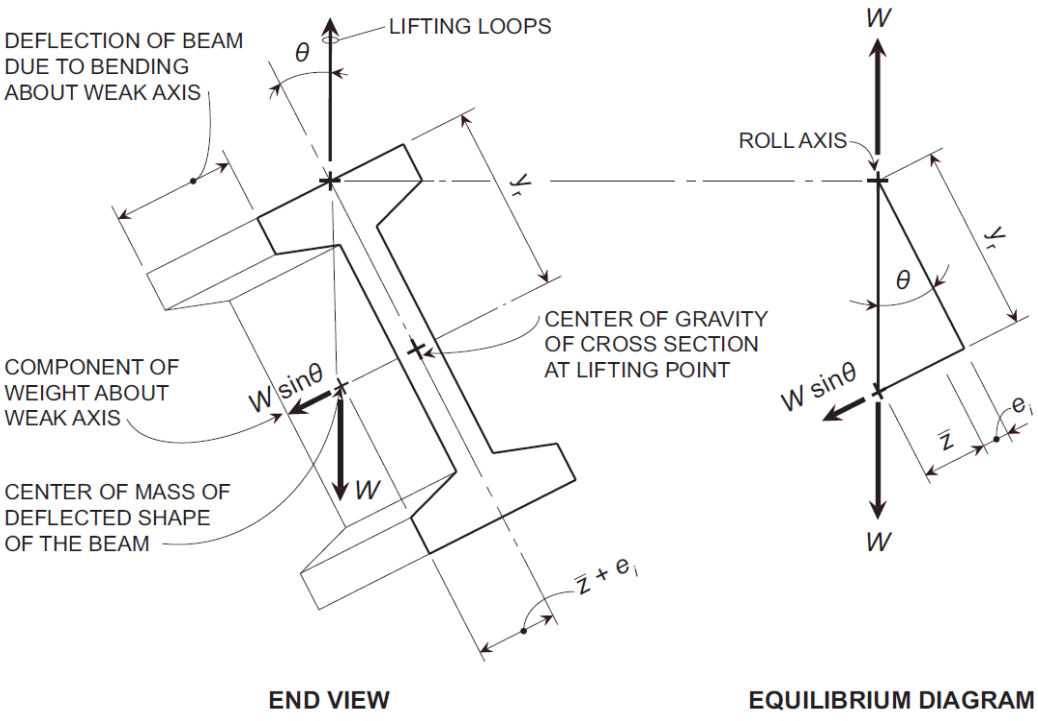

Lift Analysis for PCI BT-72 bridge girder

Girder properties

Depth	$h := 72in$		
Top flange width	$b := 42in$	Bottom flange width	$b_b := 26in$
Area	$A_c := 767in^2$	Composite section	$A_{ci} := 796.8in^2$
Major-axis inertia	$I_x := 545857 \cdot in^4$	Minor-axis inertia	$I_{yi} := 37634in^4$
Composite section	$I_{xi} := 569258.6in^4$		
Center of gravity	$CG_y := 36.6in$	Composite section	$CG_{yi} := 35.5in$
Distance to top fibers	$y_t := 36.5in$	Distance to bottom fibers	$y_b := 35.5in$
Torsion constant	$J := 12258in^4$		
Concrete weight	$\gamma_{conc} := 150 \frac{lbf}{ft^3}$		

Area of prestressing strands $A_{strand} := 0.153in^2$ $A_{ps} := A_{strand} \cdot 50 = 7.65 \cdot in^2$

Girder Length $L := 130ft$

Pickup points $a := 5ft$

$L_1 := L - 2a = 120\,ft$

The concrete has the following material properties

$f_{ci} := 8170psi$ $w_{dl} := A_c \cdot \gamma_{conc} = 0.8 \cdot \frac{kip}{ft}$

$E_{ci} := 5930ksi$ $G_c := \frac{E_{ci}}{2 \cdot (1 + 0.2)} = 2470.8 \cdot ksi$

The steel has the following material preperties

$E_s := 29000ksi$ $f_{pu} := 270ksi$

$f_{si} := 0.75 \cdot f_{pu} = 202.5 \cdot ksi$ $F_{si} := A_{ps} \cdot f_{si} = 1549.1 \cdot kip$

Stress after losses at midspan $F_{sems} := 1423.3kip$ $e_{ms} := 27.4in$

Compute initial eccentricity, e_i

This intial eccentricity is a direct result of sweep in the girder, and is calculated as the distance between the roll axis and the center of gravity of the arc of the curved girder.

Based on Mast (1993) and PCI Bridge Design Manual (2003)

$sweep := \frac{1}{2} \cdot \frac{1}{8} in \cdot \frac{L}{10ft} = 0.8 \cdot in$

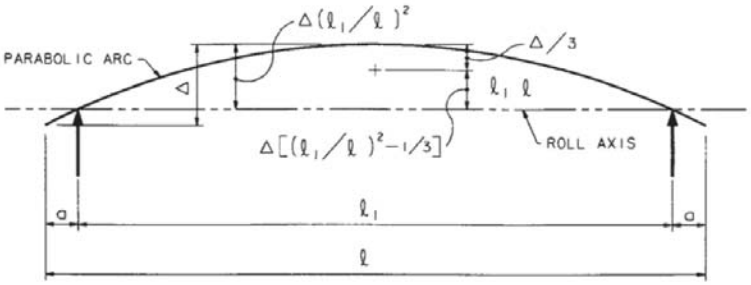

Based on Mast (1993)

$offset := \left(\frac{L_1}{L}\right)^2 - \frac{1}{3} = 0.5$

$e_i := 0.25in + sweep \cdot offset = 0.7 \cdot in$

Compute the height of the center of gravity and correct for camber

Camber can be estimated from midspan curvature

$$M_{dlms} := \frac{w_{dl} \cdot L}{2} \cdot \left(\frac{L}{4} - a \right) = 1428.1 \cdot kip \cdot ft$$

$$M_{ps} := F_{sems} \cdot e_{ms} = 3249.9 \cdot kip \cdot ft$$

$$M := M_{ps} - M_{dlms} = 1821.7 \cdot kip \cdot ft$$

$$R := \frac{E_{ci} \cdot I_{xi}}{M} = 1.5 \times 10^{5} \cdot in$$

$$camber := \frac{L^{2}}{8 \cdot R} = 2 \cdot in$$

The height of the center of gravity of the cambered arc above the roll axis yr is calculated similar to sweep

$$y_r := y_t - camber \cdot offset = 35.5 \cdot in$$

Compute Z_0

Z0 is the distance to the center of gravity of the defelected arc of the girder about the minor-axis. This takes into the accunt the distance between the girder end and the lifting point (a)

$$z_0 := \frac{w_{dl}}{12 \cdot E_{ci} \cdot I_{yi} \cdot L} \cdot \left(\frac{1}{10} \cdot L_1^{5} - a^{2} \cdot L_1^{3} + 3 \cdot a^{4} \cdot L_1 + \frac{6}{5} \cdot a^{5} \right) = 9.7 \cdot in$$

Compute θi

θi is the inital roll angle due to sweep

$$\theta_i := \frac{e_i}{y_r} = 0.0189 \qquad \theta_i = 1.084 \cdot deg$$

Compute the tilt angle θmax at cracking

Rupture concrete stresss

$$f_r := 7.5 \sqrt{\frac{f_{ci}}{psi}} \cdot psi = 677.9 \cdot psi$$

Top and bottom stresses due to gravity loads

$$f_b := \frac{M_{dlms} \cdot y_b}{I_{xi}} + \frac{-F_{sems}}{A_{ci}} - \frac{F_{sems} \cdot e_{ms} \cdot y_b}{I_{xi}} = -3.1 \cdot ksi$$

$$f_t := -\frac{M_{dlms} \cdot y_t}{I_{xi}} + \frac{-F_{sems}}{A_{ci}} + \frac{F_{sems} \cdot e_{ms} \cdot y_t}{I_{xi}} = -0.38 \cdot ksi$$

Lateral moment that will cause cracking in the top fibers

$$M_{lat} := \left(f_r - f_t\right) \cdot \frac{I_{yi}}{\left(\frac{b}{2}\right)} = 158.7 \cdot kip \cdot ft$$

Maximum roll angle

$$\theta_{max} := \frac{M_{lat}}{M_{dlms}} = 0.111 \qquad \theta_{max} = 6.366 \cdot deg$$

Maximum tilt angle during lift to avoid cracking is 6.333 deg

Compute factor of safety

Factor of safety aganist cracking. This considers the ratios between the height of roll center to the lateral deflection and the maximum tilt angle to the initial roll angle

$$FS_{cracking} := \frac{1}{\frac{z_0}{y_r} + \frac{\theta_i}{\theta_{max}}} = 2.3$$

Factor of safety aganist failure. This considers the cracked condition of the girder

Z'0c is the distance to the center of gravity of the defelected arc of the cracked girder.

$$\theta_{maxc} := \sqrt{\frac{e_i}{2.5 \cdot z_0}} = 0.166$$

$$z_{0c} := z_0 \cdot \left(1 + 2.5 \cdot \theta_{maxc}\right) = 13.7 \cdot in$$

$$FS_{failure} := \frac{y_r \cdot \theta_{maxc}}{z_{0c} \cdot \theta_{maxc} + e_i} = 2$$

Stability Analysis during Transportation

$F_{sems} = 1423.3 \cdot kip$ $e_{ms} = 27.4 \cdot in$

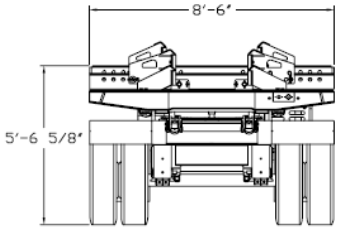

superelevation angle $\alpha := 0.06$

Trailer properties

Height of trailer $h := 68in + 4in = 72 \cdot in$

height of roll center $h_r := 24in$ assumed

height of cg above road $h_{cg} := h + CG_{yi} = 107.5 \cdot in$

Estimate the rotational stiffness of the transportation vehicle

Kθ is the elastic roatational spring constant of the vehicle

assume $K_{\theta_axle} := 4500kip \cdot in$ per radian per dual axle

Trailer has six dual axles

$K_{\theta_trailer} := 6 \cdot 4500kip \cdot in = 27000 \cdot kip \cdot in$ per radian per tariler

$K_{\theta_truck} := K_{\theta_trailer} \cdot 2 = 54000 \cdot kip \cdot in$ per radian

$$r := \frac{K_{\theta_truck}}{w_{dl} \cdot L} = 519.9 \cdot in$$

Find tilt angle

Distance between the cenetr of graviyt of the girder and the roll axis

$y := h_{cg} - h_r = 83.5 \cdot in$

account for camber $y := y \cdot 1.02 = 85.2 \cdot in$

Calculate initial eccentricity as a result of sweep for the transportation case

$$sweep_T := \frac{1}{8} in \cdot \frac{L}{10ft} = 1.6 \cdot in$$

$e_T := 1in + sweep_T \cdot offset = 1.8 \cdot in$

Since Young's modulus did not change, z0 remains the same

$z_{0T} := z_0 = 9.7 \cdot in$

Tilt angle

$\theta_T := \frac{\alpha \cdot r + e_T}{r - y - z_{0T}} = 0.078$ $\theta_T = 4.453 \cdot deg$

Check concrete compressive strength

Check stress at centerline

$F_{sems} := 1423.3kip$ $e_{ms} := 27.4in$

$f_b := \frac{M_{dlms} \cdot y_b}{I_{xi}} + \frac{-F_{sems}}{A_{ci}} - \frac{F_{sems} \cdot e_{ms} \cdot y_b}{I_{xi}} = -3.1 \cdot ksi$

$f_t := -\frac{M_{dlms} \cdot y_t}{I_{xi}} + \frac{-F_{sems}}{A_{ci}} + \frac{F_{sems} \cdot e_{ms} \cdot y_t}{I_{xi}} = -0.38 \cdot ksi$

Add lateral bending to fb

$M_{latcheck} := \theta_T \cdot M_{dlms} = 111 \cdot kip \cdot ft$

Bottom flange width

$b_b := 26in$

$f_{bT} := f_b - M_{latcheck} \cdot \frac{b_b \cdot 0.5}{I_{yi}} = -3.6 \cdot ksi$

Minimum required compressive strength

$f_{cmiin} := \frac{-f_{bT}}{0.6} = 6016.1 \cdot psi$ OK

Compute tilt angle θmax at cracking

$$M_{latT} := \frac{(f_r - f_t)\cdot I_{yi}}{\frac{b}{2}} = 158.7\cdot kip\cdot ft$$

$$\theta_{maxT} := \frac{M_{latT}}{M_{dlms}} = 0.111 \qquad \theta_{maxT} = 6.366\cdot deg$$

Compute factor of safety

Factor of safety aganist cracking

$$FS_{crackingT} := \frac{r\cdot(\theta_{maxT} - \alpha)}{z_{0T}\cdot\theta_{maxT} + e_T + y\cdot\theta_{max}} = 2.1$$

Factor of safety aganist rollover. This considers the cracked condition of the girder

Zmax is the distance between the centerline of the vehicle to the centerline of dual tire

$$z_{max} := 36in$$

$$\theta_{maxcT} := \frac{z_{max} - h_r\cdot\alpha}{r} + \alpha = 0.126$$

Z'0cT is the distance to the center of gravity of the defelected arc of the cracked girder

$$z_{0cT} := z_0\cdot(1 + 2.5\cdot\theta_{maxc}) = 13.7\cdot in$$

$$FS_{failureT} := \frac{r\cdot(\theta_{maxT} - \alpha)}{z_{0cT}\cdot\theta_{maxc} + e_T + y\cdot\theta_{maxT}} = 2$$

Girder 2: Lift and Transpotation Stability Analysis

Objective:
The objective of this sheet is to check the stability of the 130 ft long LG54 girders during lift and transportation. Long span girders are typically designed with small widths of the web and flanges to reduce the weight during handling and, therefore, they tend to have low minor-axis inertia. The latter in addition to initial imperfections such as sweep tolerance and lifting loop placement causes the girder to tip about the roll axis. Therefore, long span girders are susceptible to lateral buckling and stability problems (rolling). This often results in lateral deflection due to bending about the weak axis which, If not checked properly, may lead to cracking.

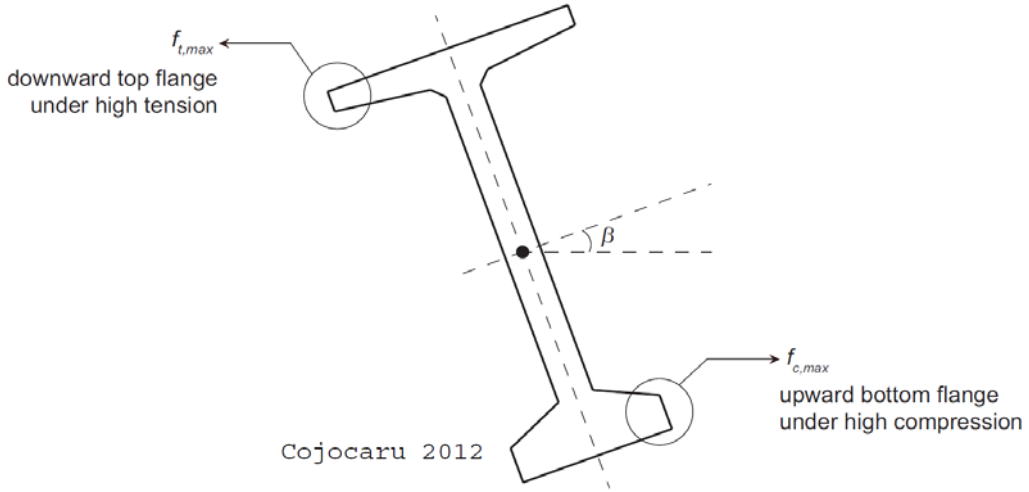

This sheet uses the theories developed by Mast (1989) to evaluate stability of girders during lift and Mast (1993) to evaluate stability of long girders during transportation. This approach is also adopted by the PCI Design Handbook 6th edition.

As discussed in Mast's papers, the main factors that contribute to girder stability are: the elastic stiffness properties of the girder, initial imperfections, location of lifting points, and properties of the support. This sheet follows Mast's approach to acquire maximum safe roll angle and factor of safety for the 130 ft long BT-72 girder.

Refernces:
Cojocaru, R. (2012). "Lifting Analysis of Precast Prestressed Concrete Beams." Thesis, Virginia Polytechnic Institute and State University.
Mast, R. F. (1989). "Lateral stability of long prestressed concrete beams, Part 1." PCI Journal, 34(1), 34-53.
Mast, R. F. (1993). "Lateral stability of long prestressed concrete beams, Part 2." PCI Journal, 38(1), 70-88.
PCI Design Handbook, 6th ed., Prestressed Concrete Institute, Chicago, IL.
PCI Bridge Design Manual (2003), 2nd ed., Prestressed Concrete Institute, Chicago, IL.

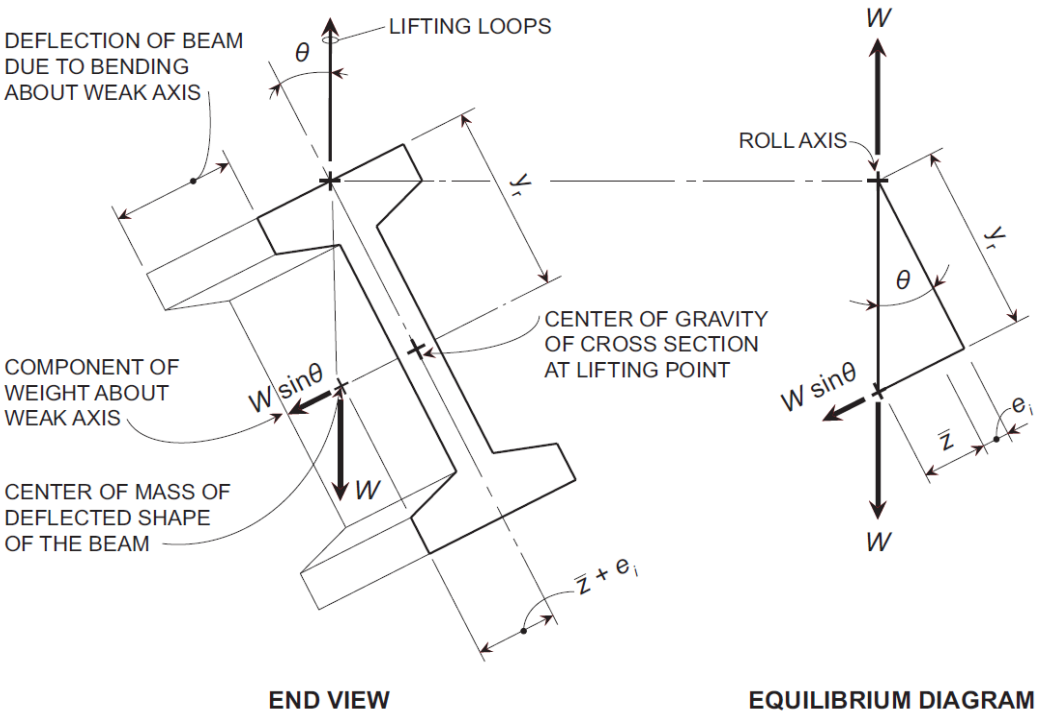

Lift Analysis for LG54 bridge girder

Girder properties

Depth	$h := 54in$		
Top flange width	$b := 48in$	Bottom flange width	$b_b := 36in$
Area	$A_c := 868in^2$	Composite section	$A_{ci} := 915.8in^2$
Major-axis inertia	$I_x := 344586 \cdot in^4$	Minor-axis inertia	$I_{yi} := 70877in^4$
Composite section	$I_{xi} := 361188in^4$		
Center of gravity	$CG_y := 25.1in$	Composite section	$CG_{yi} := 24.1in$
Distance to top fibers	$y_t := 29.9in$	Distance to bottom fibers	$y_b := 24.1in$
Torsion constant	$J := 22620in^4$		
Concrete weight	$\gamma_{conc} := 150 \frac{lbf}{ft^3}$		

Area of prestressing strands $A_{strand} := 0.217in^2$ $A_{ps} := A_{strand} \cdot 56 = 12.15 \cdot in^2$

Girder Length $L := 130ft$

Pickup points $a := 5ft$

$L_1 := L - 2a = 120\,ft$

The concrete has the following material properties

$f_{ci} := 8170psi$ $w_{dl} := A_c \cdot \gamma_{conc} = 0.9 \cdot \frac{kip}{ft}$

$E_{ci} := 5930ksi$ $G_c := \frac{E_{ci}}{2 \cdot (1 + 0.2)} = 2470.8 \cdot ksi$

The steel has the following material preperties

$E_s := 29000ksi$ $f_{pu} := 270ksi$

$f_{si} := 0.75 \cdot f_{pu} = 202.5 \cdot ksi$ $F_{si} := A_{ps} \cdot f_{si} = 2460.8 \cdot kip$

Stress after losses at midspan $F_{sems} := 2234kip$ $e_{ms} := 18.2in$

Compute initial eccentricity, e_i

This intial eccentricity is a direct result of sweep in the girder, and is calculated as the distance between the roll axis and the center of gravity of the arc of the curved girder.

Based on Mast (1993) and PCI Bridge Design Manual (2003)

$sweep := \frac{1}{2} \cdot \frac{1}{8} in \cdot \frac{L}{10ft} = 0.8 \cdot in$

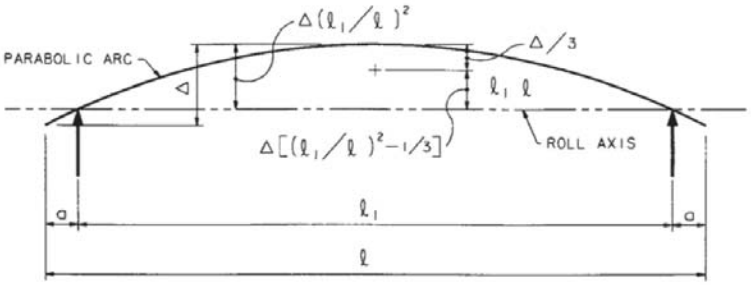

Based on Mast (1993)

$offset := \left(\frac{L_1}{L}\right)^2 - \frac{1}{3} = 0.5$

$e_i := 0.25in + sweep \cdot offset = 0.7 \cdot in$

Compute the height of the center of gravity and correct for camber

Camber can be estimated from midspan curvature

$$M_{dlms} := \frac{w_{dl} \cdot L}{2} \cdot \left(\frac{L}{4} - a \right) = 1616.2 \cdot kip \cdot ft$$

$$M_{ps} := F_{sems} \cdot e_{ms} = 3388.2 \cdot kip \cdot ft$$

$$M := M_{ps} - M_{dlms} = 1772 \cdot kip \cdot ft$$

$$R := \frac{E_{ci} \cdot I_{xi}}{M} = 1 \times 10^{5} \cdot in$$

$$camber := \frac{L^{2}}{8 \cdot R} = 3 \cdot in$$

The height of the center of gravity of the cambered arc above the roll axis yr is calculated similar to sweep

$$y_r := y_t - camber \cdot offset = 28.3 \cdot in$$

Compute Z_0

Z0 is the distance to the center of gravity of the defelected arc of the girder about the minor-axis. This takes into the accunt the distance between the girder end and the lifting point (a)

$$z_0 := \frac{w_{dl}}{12 \cdot E_{ci} \cdot I_{yi} \cdot L} \cdot \left(\frac{1}{10} \cdot L_1^{5} - a^{2} \cdot L_1^{3} + 3 \cdot a^{4} \cdot L_1 + \frac{6}{5} \cdot a^{5} \right) = 5.8 \cdot in$$

Compute θi

θi is the inital roll angle due to sweep

$$\theta_i := \frac{e_i}{y_r} = 0.0237 \qquad \theta_i = 1.358 \cdot deg$$

Compute the tilt angle θmax at cracking

Rupture concrete stresss

$$f_r := 7.5 \sqrt{\frac{f_{ci}}{psi}} \cdot psi = 677.9 \cdot psi$$

Top and bottom stresses due to gravity loads

$$f_b := \frac{M_{dlms} \cdot y_b}{I_{xi}} + \frac{-F_{sems}}{A_{ci}} - \frac{F_{sems} \cdot e_{ms} \cdot y_b}{I_{xi}} = -3.9 \cdot ksi$$

$$f_t := -\frac{M_{dlms} \cdot y_t}{I_{xi}} + \frac{-F_{sems}}{A_{ci}} + \frac{F_{sems} \cdot e_{ms} \cdot y_t}{I_{xi}} = -0.68 \cdot ksi$$

Lateral moment that will cause cracking in the top fibers

$$M_{lat} := \left(f_r - f_t\right) \cdot \frac{I_{yi}}{\left(\frac{b}{2}\right)} = 334 \cdot kip \cdot ft$$

Maximum roll angle

$$\theta_{max} := \frac{M_{lat}}{M_{dlms}} = 0.207 \qquad \theta_{max} = 11.839 \cdot deg$$

Maximum tilt angle during lift to avoid cracking is 12.5 deg

Compute factor of safety

Factor of safety aganist cracking. This considers the ratios between the height of roll center to the lateral deflection and the maximum tilt angle to the initial roll angle

$$FS_{cracking} := \frac{1}{\frac{z_0}{y_r} + \frac{\theta_i}{\theta_{max}}} = 3.1$$

Factor of safety aganist failure. This considers the cracked condition of the girder

Z'0c is the distance to the center of gravity of the defelected arc of the cracked girder.

$$\theta_{maxc} := \sqrt{\frac{e_i}{2.5 \cdot z_0}} = 0.215$$

$$z_{0c} := z_0 \cdot \left(1 + 2.5 \cdot \theta_{maxc}\right) = 9 \cdot in$$

$$FS_{failure} := \frac{y_r \cdot \theta_{maxc}}{z_{0c} \cdot \theta_{maxc} + e_i} = 2.3$$

Stability Analysis during Transportation

$F_{sems} = 2234 \cdot kip$ $e_{ms} = 18.2 \cdot in$

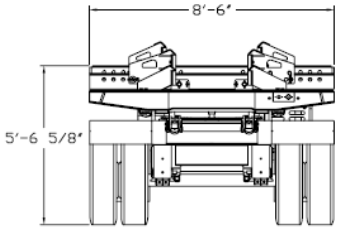

superelevation angle $\alpha := 0.06$

Trailer properties

Height of trailer $h := 68in + 4in = 72 \cdot in$

height of roll center $h_r := 24in$ assumed

height of cg above road $h_{cg} := h + CG_{yi} = 96.1 \cdot in$

Estimate the rotational stiffness of the transportation vehicle

Kθ is the elastic roatational spring constant of the vehicle

assume $K_{\theta_axle} := 4500kip \cdot in$ per radian per dual axle

Trailer has six dual axles

$K_{\theta_trailer} := 6 \cdot 4500kip \cdot in = 27000 \cdot kip \cdot in$ per radian per tariler

$K_{\theta_truck} := K_{\theta_trailer} \cdot 2 = 54000 \cdot kip \cdot in$ per radian

$$r := \frac{K_{\theta_truck}}{w_{dl} \cdot L} = 459.4 \cdot in$$

Find tilt angle

Distance between the cenetr of graviyt of the girder and the roll axis

$y := h_{cg} - h_r = 72.1 \cdot in$

account for camber $y := y \cdot 1.02 = 73.5 \cdot in$

Calculate initial eccentricity as a result of sweep for the transportation case

$$sweep_T := \frac{1}{8} in \cdot \frac{L}{10ft} = 1.6 \cdot in$$

$e_T := 1in + sweep_T \cdot offset = 1.8 \cdot in$

Since Young's modulus did not change, z0 remains the same

$z_{0T} := z_0 = 5.8 \cdot in$

Tilt angle

$\theta_T := \frac{\alpha \cdot r + e_T}{r - y - z_{0T}} = 0.077 \qquad \theta_T = 4.434 \cdot deg$

Check concrete compressive strength

Check stress at centerline

$F_{sems} = 2234 \cdot kip \qquad e_{ms} = 18.2 \cdot in$

$f_b := \frac{M_{dlms} \cdot y_b}{I_{xi}} + \frac{-F_{sems}}{A_{ci}} - \frac{F_{sems} \cdot e_{ms} \cdot y_b}{I_{xi}} = -3.9 \cdot ksi$

$f_t := -\frac{M_{dlms} \cdot y_t}{I_{xi}} + \frac{-F_{sems}}{A_{ci}} + \frac{F_{sems} \cdot e_{ms} \cdot y_t}{I_{xi}} = -0.68 \cdot ksi$

Add lateral bending to fb

$M_{latcheck} := \theta_T \cdot M_{dlms} = 125.1 \cdot kip \cdot ft$

Bottom flange width

$b_b = 36 \cdot in$

$f_{bT} := f_b - M_{latcheck} \cdot \frac{b_b \cdot 0.5}{I_{yi}} = -4.2 \cdot ksi$

Minimum required compressive strength

$f_{cmiin} := \frac{-f_{bT}}{0.6} = 7065.6 \cdot psi \qquad OK$

Compute tilt angle θmax at cracking

$$M_{latT} := \frac{(f_r - f_t)\cdot I_{yi}}{\frac{b}{2}} = 334\cdot kip\cdot ft$$

$$\theta_{maxT} := \frac{M_{latT}}{M_{dlms}} = 0.207 \qquad \theta_{maxT} = 11.839\cdot deg$$

Compute factor of safety

Factor of safety aganist cracking

$$FS_{crackingT} := \frac{r\cdot(\theta_{maxT} - \alpha)}{z_{0T}\cdot\theta_{maxT} + e_T + y\cdot\theta_{max}} = 3.7$$

Factor of safety aganist rollover. This considers the cracked condition of the girder

Zmax is the distance between the centerline of the vehicle to the centerline of dual tire

$$z_{max} := 36in$$

$$\theta_{maxcT} := \frac{z_{max} - h_r\cdot\alpha}{r} + \alpha = 0.135$$

Z'0cT is the distance to the center of gravity of the defelected arc of the cracked girder

$$z_{0cT} := z_0\cdot(1 + 2.5\cdot\theta_{maxc}) = 9\cdot in$$

$$FS_{failureT} := \frac{r\cdot(\theta_{maxT} - \alpha)}{z_{0cT}\cdot\theta_{maxc} + e_T + y\cdot\theta_{maxT}} = 3.6$$

This public document is published at a total cost of $250
42 copies of this public document were published in this first printing at a cost of $250. The total cost of all printings of this document including reprints is $250. This document was published by Louisiana Transportation Research Center to report and publish research findings as required in R.S. 48:105. This material was duplicated in accordance with standards for printing by state agencies established pursuant to R.S. 43:31. Printing of this material was purchased in accordance with the provisions of Title 43 of the Louisiana Revised Statutes.